UNIVERSITY OF GENOVA

PHD PROGRAM IN BIOENGINEERING AND ROBOTICS

Assessment and enhancement of proprioception

by

Giulia Ballardini

Thesis submitted for the degree of *Doctor of Philosophy* (34° cycle)

May 2022

Maura Casadio	Supervisor
Giorgio Cannata	Head of the PhD program

Thesis Jury:

Lorenzo Masia, *Heidelberg University*	External examiner
Michela Bassolino, *HES-SO Valais Wallis, Institute of Health*	External examiner

Dibris

Department of Informatics, Bioengineering, Robotics and Systems Engineering

Declaration

I hereby declare that except where specific reference is made to the work of others, the contents of this dissertation are original and have not been submitted in whole or in part for consideration for any other degree or qualification in this, or any other university. This dissertation is my own work and contains nothing which is the outcome of work done in collaboration with others, except as specified in the text and Acknowledgements. This dissertation contains fewer than 65,000 words including appendices, bibliography, footnotes, tables and equations and has fewer than 150 figures.

Giulia Ballardini
May 2022

Abstract

In daily living activities, proprioception is fundamental to interact with the environment and rapidly react to changing circumstances. The ability to coordinate force and position in bimanual tasks is essential for manipulating objects out of view and preventing their slippage. The work carried out in my Ph.D. research project aims to highlight the importance of assessing proprioception in both people with sensorimotor deficits and unimpaired and provide guidelines on how to design an effective supplementary vibrotactile feedback to enhance proprioception and the associated motor outcomes.

In the usual formulation of assessment protocols, either in research or clinical environments, position and force sense are mainly evaluated separately while their possible interactions and interference have received less attention. In my Ph.D. research project, I did a step toward filling this gap, identifying the reciprocal interaction between position sense and force control in bimanual tasks performed by unimpaired participants. I found that position sense is influenced by the symmetry of the loading condition, while force control is mostly affected by the position of the non-dominant hand. I also found that this latter result was not determined by handedness, but more likely by the specialization of the brain hemispheres. However, handedness influenced the overall proprioceptive performance since left-handers had a more asymmetrical performance than right-handers.

In the neurological assessment protocols commonly used in the clinical practice, proprioceptive functions are mainly assessed subjectively by clinicians referring to qualitative clinical scales. However, reliable methods to quantify proprioceptive deficits are crucial for better enhancing the detection of early symptoms, developing effective neuro-rehabilitative treatments, and monitor the progress of both disease and treatments. Furthermore, after stroke the main focus of clinical assessment is on the contralesional side of the body. Less attention is dedicated to the ipsilesional side and to the bimanual coordination. To this end, in my Ph.D. project, I investigated the position sense deficits of the two upper limbs taking into account also the location of the lesion. I found that the ipsilesional arm of stroke survivors had similar matching accuracy but higher precision than the contralesional arm. The accuracy of the two arms inter-correlated in the left and central regions of the peripersonal space for all

the stroke survivors independently of the location of the brain lesion. This findings highlight that after stroke the two arms have different proprioception and motor capabilities. As results, one of the main consequences is a defective bimanual coordination, which impacts the ability to perform many daily living activities. Despite its importance, the current formulation of the neurological assessment and rehabilitative protocol is more focused on unimanual task, limiting the possibility to investigate the interaction and interference that arise from the inter-limb coordination. This could be due to the limited availability of devices to assess the bimanual proprioception. In this context, in my Ph.D. research project I optimized a device to assess proprioception and the reciprocal interaction between position sense and force control in bimanual tasks. Its usability has been tested on stroke survivors, which performed force matching tasks and a lifting task. In the matching task, I found that the stroke survivors had higher difficulty to match a level of force required, even when it was tailored on their capability, while their ability to maintain the force was not affected. In the lifting task, I found that stroke survivors applied more force than age-matched unimpaired participants to lift the device. However, the timing in which the force was applied was not significantly different between the two populations.

Due to impact of the proprioceptive deficits, several solutions have been proposed to mitigate them and enhance the related motor outcome. Among all, the application of supplementary somatosensory feedback has been shown to be an effective resource to enhance sensorimotor ability in unimpaired participants as well as in people with sensorimotor deficits. This type of feedback is an strong modulator of plasticity, enhances motor (re-)learning and control, and can also temporally reduce position sense disorders. However, how to convey the proprioceptive information in the supplementary feedback (i.e., encoding method) and the importance of the information conveyed by the feedback (i.e., informational content) are not well investigated. In this context, my Ph.D. research project aims at deepening the actual knowledge on how to encode information in supplementary vibrotactile feedback to enhance proprioception and related motor outcomes. To this end, I compared the effects on postural control of two methods for encoding the amplitude and direction of the acceleration of the body center of mass in the activation of two vibration motors placed on the back and on the abdomen of the participants. I also evaluated the importance of the informational content of the feedback by applying a vibrotactile feedback that was uncorrelated with the actual oscillations of the center of mass. The results show that synchronized vibrotactile feedback significantly reduced the sway amplitude while increasing the frequency in anterior-posterior and medial-lateral directions. The presence of uncorrelated vibration, instead, increased

the sway amplitude, highlighting the importance of the informational content. In a second study, I tested the effects of applying two types of supplemental vibrotactile feedback on the ipsilesional arm in stroke survivors while they performed goal-directed movements with their contralesional arm. I found that all the three stroke survivors were able to perceive the vibrotactile feedback and to perform the motor tasks (i.e., reaching and stabilization) when it was applied, but they reached various levels of capability in distinguishing and using it during the motor tasks. Indeed, all of them improved their performance in the stabilization task using one encoding scheme. The stroke survivor with the better sensory assessment score also improved in the reaching performance when one supplemental feedback was applied. These preliminary results encourage investigating the effects of a longer multi-session training with a personalized vibrotactile feedback design.

The findings of my Ph.D. research project enlarge the actual knowledge on interaction between the upper limb position sense and force control, and its asymmetries related to handedness and how it is affected after stroke. My Ph.D. research project also provide evidences to support the need to a assess both ipsilesional and contralesional proprioceptive deficits separately and concurrently during bimanual tasks.

Journal publication

- Marchesi G.*, Ballardini G.*, Barone L., Giannoni P., Lentino C., De Luca A., Casadio M. *'Modified Functional Reach Test: upper-body kinematics and muscular activity in chronic stroke survivors'*, Sensors 22 (1): 230 (2022). doi.org/10.3390/s22010230

- Ballardini G., Krueger A., Giannoni P., Marinelli L., Casadio M., Scheidt R. A. *'Effect of short-term exposure to supplemental vibrotactile kinesthetic feedback on goal-directed movements after stroke: a proof of concept case series'*, Sensors 21(4): 1519 (2021). doi.org/10.3390/s21041519

- Handelzalts S., Ballardini G., Avraham C., Pagano M., Casadio M., Nisky I. *'Towards the integration of somatosensory augmentation technologies into home-based neurorehabilitation: opportunities and challenges in light of COVID-19 pandemic'*, Frontiers in Neurorobotics 15:4 (2021). doi.org/10.3389/fnbot.2021.617636

- Ballardini G., Florio V., Canessa A., Carlini G., Morasso P., Casadio M. *'Vibrotactile feedback for improving standing balance'*, Frontiers in Bioengineering and Biotechnology (2020). doi:10.3389/fbioe.2020.00094

- Ballardini G., Ponassi V., Galofaro E., Carlini G., Marini F., Pellegrino L., Morasso P., Casadio M. *'Interaction between position sense and force control in bimanual tasks'*, Journal of NeuroEngineering and Rehabilitation 16.1 (2019): 1-13. doi:10.1186/s12984-019-0606-9

Peer-reviewed conference

- Mohamed Y., Ballardini G., Parreira M. T., Lemaignan S., Leite I. *'Automatic frustration detection using thermal imaging'*, ACM/IEEE International Conference on Human-Robot Interaction (HRI), virtual. (March 7-10, 2022)

- Viola L., Lagazzi E., Ballardini G., Drogo A., Bonetti M., Marrone E., Chirico M., Ricci S. *'Design of a system to detect the force applied by tourniquets in a manikin's limb'*, Annual International Conference of the IEEE Engineering in Medicine and Biology Society (EMBC), virtual. (October 31-November 4, 2021)

- Giordano M., Rizzoglio F., Ballardini G., Mussa-Ivaldi F., Casadio M. *'Controlling an assistive robotic manipulator via a non linear body machine interface'*, International Conference on NeuroRehabilitation (ICNR), virtual. (October 13-16, 2020)

- Reboli T., Meloni S., Ballardini G., Carlini G., Casadio M., Sante F., Serafica M., Vigo G., Schiatti L. *'Hybrid actuation mechanism for an ultra-low-cost transhumeral prosthesis: preliminary study'*, International Conference on NeuroRehabilitation (ICNR), virtual. (October 13-16, 2020)

- Ballardini G., Casadio M. *'Isometric force matching asymmetries depend on the position of the left hand regardless of handedness'*. In International Conference on Human Haptic Sensing and Touch Enabled Computer Applications (pp. 194-202). Springer, Cham. Eurohaptics Conference, Leiden, Netherlands. (September 6-9, 2020)

- Ballardini G., Ponassi V., Galofaro E., Pellegrino L., Solaro C., Muller M., Casadio M. *'Bimanual control of position and force in people with multiple sclerosis: preliminary results'*. IEEE 16th International Conference on Rehabilitation Robotics (ICORR, pp. 1147-1152), Toronto, Canada. (June 24-28, 2019)

- Galofaro E., Ballardini G., Boggini S., Foti F., Nisky I., Casadio M. *'Assessment of bimanual proprioception during orientation matching task with a physically coupled object'*. IEEE 16th International Conference on Rehabilitation Robotics (ICORR, pp. 101-107), Toronto, Canada. (June 24-28, 2019)

- Marchesi G., Casadio M., Ballardini G., De Luca A., Squeri V., Vallone F., Giorgini C., Crea P., Pilotto A., Sanfilippo C., Saglia J., Canessa A. *'Robot-based assessment of sitting and standing balance: preliminary results on Parkinson's disease'*. IEEE 16th International Conference on Rehabilitation Robotics (ICORR, pp. 570-576), Toronto, Canada. (June 24-28, 2019)

Other conferences

- Ricci S., Saporetti C., Ballardini G., Torrigino D., Chirico M., Borgonovo G., Torre G., Minuto M., Casadio M., *'Design and implementation of an open source visuo-haptic simulator for surgical training'*, Annual Meeting of Society for Simulation in Europe (SESAM). (June 15-17, 2022) (Accepted)

- Viola L., Lagazzi E., Drogo A., Bonetti M., Marrone E., Ballardini G., Torre G., Chirico M., Ricci S. *'Force monitoring during tourniquet positioning. Is this the future of stop the bleed courses and bleeding control medical simulation?'*, International Meeting on Simulation in Healthcare (IMSH). (January 15-19, 2022)

- Wagner J. C., Ballardini G., Bommarito G., Inglese M., Casadio M., Canessa A., Scheidt R. A., Beardsley S. A., *'Hidden Markov modelling of altered cortical networks during reach in people with multiple sclerosis and intention tremor'*. Society for Neuroscience Annual Meeting (SfN), Chicago (IL), USA and virtual. (November 8-16, 2021)

- Delrio R., Ballardini G., Casadio M., Mastrogiovanni F., Nisky I. *'Stiffness discrimination performance in a virtual surgical incision task'*. Workshop on learning of manual skills in humans and robots, International Conference of Robotics and Automation (ICRA), virtual. (May 31, 2020)

- Ballardini G., Casadio M. *'Behavioral asymmetries in bimanual isometric force matching task is influenced by the position of the left hand'*. Karniel Computational Motor Control Workshop (CMCW), Be'er Sheva, Israel. (Accepted – March 2020 - workshop cancelled)

- Ballardini G., Ponassi V., Galofaro E., Carlini G., Pellegrino L., Marini F., Muller M., Solaro C., Morasso P., Giannoni P., Nisky I., Casadio M. *'Interaction between position and force control in bimanual tasks in unimpaired subjects and people with multiple sclerosis'*. Society for Neuroscience Annual Meeting (SfN), Chicago (IL), USA. (October 19-23, 2019)

- Wagner J., Ballardini G., Bommarito G., Inglese M., Casadio M., Canessa A., Iurato M., Scheidt R.A., Beardsley S. *'Neural correlates of decreased functional connectivity related to sensorimotor control dysfunction in persons with multiple sclerosis'*. Society for Neuroscience Annual Meeting (SfN), Chicago (IL), USA. (October 19-23, 2019)

- Thomas A., Shah V.A., Ballardini G., Stoeckmann T., Casadio M., McGuire J.R., Scheidt R.A., Mrotek L.A. *'The utility of vibrotactile cues as supplemental movement feedback varies across application site and individuals after stroke: A pilot study'*. Society for Neuroscience Annual Meeting (SfN), Chicago (IL), USA. (October 19-23, 2019)

- Shah V.A., Thomas A., Ballardini G., Casadio M., Mrotek L.A., Scheidt R.A., *'Impact of extended training on vibrotactile feedback guided reaching'*. Society for Neuroscience Annual Meeting (SfN), Chicago (IL), USA. (October 19-23, 2019)

- Wagner J., Ballardini G., Bommarito G., Inglese M., Casadio M., Canessa A., Iurato M., Scheidt R.A., Beardsley S. *'Decreased functional connectivity in sensorimotor*

brain networks in persons with Multiple Sclerosis and upper extremity dysfunction'. Rocky Mountain Bioengineering Symposium (RMBS), Milwaukee (WI), USA. (April 12-14, 2019)

- Ponassi V., Ballardini G., Galofaro E., Carlini G., Pellegrino L., Marini F., Muller M., Solaro C., Morasso P., Casadio M. *'Interaction between position and force control in bimanual tasks'*. Karniel Computational Motor Control Workshop (CMCW), Be'er Sheva, Israel. (March 24-26, 2019)

- Ballardini G., Florio V., Carlini G., Canessa A., Morasso P., Casadio M. *'Vibrotactile feedback for improving standing balance: effects of different encoding methods and importance of information content'*. Karniel Computational Motor Control Workshop (CMCW), Be'er Sheva, Israel. (March 24-26, 2019)

- Ballardini G., Florio V., Carlini G., Canessa A., Morasso P., Casadio M. 'The influence on the postural sway of a vibrotactile feedback provided by a novel low-cost and portable device'. Innovation in Rehabilitation Technologies (IRT), Genoa, Italy. (March 5, 2019)

Honor and award

- 2021: Won the C.M. Lerici Foundation scholarship for carrying out a research project in Sweden at the Robotic, Perception and Learning Division of KHT - Royal Institute of Technology in Stockholm.

- 2020: Member of the 'Best poster award' committee and student volunteer at the Eurohaptics 2020.

- 2019: Travel award for the Karniel Computational Motor Control Workshop from in Be'er Sheva, Israel.

Table of contents

List of figures

List of tables

Nomenclature

Acronyms / Abbreviations

ADC Analog to Digital Converter

AO Always On feedback method

AP Anterior-Posterior direction

ARAT Action Research Arm Test

AU Action Unit

BE Bias Error

CAHAI Chedoke Arm and Hand Activity Inventory

CNS Central Nervous System

CoM Center of Mass

cUL contralesional Upper Limb

CV Coefficient of Variance

D Dominant arm

DZ Dead Zone feedback method

EDA ElectroDermal Activity

EEG Electroencephalography

EMG Electromyography

ERM Eccentric Rotating Mass

F95 Frequency at which the power spectral density reaches the 95th percentile

ARAT Frenchay Arm Test

FMA-UE Upper Extremity portion of the Fugl-Meyer Assessment

FS Full Scale

FSR Full Scale Range

GUI Graphical User Interface

HC1-HC2-HC3-HC4 Hand Configuration in the bimanual force matching task

HRI Human-Robot Interaction

IMU Inertial Measurement Unit

iUL ipsilesional Upper Limb

JND Just Noticeable Difference

KNN K-Nearest Neighbors

LBD stroke survivors with Left Brain Damage

LC1-LC2-LC3-LC4 Loading Conditions in the bimanual position matching task

L Left

MAS Modified Ashworth Scale

ML Medial-Lateral direction

MS Multiple Sclerosis

MVF Maximum Voluntary Force task

NSA Nottingham Sensory Assessment

PCB Printed Circuit Board

PLA PolyLactid Acid

PwMS People with Multiple Sclerosis

RAMIS Robot-Assisted Minimally Invasive Surgery

RBD stroke survivors with Right Brain Damage

RMSE Root Mean Square Error

RMS Root Mean Square acceleration

ROI Regions Of Interest

R Right

SFFS Sequential Forward Floating Selection

SPI Serial Peripheral Interface

S Sham feedback

TB Trigger-Box

T vibroTactile feedback

V Visual feedback

Introduction

Somatosensation is vital to daily-living activities, critical for independence in the environment and purposeful interaction with the external world. It allows, for example, to maneuvering our way around obstacles in the dark and be able to manipulate objects out of view and prevent their slippage.

Somatosensation is mediated by two subsystems: proprioception (kinesthetic) and tactile (cutaneous) system. The tactile system provides information about contact with objects using mainly four types of myelinated cutaneous mechanoreceptors that are sensitive to mechanical pressure and skin deformation (Merkel cells, Ruffini corpuscles, Meissner corpuscles, and Pacinian corpuscles) [1]. It is essential for sensing the proprieties of the objects and helps in the object manipulation [2]. Proprioception includes the senses of position and motions, and the senses of effort, and force. The proprioceptors are located in the skin (Ruffini corpuscles and Pacinian corpuscles), skeletal striate muscles (muscle spindles) and junctions between tendons and muscles (Golgi tendon organs) [1]. The signals from those two subsystems follow the same pathway for the central nervous system that ends in the primary somatosensory cortex (S1, or Brodmann area 3, 1 and 2) located in the parietal lobe [1].

Proprioception is fundamental to perform efficient movement, to interact with the environment, and react rapidly in changing circumstances. Furthermore, afferent proprioceptive signals generated during movements are processed and used in both feedback and feedforward control loops. Indeed, in the feedback loop, proprioceptors have a role in rapid adaptation mechanisms during motor task execution, while in the feedforward loop they contribute to motor planning [3]. They help in the formation and maintenance of the internal body schema to produce accurate motor command and predict the consequences of the actions [4]. Proprioceptive information is perceived both at the conscious and unconscious level. Conscious proprioception is helping in performing complex motor tasks, while unconscious information is important for the reflexive control of muscle tone and the control of posture [4]. Indeed, information about the muscle contraction concomitant with the action establish the force exterted and required to successfully accomplish the action. The ability to coordinate

bimanual force and position control is essential for completing several daily-living activities, such as manipulate objects out of view, preventing their slippage. To successfully accomplish bimanual tasks our central nervous system has to process and integrate visual, tactile and proprioceptive inputs coming from both sides of the body's midline and coordinates the actions of the two hands [1]. Even if sense of force and position share neural pathways and sensory receptors, in the usual formulation of assessment protocols, either in research or clinical, position and force senses are mainly evaluated separately with qualitative tests. Moreover, while bimanual actions have been widely investigated in general terms, the impact of discordant motion and/or of different force feedback arising from the two arms has received less attention. The first aim of my Ph.D. research project is a first step toward to filling this gap, deepening the knowledge identifying of the reciprocal interaction between position sense and force control.

Previous studies on people with proprioception deafferentation have shown that the loss of proprioception results in deficits in inter-joint coordination [5] and limb stabilization also in presence of visual feedback [5, 6]. However, proprioception is affected by many neurodegnerative diseases and traumatic events, such as Multiple Sclerosis, Parkison's disease and stroke. Proprioceptive deficits affects motor planning, control, and (re-)learning and limit functional recovery in various motor tasks [3–8]. As consequence, reliable methods to quantify proprioceptive deficits are crucial to assess sensorimotor abilities during the progress of the disease, enhance the detection of early symptoms and designing neuro-rehabilitative approaches to improve upper limb functions and quality of life.

Moreover, in the current formulation of the neurological assessment protocol, proprioceptive functions are most often subjectively assessed by clinicians using qualitative clinical scales [7, 9]. In addition to that, the different aspects of proprioception and the two upper limbs are mainly evaluated separately without taking into account the bimanual coordination. This limits the evaluation of the possible interactions or interference that arise from the inter-limb coordination [10–12], which is one of the main outcome of proprioceptive deficits.

Furthermore, after stroke, the two upper limbs had different somatosensory [13, 14] and motor [15, 16] deficits in the ipsilateral and contralateral hemi-body sides with respect to the brain lesion side. Recent studies suggested that hemispheric specialization influences differently the motor deficits in both arms following unilateral stroke [17–23], the dependency on this in proprioceptive deficits is less investigated [24]. The previous studies on differences in somatosensory deficits due to hemisphere of the lesion reported discordant and task-specific findings.

In my Ph.D. research project I did a first step toward filling those gaps, deepening the knowledge on the proprioceptive performance of stroke survivors while performing uni and bimanual tasks.

Somatosensation and motor control could be enhance using wearable technologies in unimpaired people by guiding ongoing movement with supplemental kinesthetic cues in various forms: vibrotactile, skin stretch cues, and force feedback [25, 26]. Providing supplemental haptic cues may also be a way to mitigate the impact of proprioceptive deficits on upper limb control after stroke. It is well known that this type of feedback is an effective modulator of plasticity, enhances motor (re-)learning and control, and it can also temporally reduce position sense disorders [27–34]. As consequence, several research groups developed devices and technologies for applying supplementary somatosensory feedback [35–38]. Among all, vibrotactile feedback is widely used because it the simplest tactile stimulation from the technological point of view. For that reasons, there is a spreading of devices that apply different stimulation patterns ranging from a simple on-off stimulation provided by one actuator [39–41] to a complex pattern of stimuli provided by an array of actuators [42, 43]. However, the effectiveness of the supplementary feedback in enhancing the performance is strictly related to the stimulation pattern, since it could result difficult to interpret and integrate in the neural control [26]. One reason is that the patterns of somatosensory stimuli could result not intuitive or complex, due to either the number of vibration motors, thus forcing the user to process a redundant set of signals, or to the encoding methods that may require specific attention [44]. While from the technological point of view there are several solutions for providing supplemental vibrotactile feedback, while which information is more effective to enhance proprioception and how to encode it has received less attention. To this end, in my Ph.D. research project, I focused on the supplementary vibrotactile feedback, and I compared the efficacy of different econding method in enhancing sensorimotor abilities and the related motor outcome in both unimpaired individuals and people with sensorimotor deficits.

In detail, this Ph.D. thesis is divided into three main parts:

Part I Part I is about the interaction in unimpaired participants between the ability to perceive and control concurrently the position sense and the force control in a bimanual task (Chapter 1 and 2).

Part II is about the influence of sensorimotor deficits in stroke survivors in the ipsilesional arm (Chapter 3) and the bimanual coordination (Chapter 4);

Part III is about supplementary haptic feedback to enhance motor proprioception and motor performance. After a review of the supplementary haptic feedback used in literature (Chapter 5), I report the studies on the effect of different encoding methods for the vibrotactile feedback to improve position sense in unimpaired participants (Chapter 6) and in stroke survivors (Chapter 7).

Part I

Interaction between the ability to perceive and control concurrently the position sense and force control

Introduction

The ability to lift objects and to apply coordinated bilateral forces is essential for completing several daily living activities. To successfully accomplish ordinary bimanual tasks our Central Nervous System (CNS) has to process the sensory inputs coming from both sides of the body's midline and coordinate the actions of the two hands, integrating haptic information. For that reason, asymmetric conditions might influence task execution due to cross-modal interference [45–48]. This is the case, for example, of when the two hands have to simultaneously perform different actions or achieving the same goal in the presence of different sensory inputs from the two sides of the body.

Both position and force sense contribute to efficient neural control of actions that imply interaction with the environment at different levels: they have a role in reflex responses at both spinal and cortical levels, are fundamental for the control of all purposeful movements [1, 49–53] and influence motor (re-)learning [4, 7, 54].

Force and position control have different neural correlates [55–57] and contribute to different action features (e.g. pushing and reaching), but they share neural pathways and sensory receptors [58]. For example, muscle spindles are responsible for the position sense and are also involved in the perception of force and heaviness [59–61]. Thus, the simultaneous processing of motions and forces could represent a challenge and it might also lead to reciprocal interference, a crucial topic that was rather recently disregarded [58, 62].

Nevertheless, in the usual formulation of assessment protocols, either in research or clinical environments, position and force sense are mainly evaluated separately, without accounting for their possible interactions or interference [7, 63, 64]. The most used protocols are based on matching tasks, where blindfolded participants are required to match a reference joint position [58, 63, 65, 66] or a level of muscle contraction [52, 58, 67] with the same or with the other arm, either sequentially or concurrently. These protocols allowed investigating the asymmetries in the upper-limbs position [68, 69] and force [70] control associated with handedness and hand preferences [71, 72]. They were also used to establish indicators for intrinsic cerebral asymmetry at functional and structural levels [73–76] and to find similarity of pathways and sensory receptors between force and position sense [58].

In position matching tasks, few studies demonstrated that changing the sensory inputs affects performance [77]. For example, eliminating the antigravity support or adding weights to the reference arm provided an additional position sense cue that improved matching outcomes [77]. However, to the best of our knowledge, this sensory effect has not been evaluated in bimanual tasks with both hands active and engaged toward a common goal.

In other words, there is a lack of knowledge on how additional sensory inputs provided symmetrically or asymmetrically to the two hands impact concurrent bimanual control; this is the case for the influence of the loading conditions on position control as well as for the influence of position sense on force control.

More specifically the purpose of this project was: to investigate - in healthy participants and people with MS - how the sense of effort influences the ability to sense and control the position of the hands to investigate how the configurations of the arms have an impact on the ability to produce isometric force in tasks where the two hands share a common goal. Our hypothesis was that asymmetric loading conditions and asymmetric arm configurations might affect, respectively, the accuracy of lifting the two hands at the same height and/or applying bilaterally equal isometric forces. In fact, in mirror-symmetric conditions, the CNS could simply solve the task of guiding the two hands toward the common goal by transmitting the same motor commands to both sides of the body [78–80]. Conversely, in the presence of different sensory feedback from the two arms, the CNS must take into account this difference and compensate for it, producing different bilateral motor commands for achieving the same common goal. we wonder whether the CNS might not account correctly for the mismatch on the sensory inputs between the two limbs when pursuing a bilateral equal force or position goal; the differences in performance among task conditions would highlight this effect. In order to investigate these hypotheses, we designed and built a device that allowed to implement two bimanual matching tasks: a first task investigating position control where the two hands had to be placed in the same position under different loading conditions; and a second task where participants had to produce an equal isometric force with the two arms in symmetric or asymmetric configurations. Both tasks were performed without the guidance of visual feedback.

Experimental set-up

We designed and built a device (Fig. 1) for evaluating the ability to control position, force, and their interaction in bimanual tasks, as lifting objects and applying controlled isometric forces in the upward direction. The device is composed by two wooden vertical bars, firmly attached to a base plane. Each bar has a metal linear guide where a custom-made handle can slide or be locked in specific positions. The vertical motion of each handle is transmitted to a potentiometer (Vishay; maximum resistance of 500 Ω, linearity of ±0.25% FS) via a belt and a pulley in order to provide a precise measurement of the handle position (resolution of 0.27 mm). The friction of the sliding motion of the handle is minimized by a custom-designed

bearing block. The handle can be locked in fixed positions by a mechanical block and in such case, the isometric force exerted by the participant in the upward direction is measured by a micro load cell (mod. CZL635, Phidgets Inc.; full range scale of 5kg; precision of 0.05%; linearity of 0.05% FS). The analog signals from the potentiometers and the load cells are recorded by a DAQ board (NI USB-6008, National Instruments) that is used also to power them. The vertical range of motion of each sliding guide is 0.60 m and the lateral distance of the two guides is 0.50 m, approximately equivalent to the average shoulder-to-shoulder distance.

The handle has a cylindrical shape (90 mm height, diameter of 20 mm) and a weight of 50 g: it is 3D-printed in a rigid and low-weight material (polylactic acid) and covered with high-density foam to increase comfort. It is designed to be easy-to-grasp also by people with low to moderate motor deficits affecting upper limbs or hands. The upper side of the handle terminates with a plate where additional weights could be placed to change the loading condition during the bimanual position matching task (see subsection 1.1.2 for more details). Two conditions were used: (i) no weight, and (ii) additional weights (250 g or 500 g). Both the types of weights are shaped as cylindrical containers with the same dimension (30 mm height and diameter of 60 mm): the weight difference is obtained by homogeneously filling the containers with different percentages of clay and lead.

The DAQ board is connected to a laptop via USB. The control software is developed in LabVIEW (National Instrument): it acquires the data from the board at a sampling frequency of 100 Hz and sends the corresponding visual information to the screen placed between the two vertical bars.

During the tasks (bimanual position and force matching tasks, see also subsection 1.1.2) the device was placed on a table and the participants were seated on a 0.50 m high chair in front of it (Fig. 1). Participants grasped the cylindrical part of the device's handles, maintaining their hands (thumb and index fingers) in contact with the bottom surface of the plates. The distance between the participants and the device was slightly adjusted for each participant, such that their arms were completely extended at the top of the metal guide. The base plane of the device provided a surface where the arms could rest during breaks. A black curtain prevented the visual feedback of shoulders, arms, and hands for the entire duration of the experiments. Our goal was to assess proprioceptive ability in terms of position and force control as well as their interaction without visual influence. We designed two separate experiments that required the coordination of the two hands. Participants were allowed and encouraged to rest anytime they needed during the execution of each experiment, but they did not ask for any pause. Between the two tasks a break between them to prevent fatigue.

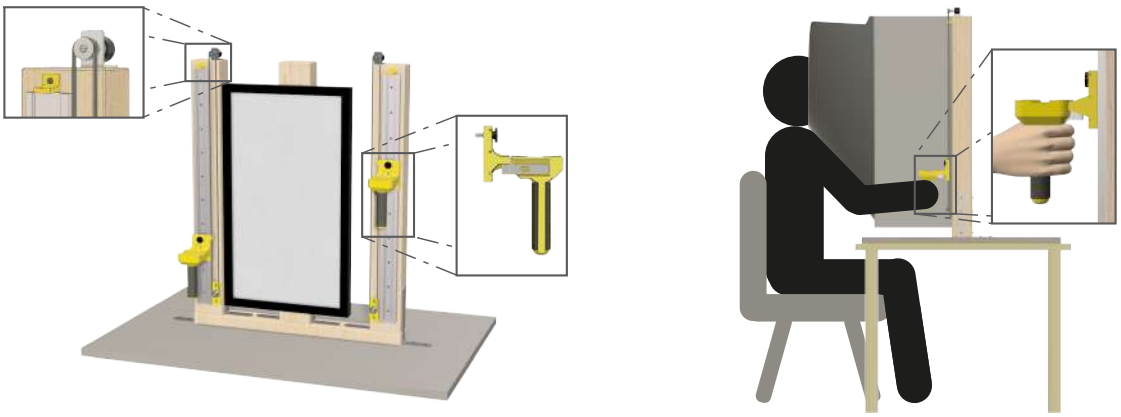

Figure 1 (left) Render of the device with a screen placed in the middle of the two lateral poles, with metal guides where custom-made handles could slide. The motion of each handle was transmitted through a belt and a pulley to a potentiometer that measured its position (left detailed view). Each handle enclosed a load cell (right detailed view) to record the force applied to the handles after fixing them with a screw in specific positions on the guide. The load cells recorded the force applied in the upward direction (i.e., the participants had to push the handle upward). (right) Experimental set-up. The device was placed on a table and the Participants were seated in front of the screen. A black curtain was attached to the device in order to prevent the visual feedback of their arms.

Chapter 1

Study I: Right-handed participants

This study has been published in: Ballardini. G., Ponassi V., Galofaro E., Carlini G., Marini F., Pellegrino L., Morasso P., Casadio M. *'Interaction between position sense and force control in bimanual tasks'*, Journal of NeuroEngineering and Rehabilitation 16.1 (2019): 1-13. doi:10.1186/s12984-019-0606-9

1.1 Material and methods

1.1.1 Participants

Twenty people participated in both tasks (mean $\pm$ std age: 31 $\pm$ 14 years old; 12 females). Five additional people participated only in Task 2 (i.e., bimanual force matching task), with a total of 25 participants (mean $\pm$ std age: 30 $\pm$ 12 years old; 14 females). Participants of both experiments performed first Task 1, then Task 2. We verified that the performance of the twenty participants performing both experiments was not different from the performance of the other five participants (repeated-measure ANOVA group effect: $p=0.115$, all interactions $p>0.21$), i.e., We did not detect any fatigue effect or carryover effects of Task 1 on Task 2.

Inclusion criteria were: (i) no evidence or known history of neurological diseases; (ii) normal joint range of motion and muscle strength; (iii) no problems of visual integrity that could not be corrected with glasses or contact lenses, as they could clearly see the targets that were displayed on the computer screen; (iv) right-hand dominance. All participants resulted right-handed from the 10-item Edinburgh Handedness Inventory [81], which has a Laterality Quotient (LQ) score ranging from -100 to 100 (LQ score: 86 $\pm$ 17 for the population of Task 1 and 87 $\pm$ 16 for the population of Task 2). Each participant signed a consent form to participate in the study and to publish the results of this research. The research and the

consent form were conformed to the ethical standards of the 1964 Declaration of Helsinki and approved by the local Ethical Committee.

1.1.2 Protocol

Task 1: Bimanual position matching task

During this task, the handles were free to be moved up and down sliding on the vertical guides. Each trial started with both handles placed in the starting position i.e., with both handles in contact with the base plane (Fig. 1.1a). Participants were asked to lift the handles reaching with both hands the same height indicated by a horizontal red line displayed on the screen. The actual positions reached by the two hands were measured when participants communicated verbally to the experimenter that they had reached the requested target and maintained it for 0.50 s (holding time interval). Participants were instructed to reach the required height with both hands, without any time constraint or additional information, so they could choose the strategy they preferred.

The visual target line could appear in three different target positions placed respectively at 0.15 m, 0.30 m, and 0.45 m from the starting position (Fig. 1.1b). Two different additional weights (250 g and 500 g) could be placed on top of the left (L) and the right (R) handles, i.e., participants lifted the two handles with on top an additional weight. These weights could be equal on the two handles (symmetric loading conditions LC1: 250 g; LC2: 500 g on both handles) or different (asymmetric loading conditions LC3: L=250 g and R=500 g; LC4: L=500 g and R=250 g), for a total of four loading conditions.

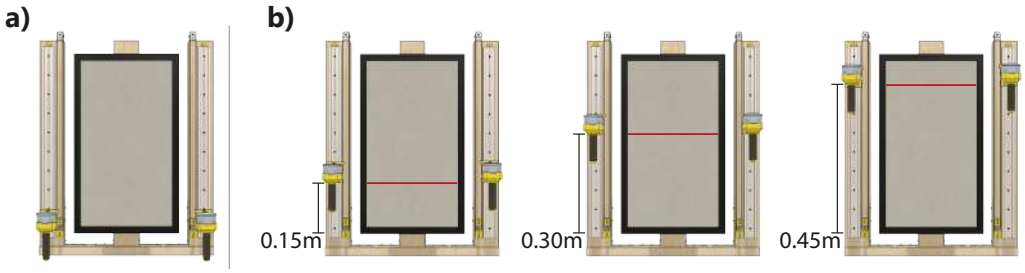

Figure 1.1 a) Starting position. Every trial started with the handles placed in contact with the base plane. b) Target positions placed respectively 0.15 m, 0.30m, and 0.45 m above the starting position. The target position was displayed on the screen with a horizontal red line that the participants had to match bilaterally with the bottom surface of the handle's plate, which was in contact with their thumb and index fingers.

Each loading condition was tested five times for each target position for a total of 60 trials (4 loading conditions $*$ 3 target positions $*$ 5 repetitions). The loading conditions and the target positions were presented in randomized order. During the test phase, participants did not receive any feedback about their performance and their hands' positions.

The task included a familiarization phase, prior to the test, where participants were required to reach once each target position without any additional weight on the handles. They received visual feedback about their hands' position through a black line connecting the position of the two handles. The trial was performed correctly when the black line perfectly overlapped the target red line. They were aware that in the following test the black line would be removed. At the end of the familiarization phase, we asked the participants if they correctly understood the task, otherwise, they could extend the familiarization phase.

Task 2: Bimanual force matching task

In Task 2, participants were asked to apply the same amount of isometric force with the two arms pushing up the handles, which were rigidly fixed on the metal guide (Fig. 1, right detailed view). They had to perform this task with the hand placed in different positions and to reach a total amount of force. The participants receive feedback only of the total force exerted, i.e. the sum of the forces of the two hands. It was visible on the video screen as a vertical bar, together with a horizontal line expressing the force target level (Fig. 1.2). Two different target force levels were requested: 9.8 N or 19.6 N. Two different hand positions were used (0.10 m or 0.30 m above the starting position) for four symmetric (HC1: 0.10 m; HC2: 0.30 m for both hands) and asymmetric (asymmetric HC3: L=0.10m and R=0.30 m; HC4 L = 0.30 m and R=0.10 m) hand configurations (Fig. 1.2).

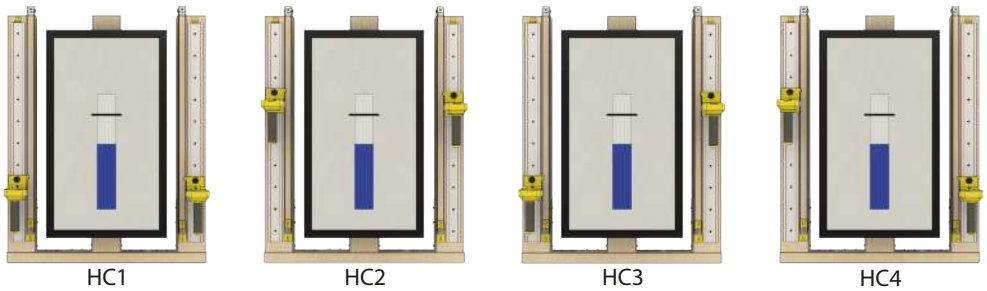

Figure 1.2 Hand configurations in the bimanual force matching task and examples of the real-time visual feedback provided during each trial. The height of the blue bar displayed on the screen was proportional to the sum of the force applied by the two hands. The black line indicated the desired target force that had to be reached with equal force contribution of the two hands.

The four hand configurations were presented five times for each target force in random order for a total of 40 trials (4 hand configurations $*$ 2 target forces $*$ 5 repetitions). The participants were instructed to apply the force simultaneously with both hands: if they attempted to do it sequentially, an error message was provided, and the trial was repeated. Participants were also instructed to verbally communicate to the experimenter that they had reached the required amount of force and then they maintained that level of force for 0.50 s (holding time interval). There was no time constrain for completing the trials.

As in Task 1, there was a familiarization phase before the test. During this phase, we provided the participants with the visual feedback of the force applied by each hand by displaying two lateral bars in addition to the central bar of the total force. Each additional bar had a height proportional to the force exerted by the corresponding hand. Participants were aware that the two additional bars would be not displayed during the test. In the familiarization phase the participants were asked to perform four of the eight possible combinations of the four hand configurations and two force levels (i.e., each participant experienced all the hand configurations and all the target forces, but not all combinations), to minimize the duration of this phase while allowing the participants to experience all the experimental conditions. Then we asked them if they correctly understood the task, otherwise, they could extend the familiarization phase.

Each task lasted about 30 minutes. In every trial to evaluate the participants' performance, we focused on the holding time interval.

1.1.3 Data analysis

Our primary outcome was the systematic difference between the two hands in terms of position in Task 1 and force in Task 2. For this purpose, we computed two types of bias error, related to position or force control, as the signed difference between the position/force of the two hands, averaged for each participant over the trials performed in the same conditions:

$$\bar{\gamma} = \frac{\sum_{i=1}^{N}(\gamma_L - \gamma_R)}{N} \tag{1.1}$$

where $\bar{\gamma}$ is the signed difference between the positions reached or the forces applied by the left (γ_L) and right (γ_R) hands, during the N trials for the same experimental conditions: target position and loading condition (Task 1), target force and hand configuration (Task 2). This indicator is also a measure of symmetry between the two hands in the two tasks: the lower the error the higher the degree of symmetry.

In addition to the bias error, for each experimental condition we also computed the variable error 1.2 as the standard deviation of the difference between the two hands at the end of each trial, in terms of position for Task 1 and force for Task 2:

$$\sigma_\gamma = \sqrt{\frac{\sum_{i=1}^{N}(\gamma_i - \bar{\gamma})^2}{N}} \tag{1.2}$$

this indicator is a measure of performance variability, independent of the degree of correctness of each trial, i.e., it is zero if a participant reaches the same value in each trial, even if it is far from the correct one.

We computed also additional indicators to take into account any apparently minor difference between the two matching tasks. In Task 2, due to the experimental design, the participants always reached the required target force (i.e., visual feedback of the sum of two forces) and the performance of the two arms are balanced, i.e., if one hand exceeded half of the target force, the other undershoot it by the same amount. In contrast, the performance of the two hands in Task 1 was independent, i.e., one hand could undershoot or overshoot the target position to different extents independently of the behavior of the other hand. Thus, in order to better understand the results of Task 1, we also verified whether each hand overshoot or undershoot the target position by computing the bias error (with 1.1) and the variable error (with 1.2) of each hand position with respect to the target position, namely the 'target bias error' and the 'target variable error'. As a final indicator, only for Task 2, we computed the absolute error, as the unsigned difference between the forces applied by the two hands averaged for each participant over the trials performed in the same conditions.

Lastly, since participants were free to choose the strategy that they preferred for accomplishing the tasks, we investigated the chosen strategies in order to understand to which extent they can provide further explanations of the results.

In Task 1 we analyzed the speed profiles of the two hands in each trial, which were characterized by a single dominant peak and by a series of small peaks (e.g., Fig. 1.3a). Then, we divided the hand movement in each trial a ballistic phase followed by an adjustment phase. In particular, the ballistic phase started when the speed exceeds 10% of its peak speed and terminates when it crosses downward the same threshold. The adjustment phase went from this latter instant to the end of the holding time. For each phase, we computed the duration. In the ballistic phase, we also computed the amplitude and the time of the peak speed. In the adjustment phase, we computed the standard deviation of the speed profile (std speed adjustment).

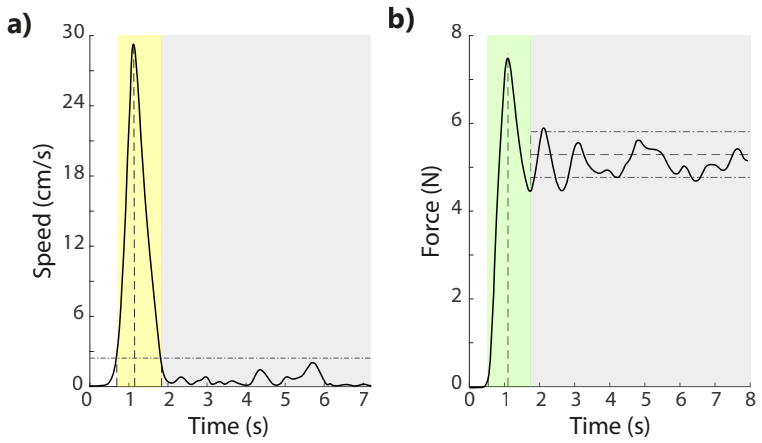

Figure 1.3 Example of a) speed profile from Task 1 and b) force profile from Task 2 for a participant. In a) the yellow area highlights the ballistic phase, which is initiated when the speed exceeds the threshold of 10% of the first peak (horizontal dashed line) and terminates when it crosses downward which started when the speed exceeded the relative threshold. The gray area indicates the adjustment phase. In b) the green area highlights the first part of the force profile, characterized by the main force peak. This is followed by the adjustment phase (gray area) where the mean value is indicated by a horizontal dashed line and the standard deviation by a dashed and dotted line.

In Task 2 we analyzed the force profiles separately for two hands, considering as starting time the instant when the force applied by both hands exceeded for the first time the threshold level of 0.50 N. The force profiles were characterized by a first phase in which they reached the main peak, and the following adjustment phase in which the force level remained high (e.g. Fig. 1.3b). We computed the amplitude and the timing of the first peak. We considered that the adjustment phase started with the first minimum of the force profile after the main peak and ended with the holding time. For this phase, we computed the duration and the amplitude of the force profile, characterizing the latter with the standard deviation (std force adjustment) and the corresponding coefficient of variance (CV), i.e., the standard deviation divided by the mean value.

Statistical analysis

Our primary goal was to assess in:

Task 1 the influence of the loading conditions of the two hands on the ability to lift them at the same height in the absence of visual feedback;

Task 2 the influence of the hand configurations on the ability to push upward, applying equal force with the two hands.

Specifically, using Statistica 7.1 (Statsoft) we tested in Task 1 the hypothesis that the loading conditions could influence the position sense, whereas in Task 2 we tested the hypothesis that the hand configurations could influence the force applied by the hands. To test both hypotheses we performed a repeated-measures ANOVA (rm-ANOVA) on the two types of bias error with two within-subjects factors: the 'loading condition' (4 levels: LC1, LC2, LC3, LC4) and 'target position' (3 levels: 0.15, 0.30, 0.45 m) for Task 1; 'hand configuration' (4 levels: HC1, HC2, HC3, HC4) and 'target force' (2 levels: 9.8, 19.6 N) for Task 2. A significant effect of the first factor in each task would support our hypotheses. To further understand our outcomes, we applied the same analysis to the variable error in both experiments and to the absolute error only in Task 2.

Moreover, to evaluate to what extent the two hands matched the target positions in Task 1, we performed an rm-ANOVA on the target bias error and target variable error with two within-subjects factors: 'hand' (2 levels: right and left) and the 'loading condition' (4 levels). For the analysis of the strategy, we used two separated rm-ANOVA, one for each task. For Task 1 we performed an rm-ANOVA with three within-subjects factors: 'hand' (2 levels), 'target position' (3 levels) 'weight' (4 levels: the additional weights added on one hand (250 g and 500 g) considered both in symmetric and asymmetric loading conditions). For Task 2 weperformed an rm-ANOVA using three within-subjects factors: 'hand' (2 levels: left, right), 'hand configuration' (4 levels), and 'target force' (2 levels).

We verified that all data were normality distributed by the Lilliefors test. we tested for the sphericity of the data using Mauchly's test and the Greenhouse-Geisser correction was applied when the assumption of sphericity was rejected. Specifically, the sphericity assumption was rejected only for the bias error in Task 1 and for some strategy indicators (Task 1: peak time and peak amplitude - Task 2: CV and duration of the adjustment phase).

we performed a post-hoc analysis (Fisher's LSD test) to further investigate statistically significant main and interaction effects. Statistical significance was set at the family-wise error rate of α=0.05. The p-values are reported without the correction for multiple comparisons, however, we verified that the significant results were robust to Bonferroni-Holm corrections and we reported in the text when it was not.

1.2 Results

All participants successfully participated in this study and did not report any adverse event in terms of muscle aches, fatigue, or misunderstanding of the tasks.

Task 1: Bimanual position matching task

The bias error was influenced by the loading condition ($F_{3,57}$=13.47; p<0.001), regardless of the target position (target position effect: $F_{2,38}$=1.67; p=0.210; interaction target $*$ load effect: $F_{6,114}$=1.366; p=0.234). Indeed, in the symmetric loading conditions, when both held either lighter (250 g) or heavier (500 g) weights, the bias error was close to zero and there was not a statistical difference in height between two hands (LC1-LC2: p=0.403; Fig. 1.4a, top row). Conversely, a significant difference emerged between the two asymmetric conditions (LC3-LC4: p<0.001; Fig. 1.4a, bottom row): the hand with the lighter weight reached systematically a lower height than the hand with the heavier weight, as indicated by the different sign of the bias error of LC3 and LC4. This effect was more marked when the left hand had the lighter weight (LC3), in fact, this condition was significantly different from all the others (p$\leq$0.001 in all cases). In LC4, i.e., when the lighter weight was on the right hand, the bias error changed sign with respect to LC3, but its absolute value was lower. The difference between LC4 and LC2 was statistically significant (LC2-LC4: p=0.007), while the difference between LC4 and LC1 was close to the threshold of significance (LC1-LC4: p=0.058). Neither the loading condition nor the target position had a significant effect on the variable error computed for the difference in height between the two hands (Fig. 1.4b).

To further understand the effect of the loading condition, we analyzed also the difference between each hand and the target position. The target bias error highlighted that both hands in all the conditions undershoot the target position (mean $\pm$ SE: 15.5 $\pm$ 6.0 mm; Fig. 1.4). This undershoot was equal for the two hands in both the symmetric conditions (Fig. 1.4c, top row). Conversely, in the asymmetric conditions (Fig. 1.4c, bottom row) this undershoot increased for the hand that held the lighter weight, i.e. the left in LC3, and the right in LC4, determining a highly significant hand $*$ load effect ($F_{3,5}$=14.94; p<0.001). More specifically, the hand with lighter weight reached a significantly lower height with respect to the other hand and also the height reached by both hands in symmetric conditions (p<0.005 in all cases). The target variable error (Fig. 1.4d), instead, revealed only a significant difference across the loading conditions ($F_{3,57}$=5.19; p=0.003). Specifically, it was lower in LC1 and LC3 with respect to LC2 and LC4, i.e. the variability of the height reached by both hands was lower when the left hand held a lighter weight (LC1-LC2: p=0.008; LC1-LC4: p=0.001; LC3-LC4: p=0.009; LC2-LC3: p=0.042 - not robust to Bonferroni-Holm correction; other comparisons p>0.50).

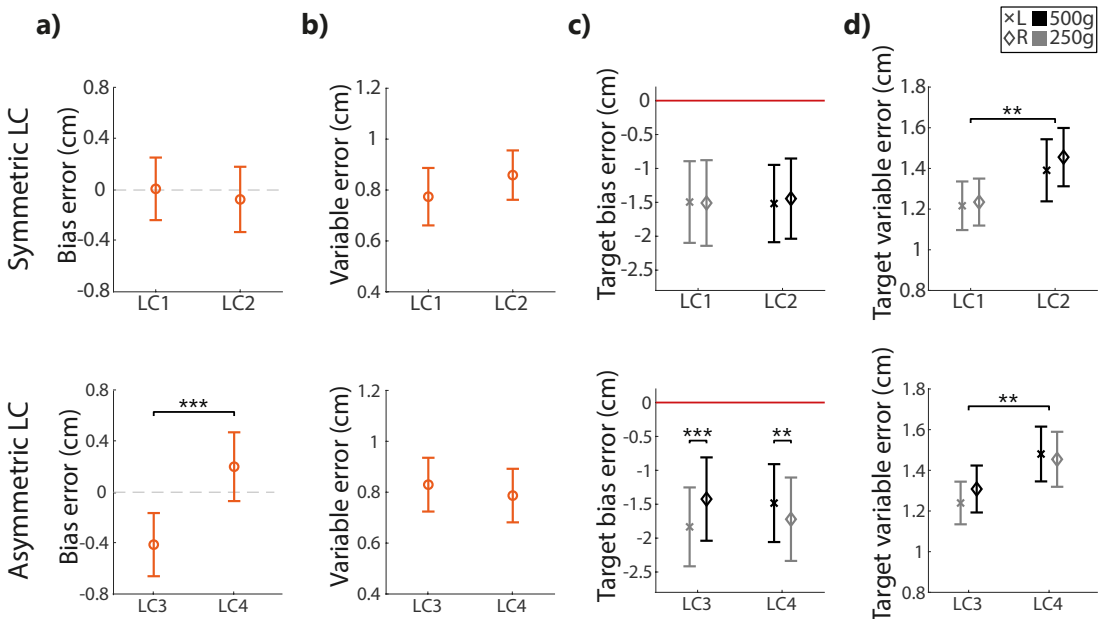

Figure 1.4 Indicators of performance in the bimanual position matching task averaged over the three target positions divided in symmetric (top) and asymmetric (bottom) loading conditions (x-axis). a) Bias error and b) Variable error computed on the difference between the heights reached by the two hands (L – R). In a) the dashed line indicates no difference between the two hands (i.e., the desired performance). c) Target bias error and d) Target variable error, computed on the difference between the heights reached by each hand and the target position. The left hand is represented by an 'x' symbol, right hand by a 'diamond' symbol. In c) the red line represents the target position. Colors indicate the loading conditions of the hand: gray is for the lighter weight and black is for the heavier. All the panels show the population results (mean value $\pm$ SE). $*$ indicate statistical significance: $**$ $p< 0.01$ and $***$ $p<0.001$.

Analysis of the strategy

From the analysis of the strategies adopted by the participants to match the target position, we found that the two hands rose concurrently, i.e., no statistically significant difference between the two hands in the peak time as well as in the onset time (all $p>0.18$). Also, all the other parameters were not different for the two hands (all $p>0.07$; Table 1.1). Conversely, all the parameters depended on the weights placed on the handles except for the duration of the adjustments ($F_{3,57}=1.93$; $p=0.134$). In the symmetric conditions with heavier weights, the mean speed, the std in the adjustment, and also the peak speed were significantly lower than in presence of lighter weights, while the duration of both phases was longer. Instead in the asymmetric conditions, the speed of both hands decreased, assuming intermediate values with respect to the two symmetric conditions for all the parameters, except for peak time, and for

Table 1.1 F and p values of the position strategy parameters in Task 1

	Hand		Weight		Target	
	$F_{1,19}$	p	$F_{3,57}$	p	$F_{2,38}$	p
Peak amplitude	1.72	0.205	29.38	<0.001	167.81	<0.001
Peak time	1.31	0.267	11.75	<0.001	8.72	0.005
Onset time	1.14	0.300	53.67	<0.001	27.25	<0.001
Mean speed	0.14	0.715	13.25	<0.001	91.30	<0.001
Ballistic duration	1.63	0.217	23.10	<0.001	19.88	<0.001
Std speed adjustment	3.48	0.078	16.95	<0.001	39.92	<0.001
Adjustment duration	2.42	0.136	1.93	0.134	0.27	0.764

the duration of the adjustment phase. Comparing symmetric and asymmetric conditions, we found that the hand holding 250 g had a delayed velocity peak in the asymmetric condition, while for the heavier weight there was no change. As expected all the parameters differed for the target positions, ($p \leq 0.005$ in all cases; Table 1.1), except for the duration of the adjustment phase ($F_{3,57}$=0.27, p=0.764).

Task 2: Bimanual force matching task

The absolute error (Fig. 1.5a) computed as the absolute difference between the force applied by the left and right hand was influenced by two factors:

- the target force ($F_{1,24}$=9.11; p=0.006), i.e., higher force corresponded to higher absolute error;
- the hand configuration ($F_{3,72}$=4.22; p=0.008), i.e., the left hand in the lower position corresponded to higher absolute error (left hand at lower vs higher position: $F_{(1,99}$=12.25; p=0.001)

The effect of the target force was due to the variable error, i.e. higher target force led to significantly higher variable errors ($F_{1,24}$=30.36; $p<0.001$). Instead, the bias error had an opposite and significant behavior: the systematic difference between the two hands was lower for the higher target force ($F_{1,24}$=15.67; $p<0.001$, no interaction effects were observed $p>0.11$ in all cases).

Conversely, the effect of the hand configuration was due mainly to the systematic component of the error, i.e. to the bias error (hand configuration effect: $F_{3,72}$=6.72; $p<0.001$; left hand at lower vs higher position: $F_{1,99}$=20.63; $p<0.001$; Fig. 1.5b). This effect was significant in both the symmetric (HC1-HC2: p=0.028) and asymmetric (HC3-HC4: $p<0.001$)

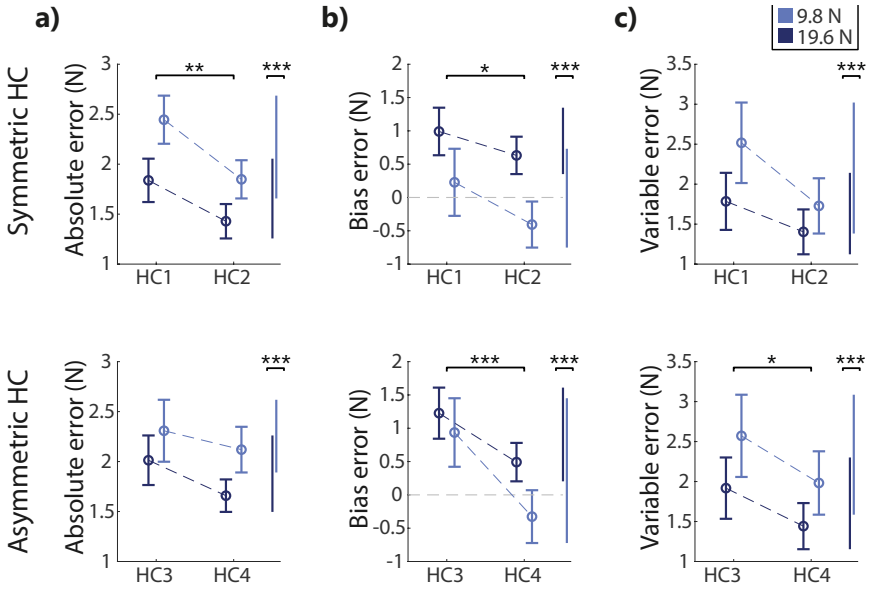

Figure 1.5 Indicators of performance in the force matching task: the difference between the forces applied by the two hands (L - R). Top row: symmetric hand configurations (HC1 and HC2). Bottom row: asymmetric hand configurations (HC3 and HC4). All the panels show the population results (mean value $\pm$ SE). In each panel, data is reported separately for each target force (dark blue for the lower force, light blue for the higher). a) absolute error; b) bias error, where the gray dashed line represents the null difference between the two hands (i.e., the desired performance). c) variable error. $*$ indicates statistical significance: $*$ $p<0.05$, $**$ $p< 0.01$ and $***$ $p<0.001$.

configurations, indicating that when the left hand was in the lowest position, it applied systematically more force than the right, independently on its position. This overshoot remarkably decreased when the left hand was in the highest position, to the point that for the higher target force, this trend was inverted, i.e., the right hand applied more force than the left. The variable error had the same trend without reaching the significance threshold ($F_{3,72}$=2.14; p=0.102; Fig. 1.5c). When we considered the two conditions separately, the absolute error (Fig. 1.5a) was statistically significant only for the symmetric hand configurations (HC1-HC2: p=0.001; HC3-HC4: p=0.114). For all the parameters no significant differences were found between symmetrical and asymmetrical hand configurations (p>0.10).

Analysis of the strategy

From the analysis of the strategies adopted by the participants to accomplish this task, we found that almost all the parameters computed on the force profiles were significantly different between the two hands (Table 1.2). In particular, the left hand had a higher ($F_{1,24}$=9.52, p=0.005) and delayed ($F_{1,24}$=5.43, p=0.028 - not robust to Bonferroni-Holm corrections)

Table 1.2 F and p values of the force strategy parameters in Task 2

	Hand		Target force		HC	
	$F_{1,19}$	p	$F_{3,57}$	p	$F_{2,38}$	p
Peak amplitude	9.52	0.005	483.35	<0.001	2.50	0.066
Peak time	5.43	0.028	183.13	<0.001	3.55	0.019
CV adjustment	14.43	0.001	6.13	0.021	7.35	0.001
Std force adjustment	0.37	0.548	49.42	<0.001	10.10	<0.001
Adjustment duration	5.20	0.032	14.20	0.001	2.58	0.060

force peak than the right hand. In the adjustment phase, the left hand had a longer duration ($F_{1,24}$=5.20, p=0.032, not robust to Bonferroni-Holm corrections) and lower CV ($F_{1,24}$=14.43, p=0.001), but the latter was due to the higher mean values of the force since the std was equal between the two hands (p>0.54).

Also, the target force level significantly influenced the strategy adopted to accomplish the task. Specifically, an higher target force induced a delay in the peak force ($F_{1,24}$=183.13, p<0.001), a longer duration of the adjustment phase ($F_{1,24}$=14.20, p=0.001), and a lower CV ($F_{1,24}$=6.13, p=0.021 - not robust to Bonferroni-Holm corrections). Also, in this case, the latter was due to a higher mean value.

The hand configuration did not affect the amplitude of the force peak ($F_{1,24}$= 2.50, p=0.066), while its timing was significantly higher when both hands were at the lower position with respect to all the other conditions (all p<0.02). In the adjustment phase, both the CV and the std were affected by the hand configurations (CV: $F_{3,72}$=7.35, p=0.001; std: $F_{3,72}$=10.10, p<0.001), specifically both parameters were higher when the left hand was higher than the right hand, with respect to all the other hand configurations (p<0.05)

1.3 Discussion

We designed two tasks to investigate the interaction between position and force control in bimanual tasks. Indeed, in Task 1, the participants had to lift both hands at the same height under different loading conditions; in Task 2, they had to apply equal isometric forces in the upward direction, with the hands in different configurations. In both cases, the participants could perform the matching task without relying on visual feedback, but only on proprioception. Our hypotheses were that:

- asymmetric loading conditions, i.e. different weights held by the two hands, would affect bimanual position control in Task 1;

- asymmetric configurations of the hands/joints would influence bilateral force control in Task 2.

For both conditions, we also expected decreased performance with respect to the corresponding symmetric ones. The results confirmed the first hypothesis, demonstrating that an asymmetric loading condition determined a systematic bias error between the heights reached by the two hands. As expected, the target height did not influence the performance. Conversely, the second hypothesis had to be rejected because our results showed that the configuration of the hands affected the ability to apply the desired bimanual force, but this effect was dominated by the position of the left hand, regardless of the position of the right.

Task 1: Bimanual position matching task

The reported ability to lift both hands at the same height in symmetric loading conditions is probably due to an underlying synchronization tendency between the hands, well established in several bimanual tasks [10, 82–84]. Indeed, in this task temporal and spatial parameters constrain the limb movements [78, 84, 85], inducing intermanual coordination and leading to a systematic bias toward similar patterns [82, 86].

In the asymmetric conditions, the hand holding the lighter weight reached a position farther from the target, i.e., had a higher target bias error than the other hand. This is in agreement with previous findings suggesting that the effort required to hold a limb against the force of gravity or weight in static condition provide a positional cue that improves performance in upper limb joint matching tasks [77, 87, 88]. Moreover, holding bigger heavier weights increases muscular activation of the same muscle groups [1, 89], determining a higher proprioceptors' activation [1], that leads to better performance in position matching tasks [76].

However, in the symmetric loading conditions, we did not find any significant difference between the trials cases in which both hands held heavier or lighter weights. Thus, in our task based on additional light-weights but with a marked relative difference between them, the position control was influenced by the different weights, only when they were unbalanced, i.e. in asymmetric loading conditions, but not when they were balanced, i.e. in symmetric loading conditions.

As for the variable error, the two hands were coupled, i.e. the variability of the two hands with respect to their average error was similar in all the conditions. Specifically, in symmetric conditions (LC1 and LC2) both hands had higher target variable error when holding heavier than lighter weights. In symmetric conditions, the two hands received

the same additional feedback (i.e., the position of the other hand) and since the variability associated with force/heaviness perception is known to be higher for higher forces/weights [79, 80]), we expected the two hands to have higher variability when holding heavier weights. In the two asymmetric conditions (LC3 and LC4), the two hands received different feedback depending on the weight they were holding. If the CNS when controlling one hand was unable to integrate the information of the other, each hand would maintain higher target variability holding the heavier weight. However, the latter was only the behavior of the left hand, while the right hand modified its behavior to match the performance of the left. Thus, the CNS when controlling the right hand is integrating and accounting for the information coming from the left hand holding a different weight. Conversely, when controlling the left hand, the CNS did not account for the feedback from the right hand, relying only on the left hand's proprioceptive information. This result suggests a 'leading role' of the left since the variability of the two hands was coupled in all conditions, independently of the weight held by each hand, and this behavior seems to be determined by the left hand, at least in right-handed participants.

The dominant role in proprioceptive tasks of the left hand has been previously reported in the literature [72, 90] and also the results of the second task, discussed in the next paragraph, supported this conclusion.

The results of the analysis on the strategies suggest that in Task 1 the loading condition influences the kinematic strategy during the execution of the task and this may cause the changes in the bimanual position performance observed in the experiments. Specifically, the movements' strategies support the following considerations: (i) in symmetric loading conditions, the movement speed was influenced by the heaviness of the weight on the handle; (ii) in asymmetric conditions, the difference between the hands' speed due to the weights decreased. Most features of the movement converged toward intermediate values with respect to those observed when both hands hold the same weights, in accordance with the inter-limb interference; (iii) in asymmetric conditions, the hand holding the lighter weight has a delayed peak speed. This supports the main result that, in this case, the mismatch in the proprioceptive inputs results in difficulty for the subjects in performing the task, as also highlighted by the residual bias error in the steady-state phase.

Task 2: Bimanual force matching task

The force outcomes mainly depended on the position of the left hand, regardless of the right hand, i.e. for this bimanual isometric force task we found a leading role of the left hand

and not an effect of hand configuration symmetry. This result is surprising and in apparent contrast with the initial assumption that the equal position of the two hands would imply better performance as it corresponded to equal joint configurations that require a similar motor command for the two sides of the body.

However, this paradoxical result may be explained by the dichotomous model proposed by Goble et al. [72]. The model suggests that the upper limbs' differences found in the behavioral performances are based on the different key sources of movement-related sensory feedback, which they rely more on: vision or proprioception. According to such model, during bimanual activities, the dominant (right) arm relies more on visual feedback, whereas the non-dominant (left) arm is better off with proprioceptive feedback [72, 90]. Thus, in our experimental paradigm, where the task could not be solved relying on visual feedback, the left arm may be advantaged and consequently assume a leading, dominant role. Further support to this interpretation comes from another similar study demonstrating that the non-dominant limb is specialized in controlling static exertion of forces [47, 91, 92].

However, this finding is supported by Johansson et al. [93]. They found that during bimanual object manipulation the brain selects one hand as prime actor even when the two hands has to apply symmetric forces, i.e., there is an asymmetric control of the two hands even if the same force outcome is required. Indeed, the hand that experiences the most natural directional relationship between forces generated and desired motion consequences, whether left or right, is appointed as prime actor while the other hand plays an assisting, or postural, role. The asymmetric control of the hands is manifest from the cortical level all the way down to specific muscles. Thus, besides supporting the notion that there is a dual coordinated control scheme for goal oriented behaviors, with one system for goal motions and one for postural support [94], these systems are segregated throughout the motor system and can be flexibly rearranged between the hands depending on task constrains.

Another result worth consideration is that the errors, and especially the bias error, were lower when the left hand was in the higher position. we may speculate that the better performance of the leading hand in the highest position could be due to muscular activation. In particular, for exerting the required isometric forces, participants may need to recruit motor units at the shoulder/trunk level when the hand is in the higher position compared to when it is in a lower position: this may imply an increase of the motor commands to produce the same amount of force that could lead to a better force perception [70, 95, 96], explaining the lower errors. Notice also that in different arm configurations, different muscle groups contribute to produce the same level of force, thus the variability (i.e., variable error) of the resulting force could change depending on which specific muscles are recruited and how

they are activated: in our task the recruitment of shoulder and trunk muscles determined also a decreased variability. For different levels of force, the results confirmed that the variable error depended on the applied force: the variability increased when higher force was required. Indeed, for biological signals it is common to have larger variability associated with higher amplitude of the signals. It is well known for force applied by the fingers or in unimanual tasks [48] as well as for bimanual matching tasks [78, 79].

The magnitude of the desired force had also another relevant effect: the left hand applied more force than the right hand for the lower target force, but for higher target force such effect was decreased and even inverted. This result is consistent with the literature about sequential matching tasks, where the force applied by the left hand is significantly altered by the amount of force required [76].

The results of the analysis on the strategies suggest that in Task 2 the force strategy appeared to be unaffected by the symmetry of the hand configuration, this might be an additional explanation for the independence of the accuracy of performance from this parameter. Furthermore, as for the bias error, almost all the strategy indicators were different between the two hands: the left hand had a higher and delayed force peak and longer adjustment phase with higher mean force. These features support the hypothesis of a leading role in force control for this hand.

The results of this study would be relevant for clinical evaluations and rehabilitative applications. While providing new insights about the interaction between force and position control in unimpaired individuals, they can be also used to define a quantitative evaluation of proprioception in bilateral tasks for people with neurological disorders and stroke survivors.

Limitations

A concurrent acquisition of muscle signals was not performed. This could allow a deeper understanding of the neural mechanism underlying our results, providing further support for the explanations proposed in the section 1.3. Thus, future studies might focus on recording surface electromyographic data, especially to further investigate the relation between the number of recruited muscle fibers and proprioceptive errors. In addition, the results we found in Task 1 could be valid only for lighter and not for heavier weights, due to no linear relations between proprioceptive errors and muscle fiber activations.

Chapter 2

Study II: The influence of handedness on bimanual isometric force matching task

This study has been published in: Ballardini G., Casadio M. *'Isometric force matching asymmetries depend on the position of the left hand regardless of handedness'*. In International Conference on Human Haptic Sensing and Touch Enabled Computer Applications (pp. 194-202). Springer, Cham. Eurohaptics Conference, Leiden, Netherlands. (September 6-9, 2020)

2.1 Introduction

In the previous study on right-handed participants (Chapter 1) we found that the ability to simultaneously apply an equal amount of isometric force in the upward direction with the two arms was influenced by the position of the left hand, indicating a leading role of the non-dominant limb on the bimanual performance of such task. We hypothesize that this effect is related to the participants' handedness and therefore that the results would be mirrored in left-handed individuals.

Since about 89.5% of the world population prefers using the right hand [97] in the execution of various uni-manual motor tasks, there is a bias also in the study of sensorimotor abilities and motor control [98, 99]. The majority of research on the upper limb focused only on right-handed individuals performing uni-manual tasks with their preferred arm, also called the dominant arm. This approach reduces the experimental design complexity but does not take into account the interaction between the two arms [100]. In addition, it limits the possibility to determine sensorimotor differences between left- and right-handed individuals (see also [98] for a review) and the ability to determine whether the upper limb asymmetries

were due, to the hand dominance or to a specialization of the brain hemisphere unrelated to handedness. Actually, some tasks showed upper-limb behavioral asymmetries in left-handed individuals identical to the right-handers, suggesting that these observed effects were not determined by handedness, but likely by the specialization of the brain hemisphere. For example, this is the case of stiffness perception [101] and weight perception [102]. In other tasks, instead, the upper-limb behavioral asymmetries, such as target reaching accuracy [90] and finger pinch movement discrimination [100], were found mirrored with respect to right-handers, suggesting that the observed effects were due to handedness. However, to the best of our knowledge, the handedness effect on behavioral asymmetries has not been evaluated in bimanual force control tasks with both hands are actively engaged toward a common goal.

For testing my hypothesis, i.e., the leading role of the left-hand position in the bimanual isometric force task is related to handedness, in this study, we repeated the same experiment on a population of young left-handers and on an age-matched group of right-handers. My hypothesis will be supported if in both populations the performance will depend on the position of the non-dominant hand. Conversely, if force performance will depend on the position of the left hand, results will indicate a hemispheric specialization in the brain, independent of handedness.

2.2 Material and methods

2.2.1 Participants

36 participants (20 females, age range: 23-33 years old) voluntarily participated in this study. For all participants, we evaluated the hand dominance by the 10-item Edinburgh Handedness Inventory [81]. Based on this score, we divided them into two age-matched groups (Table 2.1): 13 left-handers (LQ score $<$ -50) and 23 right-handers (LQ score $>$ 50).

Inclusion criteria were: (i) no evidence or known history of neurological disease; (ii) normal joint range of motion and muscle strength; (iii) no problems of visual integrity that could not be corrected with glasses or contact lenses, as i.e. they could see the feedback displayed on the device's screen. Each participant signed a consent form to participate in the study and to publish the results of this research. The research and the consent form were conformed to the ethical standards of the 1964 Declaration of Helsinki and approved by the local Ethical Committee.

Table 2.1 Demographic data

	Sex	Age	LQ score
Left-handed	8 F, 5 M	25 ± 3	-86 ± 14
Right-handed	12 F, 11 M	26 ± 2	75 ± 14

Age and LQ scores are reported as mean ± std

2.2.2 Protocol

The experimental set-up and protocol are the same as the bimanual force matching task described in section I and subsection 1.1.2 respectively. Here, we decided to perform only Task 2, since we did not find any limb asymmetry in right-handed participants.

Briefly, participants were sat in front of our device (Fig. 1) and they were required to apply simultaneously the same amount of isometric force on both handles. In each trial the handles were placed in one of the four different configurations (HC; Fig. 1.2) corresponding to all the possible combinations of two different heights, respectively 0.10 and 0.30 m above the baseline position, i.e. handle in contact with the base plane. During each trial, participants did not receive any feedback of the force applied by each hand, but they could see on the device's screen the total force exerted as a vertical bar whose height was equal to the sum of the two forces. On the screen, they can see the target force to match, as a horizontal line that has to be reached by the bar controlled by the bilateral force applied by the participants. Two different target force levels were presented: 9.8 N or 19.6 N. Each target force was presented five times for each hand configuration, in random order, for a total of 40 trials (4 hand configurations*2 target forces*5 repetitions). To complete each trial, participants had to communicate to the experimenter when they reached the required amount of force and to maintain it for 0.5 s (holding time interval). There was no time constrain to complete each trial.

2.2.3 Data analysis

We focused on the difference of force applied by the two hands in the holding time interval. Our primary outcome was the absolute error defined as the absolute value of the difference between the left and the right hand (2.1) computed in terms of upward isometric force:

$$\gamma = \frac{\sum_{i=1}^{N} |\gamma_L - \gamma_R|}{N} \tag{2.1}$$

Eq. 2.1. where N (=5) is the number of trials repeated under the same condition, γ is the measured force for the right (R) and left (L) hand. This difference was evaluated in the holding time, i.e., 0.5 s after the participants declared to have matched the required force.

It could be influenced by two concurrent factors: (1) a systematic tendency to exert more force with one arm, i.e. the bias error, computed as in Eq. 1.2; (2) a variable component accounting for trial-to-trial consistency, i.e. the variable error, computed as in Eq. 1.2.

Statistical analysis

Our primary goal was to investigate whether the ability to exert equal isometric forces with the two arms in different configurations was influenced by handedness. The secondary goal was to verify if the performance of left-handed participants depended on the symmetry of the hand configuration, the position of the left hand, and the target force. Using IBM SPSS Statistics, we performed a repeated-measures ANOVA on the three indicators (absolute, bias, and variable error) with one between-subjects factor: 'handedness' (2 levels: left- and right-handed participants) and with three within-subjects factors: 'symmetry' (2 levels: symmetric HC and asymmetric HC), 'left hand position' (2 levels: up and down), and 'target force' (2 levels: 9.8 N and 19.6 N). We verified the normality of the data using the Anderson-Darling test [103]. The null hypothesis was rejected for the absolute and the variable error, thus these data were corrected applying the fractional rank method [104]. We tested for the sphericity of the data using Mauchly's test, and it was verified for all indicators. We performed a post-hoc analysis (Tukey's method) to further investigate statistically significant effects. Statistical significance was set at the family-wise error rate of α=0.05.

2.3 Results

Left-handed participants had worse performance in the bimanual force matching task

The absolute error (Fig. 2.1a) was influenced by handedness ($F_{1,34}$=6.75; p=0.014). Specifically, left-handers performed the task with a higher difference of force between the arms than right-handers. However, this population effect for each participant could be due to the bias or to the variable error, as well as to their combination, regardless of handedness. Indeed, for both the bias and the variable errors (Fig. 2.1b and 2.1c), the handedness main factor did not reach the threshold of significance.

The bimanual performance was influenced by the position of the left hand regardless of handedness

In left-handed participants, the difference of force applied by the two hands depended on the position of the left hand and not of the non-dominant (right) hand. The absolute error significantly depended on the position of the left hand for both groups (left hand position effect: $F_{1,34}$=22.09; p<0.001), i.e. when the left hand was in the lower position the absolute error was higher for all participants. This could be explained by the bias error, which showed that participants of both groups tended to apply more force with the left hand when it was in the lower position (left hand position effect: $F_{1,34}$= 16.44; p<0.001). However, this effect was more marked when the hands were in asymmetric configurations, i.e., the performance was not different in symmetric configurations (symmetry*left hand position interaction: $F_{1,34}$=16.00; p<0.001; post-hoc: HC1-HC2: p=0.759; HC3-HC4: p<0.001). As for the variable error, no effect of the left hand position was found in the overall population (left hand position effect: p>0.05), while only the left-handers in most configurations (3 out of 4) had a higher variable error when the left hand was in the lower position (left hand position*group interaction: $F_{1,34}$=11.86; p=0.002). For all the three indicators there was no significant main effect of the symmetry of the hand configuration, consistently for both groups.

The error was influenced by the required total amount of force, regardless of handedness

The level of the target force had a significant - or close to significance - effect on all the three indicators (absolute error: $F_{1,34}$= 6.89; p=0.013; variable error: $F_{1,34}$=11.86; p=0.002; bias error: $F_{1,34}$=6.22; p=0.018), i.e. as expected these indicators were higher for higher target force, regardless of handedness, symmetry of the hand configuration and position of the left hand.

All the above-mentioned results were confirmed also in the sex-matched subgroup.

2.4 Discussion

In this study, we wanted to test our hypothesis that the leading role of the left hand position in bimanual isometric force task is related to handedness. To do so, we repeated the same experiment performed chapter 1 on a population of young left-handers and an age-

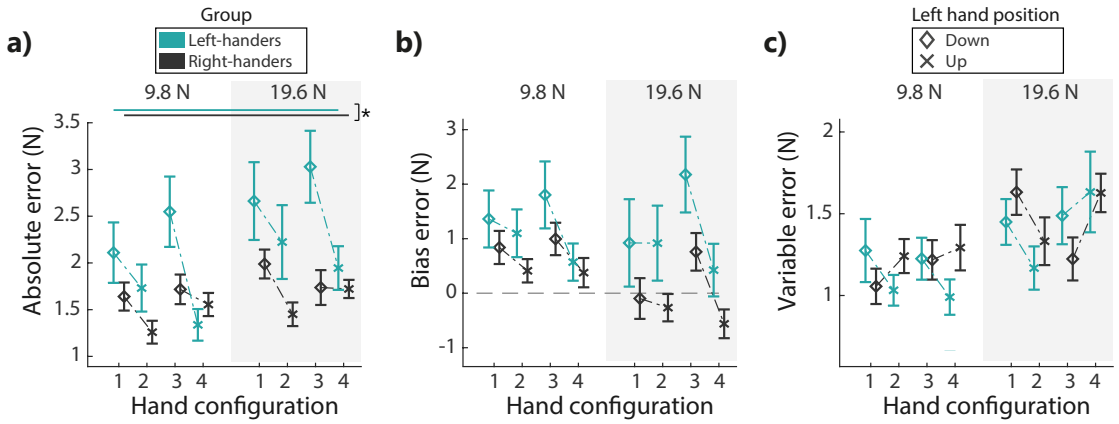

Figure 2.1 Indicators of performance computed on the difference between the forces applied by the left and the right hand in terms of a) absolute error, b) bias error and c) variable error. Each indicator has been reported for the four hand configurations (symmetric: HC1 and HC2; asymmetric: HC3 and HC4, see 1.2). The left hand in the higher position is represented by the 'x' symbol, while in the lower position by the 'diamond' symbol. Data is reported separately for each target force: white background indicates 9.8 N, light gray background 19.6 N. All the panels show the results (mean ± SE) separately for the left- (blue) and the right- (gray) handed population. * indicates a $p<0.05$

matched group of right-handers. Our hypothesis will be supported if in both populations the performance will depend on the position of the non-dominant hand. Conversely, if force performance will depend on the position of the left hand, results will indicate a hemispheric specialization in the brain, independent of handedness. Interestingly, our results showed an effect of the handedness on the force applied by the two hands, but not on the leading role of the left hand position.

The difference of force applied by the two hands in terms of absolute error was influenced by handedness in all the experimental conditions

Left-handed participants had higher absolute error than right-handed participants. This result supports the conclusions of previous studies, such as [100], suggesting that bimanual proprioception was less accurate in left-handed individuals. This study extends this finding to a bimanual isometric force matching task, where participants integrated the proprioceptive information from their arms positioned in symmetric or asymmetric configurations, not relying on visual feedback.

Bimanual force matching performance depended on the position of the left hand regardless of the handedness

The performance seemed to be influenced by the specialization of the brain hemisphere, evolving independently from handedness. The significant effect of the left hand position in right-handed individuals was supported by the dichotomous model theorized by Goble et al. [99] and observed in motor [90] and force tasks [70, 76]. This model suggests that during bimanual activities, the dominant right arm relies more on visual feedback, while the non-dominant left arm on proprioceptive feedback. Thus, in our experiment, where participants could not rely on visual feedback, the left arm might be advantaged and play a key role in solving the task. The present study on left-handed individuals extends this finding, suggesting that the observed asymmetry in bimanual force matching performance with different arm configurations could be due to a specialization of the right hemisphere, evolving independently from handedness. This result is also supported by a study by Kang et al. [105] on people with unilateral stroke, suggesting a specific contribution of the right hemisphere in controlling the production of bilateral force. Also other studies found a specialization of the right hemisphere in different but related tasks, such as controlling limb impedance for stabilizing limb position at the end of movement [19] and generating force for adapting to dynamic variation, such as unexpected perturbation [106]. Note that the signed difference between the forces applied by the two hands was higher and significant when the two arms were in asymmetric configurations. This was expected, since in this case the central nervous system has to apply different neural commands for each side of the body, accounting for the difference in arm configuration. However, humans have a universal tendency to perform coordinated bimanual movements, by synchronized activation of homologous limb muscles (e.g. in [10]). The present results suggest that this tendency could be present also in bimanual isometric force matching tasks, explaining at least in part the more similar performance in symmetric configurations. we also found that the performance variability was partially influenced by handedness, since only left-handed individuals tended to have higher variability when the left hand was in the lower position than in the other configurations. A crucial role of the right hemisphere for variability of bilateral force control has been suggested in [70], but its interaction with handedness has not been extensively studied.

The error is influenced by the required total amount of force, regardless of handedness

The total amount of the requested force had a relevant effect on the performance, increasing the difference between the two hands and its variability. Further, the bias error highlighted that the left hand applied more force than the right for the lower target force, but this effect was decreased and even inverted for the higher target force, consistently with previous results in the sequential [70, 76] and concurrent matching task. The results of the present study extend the previous findings, highlighting that this effect was not influenced by handedness.

2.4.1 Limitations

The results obtained in the right-handers were consistent with what was reported in Chapter 1 for both the absolute and the bias error. Instead, the variable errors in our young participants were lower and in a different relation to hand configurations. The difference was due to the older participants included in the previous study who had significantly higher variable errors, as found also in [107]. We plan to further investigate the influence of aging on this specific task in a future study.

Part II

Assessment of proprioception in stroke survivors

Introduction

Stroke is characterized as a neurological deficit attributed to an acute focal injury of the central nervous system by a vascular cause. There are two main types of stroke: the ischemic, which is caused by a lack of blood, and the hemorrhagic, due to the rupture of a vascular structure. It results in the localized death of the nervous tissue leading to a not proper functionality of the brain in that region. The long-term effect of stroke is mainly determined by the site and size of the initial stroke lesion and by the extent of subsequent recovery [56].

Stroke is the second cause of disability worldwide [108]. One of the most common deficit after stroke is hemiparesis of the upper limb contaleral with respect to the brain lesion side, with more than 80% of those with stroke experiencing it acutely and more than 40% chronically. Furthermore, more than 50% of stroke survivors exhibit long-term weakness or paresis in their contralesional arm [109, 110], while 50% ehibit proprioceptive deficits [111]. It is well known that the loss of proprioception affects motor planning, control, and (re-)learning limiting functional recovery in various motor tasks [3–8]. In fact, many survivors present with deficits of proprioception perform movement trajectories that are often less accurate and stabilization strategies that are less effective compared to unimpaired people [50]. This limits physical interaction with people and the environment, thereby reducing their quality of life [112].

Thus, the recovery of upper limb functions in stroke survivors is an important rehabilitative goal [113]. To achieve this goal, it is essential to assess and consider abnormal patterns of movements, altered strength, and sensory perception of both ipsilesional and contralesional arms [114, 115]. The first necessary step for achieving this goal is a complete and effective assessment of the capability of the person. This will allow to design specific rehabilitative treatment, and also monitoring the progress. Despite that, in the current formulation of the neurological assessment protocol, proprioceptive functions are most often subjectively assessed by clinicians using qualitative clinical scales [7]. In addition to that, the different aspects of proprioception and the two upper limbs are mainly evaluated separately and the main focus of the rehabilitation and the assessment protocol in stroke survivors is on the contralesional arm. This limits the evaluation of the possible interactions or interference that arise from the inter-limb coordination [12], which is one of the main outcome of proprioceptive deficits in stroke survivors.

In relation to the cerebral lesion, the ipsilesional Upper Limb (iUL) is often termed ‘unaffected’ or ‘unimpaired’ and used as a reference for the assessment of the ‘affected’ or ‘impaired’ contralesional Upper Limb (cUL) [116, 117]. However, there is increasing

evidence that also ipsilesional deficits can persist and be functionally limiting from the acute to the chronic stage of stroke (see [115] for a review).

In general, most studies on iUL focused on motor deficits, while limited attention has been devoted to somatosensation. Early studies found ipsilesional muscle weakness [117–119], while recently degradation of motor performance was mainly investigated in tasks requiring accuracy, dexterity or coordination [17–20, 22, 23, 114, 120]. Previous studies on ipsilesional tactile and proprioceptive deficits in stroke survivors highlighted impairments in stereognosis [121], tactile-perceptual ability [13], as well as altered thresholds for light-touch [14, 16], motion detection [122], point localization [121, 123], two points discrimination [15, 124] and pressure sensitivity [15, 125, 126]. Those can be detected with standard clinical methods, e.g., the nine-peg hole test [127, 128], the Jebsen hand function test [114, 116], the pegboard test [129, 130].

In addition to that, recent studies suggested that hemispheric specialization influences differently the motor deficits in both arms following unilateral stroke [18, 19, 131–135], the dependency on this in proprioceptive deficits is less investigated. The previous studies on differences in somatosensory deficits due to hemisphere of the lesion reported discordant and task-specific findings [13–16].

In my Ph.D. research project I did a first step toward filling those gaps, deepening the knowledge on the proprioceptive performance of stroke survivors while performing uni and bimanual tasks.

Chapter 3

Study I: The influence of brain laterality on unimanual passive position matching task

This study has been done in collaboration with the with Robotic Research Center, Mechanical and Aerospace Engineering and the School of Physical and Mathematical Sciences of Nanyang Technological University (Singapore), and the Clinic for Advanced Rehabilitation Therapeutics, Tan Tock Seng Hospital Rehabilitation Centre, (Singapore).

3.1 Introduction

Hemispheric specialization is a defining characteristic of the human brain organization [136]. It can be defined by asymmetries of intra-hemispheric functional and effective connectivity. Hemispheric specialization is based on the interplay of two complementary aspects: (i) functional specialization, i.e., each hemisphere hosts specialized networks that have unique functional properties. From the evolutionary point of view, the lateralization of specific functions in one hemisphere seems to be beneficial in reducing conduction delays [137] or downgrading interference from incompatible processes [138]; (ii) functional integration, i.e., mechanisms that enable the inter-hemispheric coordination necessary to efficiently process the information of both hemispheres [139–141]. Anatomical and developmental studies highlighted hemispheric asymmetries in structural connectivity, which are a fundamental constraint of brain architecture and may be the cause for functional hemispheric specialization [142].

Traditionally, emphasis has been on left hemisphere supremacy for language versus right hemisphere dominance for visuo-spatial representation and attention [140, 143]. Recently, it has been proposed that this specialization is relative because, with only few exceptions, both hemispheres can process all types of information, although they do it in fundamentally different manners [136]. This can be explained by the differences in anatomical connectivity, which have been described both within and between cortical areas in the two hemispheres [142]. However, the view that specialized functions of the left hemisphere are essential for skilled movement and language, is quite well established for right-handers unimpaired people [140, 144, 145].

With respect to human motor control and execution, the hemispheric specialization is closely tied to handedness [140], i.e., the preferred and non-preferred arms have complementary roles during motor performance.

Two main theories have been proposed for how motion and impedance is coordinated among human hands. Global dominance theory states that the hemisphere contralateral to the dominant arm (left hemisphere for right-handers) specializes in all aspects of motor control, while dynamic dominance theory suggests that each hemisphere specializes in different control aspects [94].

This dynamic-dominance hypothesis of handedness is based on differences in movement strategy observed between the preferred and non-preferred arms of right-handed individuals. This hypothesis suggests that each arm is specialized for a different aspect of movement control: the dominant (right) arm system is specialized for the predictive control of trajectories, and the non-dominant (left) arm system for the stabilization controlling the limb impedance [69, 94, 146].

Studies on behavioral performance of individuals with unilateral brain injury supported the hemisphere-limb specialization for motor control finding different deficits in both the ipsilesional [18, 131] and contralesional [19] arm depending on the brain lesion side. Left hemisphere damage resulted in deficits in the early stages of movement, such as increased reaction times [132, 133] and a slower initial movement component [134]. In contrast, individuals with damage to the right hemisphere showed poorer feedback-dependent control, as would be necessary for accurately achieving a final target position [134, 135].

Despite their importance, there is limited evidence about the dependency of upper limb position sense performance on the brain hemispheric location and the arm position in the workspace. Vallar et al. [147] addressed this issue, but they focused on the difference between stroke survivors with and without spatial neglect and the effects of supplementary optokinetic stimulation. More in general, previous studies on differences in somatosensory

deficits due to hemisphere of the lesion reported discordant findings. For example, tactile sensation in stroke survivors with a Right Brain Damage (RBD) was better [16, 15], equal [14] or even worst [13] than survivors with Left Brain Damage (LBD).

Furthermore, to assess position sense, nowadays, both in clinical and research, there are about fifty standardized methods [148], which applying different methods have discrepancies in their findings [148–150]. One of the most common paradigm to study perception ability in stroke survivors is the mirror position matching task. Specifically, it allows to quantify the spatial component of the proprioception ability after stroke. There, a physiotherapist or a robotic device moves the contralesional arm in specific positions that the participants have to mirror with the ipsilesional arm [7, 151–153]. However, this type of test, as our previous bimanual position matching tasks (subsection 1.1.2), accounts concurrently for the proprioception of the two arms [90, 99, 149], not allowing us to determine independently the deficits of each arm and their mapping in the workspace. For this reason, we focused on the comparison of performance on unilateral position matching tasks. However, in this case, the memory component plays an important role [65], since the same arm is used as both reference and matching in sequential phases.

This study aims at filling these gaps by assessing the iUL position sense after stroke during a passive unimanual position matching task. We compared the iUL proprioceptive performance with those of the cUL and we also investigated the dependency of this performance on the hemisphere of the brain lesion, accounting for the hand position in the workspace. Moreover, we compared the iUL proprioceptive performance with those of the dominant arm of a group of slightly younger unimpaired participants.

3.2 Material and methods

3.2.1 Participants

40 stroke survivors (age range: 31-72 years old, see also Table 3.1) and 24 participants without any known sensorimotor impairment or history of neurological, psychiatric, or neuromuscular disorders (age range: 21-58 years old, mean age ± std: 37.2 ± 14.2 years old; 10 females) completed the proprioceptive test.

For stroke survivors, the inclusion criteria: (i) first-ever stroke event diagnosed by neurologists or neurosurgeons and brain imaging; (ii) age ranged between 21 and 85 years old; (iii) being between 3 and 24 months after the stroke event, i.e., post-acute stroke phase; (iv) Upper Extremity portion of the Fugl-Meyer Assessment (FMA-UE) < 20 or presence of

motor ataxia; (v) ability to understand instructions and give informed consent; (vi) absence of uncontrolled medical illnesses and pregnancy; (vii) more than 6 months of life expectancy; (viii) ability to sit upright with support for more than 90 minutes; (ix) absence of arm related contraindications to robot aided therapy such as shoulder pain (Visual Analog Scale for pain ≤ 4); (x) absent or low level of spasticity (Modified Ashworth Scale ≤ 2); (xi) absence of hemi spatial neglect assessed using the line bisection test; (xii) mini-mental state examination score ≥ 27.

Inclusion criteria for all participants were to be naïve to the study and right-handed; this latter requirement for stroke survivors was referred to their hand dominance before the stroke event. This was motivated by the fact that hand dominance could be a confounding factor in this experiment, accounting for the hemispheric localization of the lesion.

41 stroke survivors matching the inclusion criteria were enrolled for the assessment. However, one of them was excluded from the analysis because he/she did not complete the assessment, performing the test only with one arm. According to the clinical history, 28 stroke survivors had left-hemisphere damage and 12 had right-hemisphere damage (Table 3.1).

As preliminary analysis, we verified that there was no difference in age or clinical scores between the LBD and RBD stroke survivors, using the Wilcoxon rank-sum test. We did not find any difference between the two groups neither in the age ($p=0.701$) nor in their clinical scores (Table 3.1; FMA-UE $p=0.111$; ARAT $p=0.360$; FAT $p=0.169$). Instead, stroke survivors and unimpaired participants had different age ($p<0.001$) and they cannot be considered age-matched groups. This limit was considered in the analysis and in the section 3.5 (further analysis on the effects of age in unimpaired participants are reported in the section 3.3).

Ethical approvals for all procedures were obtained from the Domain Specific Review Boards (NHG-DSRB 2014/00122) of the National Healthcare Group for stroke survivors, and of Nanyang Technological University for unimpaired participants before recruitment. All participants gave written informed consent to participate in the study, in conformity with the 1964 Declaration of Helsinki. The study was carried out in the outpatient clinic of a tertiary rehabilitation centre with links to an acute stroke unit.

Table 3.1 Demographic data and clinical test results

Brain lesion side	Sex	Age	FMA-UE (0-66)	ARAT (0-51)	FAT (0-5)
Left	13F, 15M	57 ± 9	40.4 ± 10.5	24.4 ± 15.9	1.5 ± 1.5
Right	5F, 7M	54 ± 13	33.7 ± 8.0	18.4 ± 14.7	0.8 ± 1.3
All		56 ± 10	38.4 ± 10.3	22.6 ± 15.8	1.32 ± 1.5

Abbreviations: FMA-UE: Upper Extremity portion of the Fugl-Meyer Assessment; ARAT: Action Research Arm Test; FAT: Frenchay Arm Test. Data are reported as mean ± std

3.2.2 Experimental set-up

The proprioceptive assessment was performed using H-Man, a planar end-point robot designed for assessing and training the upper-limb sensorimotor function, already used in studies with unimpaired participants and stroke survivors [154–157].

The experimental set-up and the protocol were the same used in [155, 156]. Briefly, participants were seated in front of H-Man in a height-adjustable chair, with their sternum centered to the robot's workspace. Their hand grasped or was strapped to the robot's handle, which in the starting position was on the participants' midline, approximately 25 cm far from their sternum, requiring an elbow angle of approximately 90° (Fig. 3.1). Shoulder straps attached to the chair prevent trunk movements, allowing only rotations of the shoulder and flexion/extension of elbow joints.

3.2.3 Protocol

During the experiment, they were required to keep the eyes closed and the arm muscles relaxed.

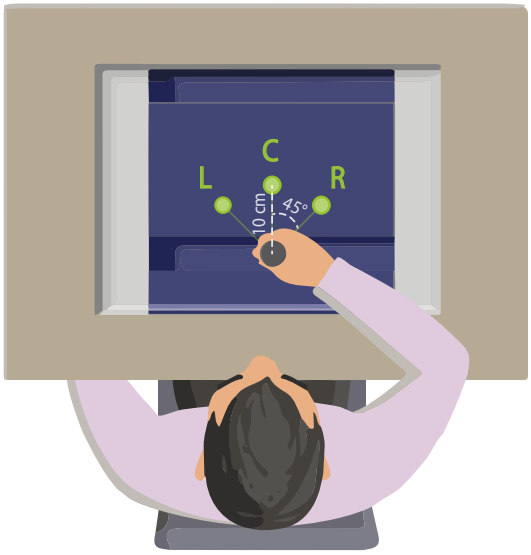

Figure 3.1 Experimental set-up. Participants were seated in front of H-Man, with their sternum's center aligned with the center of the robot's workspace and with the hand's starting position (gray). They had to grasp the robot's handle, which in each trial was moved by the robot in one of three possible target locations (green) set 10 cm far from the starting position and with an angle of 0° (Central: C) and ± 45° (Left: L; Right: R) with respect to the participant's midline.

Each trial was divided into two phases: 'reference' and 'match'. In the reference phase, the robot's handle was moved from the starting position to a target position at a constant velocity of 7 cm/s and held there for 2 seconds. Then, the handle returned to the starting position at the same velocity. After 1s, the match phase started. In this phase, the robot's handle was moved again in the direction of the same target at a constant velocity of 2 cm/s. Participants had to verbally notify when they felt that their hand reached the target position (perceived target position). The experimenter immediately ended the trial stopping the handle motion. After that, the handle returned to the starting position. The participants did not receive any feedback about trial performance. The three targets were placed 10 cm far from the starting position in three different directions at 0° (central target), and ± 45° (left and right lateral targets) with respect to the participants' midline. Each target was presented 6 times in random order for a total of 18 trials. The stroke survivors performed the same task with both the contralesional and the ipsilesional arm. The order in which the arms were tested was balanced among them. The unimpaired participants performed the task only once, with the dominant (right) arm . All the participants performed up to 10 trials (minimum 3) for familiarizing themselves with the task before performing the test.

3.2.4 Data analysis

First, we computed the matching error as the signed difference between the perceived (i.e. the point where the participant indicated their hand reached the target position) and the true target position as in [158]. Then, to assess the proprioceptive performance we estimated the following indicators:

- Constant error, as the mean value of the matching error across trials toward the same target. Before averaging across participants, we considered the unsigned value of the matching error, since we were interested in evaluating the overall accuracy, not the tendency of the participants to overshoot or undershoot the target distance;
- Variable error, as the standard deviation of the matching error, computed across trials toward the same target. This represents the precision, i.e., the repeatability (consistency) of the performance across trials.

The difference between cUL and D was not studied here, because it has been already investigated in several studies and reported in [159, 156] with this experimental set-up and protocol.

Statistical analysis

Our main goal was to evaluate if in stroke survivors there were differences between the proprioceptive performance of the two arms during a passive position matching task, where the hand was moved by an endpoint robot. To do so, we compared the proprioceptive performance of iUL and cUL, performing a repeated measure ANOVA with two within-subjects factors: 'arm' (2 levels: 'iUL' and 'cUL') and 'target' (3 levels: 'left', 'central' and 'right'). In addition, we also compared the performance of iUL and Dominant arm (D) of unimpaired participants, performing a mixed-design ANOVA with 'population' as a between-subjects factor (2 levels: 'unimpaired' and 'stroke') and 'target' as a within-subjects factor (3 levels). Before running the ANOVA, we checked the normality of data using the Anderson-Darling test [103]. When the null hypothesis was rejected, the data were corrected by applying the fractional rank method [104]. For the rm-ANOVA, we tested the sphericity using Mauchly's test and for the mixed ANOVA we tested the equality of variances using Levene's test , both were not rejected for any metric. Statistical significance was set at the family-wise error rate of α=0.05 and applying the Bonferroni correction for multiple comparisons the threshold required for the significance of each of the two ANOVAs was set to $\alpha = 0.05/2 = 0.025$. Finally, we investigated if there was a correlation between the

proprioceptive performance of the two arms in stroke survivors and if this correlation was influenced by the brain hemisphere of the lesion and by the target position in the workspace. For the latter, we considered targets positioned in the central, left and right workspace with respect to the participants' midline (see Figure 3.1), regardless of their brain lesion side). To this end, we computed Spearman's correlation coefficient between the performance of the iUL and cUL, considering as separate factors: (i) the brain hemisphere of the lesion (LBD and RBD stroke survivors); (ii) the target position (right, central, left). Spearman's correlation coefficient (ρ) ranging from 0.20 to 0.39 was considered as moderate, from 0.40 to 0.59 as relatively strong, from 0.60 to 0.79 as strong, and higher as very strong correlation [160].

3.3 Preliminary results on unimpaired participants

Differences between the position sense of the two arms

9 right-handed unimpaired participants (age range: 21-34 years, mean age ± std: 26.2 ± 4.8 years; 2 females) performed the task with both the dominant and non-dominant arm. As a preliminary analysis, we evaluated if there was any difference in performance between the two upper limbs in terms of accuracy and precision, computed as described in the Data analysis section in the manuscript. Thus, we performed an rm-ANOVA with two within-subject factors: 'arm' (2 levels) and 'target' (3 levels). Before running the rm-ANOVA, we checked the normality of data using the Anderson-Darling test. When the null hypothesis was rejected, the data were corrected by applying the fractional rank method. We tested also the sphericity using Mauchly's test. We found that there was no significant difference between the performance of the two arms (Fig. 3.2a), neither in terms of accuracy ($F_{1,8}$=0.061 p=0.812) nor of precision ($F_{1,8}$=0.248 p=0.632). Thanks to this finding, we can compare the performance of stroke survivors with only the dominant arm of unimpaired participants. This is in line with other proprioceptive evaluations, as a mirror-matching task [151, 161] and single-joint 2-alternative choice paradigm [162].

Effect of age on position sense performance in unimpaired participants

We compared position sense performance of unimpaired participants, dividing them into 'younger' (15 people; age range: 20-34 years, mean age ± std: 26.7 ± 4.0 years; 4 females) and 'aged' (9 people; age range: 46-58 years, mean age ± std: 54.8 ± 3.7 years; 6 females). For doing that, we performed a mixed-design ANOVA with 'age' as a between-subjects factor

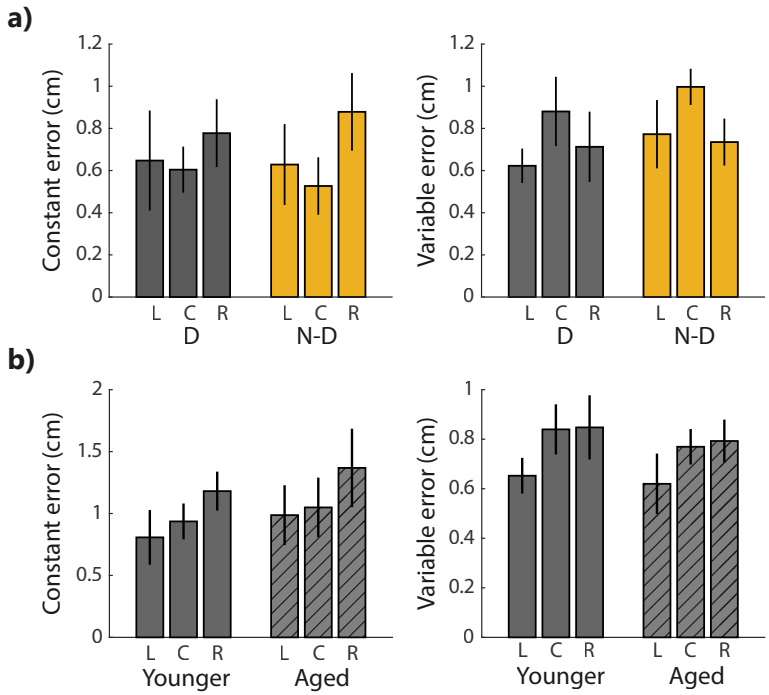

Figure 3.2 a) Comparison between the dominant (D) and non-dominant (N-D) arms in unimpaired participants in term of constant (left) and variable (right) error; b) Comparison between the dominant (D) arms of the younger and aged group of unimpaired participants in term of constant (left) and variable (right) error;

(2 levels) and 'target' as a within-subjects factor (3 levels). Before running the ANOVA, we checked the normality of data using the Anderson-Darling test. When the null hypothesis was rejected, the data were corrected by applying the fractional rank method. We also verified the equality of variances using Levene's test. As shown in Fig. 3.2b, we found no difference between them neither in accuracy ($F_{1,22}$=0.362 p=0.554) nor in precision ($F_{1,22}$=0.231 p=0.636). This is in line with previous findings in a smaller population [155].

3.4 Results on stroke survivors

To understand if in stroke survivors the iUL had impaired position sense in unimanual position matching tasks, we compared the performance indicators, i.e., constant error (Fig. 3.3a) and variable error (Fig. 3.3c) of this arm with those (i) of the cUL and (ii) of the dominant arm of unimpaired participants.

As for two arms of stroke survivors, we found that the iUL and cUL (Table 3.2) had different performance in terms of precision (variable error: $F_{1,39}$=6.94 p=0.012), but not in

terms of accuracy (constant error: $F_{1,39}$=0.05 p=0.823). Specifically, compared to the cUL, the iUL had no significantly different accuracy, but higher precision, i.e., a lower variability when identifying the same position in space.

The fact that the iUL arm of stroke survivors had lower accuracy ($F_{1,62}$=5.57 p=0.021) than the dominant arm of unimpaired participants, but no significantly different precision ($F_{1,62}$=0.78 p=0.379; Table 3.3) confirmed that the iUL precision was not significantly affected by stroke in our population, while the accuracy worsened also in the iUL.

Table 3.2 Comparison between the ipsilesional and contralesional arm

	Constant error		Variable error	
Factor	F	p	F	p
Arm	0.05	0.823	6.94	0.012
Target	1.23	0.297	3.94	0.024
Arm*Target	0.58	0.561	0.61	0.548

Table 3.3 Comparison between iUL of stroke survivors and D of unimpaired participants

	Constant error		Variable error	
Factor	F	p	F	p
Population	0.78	0.379	5.57	0.021
Target	3.47	0.034	1.19	0.147
Population*Target	2.98	0.055	4.21	0.017

As for the dependence of the proprioceptive performance on the workspace region, comparing iUL and cUL, we found that the variable error ($F_{2,78}$=3.94 p=0.024), but not the constant error ($F_{2,78}$=1.23 p=0.297) significantly depended on target positions.

Specifically, the variable error of the stroke survivors was slightly, but significantly higher for the central target. This was observable for both arms, i.e., there were no significant interactions between arm and target ($F_{2,78}$=0.61 p=0.548). This latter trend was not present in the unimpaired participants. However, when directly comparing the stroke survivors and the unimpaired participants, the effects of the population * target interaction and the target factor did not reach the threshold for significance after applying Bonferroni corrections (p=0.055 and p=0.034, respectively).

Interestingly, the interaction effect between population and target was significant only for the constant error ($F_{2,124}$=4.21 p=0.017). In fact, for unimpaired participants, the error increased from the left to the right workspace, while this effect did not present among the stroke survivors whose lower errors were reached on average for the central target.

To understand if there was a correlation between the proprioceptive performance of the two arms in stroke survivors and if that correlation depended on the hemisphere of the brain lesion, we computed the Spearman's correlation between the performance of iUL and cUL, separately for survivors with RBD and LBD and the three targets (Table 3.4), i.e., central, left and right with respect to the subject midline.

For the central target, the matching performance of the two arms correlated in terms of accuracy for all survivors (both $\rho > 0.40$, Fig. 3.3b - central panel), but not in terms of precision (both $\rho < 0.30$, Fig. 3.3d - central panel). Specifically, the correlation between the constant errors of the two arms was relatively strong for the LBD group (ρ=0.41) and strong for the RBD group (ρ=0.71). These results were maintained for all survivors on the left workspace (Fig. 3.3b - left panel), i.e., the constant error had a higher (relatively strong) correlation between the two arms for the LBD group (ρ=0.56) and lower (moderate) for the RBD group (ρ=0.34), while the variable errors had almost no correlation for all the stroke survivors (ρ<0.10). In the right workspace, the only correlation was for the variable error for the RBD group (ρ=0.54, Fig. 3.3d - right panel, others ρ<0.20).

When we found a correlation with $\rho \geq 0.30$, we also computed a curve fitting by using monotonic least-squares splines (Fig. 3.3b and 3.3d, Table 3.4).

Table 3.4 Spearman's correlation coefficient and R^2 of the curve fitting when $\rho \geq 0.30$

	Constant error		Variable error	
	LBD	RBD	LBD	RBD
Left target	ρ=0.56 R^2=0.36	ρ=0.34 R^2=0.22	ρ=-0.02	ρ=0.08
Center target	ρ=0.41 R^2=0.30	ρ=0.71 R^2=0.63	ρ=0.29	ρ=0.24
Right target	ρ=0.19	ρ=-0.04	ρ=-0.03	ρ=0.54 R^2=0.63

3.5 Discussion

We investigated the iUL position sense in stroke survivors during a unimanual position matching task, requiring movements of both shoulder and elbow. Our results suggest that in this task stroke did not affect the two arms in a similar way in terms of precision, since the ipsilesional arm had matching variability lower than contralesional and comparable to that of

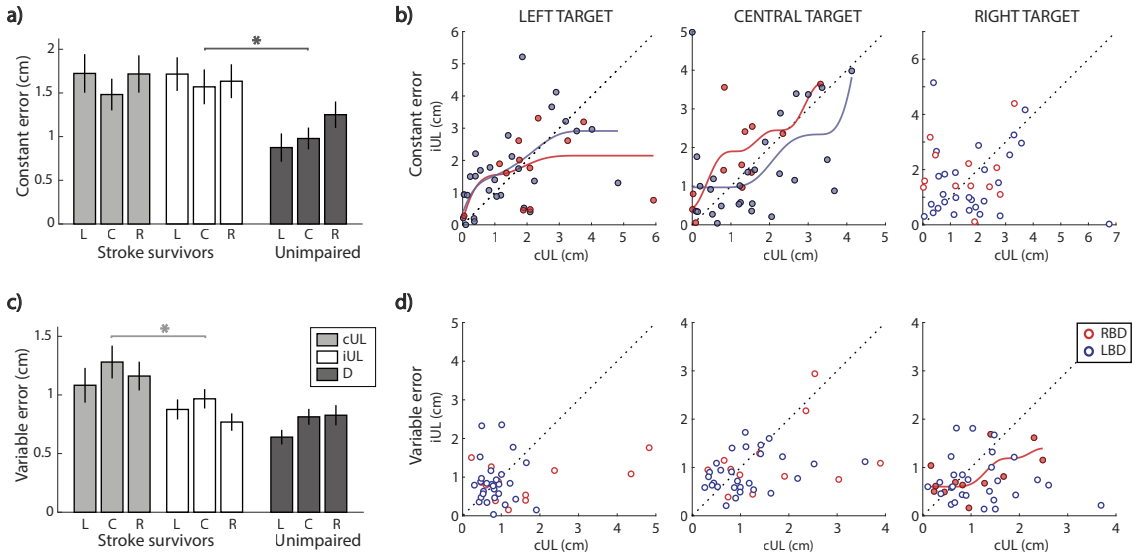

Figure 3.3 a,b) Constant error - unsigned value of the constant error averaged across participant – c,d) variable error. a,c) report the comparison between the ipsilesional (white) and contralesional (gray) arms of stroke survivors and between dominant arm of unimpaired (dark gray) participants for left central and right targets with respect to the subject midline. * indicates statistical significance, $p<0.025$; Error bars indicate SE. b,d) report the correlation between the two arms of stroke survivors for left (left panel), central (central panel) and right (right panel) targets. Red and blue indicate respectively RBD and LBD stroke survivors. The circles are filled when there is at least a moderate correlation (Spearman's coefficient ≥ 0.30). In these cases, we also displayed a monotonic fitting curve, i.e., a monotonic least squares splines, to highlight the trend. The dashed line represents the equal performance for the two arms.

unimpaired participants. The precision of the two arms was also not correlated, with the only exception of a weak relationship in the right workspace for the RBD group.

Conversely, the two arms had similar matching accuracy, that correlated along the midline and in the left workspace for all the stroke survivors, independently of the hemispheric localization of the brain lesion. The iUL accuracy in stroke survivors was lower than in the group of unimpaired participants, highlighting a significant decrease in this performance metric.

In the following, we discuss in detail these findings.

In unilateral passive hand matching, the precision of the ipsilesional arm is affected after stroke, while its accuracy is not

We found proprioceptive differences between the two arms of stroke survivors in terms of precision, but not of accuracy, suggesting that stroke impacts the ipsilesional arm proprioception in a different way than the contralesional arm. Our results support the findings that after stroke the iUL has not an 'unaffected', but a 'less-affected'. These findings could also indicate a degree of dissociation between accuracy and precision for passive matching task involving multiple joints, as already observed for single-joint matching task with active matching movement [152]. This dissociation between accuracy and precision in proprioceptive performance affected by stroke and/or age. We acknowledge that in this study the unimpaired group was slightly younger than the stroke survivor group and it is well known that there is a deterioration of the proprioceptive mechanisms with age [65, 163, 164]. Our preliminary results within the unimpaired participants (Section 3.3) did not highlight any significant difference due to age on a limited number of participants. Consequently, we cannot ensure that significant difference in accuracy between the two groups was due to stroke. Likely, it was due to a combination of both factors, age and stroke. Hence, future investigations including an age-matched control group are necessary to address this important point.

Therefore, our results support and enlarge the actual knowledge, highlighting the precision asymmetry between the two arms in this passive proprioceptive task following stroke. In fact, most of the methods used in literature to assess the position sense relays on active movements, which activate neural patterns different than the passive tasks [165, 166, 65, 167, 149]. In fact, proprioception differs in active and passive tasks due to many factors, such as (i) the more predominant role of thixotropy in passive than in active movements [52]; (ii) the sensitivity of passive spindle with is related to the muscle contraction [52]; (iii) the difference sources of signals, e.g., performance in passive movements resulted primarily from processing of afferent inputs, while during active movement also the efferent copy of the motor commands plays a key-role [168].

The correlation between the position sense performance of the two arms depends on the workspace region

We found a correlation between the proprioceptive performance of the two arms considering all our stroke survivors only in the central and left workspace regions with respect to the body midline. This finding confirmed the in-homogeneity of perception acuity across the 2D

workspace, highlighted by previous studies in both unimpaired participants [36, 158, 169–171] and stroke survivors [7, 20, 151–153] also with the same experimental set-up and protocol [172]. Furthermore, Contu et al. [172] highlighted that the matching precision and accuracy for both the contralesional arm of stroke survivors and the dominant (right) arm of age-matched unimpaired participants is lower for the 'external' target (i.e., right (left) target for the right (left) arm). In addition, previous works on stroke survivors highlighted that most stroke survivors had spatial contraction [7, 151] greater variability and higher systematic shift than controls [7]. However, previous works on stroke survivors were mostly based on the position sense of both arms [7, 151–153] or single-joint [20] paradigms and focused mainly on the contralesional arm.

These differences across the space are due to an interplay of many factors, such as limb geometry [169, 173], limb anisotropy [3], spatial biases in muscle spindle firing rates [174, 175] also depending on the amplitude of the joint angles (e.g., there is a tendency to overestimate large joint angles [170]) and the coupling between joints (e.g., the elbow extension is overestimated only when the shoulder is abducted [170]). Therefore, there is still the need for deeper investigating position sense in a task involving multiple joints, because it is not a mere byproduct of results obtained for single joint tasks. Furthermore, tests accounting concurrently for the proprioception of the two arms do not allow to determine independently the deficits of each arm and thus do not lead to a clear understanding of possible sensory deficits in the ipsilesional arm and their mapping in the workspace.

The mapping of proprioception accuracy across a 2D horizontal workspace does not depend on the hemisphere of the stroke lesion

The accuracy of the two arms correlated in the central and left workspace regions with respect to the body midline, independently of the hemisphere of the brain lesion. Instead, for the matching precision, there was a correlation between the performance of the two arms only for the RBD group and limited to the right workspace.

In stroke survivors with unilateral brain damage, the effects of the brain hemisphere on the neural control of movements have been extensively investigated and several studies highlighted that the spatial and temporal alteration of arm movement depends on the side of the lesion [17, 18, 23, 120, 128, 131, 176]. Specifically, in relation to the ipsilesional arm, Schaefer et al. [131] reported that in reaching movements in the ipsilateral workspace, RBD had lower final position accuracy, a sign of deficits in controlling the hand position while LBD had deficits in controlling the trajectory, a sign of deficits in multi-joint coordination.

Conversely, to date, the sensory deficits have been less investigated than the motor deficits in terms of dependency on the brain lesion side. There are studies, as [52, 168], suggesting that RBD have higher probability to develop contralesional somatosensory, proprioceptive deficits or even neglect [177, 178]. However, the actual literature often provides task-dependent and/or discordant results. For example [15, 16] reported that RBD had a reduced tactile sensibility with respect to the LBD group, while [13] found the opposite result. Instead [14, 126] did not find any difference between RBD and LBD groups. This discrepancy in results could be due to differences in several factors, such as the experimental methods, and/or the characteristics of the participants, e.g., age and impairment level.

To the best of our knowledge, the relationship between the upper limb position sense deficits and the brain lesion side has been considered in only few studies. [161] did not find any difference between RBD and LBD in the mirror position test. [162] evaluated hand proprioception in a single-joint experimental design finding more severe proprioceptive deficits in RBD than LBD only for contralesional hand, i.e., they did not find differences in the ipsilesional hand between the two groups. They also reported that all the stroke survivors had lower proprioceptive performance only with the left hand than control participants.

Thus, these previous results specifically focusing on position sense, although not directly comparable with our finding, are not in contrast, but they rather support our main findings. Indeed, our finding on the correlation in the accuracy is supported by the [161]. Instead, the slight difference in the precision between the two groups observed only in the right workspace could be due to an interplay of many factors, as (i) the handedness, since only for the LBD group had the dominant arm as a contralesional arm; (ii) difference in position sense found in single-joint tasks [162]; (iii) difference in tactile ability between the two sides [13] and future investigations on larger of RBD and LBD groups are needed to better understand this latter point.

Implication for functional evaluation and rehabilitation

Findings from this study enlarge the actual knowledge on the upper limb position sense asymmetries in stroke survivors relating to passive unilateral matching tasks, their mapping in the 2D workspace, and the relation with the hemisphere of the brain lesion. It also provide evidence to support the need to quantitatively assess both ipsilesional and contralesional proprioceptive deficits to have a more complete evaluation, which is essential to design and tailor an effective rehabilitative treatment. In addition to that this robot-aided assessment

could be useful to monitor the efficacy of the rehabilitation treatment and to correlate the motor rehabilitation outcomes to the proprioceptive abilities.

Limitations

We acknowledge that, in our proprioceptive test participants have to rely on memory to complete the task [65], since the same arm is used to provide a reference to match in sequential phases. To mitigate this issue one of the inclusion criteria to be enrolled in this study was to have a score in the mini-mental state examination above 27.
Another limitation of this study is the lack of clinical evaluation of the bilateral proprioceptive and sensory ability prior to the proprioceptive test performed with the robot. Finally, the dependency of performance on the workspace region could underline mechanism related to the handedness of the participants which remains predominant despite the stroke, as [162] found lower performance for the left hand in all stroke survivors despite their brain lesion side. This point could be addressed by further investigations involving left-handed participants from both groups, unimpaired and stroke survivors.

Chapter 4

Study II: Development of a device to assess proprioception during bimanual tasks, and preliminary results on stroke survivors

This study has been done in collaboration with the Department of Neurosciences, Biomedicine and Movement Sciences, Verona University (Verona, Italy).

4.1 Introduction

Recently, bimanual movement training has emerged as an effective tool in neuro-rehabilitation to facilitate and enhance functional recovery and bimanual coordination. It is a general term that includes different training techniques requiring the simultaneous use of both upper limbs to solve a specific task [179, 180]. Bimanual movement training potentially can encourage inter-hemispheric communication and improve unilateral motor cortex activation enhancing also both the uni- and bi-manual motor control [179]. This can be explained by the inherent dependencies between arms [181–183], which activate similar neural distributed networks in both hemispheres during symmetrical movements [184–186]. Previous studies demonstrate that this type of training is effective in improving ipsilesional and bimanual motor ability after stroke [179, 187].

Bimanual tasks could be categorized in (i) physically coupled task when the action of one limb affects the dynamic of the other [188], i.e., there is a direct transfer of forces between

the two limbs and direct proprioceptive feedback of the opposite side action; (ii) uncoupled task, when the movement and action of each limb are independent, e.g., when the two limbs are interacting with two different objects.

Although arguably more realistic, coupled bimanual tasks are less investigated than uncoupled tasks. Several previous studies used uncoupled bimanual tasks to investigate the ability to orient objects in the space [189, 190], matching a specific position or exerting a required level of force [Chapter 1 and 2]. Examples of coupled bimanual tasks can be found in [191] and in [192]. In the first study [191], children were required to use both hands for lifting a small cube, which recorded the force applied and movement performed. This device has been used to assess proprioception, but it is less suitable for training since the device seems to not provide any type of online feedback. In [192], a box was used to evaluate the proprioception ability in unimpaired participants, the device was able to measure the force applied and fatigue during an orientation-matching task under different loading conditions. The system can also provide online visual feedback about the performance and the 3D orientation of the device in the space.

However, from a technological point of view, the previously mentioned devices for physically coupled tasks obtained information only about the orientation of the device in the space from the Inertial Measurement Units (IMUs). From there, it is theoretically possible to obtain information about the 3D position by integrating the IMU signals. These estimates are accurate on a short time scale but suffer from integration drift over longer time scales [193]. Since, we were interested in a tool that could directly measure its 3D position, we re-designed the device used in [192], by substituting the IMU with a tracking camera. As result, our new device directly measures the force applied to the device, its orientation in the space, but also its 3D position for log-time without suffering of the drift typical of IMUs. It could be used standalone, and it can provide online visual feedback about performance, and it can also be coupled with an electromyograph to synchronize the recording of behavioral data and physiolocial signals, such as electromyographic (EMG) or electroencephalographic (EEG) signals during the task execution. In addition to that, with simple modification the device could be suitable for both coupled and uncoupled bimanual tasks, allowing a more comprehensive assessment with only one device.

Here , we reported the design and development of this new device from both the hardware and software point of view, and the preliminary tests performed in stroke survivors.

4.2 Material and Methods

4.2.1 Design and development of the device

Hardware components

We re-designed a low-cost sensorized device shaped like a rectangular box (Fig. 4.1) of 15 × 35 × 25 cm (height × width × depth). The width of 35 cm has been chosen to match the average human anthropometric inter-shoulder distance.

The device has been designed to be handled by placing the hands on the lateral sides, which are separated by four polymeric rods, allowing to fix their distance and reducing the weight of the device. Each lateral side is composed of two rigid plates 3D-printed in PolyLactide Acid (PLA), which keep in place three load cells (Micro Load Cell CZL635; full-range scale of 5kg; precision of 0.05% and linearity of 0.05% FS) in a triangular configuration. Due to this configuration, the force applied by the user on the external plate of the device is sensed by the load cells and measured by the device.

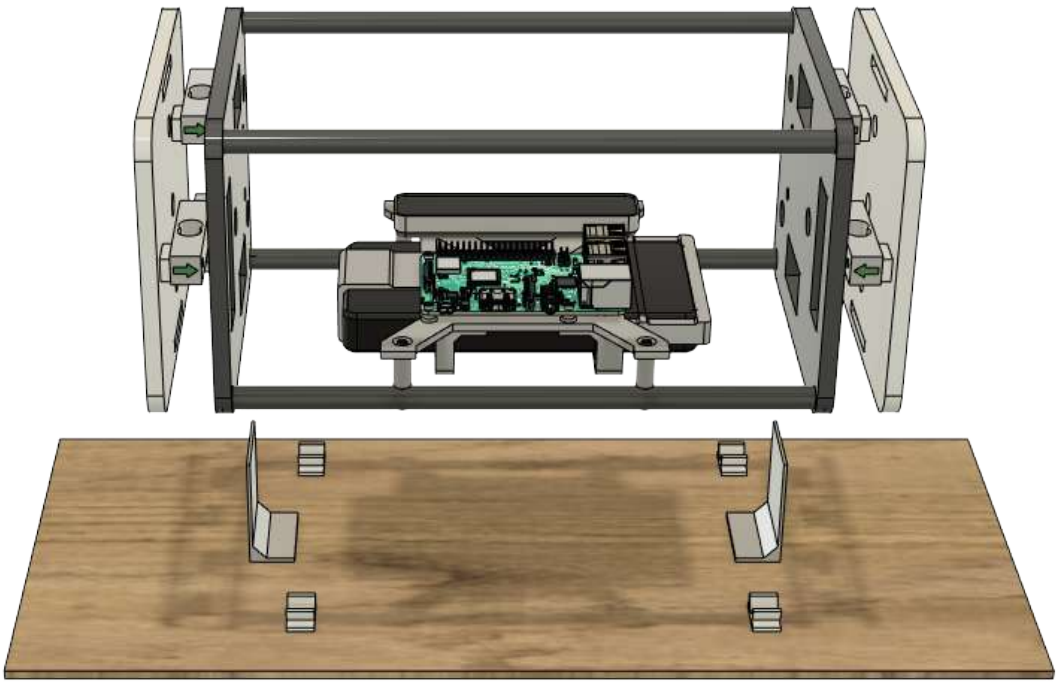

Figure 4.1 CAD model of the device (above) with the tool to make it suitable for uncoupled bimanual tasks (below).

At the center of the bottom part of the device, there is a 3D-printed rigid plate made of PLA. It encloses a micro-controller (Raspberry Pi, model 3B+, CPU frequency: 1400MHz) and a tracking camera (RealSense™ T265, Intel) on the upper side, and a battery (24800mAh, output of 3.1A) on the bottom side. The camera measures both the 3D position and orientation of the device, thanks to its two fisheye lenses (OV9282, with 163±5° field of view), a visual processing unit (Intel® Movidius™ Myriad™ 2.0), and an Inertial Measurement Unit (IMU, BMI055). The micro-controller is connected via USB to both the tracking camera and the external battery.

The force exerted by the user on the external lateral side is sensed by the three load cells placed between the two rigid plates. The analog signals from the three load cells of each side are sent to a customized Printed Circuit Board (PCB), where are converted into digital signals. Furthermore, in each PCB (Fig. 4.2) the analog signal from each load cell is amplified (Instrumental Amplifier INA 122, Texas Instruments, gain of 2005) and then converted into digital by to a single-ended input Successive Approximation Register Analog to Digital Converter (SAR ADC: MCP 33111-05, Microchips, sample rate: 500 kSPS, resolution: 12-bit). Thanks to the PCB design, all the load cells are sampled on the rise edges of the chip selector signals of the micro-controller. Then, after the sampling the analog-to-digital conversion - requiring 12 clocks due to the resolution of the ADC - is performed sequentially for all the six load cells and the digital signals are transmitted to the micro-controller on the same wire of the Serial Peripheral Interface (SPI).

The device can be used for physically coupled bimanual tasks, without any modification, or for uncoupled task. For this latter option, we designed and developed an additional tool (bottom part of Fig. 4.1) that can hold the device and make the two lateral sides independent. It is composed of a base plate, where there are four grippers, which can fix the two bottom rods of the device. On the same base plate there are two L-shaped metallic parts. Their distance matched the distance between the two internal plates of the lateral sides of the device to ensure that the force applied on one side will not be transmitted on the other side, ensuring that the device will be in an uncoupled configuration when the hands of the user would be placed on them.

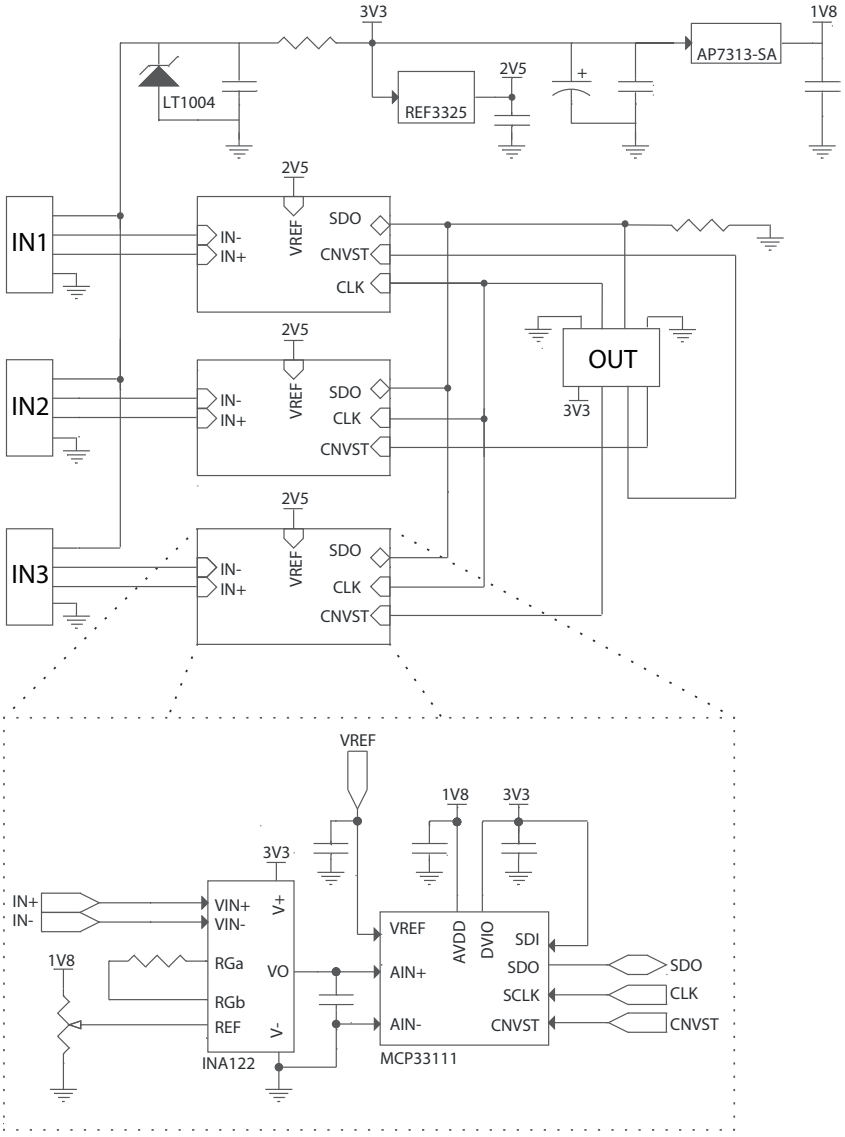

Figure 4.2 Design of the PCB in each lateral side, which sampled the analog signals from the load cells on the edge of the same signals, sequentially convert them into digital signals, given as output of the PCB on the same bus of the SPI.

We also developed an optional 'expansion kit' that can be easily integrated with the device. It allows to couple the acquisition of behavioral data and electro-physiological signals acquired during the execution of the task with the device. In this case, a programmable Trigger-Box (TB) has to be connected to same laptop. Any EMG or EEG device that could accept an external trigger to start and stop the data acquisition could be then connected to the TB, which will synchronize the acquisition of the two devices. A scheme of the connections between all the components is reported in Fig. 4.3.

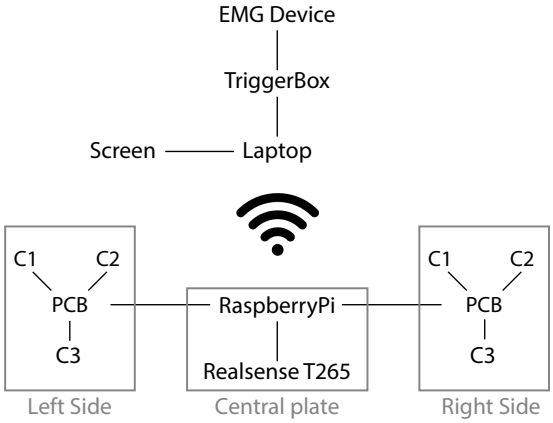

Figure 4.3 Scheme of the connection between all the system's components.

Software

The software is divided into two main parts: (1) on the Raspberry, which is responsible to acquire the data, save it and send it to the laptop when needed, e.g., for visual feedback, and (2) on the laptop, where there is the Graphic User Interface (GUI). The micro-controller and the laptop are connected via Wi-Fi using a socket connection. The Raspberry-laptop communication is bi-directional, i.e., the roles of 'sender' and 'receiver' are exchanged during the experimental protocol according to the the need and the phase of the experiment.

The software on the Raspberry is developed in Python 3.0. It is responsible to set the socket connection with the laptop, acquire the positional and force data, and saving the data on its memory at a frequency of 100Hz. In details, it is made of an initial setting for the connection and then it is composed of three parallel and synchronized threads.

i The first thread is mainly responsible for acquiring the positional data from the Realsense Camera. Every time that new data is available, it acquires a data vector with 7 elements: three for the 3D position in the camera reference system and four data for the quaternion, i.e., the camera orientation in its reference system. When the camera is switched on, it perform an auto-calibration, i.e., its initial position is taken as reference. For this reason, at the beginning of the experimental session, the device has to keep horizontally in a position, that will be set as starting position.

ii The second thread is mainly responsible for acquiring the data from the six load cells. It rises the six chip selector signals (one for each load cells), and on the rising edges the six load cells are sampled. Then, the signals from the six load cells are sequentially converted into digital signals, when the chip selector is lowered the data from the

correspondent load cell is converted from analog to digital in 12 clock cycles. The data acquired from the six load cells are then packed in a vector with 6 elements, which contains in order the data from the three load cells of left and right sides respectively. At the beginning of each experimental session, the user is asked to not touch the device for 250 ms. In this time, the device collected the force data, and the average value is set as a 'zero' reference for that experimental session and use to tare force acquired during the session. This data is stored and used as the header of the data file stored in the Raspberry, together with the calibration data, i.e., to transform the data collected by the load cells (bit) in force data (N).

iii The third thread is mainly responsible for saving the data (and the trial information) on the Raspberry in ASCII format at the end of each trial, so the task can be interrupted at the end of any trial without losing the data collected until there. It is also responsible for sending the data needed for the visual feedback to the laptop application, at a frequency of 60Hz. This function is done only when is needed, i.e., in accordance with the task selected by the experimenter on the application that run on the laptop (see below).

The software on the laptop is an application developed in Unity (unity Technology), based on C#. When the application starts, it set up the socket connection with the Raspberry. After that, there is a page to insert the users' data and the information about the experimental session. After that, the GUI provided a new page where the experimenter can choose the experimental task to perform and according to that, the Raspberry wuld send the data needed for the visual feedback when necessary, which would be displayed on the screen (see Table 4.3.2 for more details). At the beginning and the end of each trial, the application sends a trigger to the EMG/EEG device via the trigger-box to start and end the acquisition of physiological signals.

4.3 Preliminary tests on stroke survivors

We re-designed a low-cost and easy-to-use device that could be used to quantitatively assess the position and force sense as well as their interaction in various bimanual tasks. There, we presented a first proof of concept that this device could also be used to assess proprioceptive deficits in stroke survivors.

4.3.1 Participants

10 stroke survivors (mean age ± std: 67.5 ± 12.3 years old, 2 females, see 4.1 for more details) and 10 participants without any known sensorimotor impairment or history of neurological, psychiatric, or neuromuscular disorders (mean age ± std: 65.2 ± 7.2 years old; 5 females) participated in the study. All participants were right-handed, for stroke survivors it was referred to their hand dominance before the stroke event. This study was conformed to the ethical standards of the 1964 Declaration of Helsinki. The study procedures were approved by Verona University Institutional Review Board (CARU n. 22/2019).

As preliminary analysis, we verified that there was no difference in age between the two populations of participants, using the Wilcoxon rank-sum test. We did not find any difference between the age of the two populations (p=0.947).

4.3.2 Experimental protocol

Participants sat in an height-adjustable chair in front of the screen placed about 50 cm far from their chest. The height of the chair was adjusted to let the forearms rested on the table with shoulders in 20° flexion and elbows at 110° flexion. The hands were positioned fully open on the lateral sides of the device.

Table 4.1 Demographic data and clinical test results

Participant	Sex	Age	Time after event (days)	FMA-UE (A-D) (0-66)	FMA-UE (H) (0-24)	AFE (0-5)
S01	M	47	649	59	12	4+
S02	M	89	226	61	12	5
S03	M	69	125	62	12	5
S04	M	65	106	56	12	4
S05	M	71	67	60	12	5
S06	F	63	108	50	10	5
S07	M	81	241	66	12	5
S08	M	80	58	62	12	5
S09	M	55	264	62	9	4+
S10	F	71	158	53	10	4+

Abbreviations: FMA-UE: Upper Extremity portion of the Fugl-Meyer Assessment (A-D): motor assessment, H: sensory assessment; AFE: Active Finger Extension [194]

The experimental protocol was composed by four experimental tasks, in all of them, the pause between the trials is chosen manually, so the task would be suitable for people with different sensorimotor abilities without inducing fatigue.

1. Maximum Voluntary Force (MVF). It is composed of three sequential 7-second long trials. In each trial the user is asked to apply the maximum force on the lateral side of the device. This task could be performed under three different visual feedback conditions: no visual feedback, visual feedback about the total force exerted on the lateral sides, visual feedback about the force exerted on each lateral side separately. At the end of this task, the mean MVF (i.e., averaged across the three trials) is computed and sent to the laptop, since it is required to perform the force matching tasks (see below), but it can also manually set by the experimenter using the GUI.

2. Coupled bimanual force matching task. In each trial, the user is asked to match a target force apply simultaneously the same amount of force on the two lateral sides of the device. Then, it has to maintain this target force until the end of the trial, which has a duration of 5 seconds. The user has a visual feedback about the total force applied, it is coded coded in the height of a white bar that has to reach the red bar coding the target force. The target forces presented in the tasks corresponded to the 10, 25 and 50 % of the MVF recorded at the beginning of the experimental session or set by the experimenter. Each target force is presented 7 times in random order, for a total of 21 trials.

3. Dynamic bimanual force trajectory task (already reported in [124]): in each trial, the user has to dynamically match a temporized force profile which was displayed on the screen. Indeed, the total force applied by the user is coded in the height of a white cursor that had to match the height of a red cursor, which is following the target force profile (F_y). The target force is shaped as an isosceles trapezoid. Indeed, the trial was divided in five sequential phases (Figure 4.4):

   (a) Rest (2 s): no force was required,

   (b) Increment phase (3.5 s): the force constantly increased from 0 to the maximum target force level, corresponded to the 10, 25 or 50% of MVF depending on the trial. In this phase, the cursor on the screen should move upward and rightward along one leg of the trapezoid.

   (c) Holding phases (7 s): the maximum target force level was required (notice that this phase in the following test is divided into two sequential phase of 3.5s, i.e.,

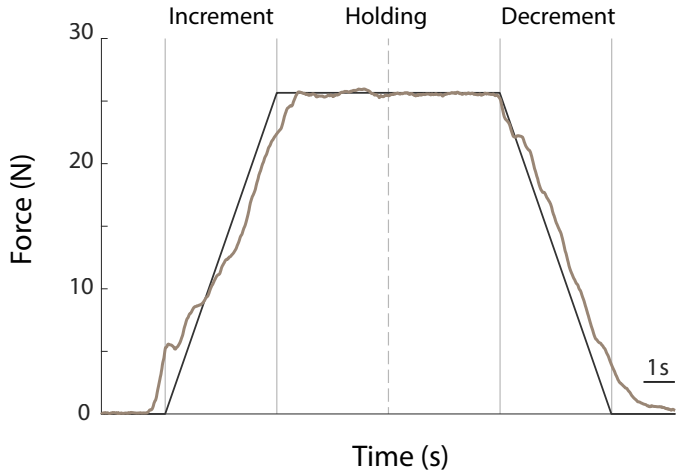

Figure 4.4 Example of dynamic bimanual force trajectory trial, with the target trajectory force (black) and the measured trajectory force (brown) for one target force level for one unimpaired participant. The trial is divided by vertical gray lines in the four phases used in the data analysis.

the same duration of the up and down phases). In this phase, the cursor on the screen should stay at the same height, moving rightward along the top side, i.e., the minor base of the trapezoid.

(d) Decrement phase (3.5 s): the force constantly decreased from the maximum target force level to 0. In this phase, the cursor on the screen should move downward and rightward along the other leg of the trapezoid.

(e) Rest (2 s): no force was required.

Each maximum target force is presented 7 times in random order, for a total of 21 trials.

4. Lifting task. In each trial, the user can handle the device in a manipulation task imposed by the experimenter, while the force applied on the lateral sides and the 3D position and orientation are saved. No visual feedback is displayed. The duration of each trial is decided by the experimenter according to the performance required. In our protocol, the participant performed a lifting task. In this task, the participants were asked to lift the device of approximately 30 cm height, holding there for 3 seconds and then bring the device back to the starting position, i.e., on the table. They repeated this task 21 times.

4.3.3 Data analysis

To evaluate the proprioceptive performance during the force matching tasks, we firstly identify the holding phase, i.e., the last 2.5 s for the coupled bimanual force matching task, as in [], and we focused only on that phase. In the dynamic bimanual force trajectory task, we divided the whole trial in 4 sequential phases: increment, holding divided in two parts to match the duration of the other phases (3.5 s), and decrement, and we analyzed the performance separately in all of that phases. For both the force matching tasks, we computed the same following metrics:

- Root-Mean-Square Error (RMSE) of the difference between the force applied by the participants and the target force [195], i.e., matching error. The RMSE measures the accuracy of the matching, i.e., higher values of RMSE indicate less accuracy. It is defined as in Eq. 4.1:

$$RMSE = \sqrt{\frac{\sum_{i=1}^{N}(F_M i - F_{Ti})^2}{N}} \tag{4.1}$$

  where: F_{Mi} is the measured force applied at the sample i, F_{Ti} is the corresponding target force, and N is the total number of samples considered.

- Bias Error (BE), i.e., the systematic component of the matching error. It is computed as the signed difference between the total force applied by the participants and the target force (see Eq. 1.1). Positive values indicate an overshoot, while negative values indicate an undershoot.

- Coefficient of variation, it is a measure of force variability of the force expressed as a percentage of the mean force [196], i.e., it is computed as the standard deviation of the total force after removing the best straight-fit line from the data (least-squares method, Matlab function detrend) divided by the total mean force applied.

For the lifting task, in stead, we divided each trial in 3 sequential phases: up, hold, down. To evaluate the performance, we computed the following metrics:

- Maximum total force, computed as the maximum applied on the device in each trial divided by the Maximum Voluntary Force of the participant recorded in the MVF task,

- Coefficient of variation of the force during the holding time, i.e., where the device was hold in the higher position,

- Difference in time between the onset of the movement and the onset of the force, computed at the first time that the force exceed the 10% of its peak velocity.

Statistical analysis

Our main goal was to evaluate if our device was able to detect differences in performance between the stroke survivors and the unimpaired participants in all the tasks.

As preliminary analysis, we verified if there was a difference between the maximum voluntary force applied by the two populations of participants, by using the Wilcoxon rank-sum test, since the data was not normally distributed according to Anderson-Darling test [103].

In the coupled bimanual force matching task, we wanted to compare the performance metrics between the two groups of participants taking into account also the target force level. To do so, we performed a mixed-design ANOVA with one within-subjects factors: 'target' (3 levels: '10', '25', and '50' % of MVF) and one between-subjects factors: population (2 levels: 'unimpaired participants', and 'stroke survivors'). For the dynamic bimanual force trajectory task, we wanted to compare the performance metrics between the two groups of participants taking into account also the target force level and the phase of the trial. To do so, we performed a mixed-design ANOVA with two within-subjects factors: 'target' (3 levels: '10', '25', and '50' % of MVF), and 'phase' (4 levels: 'increment', 'holding1','holding2', and 'decrement') and one between-subjects factors: population (2 levels: 'unimpaired participants', and 'stroke survivors'). Before running the two ANOVAs, we checked the normality of data using the Anderson-Darling test [103]. When the null hypothesis was rejected, the data was corrected by applying the fractional rank method [104]. we tested for the sphericity of the data using Mauchly's test and the Greenhouse-Geisser correction was applied when the assumption of sphericity was rejected.

For the lifting task, we evaluated the difference in performance between the two population of participant, performing the Wilcoxon rank-sum test, since the data was not normally distributed according to Anderson-Darling test [103].

Statistical significance was set at the family-wise error rate of α=0.05 and the Bonferroni correction for multiple comparisons was applied.

4.4 Results

There is no significant difference (p=0.186) between the MVF for unimpaired participants (mean $\pm$ std: 157.08 $\pm$ 31.43 N) and stroke survivors (139.47 $\pm$ 21.92).

Coupled bimanual force matching task

To evaluate if the bimanual performance stroke survivors during the coupled bimanual force matching task was affected, we compared the performance indicators (root-mean-square error, bias error, and coefficient of variation) computed in the holding phase of 2.5 s between the two group of participants (Fig. 4.5).

We found that the coefficient of variation of the force was significantly different between the two populations ($F_{1,18}$=7.94 p=0.011), with an higher variation for the stroke survivors. The errors between the force applied by the participants and the target force in term of RMSE was close to the significance threshold ($F_{1,18}$=4.35 p=0.051), while the bias error was not significantly different between them ($F_{1,18}$=0.01 p=0.973).

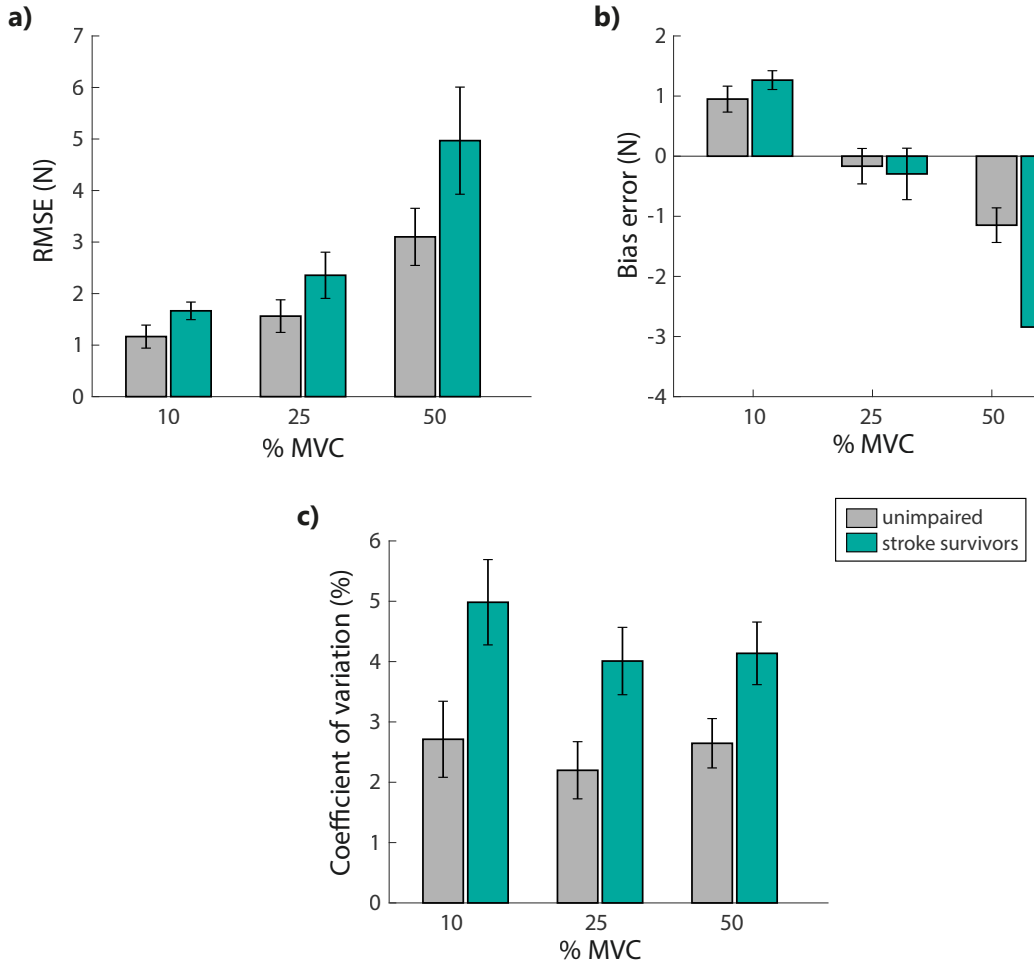

Figure 4.5 Performance indicator for the coupled bimanual force matching task. a) Root-Mean-Square Error, b) bias error, and c) coefficient of variation are reported separately for the three target force levels and the two populations. Bars and error-bars indicate mean and standard error.

With respect to the target force level, instead we found that the level of force required significantly affected the accuracy of the matching both in terms of RMSE and bias error (RMSE: $F_{2,36}$=24.96 p<0.001, BE: $F_{1.32,23.78}$=72.57 p< 0.001). However, the trend of those error is not significantly different for the two populations (target*population interaction: RMSE: $F_{2,36}$=0.05 p=0.955, BE: $F_{1.32,23.78}$=3.45 p=0.065). Indeed, both the groups of participants had higher errors when an higher target force was required. Also the coefficient of variation of the force applied during the holding phase, was affected by the level of force required ($F_{2,36}$=4.21 p=0.023), without a significantly difference between the two groups of participants (target*population interaction: $F_{2,36}$=0.59 p=0.559).

Dynamic bimanual force trajectory task

To evaluate if the bimanual performance stroke survivors during the dynamic bimanual force trajectory task was affected, we compared the performance indicators (root-mean-square error, bias error, and coefficient of variation) between the two group of participants. We also accounted for the level of force required and the phase of the task (Fig. 4.6).

We did not find any significant difference between the two populations in any metric computed (RMSE: $F_{1,18}$=0.40 p=0.845, BE: $F_{1,18}$=0.01 p=0.998, CV: $F_{1,18}$=0.36 p=0.555).

Instead, we found that the level of force required significantly affected the errors between the force applied by the participants and the target force (RMSE: $F_{2,36}$=159.04 p<0.001, BE: $F_{2,36}$=14.12 p<0.001), for all the participants (target*population interaction: RMSE: $F_{2,36}$=0.40 p=0.675, BE: $F_{2,36}$=0.40 p=0.998). Both the groups of participants had higher errors when an higher target force was required. Those metrics were also significantly different across the trial phases (RMSE: $F_{3,54}$=133.66 p<0.001, BE: $F_{1.97,35.46}$=74.41 p<0.001), with no difference between the two populations (phase*population interaction: RMSE: $F_{3,54}$=0.61 p=0.609, BE: $F_{1.97,35.46}$=0.09 p=0.910). Both groups had higher matching error in the increment and decrement phases than in the holding phase, i.e., when the force required incremented or decremented in time. Both groups of participants had also higher matching error for higher target force level. Furthermore, the bias error increased more for the decrement phase in relation to the force level required than the other phases (significant phase*target interaction: $F_{3.02,54.29}$=21.94 p<0.001). The RMSE, instead did not show this trend (phase*target interaction: $F_{3.84,9.06}$=1.53 p=0.206).

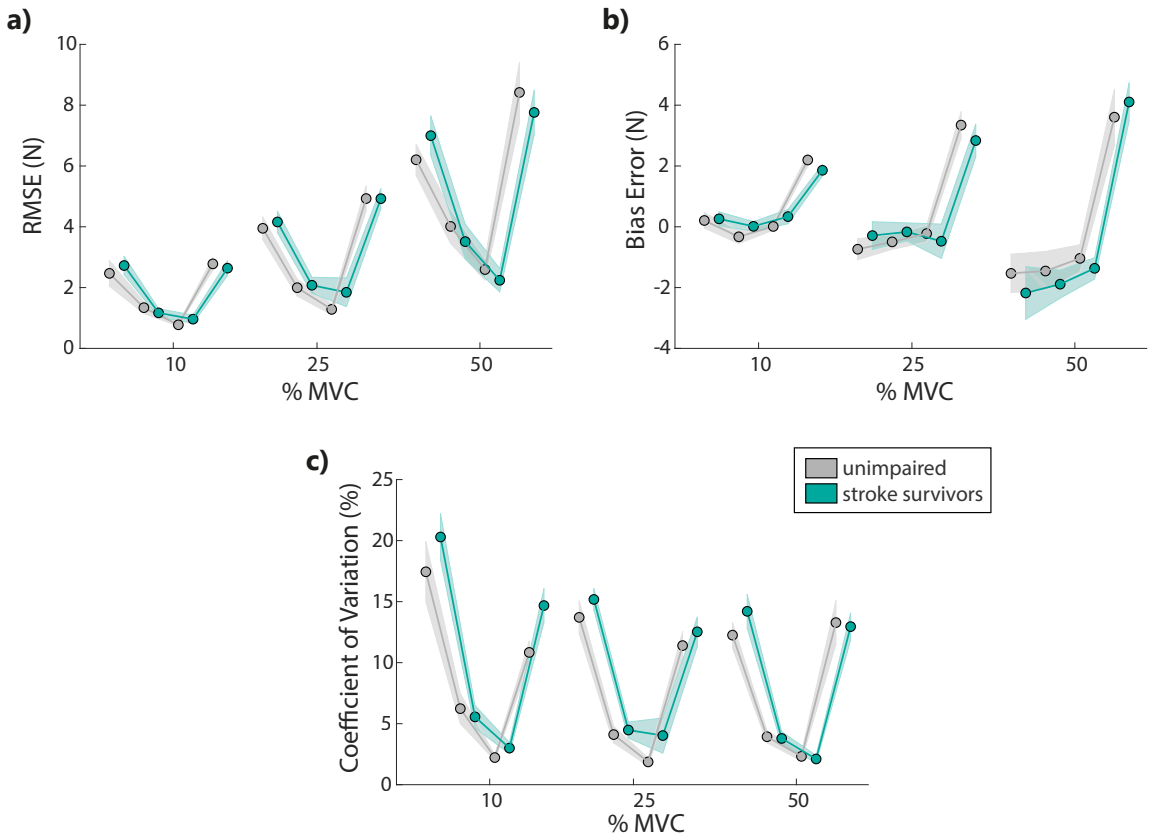

Figure 4.6 Performance indicator for the dynamic bimanual force trajectory task. a) Root-Mean-Square Error, b) bias error, and c) coefficient of variation, computed separately for the three target force levels, the four phases (increment, holding1, holding2, decrement) and the two populations. Dots and patches indicate mean and standard error.

The level of force required and the trial phase significantly affected also the variation of the force (target effect: $F_{2,36}$=8.78 p=0.001, phase effect: $F_{1.85,33.27}$=104.78 p<0.001) with a no significantly different trend between the two populations (target*population interaction: $F_{2,36}$=0.88 p=0.425, phase*population interaction: $F_{1.85,33.27}$=0.28 p=0.741). Indeed, both the effects were driven by the higher variability in the up and down phases, which were higher for higher target force levels (significant phase*target interaction: $F_{3.75,67.53}$=2.90 p=0.012).

Lifting task

To evaluate if in stroke survivors the performance during the lifting task was affected and to characterize them, we compared the performance indicators between the two populations, i.e., difference between the force and the movement onset time, coefficient of variation during the

holding phase in the higher position, and the maximum force applied in the trial normalized for the MVF (Fig. 4.7).

We found that neither the difference in time between the onset of the movement and the force nor the coefficient of force variation during the holding were significantly different between the two populations (both p>0.23). Instead, we found that the maximum total force applied in the trial was significantly higher for the stroke survivors (p=0.016). This population trend is in accordance to the example of trajectory reported in Fig. 4.7a. Furthermore, there we reported an example of force and elevation profiles acquired during a trial for one stroke survivors (right) and an age-matched unimpaired participant (left). There, we can notice that the stroke survivors applied more force than the corresponding control subject to lift the same device.

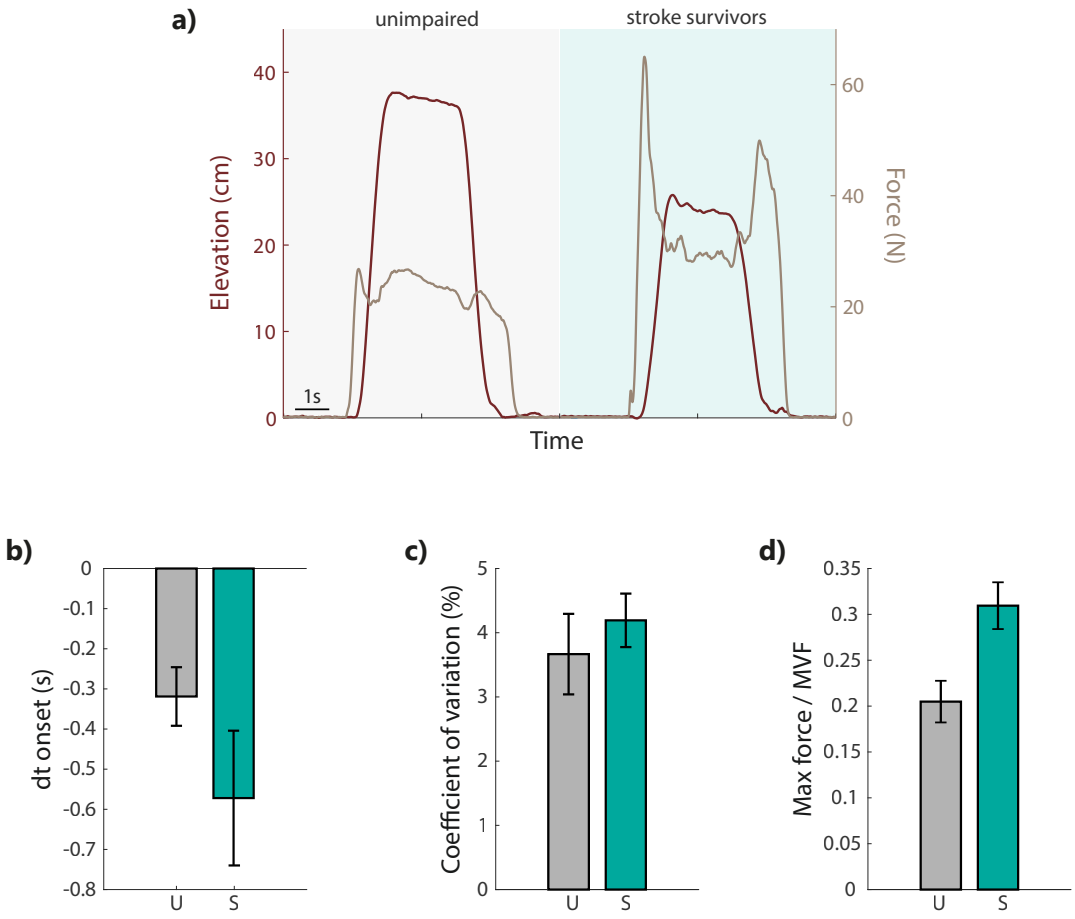

Figure 4.7 a) Example of total force and elevation profiles acquired during a trial of the lifting task for a unimpaired participant (left) and a stroke survivor (right). b) difference between the force and the movement onset time, b) coefficient of variation during the holding phase in the higher position, and c) the maximum force applied in the trial normalized for the MVF. Bars and error-bars indicate population mean and standard error.

4.5 Discussion

In this study, we re-design and develop a device able to directly measure the force applied on it and concurrently its position and orientation in the space even during long-time recording without suffering of the drift typical of IMUs [193]. This allow the experimenter to design bimanual functional evaluation of the participants' ability during the object manipulation. Furthermore, the device is designed to provide online feedback to both the experimenter and the participants, making the device suitable for bimanual training. We also implemented a set of additional tools that can be easily coupled to the device: (1) a base support, which fix the device in a stable position and allow the the device to be used for uncoupled bimanual tasks while measuring the force applied on each side, (2) a trigger-box that could synchronize the acquisition of physiological signals, such as EMG or EEG, with the task execution, allowing a more complete assessment of the proprioception and characterization of the physio-pathology of the disease and progress of the rehabilitation.

The device is also provided with a GUI that allow the experimenter to customize the experimental protocol. For example, the experimenter could choose the order and the tasks that the participants has to perform and the pause within and between the different tasks. Furthermore, at the current stage the experimenter can choose between four different task designed in collaboration with a team of physiotherapists, which could be performed in uni or bi-manual condition and coupled or uncoupled configuration. The chosen tasks allows the characterization of different proprioceptive abilities: (1) the maximum force that the participants are able to exert by pushing on the lateral sides of the device, which can be performed in different visual feedback conditions; (2) the ability to match a required target force and maintain it; (3) the ability to adapt the force to match a target force level that is constantly increasing, decreasing and fixed; (4) the interaction between the force applied on the device and its position in the space during the free manipulation of device.

We tested the device on stroke survivors and unimpaired participants as proof of concept of the potentialities of the device to assess proprioception during the various bimanual tasks in coupled configuration.

In the coupled bimanual force matching task, i.e., where we evaluated the ability to match a required target force and maintain it, we found that stroke survivors had higher difficulty to match the level of force required, even if it was tailored on their ability. Indeed, for all the participants, the matching error depended on the level of force required, as already shown in other similar task [Chapter 2], [68]. Indeed, looking at the sign of the error, all the

participants overshot the lower level of force (10% MVF), while undershot the higher level of force (50% MVF). Interestingly for the middle target force (i.e., 25% MVF: 39.27 $\pm$ 7.86 N - mean $\pm$ std - for unimpaired participants, and 35.21 $\pm$ 5.48 N for stroke survivors), the bias error is close to zero for both the populations. In addition, we also found that stroke survivors had greater variability in the force exerted. This is in line with previous studied on position matching tasks in stroke survivors [152, 153], [Chapter 3] and also in bimanual force matching task in people with Multiple Sclerosis [197], however to the best of our knowledge, this assessment on force matching task in stroke survivors was not performed before.

In the dynamic bimanual force trajectory task, we evaluated the ability to adapt the force to match a target force level that is constantly increasing, decreasing and kept constant in four separate phases of each trial. There, we found that the target and the phase of the trial (i.e., the profile of the target force to match) significantly affect the matching ability of the two populations, both in term of matching errors and force variability. Furthermore, the RMSE and the force variability are higher in the increment and decrement phases, where the participants are required to match a force that is changing in time, while are lower for the holding phase. Indeed, looking at the sign of the matching error, all the participants overshot the decrement phase indipendently on the level of force required. Conversely, in the increment phase, they tended to undershot more when the force required is higher. Interestingly, in this task we did not find any difference between unimpaired participants and stroke survivors neither in terms of matching errors, nor in the coefficient of variation of the force. This lack of significance could be related to the age of the participants, since it is well known in literature there is a deterioration of the proprioceptive mechanisms with age [65, 163, 164], which could be related to the effects of the age on the number of cutaneous mechanoreceptors [198] and the brain volume loss [199]. However, further analysis are needed to deeply investigate this hypothesis.

In the lifting task, we assessed the interaction between the force applied on the device and its position in the space during a lifting and holding task when the the action of one limb affects the dynamic of the other. There, we found the stroke survivors applied more force than age-matched unimpaired participants to lift the device. However, the timing in which the force was applied and its variability during the holding phase were no significantly different between the two populations.

Taken all together our preliminary findings suggested that our device is a potential useful device to assess proscription in various bimanual tasks in people with sensorimotor deficits and limited range of motion. Giving online feedback about the performance, i.e., the force applied by each arm, the device position and orientation, it could also be used as training

device to enhance proprioception and used to monitor the change in time of the participants abilities.

Limitations

The small number of research participants, limits the possibility to draw a general conclusion. To overcome this limitation, we are planning to collect data from more stroke survivors as well as age-matched unimpaired participants. Further investigation should be also include younger participants to investigate if there is an effect of age on the performance during those tasks as shown in other tasks [65]. Another important factor that has to be taken into account in future analysis is the time after stroke, since it is well known that also the recovery stage after stroke affect both the sensory and motor abilities in both arms [115].

Part III

How to encode information in supplementary somatosensory feedback to enhance proprioception and motor performance

Chapter 5

Introduction to supplementary somatosensory feedback

Part of this chapter has been published in: Handelzalts S., Ballardini G., Avraham C., Pagano M., Casadio M., Nisky I. *'Towards the integration of somatosensory augmentation technologies into home-based neurorehabilitation: opportunities and challenges in light of COVID-19 pandemic'*, Frontiers in Neurorobotics 15:4 (2021). doi.org/10.3389/fnbot.2021.617636

Introduction

Somatosensory impairment is considered to have a negative prognostic impact on rehabilitation interventions and overall motor function recovery [200–202]. Not only proprioceptive deficits interfere with motor learning, but people with proprioceptive impairments also have sub-optimal functional recovery [7, 4] and move by relying on visual feedback, which come with delays of 100-200 ms [7], leading to movements that are typically slow, jerky, poorly-coordinated, and require great concentration [3, 5, 6]. A possible solution to mitigate the impact of those problems is improve somatosensory abilities and control [203] providing supplementary somatosensory feedback.

Supplementary feedback provides additional cues that complement and/or replace native sensory input from the somatosensory, visual, and/or vestibular systems [204]. It has been shown promising in providing guidance to improve movements (re)learning [42, 43, 205–208]. In this case, the supplementary feedback can be triggered by the participant's performance or can provide information continuously during the action [39, 40]. Compared with visual feedback, online tactile feedback allow to convey information without the need to shift visual attention, thus affording a more ecological movement [205]. It is used also

in virtual reality environments to increase the realism of the interaction [26, 209] and make it more engaging, enjoyable and motivating [210]. Somatosensory feedback also plays a critical role in emotional and social communication [211, 212], e.g., to enhance remote communication for reinvigorating the user's interest during practice [213] or to render realistic feelings such as comfort, affection [214, 215], attention [216], or social presence [217].

For those reasons, over the last few decades, technologies that can provide tactile feedback have become very popular and many new devices continue to be developed. From the technological point of view, there is a variety of ways to apply tactile stimulation. These can be categorized according to the mechanism evoking the tactile sensation: electrotactile, thermal and mechanical. After a brief introduction of all type of tactile feedback, I will focus on the mechanical stimulations.

5.1 Electrotactile stimulation

Electrotactile stimulation uses surface electrodes to directly activate sensory nerves under the skin by passing an electrical current through the skin [218, 219]. The evoked sensation is affected by many factors, such as: (i) the number and configuration of the electrodes [220], (ii) the property of the stimuli (e.g., voltage, current, repetition rate), (iii) the body location and the property of the skin (e.g, skin impedance and resistance [221, 222, 35]), (iv) the contact conditions (e.g., sweat and motion that induces temporal changes [223]. In rehabilitation electrical stimulation is also used to as neuromuscular stimulation. There, short duration electrical pulses are applied on the skin targeting peripheral muscle nerves. The stimulation induces a depolarization of peripheral neurons and subsequently elicits muscle contractions also in paralyzed or paretic muscles. This technique is termed also functional electrical stimulation.

Advantages and Disadvantages

A drawback of this type of stimulation is that the absolute threshold for electrotactile stimulation is quite close to the pain threshold, some solutions are proposed to increase the difference between them [224–226], but it is always an important point to take in account. Also, there is an high-variability in the perceived sensation. On the other hand, the device for the electrotactile feedback can be very small in size, energy efficient and free from mechanical resonance [223].

5.2 Thermal stimulation

Changes in temperature are detected by thermoreceptors place in the dermis, which have free, non-specialized, nerve endings [227]. In general, thermoreceptors could be separated into receptors for cold and warmth detection [227]. The human skin rests in a 'neutral' homeostatic thermal state, where both types of receptor are spontaneously active, and there is no awareness of cold or warmth [228]. The size of this zone is around 6-8°C and it is relatively constant across individuals, but the position of each individual's neutral zone varies. Detection of changes within this range is dependent more on the rate of change of the stimulus than the actual extent of the change [229], e.g. fast changes are felt stronger and sooner than slow changes. Outside of this range, the detection of temperature changes is more related on how far the stimulus is from neutrality, i.e., humans are more sensitive to changes farther from neutrality towards the pain threshold [229]. The technological solution to convey thermal stimuli is mainly based on Peltier heat pump [36, 230, 231]. It is thermoelectric cooler, i.e., solid-state heat pump, which operate according to the Peltier effect to create heat flux at the interface between the two electrical junctions.

Advantages and Disadvantages

Thermal stimulation is an ecological stimulus with strong link to social and emotional phenomena, and alarm signals. Thermal perception can be highly precise, e.g., experts are able to detect changes less than 0.2°C in ideal laboratory conditions [232]. However, the skin has poor spatial resolution compared to mechanical stimuli [233].

5.3 Mechanical stimulation

Mechanical tactile stimulations can be further divided into: vibration, skin deformation, and mid-air stimulations. Recently, the idea of wearable tactile devices that combine vibration, stretch, and pressure for conveying multimodal haptic information was introduced [234–236], highlighting the importance of understanding the unique properties of each stimulation type and harnessing the advantages of each to design devices that are more than the sum of their parts.

5.3.1 Vibration

Vibration is the simplest and most common tactile stimulation technology that has become ubiquitous and is used in a wide variety of devices such as phones, watches, games, and home appliances [26]. Typically, the actuators used in wearable devices produce vibration at frequencies above 100 Hz, which activates the Pacinian corpuscles mechanoreceptors [26]. The most common locations for applying the vibrotactile stimulation are the arm [42, 43, 208, 237] and the torso [238, 239]. Other locations include the hand [240, 241] and different locations on the lower limb [242]. The design of the device and the stimulation patterns (e.g., frequency and amplitude of the vibration) need to take into account the targeted dermatomes and the density and size of the mechanoreceptors' receptive fields which vary across the body [2, 243, 244] and across the skin type (e.g., hairy skin has a reduced number of Pacinian corpuscles compared to glabrous skin [245, 246]. Skin type can also influence the quality of stimulation via its mechanical properties and its physical propagation of the vibration [247, 248].

Vibrotactile feedback can be conveyed by a single actuator, or by an array of actuators that create an oscillating movement. The choice of the actuator affects the size, shape, cost, availability, robustness, speed of response, input requirements, and power consumption of the device [249, 250].

The stimulation patterns can be divided into two fundamental categories: (i) binary on-off state, which is triggered by specific events such as an alarm or event-cue related information [39, 40], and its intensity can be constant or vary according to the events [41]; (ii) continuous vibration, created by changing parameters of the vibration signals such as amplitude, frequency, duration, rhythm, and waveform [44, 243]. It is used to convey various types of information to the users, including: (1) state feedback, encoding position and/or velocity of limbs [42, 43, 208, 39], (2) force feedback, encoding the amount of force exerted [251], and (3) error feedback, encoding information regarding the goal of the task and the state of the end-effector [42, 252, 253].

By controlling the shape and timing of the signals from multiple static actuators, it is also possible to display illusions of movement that can enrich the design space of tactile stimulation. Prominent examples are: (1) phi (or beta) movement, where a smooth apparent motion of a single stimulus is created by the periodic activation of two spatially separated stimuli [254, 255], (2) saltatory (or rabbit) illusion, i.e., illusory sweeping movement of discrete taps that occur by activating actuators in sequence [255, 256], and (3) the tendons vibration illusion, which is an illusory perception of movement that can be evoked by triggering the muscle spindle afferents through vibrations applied to the tendon [257, 258].

Advantages and Disadvantages

A major advantage of vibrotactile devices is that the actuators can be easily integrated into wearable devices because they are small, lightweight, low-power, and low-cost [259]. On the other hand, disadvantages of vibrotactile feedback stem from the properties of the mechanoreceptors activated by vibration. (i) it is difficult to accurately locate the source of the stimulations if they are placed close together, because of the propagation of the vibration [244, 260] and the large size of the mechanoreceptors' receptive fields [261]; (ii) it is difficult to convey directional information, unless several actuators are used in a spatially and/or temporally coordinated mode [262]; (iii) its effects depend on hoe the information is coded in the feedback, e.g., if the vibration frequency or location varies, vibrotactile feedback may be less effective in conveying information than a uniform signal that alerts the user of a required response [263]; (iv) prolonged exposure to continuous vibratory stimulation could result in an unpleasant sensation [237] and has been associated with long-term nerve and tissue damage [264]; (v) choosing the right type, number, and target location of the actuators for patients with possible degradation of perception due to aging or disease might be challenging [243].

5.3.2 Pressure

Pressure stimulus triggers a response in the low frequency range of the slow adapting afferents SA-I, innervating the Merkel cells [2]. Technologies that provide this type of feedback deliver forces that cause deformation, and the strength of the stimulus is determined based on sensitivity thresholds, which vary across the body.

Pressure stimulation is commonly provided by devices that contact the skin with a single end-effector that can: (i) change its properties, such as the shape in soft actuators [38] or the viscosity in electrorheological or magnetorheological fluids [265–268], (ii) tighten a band around a body location, like the fingertip [269], wrist [270] or forearm [271], or (iii) press on the skin with a servomotor [272, 273], a hydraulic, or pneumatic actuator [274–276]. For the latter solution, it is also possible to enlarge the area of stimulation by increasing the number of end-effectors in contact with the skin using a pin array matrix, i.e., a matrix of actuators that can be activated separately. In order to provide efficient tactile stimulation it is also important to consider the size and density of the contact points, since these will affect the cost and weight of the device, as well as its perceptual effect.

Advantages and Disadvantages

Pressure stimulation enables rendering perceptual properties such as shape, curvature, orientation, and texture [277]. However, sensitivity to pressure is largely dependent on the area of stimulation [232]. In addition, while multiple actuation approaches are available for applying pressure to the skin, each approach is suitable for a different application. Therefore, the desired application should be considered in the specifications of the stimulation and device.

5.3.3 Mid-air

All the technologies described above require physical contact between the device and the body to provide somatosensory feedback, and the energy produced by the actuators is transferred to the skin through a solid medium. This allows efficient energy transduction, creating natural haptic sensations with the aid of appropriate contactors to the skin. However, these solutions present some limitations: (i) they do not exploit arbitrary body locations, i.e., can deliver feedback only at a location close to the device's end effector, (ii) they may cause undesired effects due to the continuous contact between the skin and the devices. Several recent developments address these limitations by proposing mid-air technologies. They transmit the energy of the stimulus through air, avoiding the direct contact with the skin.

Ultrasound

One of the main approaches to creating mid-air stimulation relies on ultrasonic waves, typically at 40 or 70 kHz frequencies (for survey see [37]. In this type of mid-air tactile stimulation the sensation is caused by a non-linear effect of focused ultrasound called acoustic radiation force, which induces a shear wave in the skin, creating a displacement, which triggers the mechanoreceptors within the skin and evoking mainly a pressure sensation [278]. Most ultrasound haptic systems targeting the hand trigger the Lamellar corpuscles [37]. In other body locations ultrasound can trigger other mechanoreceptors, such as Meissner corpuscles on the face [279], and Ruffini corpuscles or Merkel disks on the upper limb [280].

The most widely used technological solution to evoke tactile sensation with ultrasound is based on phased arrays of transducers, i.e., multiple transducers whose phase and intensity can be controlled individually, with a defined timing. In this way, the focused ultrasound waves can generate one or more localized regions of pressure in the 3D space, called focal points, without moving or turning the device. These focal points cannot be fully singular because of secondary peaks and wavelength limitations [37]. However, several focal points can be controlled together to create shapes [281] or textures [282, 283]. If the radiation force

is modulated at the 1–1 kHz range the ultrasound waves can also evoke a vibratory sensation in addition to the pressure sensation [284–286].

Advantages and Disadvantages

They can easily and efficiently create static or dynamic textures and volumetric shapes perceived by mechanoreceptors in the skin. However, in its current state, this technology has some inherent limitations that may have an impact on potential applications, including the size and the weight of the transducers [37] and the low intensity of the force conveyed to the user, e.g., with ultrasound it is at most 160 mN [287], and so does not allow the rendering of real-word interaction forces.

Air-jet

The air-jet tactile feedback can be created using two main methods: (i) direct compress's air through focused nozzles, which is utilized by connecting a tank of pressurized air through valves to focused outputs; and (ii) vortex based tactile actuation technology, which uses air vortices by controlling the pressure difference between the nozzle and the outside medium [288]. They are is used to realize mid-air display usually to convey non-contact force feedback which can be perceived directly by the mechanoreceptors in the skin [289–291] or mediated by an air receiver, such as a shallow cup [292], or a flexible sheet driven by the jet [293].

Advantages and Disadvantages

The air-jet method is a straightforward implementation and can give relatively acceptable force feedback [294]. However, due to the physical properties of air, their spatial and temporal properties are quite limited and they cannot provide detailed tactile feedback [295]. The reachable distance of an air jet is determined by the diameter and the velocity of the jet stream, which results in the trade-off between the spatial resolution of the pressure on the skin and the distance from the device to the skin [25].

Laser

The laser can be used as stimulation for mid-air display thanks to its ability to create mechanical waves on a biological tissue. Laser-induced stress waves are elastic waves created by the absorption of electromagnetic waves in the medium. They are generated by several mechanisms, such as:

- Laser-induced optical breakdown. Because the electric field strength of typical laser pulses is very high, the surface of an irradiated medium is susceptible to ionization and subsequent plasma formation. The high-temperature and high-pressure plasma expands rapidly, causing stress waves to propagate into the bulk medium in the form of shock waves. This mechanism, also known as photodisruption is used in medical applications, specifically lens fragmentation and lithotripsy. In [296, 297], they used femtposecond laser pulses to create optical breakdown and render aerial and volumetric graphics.

- Thermoelastic effect. An light-absorbing elastic medium (like human skin) can be heated locally by the instantaneous absorption of a short laser pulse. The temperature, and thereby the local pressure, of the heated region increases immediately, leading to a non-uniform distribution of the temperature in the tissue. As the elastic medium transitions into a new equilibrium state, stress waves are generated and propagate into the medium. Two types of photo-effects are involved according to the energy level and increasing rate of temperature: (i) photo-thermal effect, where the absorbed heat energy is enough to cause tissue coagulation or ablation; and (ii) photo-mechanical effect, where the localized instantaneous heating of tissue due to the energy absorption induces rapid a thermoelastic deformation (i.e. volume expansion). Before reaching a new equilibrium state, transient elastic (stress and strain) waves with a life time of microseconds are created and propagate into the tissue at a sound speed of about 1.5 km/s. Those waves making a mechanical displacement in the tissue and could activate mechanoreceptors. Note that it is strain (or equivalently displacement), not stress, that directly causes the physical sensations, if any. When the transient elastic waves disappear, the quasi-steady state is reached. It is followed by thermal diffusion, in which the heated region cools off over a longer period of time in the order of milliseconds, and the thermoelastic stresses eventually decay to zero. The detailed elastic dynamics during this thermal diffusion process depends on the transient behavior of the temperature distribution. However, exploratory studies [298, 299] reported that the evoked stimulus is perceived to be similar to a mechanical stimuli or touch. Such laser-induced thermoelastic effect can be nondestructive whereas laser-induced optical breakdown inevitably damage the medium. It is dominant in a linear-interaction regime with low-power radiation having a pulse width of a few nanoseconds. The detailed elastic dynamics during this thermal diffusion process depends on the transient behavior of the temperature distribution. However, exploratory studies [298, 299]

reported that the evoked stimulus is perceived to be similar to a mechanical stimuli or touch.

Advantages and Disadvantages

Compared to the air-jets and ultrasound technologies, laser can be focused on more thigh spot even across a long distance and have an extremely long transmission distance, since the energy can be transmitted with very small diffusion and attenuation [298, 300]. One main limitation of this technology is the need to use very high-cost laser devices. Another limitation is the high variability in the evoked sensation, mainly due to the inhomogeneity of the optical and mechanical properties in the human skin [298]. A possible solution to this limitation is to use indirect radiation, i.e., posing an elastic medium between the laser stimulator and the skin [300, 301].

5.4 How to design an effective supplementary somatosensory feedback

To convey effective tactile stimulations it is critical to identify the optimal method to provide the feedback. It might be difficult to interpret and integrate especially for people with neurodegenerative disease or who had traumatic event like stroke. Also, the tactile stimuli patterns might not be intuitive or might be too complex for the user, due to either the number of actuators forcing the user to process a redundant set of signals, or to the encoding methods that may require specific attention [44]. This is especially important for people undergoing rehabilitation training, who are often at the initial stages of learning that already require a relatively high degree of cognitive effort and attention [302]. Moreover, some neurological patients suffer from cognitive and attention deficits, and hence, to benefit from added information, the feedback must be simple [303]. Additionally, the cognitive load of interpreting tactile cues in applications where the patient's attention is divided among multiple tasks, and how this might reduce the saliency of the cues, should be further explored [208, 304].

Also, the optimal timing of providing somatosensory feedback also needs to be examined. For example, providing feedback for the entire duration of training can improve short term performance, but may limit motor learning. Conversely, providing feedback for only portions of training might produce poor initial performance, but improve motor skill retention [305]. Moreover, the conditions under which tactile feedback is most effective at improving task

performance should be examined (e.g., whether it is most effective when supplementing another modality), as well as the temporal and spatial patterns and the location for applying the stimulation.

Supplementary somatosensory stimulation can be beneficial even if it does not provide any information. For instance, subthreshold tactile stimulations (i.e., below the level at which a person can perceive the stimulation) add noise to proprioceptive signals and might help these signals to overcome the threshold of specific neural circuits. This phenomenon, also known as the stochastic resonance theory [306–308], which has been shown to facilitate more efficient detection of somatosensory information, and improve sensorimotor performance [309, 310]. As such, it could be used in the rehabilitation treatments of individuals with sensorimotor deficits to improve motor functions (e.g., grasp, object manipulation, balance and gait) and tactile sensation [311, 312].

To design an supplementary feedback to effectively enhance the motor performance and (re) learning, it is essential to understand the importance of the informational content in the stimulation and how to encode it in the somatosensory feedback. Therefore, for supplemental auditory or visual feedback has been demonstrated that linear and logarithmic mapping have different effects on the postural sway [313]. Despite their importance, those aspects in supplementary somatosensory feedback are not well investigated. I am filled this gap evaluating the effect of different encoding methods on motor performance in unimpaired participants and stroke survivors.

Chapter 6

Study I: Vibrotactile feedback for improving standing balance in unimpaired participants

This study has been published in: Ballardini G., Florio V., Canessa A., Carlini G., Morasso P., Casadio M. *'Vibrotactile feedback for improving standing balance'*, Frontiers in Bioengineering and Biotechnology (2020). doi:10.3389/fbioe.2020.00094

6.1 Introduction

Postural control is a complex sensorimotor skill with two main functions: stabilizing balance and maintaining the relative position of body segments [314, 315]. It requires the interaction of the sensory, muscular, and nervous systems [316]. In particular, the central nervous system must process and integrate concurrent feedback from the vestibular, somatosensory, and visual sensory channels [316, 317]. Each sensory system contributes differently to postural control; thus the impairment of a specific sense has different impacts on balance. For example, during quiet standing, the postural sway increases more when somatosensory information is unavailable than in absence of the vestibular or visual information [318–320]. However, the contribution of feedback from different modalities is known to be additive, thus it seems worth investigating to what extent providing an additional channel may further improve balance and/or compensate for balance deficits in pathological conditions. Several studies suggest indeed that, in presence of sensory deficits, providing supplemental sensory

information to the central nervous system might improve postural stability, decreasing the postural sway and even the risk of falling [252, 321–323].

For those reasons, many research groups have developed devices able to provide supplemental information through supplementary somatosensory feedback, such as vibrotactile [238, 239, 259, 323–325], or electrotactile [326, 327]. However, the feedback provided by the most common vibrotactile devices resulted difficult to interpret and integrate into the neural control [26]. One reason is that the patterns of somatosensory stimuli are not intuitive or complex, due to either the number of vibration motors, thus forcing the user to process a redundant set of signals, or to the encoding methods that may require specific attention [44].

While from the technological point of view there are several solutions for providing supplemental vibrotactile feedback, which information is more effective to reduce the postural sway and how to encode it has received less attention. For example, there is evidence that humans modify their postural sway [328, 329] in presence of vibrotactile feedback, encoding velocity and/or position of the body center of mass or the center of pressure. However, other studies have shown that also the stochastic resonance resulted in a reduction of the postural sway in elderly people [330, 331] and in people affected by vestibular impairments [267].

We designed and built a portable, low-weight, and low-cost device to provide vibrotactile feedback to improve standing balance. We used only two vibration motors placed on the opposite sides of the torso (abdomen and back) at the L5 level, namely in the CoM area. The idea was to activate them as a function of the actual sway evaluated from the accelerometric signal. As explained below the implemented system encoded in the vibrotactile feedback a combination of position and acceleration of the CoM in the sagittal plane. The main goal was to evaluate the extent to which such additional sensory feedback could reduce the sway amplitude. If the previous evaluation was positive, we also planned to test three related hypotheses about the improvements: (i) the changes depend on the time profile of the vibrotactile stimulation, comparing a continuous stimulation paradigm with a paradigm that included a dead zone (with vibration silent) around the natural stance posture. The dead zone paradigm would be preferable for prolonged use of the vibrotactile feedback, because it reduces the exposure to the stimuli, avoiding the sensory overload of the user [332]. To the best of our knowledge, this hypothesis has been tested only for auditory feedback. (ii) The changes depend on the informational content of the feedback i.e., they are not a mere effect of the vibration. In cases where feedback about postural oscillations is provided by only two vibrators, the fact that the informational content and not the vibration per se determine changes on the postural oscillations was not extensively verified by previous studies. (iii) The proposed vibrotactile feedback does not induce after effects, i.e., when the vibration is

turned off the participants recovered their normal oscillations patterns, without any influence of the previously experienced vibration. This is an important point that deserves extensive investigation, however, it has received scarce attention in the literature and with this study, we partially filled the gap.

To verify these hypotheses, we asked young healthy participants to stand upright with their eyes closed on a rigid horizontal surface wearing the device that included vibration motors and an accelerometer sensor. The acceleration profiles were analyzed, correlating them with the two different stimulation modalities.

6.2 Material and methods

6.2.1 Device

We designed a portable device that provides supplemental vibrotactile feedback synchronized with an accelerometric signal encoding information about the CoM position and acceleration. The device weighs 400 g and consists of three main components: (a) an input and recording unit, based on an Inertial Measurement Unit (IMU) sensor, (b) a processing unit, and (c) a vibrotactile output unit (Fig. 6.1).

Input and recording unit

The acceleration vector of the CoM is measured by means of the three-axis IMU (BST-BNO055-DS000-12, Bosch Sensortec GmbH, sensitivity = 0.2 mV = 1.2 mm/s^2; non-linearity = 0.5 % FS, bandwidth = 62.5 Hz), firmly attached to the participants' back at the L3 level, which approximately corresponds to the CoM position during quiet standing. The accelerometer gain was set in such a way to have a measurement in the range of 2g, appropriate for measuring the small acceleration caused by postural adjustments. The IMU was positioned as in [333, 334], with one of the accelerometer's axes aligned in the Anterior-Posterior (AP) direction, a second axis in the Medial-Lateral (ML) direction, and the third in the vertical direction. Thus, in correspondence with the natural equilibrium posture of each participant, the measurement signal in the AP direction has a null mean value, unaffected by any gravity component. In contrast, this component is not negligible when the body sways forward or backward with respect to the reference position, with an additional gravity component related to the tilt angle. As a consequence, the measurement signal in the accelerometer's AP direction is a combination of the CoM acceleration and the CoM position in the AP direction. The raw signal measured along the AP axis of the IMU is used

as input for controlling the vibration unit (see section 6.2.1) and thus the control signal used in this study encodes a combination of:

- the component of the CoM angular acceleration along the accelerometer's AP direction, characterized by high-frequency component;
- the projection of the gravity vector along the accelerometer's AP direction, related to the CoM position; thus, characterized by a lower frequency component.

Notice that the AP direction is considered with respect to the participants' body, thus is not parallel to the floor.

The processing unit

This unit is based on a microprocessor (WiPy 2.0, Pycom) which received as input the data provided by the IMU, computed the control parameters according to the control paradigms explained in the following section, and sent the command signals to the two vibration motors. A custom-made printed circuit board connected the WiPy with the IMU and the vibration motors. The WiPy had also an ESP32 expansion board, which provided the connection to the battery (lithium-ion battery: 1 S, 1200 mAh) and a MicroSD where were stored the accelerometric signals along the three axes. All the components of the processing unity were enclosed in a 14.5 x 7.5 x 4.5 mm module. The microprocessor communicated via WiFi with a laptop. The software of the WiPy was developed with MicroPython (Pymakr plug-in provided by Pycom).

Vibrotactile output unit

The AP acceleration of the CoM modulated the amplitude and frequency of the vibration provided by two micro-motors with integrated eccentric rotating mass (Pico Vibe 10 mm vibration motors; Precision Microdrives Inc, Model 310-117). Each vibration motor had an operational frequency range of 50 to 250 Hz and a peak vibrational amplitude of 2.6g. We attached the vibration motors on the back and the abdomen of the participant, at the L5 level, i.e., distant enough from the IMU (located back at the L3 level) in order to avoid interference [244]. The vibration frequency f (in Hz) of each motor was computed, as a function of the control variable a, through a second order polynomial rule:

$$f = c_1 \cdot |a|^2 + c_1 \cdot |a| + c_3 \tag{6.1}$$

where the coefficients (c_1=-212.66, c_2=293.34 and c_3=150.21) were set based on:

- the minimum level of activation of these vibration motors [42];
- the Just Noticeable Difference (JND) for this stimulus, computed according to [244, 335].

The control variable 'a' was related to the AP component of the accelerometric measurement (m/s^2) as explained in the following section.

Eq. 6.1 takes into account two components: (i) a linear relationship between the activation voltage and the acceleration signal and (ii) a second-order polynomial relationship between the activation voltage and the vibration frequency. The frequency and amplitude of the vibration are coupled: the frequency of vibration in Hz is roughly 100 times the amplitude in g and their relationship is linear in the range of activation [42]. Thus, controlling the frequency as in Eq. 6.1 implies also a change of the vibration amplitude. For simplicity, in the following, we refer to changes in intensity (its amplitude and frequency of the vibration) of the vibration and we express it only in terms of frequency. The reason for choosing this kind of coupled vibration motor was twofold: they are inexpensive and the vibration feedback is more effective when frequency and amplitude are coupled [336].

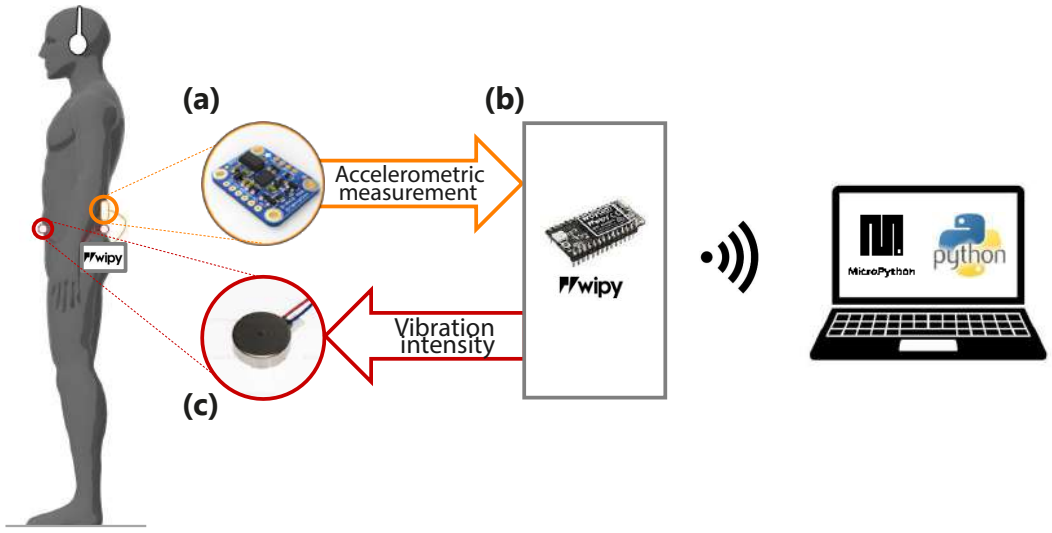

Figure 6.1 Experimental set-up. The participant was asked to stand still in the standing position, wearing headphones and our portable device composed by: (a) a sensor (IMU) placed on the back at L3 level; (b) the microprocessor unity connected to the PC via Wi-Fi; (c) two vibration motors attached to the skin of the participant: on the back and on the abdomen at L5 level. The IMU recorded the accelerometric signal and sent it to a microprocessor (WiPy) that saved them on a microSD card. The accelerometric measurement was used for controlling the vibration motors.

6.2.2 Vibrotactile feedback control

We investigated three different methods of synchronization between the vibrotactile feedback and the accelerometric signals, namely three different encoding methods of the body sway: Always On (AO), Dead Zone (DZ), and Sham (S).

More specifically, in the AO method the participants continuously felt the vibration, i.e. one of the two vibration motors was always active as explained by the following activation rule, where c_1, c_2, and c_3 are the same coefficients of Eq. 6.1:

$$\begin{cases} f_{v1} = c_1 \cdot |a_{AP}|^2 + c_2 \cdot |a_{AP}| + C_3 & f_{v2} = 0 & a_{AP} < 0 \\ f_{v1} = 0 & f_{v2} = c_1 \cdot |a_{AP}|^2 + c_2 \cdot |a_{AP}| + C_3 & a_{AP} \geq 0 \end{cases} \tag{6.2}$$

The DZ method is similar to the AO method, with the difference that vibrotactile feedback is turned off in a small region around the natural stance posture, namely if the accelerometric signal falls below a given threshold Thr. Thus the activation rule is expressed by the following equation:

$$\begin{cases} f_{v1} = c_1 \cdot |a_{AP}|^2 + c_2 \cdot |a_{AP}| + C_3 & f_{v2} = 0 & a_{AP} \leq -Thr \\ f_{v1} = 0 & f_{v2} = 0 & |a_{AP}| < Thr \\ f_{v1} = 0 & f_{v2} = c_1 \cdot |a_{AP}|^2 + c_2 \cdot |a_{AP}| + C_3 & a_{AP} \geq Thr \end{cases} \tag{6.3}$$

The acceleration threshold (Thr) was chosen to be equal to the standard deviation of the accelerometric signal recorded when the participants were standing with their eyes open during the baseline phase. In the sham feedback, the vibration had the same intensity as the other two feedback methods but did not encode any information about the actual sway of the participant. Specifically, the sham vibration encoded the direction and amplitude of the accelerometric signal in another trial. With this choice, the vibration had the same intensity (i.e. range of frequency: $150 \div 235$ Hz) already experienced during the other trials, but it did not encode any information about the CoM on the current trial.

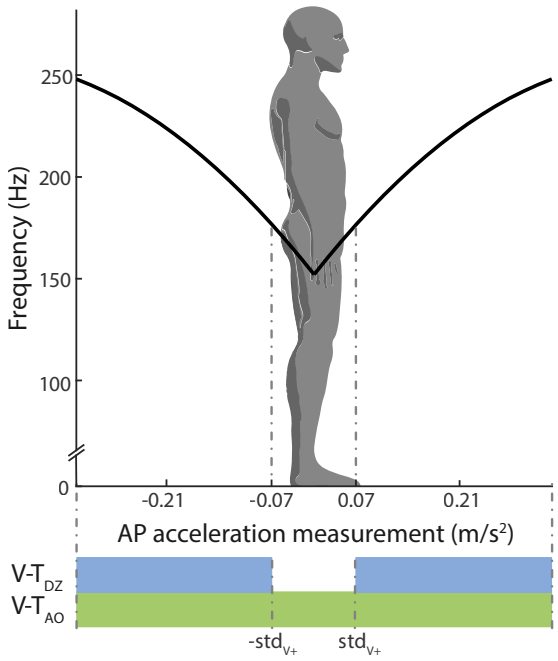

Figure 6.2 Relation between the AP acceleration and the vibration frequency. The black line represents, for the always-on method (V-T+$_{AO}$), the relation between the amplitude of the acceleration signal measured by the IMU sensor on the Anterior-Posterior (AP) direction in absolute unit (m/s^2) and the vibration frequency (in Hz) applied to one motor or the other: the motor on the abdomen, for positive acceleration respect to the natural stance, and the motor on the back, for negative acceleration. The standard deviation of the acceleration measurement recorded during the initial trial with eyes open (std$_{V+}$) was used for defining the limit of the dead zone, i.e. the region where the vibration was silent for the DZ method (V-T+$_{DZ}$): this region is represented in the figure by the two dotted lines. Outside that region the vibration was controlled in the same way for both methods (AO and DZ).

6.2.3 Participants

The 24 participants enrolled in the experiment were healthy young adults, who were divided into two groups. The first one was composed of 15 participants (25.13 means ± 2.19 std years, 8 females) who were tested with the DZ feedback method. The second group was composed of 9 participants (25.78 ± 3.49 years, 5 females) who were tested with the AO feedback method. The latter group was tested also with the sham feedback at the end of the experiment. For both groups, the inclusion criteria were the same: no known history of disease or lower limb injury, normal cognitive abilities, no problems of visual integrity that could not be corrected with glasses or contact lenses. All participants provided written consent to participate in this experiment. The study was conformed to the standard of the

declaration of Helsinki and was approved by the institutional ethical committee (Comitato etico regione Liguria).

6.2.4 Experimental set-up and protocol

Participants stood with their feet together, without shoes, and with their arms hanging at the sides of the body. They wore noise-mask headphones to avoid the influence of disturbances from the vibration sensors and/or environmental noise. The participants were instructed to stand as still as possible with their eyes open or closed depending on the trial. They were aware of whether or not the vibration was provided in a specific trial. No indication or clue about the informational content of the vibration or the encoding method was provided, but there was a familiarization phase where participants could explore the vibrotactile feedback and understand the encoded information. The experiment was divided into three phases: baseline, familiarization, and test (6.3).

Baseline

Participants performed a preliminary test, equal for both groups and composed of two trials with a duration of 50s without the vibrotactile stimulation. In the first trial they had to maintain the standing position with the eyes open (i.e. with the visual feedback: V+T-; T1). During this trial, they were placed in front of a white wall, at a distance of 1m, and they had to look at a blue dot target (0.75cm radius) on the wall. The second trial was performed with the eyes closed (i.e., without the visual feedback: V-T-; T2). Between the two trials, there was a short pause (about 30s).

Familiarization

The familiarization lasted 30s. During this phase, the participants were free to explore the vibrotactile feedback maintaining the standing position with eyes open or closed, as they preferred. Notice that this allowed the participants to understand that performing correctly the task corresponded to reduce the intensity of the vibration, till a complete silencing only in the DZ method.

Test

The first part of the test was composed of three repetitions of two trials with a duration of 50s each. The first trial was performed without vibrotactile feedback (V-T-; T3-T5-T7), and

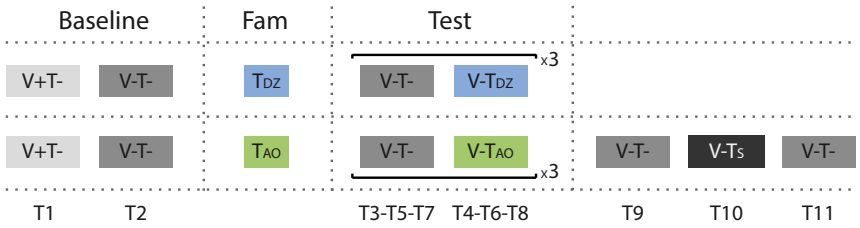

Figure 6.3 Protocol adopted for group 1 (upper row) and group 2 (bottom row). Trials were either with the visual feedback (i.e., eyes open: V+) or without it (i.e., eyes closed: V-). The vibrotactile feedback was either off (T-), or on (T+). There were three types of vibrotactile feedback: Dead Zone (DZ), Always On (AO), or Sham (S). Ti (where i goes from 1 to 9 for group1 and 11 for group 2) indicates the trial numbers.

the second with vibrotactile feedback (T4-T6-T8): dead zone method (V-T_{DZ}) for group 1 and always on method (V-T_{AO}) for the group 2.

Participants from group 2 performed also the sham test, i.e. they were asked to stand still for three additional 50s trials where the first and the last trial were without any feedback (V-T-; T9-T11), and the second trial with the sham feedback (V-T_S; T10), i.e. vibrotactile feedback where the vibration intensity was not related to the actual CoM oscillations (see Vibrotactile feedback control section). The rationale of testing the effect of sham feedback was to verify if measurable sway changes observed in our experiment were due (1) to the informational content of the supplemental vibrotactile feedback or (2) to a mere effect of vibration acting as noise and increasing the perceptive thresholds as in [337–342]. In the latter case, we expected that changes –and specifically a reduction of the postural sway during the exposure to the synchronized informative feedback, would have been maintained during the exposure to the unsynchronized sham feedback. This is because the sham feedback had the same amplitude and frequency as the informative feedback, with the only difference that was unrelated to the actual CoM oscillations. Instead, in the former case, if participants used the information encoded in the vibration in the previous trials since in the sham feedback the vibration would be not related to the actual CoM oscillations, the attempts to use the vibration content would decrease participants' stability, increasing the postural sway.

6.2.5 Data analysis

We aimed at investigating the efficacy of synchronized vibrotactile feedback for the reduction of body sway and distinguishing the specific effects of the different encoding methods. The indicators for describing the postural oscillations were extracted from the acceleration signals recorded with the IMU (see Fig.6.4 for an example) located at L3 level.

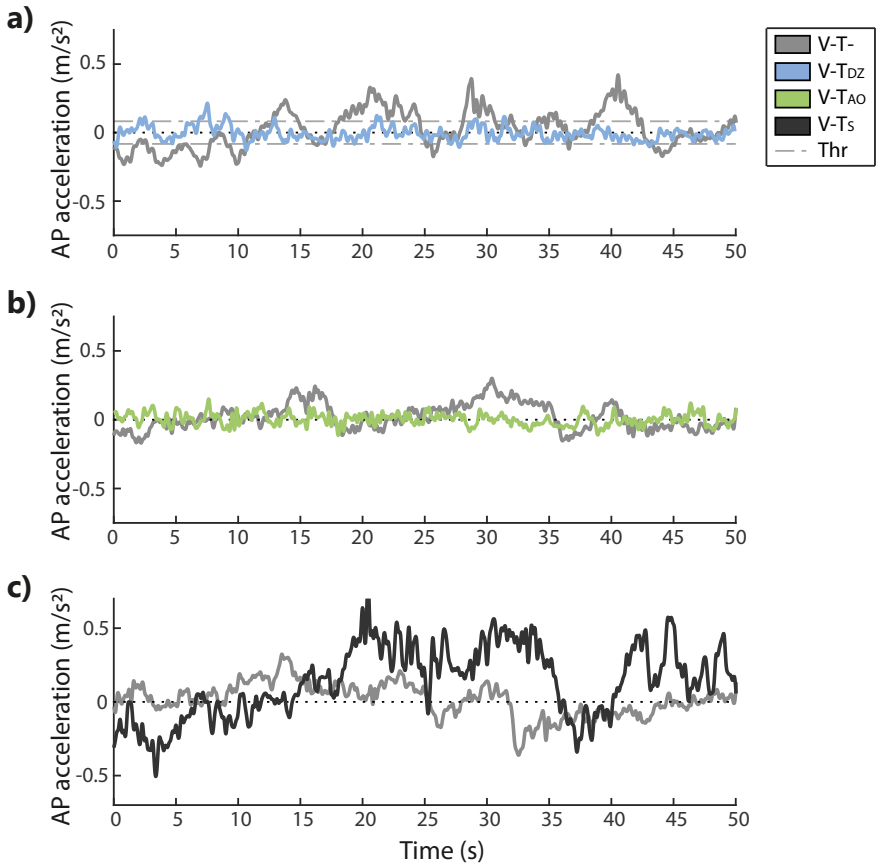

Figure 6.4 Examples of the accelerometer signals (low-pass filtered, cut-off frequency 3.5 Hz) in the absence (V-T-) and presence (V-T+) of supplemental vibrotactile feedback. Each panel compares, for one typical participant, the accelerometric signal in the (V-T-) condition with the same signal measured in the three conditions with vibration on the dead-zone method (V-T$_{DZ}$) in panel a (note that the dead zone is delimited by the two dashed lines); the always-on method (V-T$_{+AO}$) in panel b; the sham feedback (V-T$_S$) in panel c.

The accelerometric signal was sampled at a frequency of 50 Hz. During the experiment, for the online computation of the vibrotactile feedback, we used the raw data, while during the offline data analysis to evaluate the postural performance of the participants we took as reference for the signal pre-processing the studies of [333] and [343] filtered the data with a zero-phase fourth-order Butterworth low-pass filter with a cut-off frequency of 3.5 Hz. These studies demonstrated that in quiet standing we can extract reliable indicators of postural stability from the accelerometric signals in the horizontal plane and that these indicators are correlated with the ones extracted from the center of pressure, both for healthy participants and for people with Parkinson's disease. In other words, according to these studies, the higher is the amplitude of these low-pass filtered signals extracted from the accelerometric signals the greater the postural sway measured by a force platform as a shift in the center

of pressure. Therefore, in the present study, we referred to an increase/decrease of these signals as an increase/decrease of the postural sway/oscillations. To evaluate the participants' performance we computed two outcome measures from the acceleration signals [333]:

- the Root Mean Square acceleration (RMS), quantifying the magnitude of the acceleration in the spatial-temporal domain;
- the frequency at which the power spectral density reaches the 95th percentile (F95), describing the character of signal in the frequency domain.

We computed both these indicators separately for acceleration components in the anterior-posterior and medial-lateral directions.

Statistical analysis

The baseline data were used (i) to verify that there were no differences between groups before exposure to vibration and (ii) for defining the amplitude of the dead zone. We also verified the difference in performance between open and closed eyes conditions, expecting a significant worsening in performance when the visual feedback was absent. To do so, we used a repeated-measures ANOVA with one factor within participants 'Visual feedback' (open/close eyes) and one factor between participants: 'Groups' (group 1 vs. group 2). After that, for verifying if the two methods of encoding the acceleration of the CoM induced changes in the postural sway and if these changes depended on the encoding methods we analyzed the data of the test phase by using an rm-ANOVA with two within-subjects factors: 'Vibration' (2 levels: on and off) and 'Repetition' (3 levels) and one factor between participants: 'Encoding method' (2 levels: dead zone and always on). We further investigated significant main and interaction effects by performing a post-hoc analysis using Fisher's LSD. Although we could expect a sizable variability among participants in their baseline performance, we did not normalize the data for the anthropometric parameters or the baseline performance. The reason for this was that in each group the same participants were tested multiple times under different conditions and the rm-ANOVA allowed for individual differences in the baseline, i.e. it allowed testing for the effect of the supplemental feedback (and more specifically for all the factors: vibration on/off, encoding method and repetition) while excluding the influence of different baseline performance across participants. Effects were related to repetition to highlight (i) learning effects in the vibration trials, and (ii) after-effects in the no vibration trials. Therefore, when the repetition factor or its interactions were significant, we further investigated these results by comparing the first and the last trial on the same condition (presence/absence of vibration).

Specifically, in the no vibration condition this was equivalent to test if there were any after effect recorded before exposure to vibrations. For testing the importance of the informational content encoded in the vibrotactile feedback we compared (three planned comparisons - paired t-test), the performance in the sham trial with the performance (i) in the last trial with the always-on method, and (ii) in the two trials without vibration before and after the sham trial. The normality of the data was checked with the Lilliefors test. The assumption of sphericity necessary to perform rm-ANOVA was verified for all the parameters (Mauchly's test). Statistical significance was set at the family-wise error rate of α=0.05. Since we had more than one parameter extracted from the same dataset we verified that all the reported p-values – computed without corrections for multiple comparisons - were robust to the Bonferroni-Holm correction and we reported when they were not.

6.3 Results

Baseline

The first analysis that we performed was to check the performance during the baseline, where the participants had to perform two consecutive trials with (T1) and without (T2) the visual feedback. As expected, we found that all the participants worsened their performance during the closed eyes condition. Specifically, the amplitude of the acceleration signals in the AP and the ML directions significantly increased (RMS: AP: $F_{1,22}$=36.20, p<0.001; ML: $F_{1,22}$=22.05, p<0.001). For the F95 parameter there was a significant decrease in the AP direction ($F_{1,22}$=7.57, p=0.012), which was not found in the ML direction ($F_{1,22}$=3.69, p=0.068). The second preliminary analysis was aimed to check that the two groups of participants were equivalent with regard to the baseline performance during unperturbed sway. In particular, we compared the performance in the first two trials, in absence of vibration, and we found not significant differences between the two groups for all the parameters (RMS: AP: p=0.066, ML: p=0.417; F95: AP: p=0.793, ML: p=0.471).

Supplemental synchronized vibrotactile feedback reduces postural sway

For investigating the effects of the vibrotactile feedback encoding the CoM information, we analyzed the data collected during the test phase, where participants were required to stand as still as possible with eyes closed and they performed three repetitions of two trials without (T3-T5-T7) and with (T4-T6-T8) supplemental feedback.

Encoding method effect

We found that for all participants the vibrotactile feedback encoding the accelerometric measurement modified the postural sway, independently of the encoding method (encoding method effect: p>0.42 for all the parameters).

AP direction

When the vibration was applied, in the AP direction, i.e. the direction encoded in the supplemental feedback, there was a significant effect of the vibration on both the RMS and the F95 as displayed in Fig. 6.4 for a typical participant of group 1 (Fig. 6.4a) and group 2 (Fig. 6.4b). Specifically, the amplitude of the AP acceleration decreased (RMS: $F_{1,22}$=22.34, p<0.001, Fig. 6.5a and 6.5c) and its frequency increased (F95: $F_{1,22}$=72.02, p<0.001, Fig. 6.5b and 6.5d).

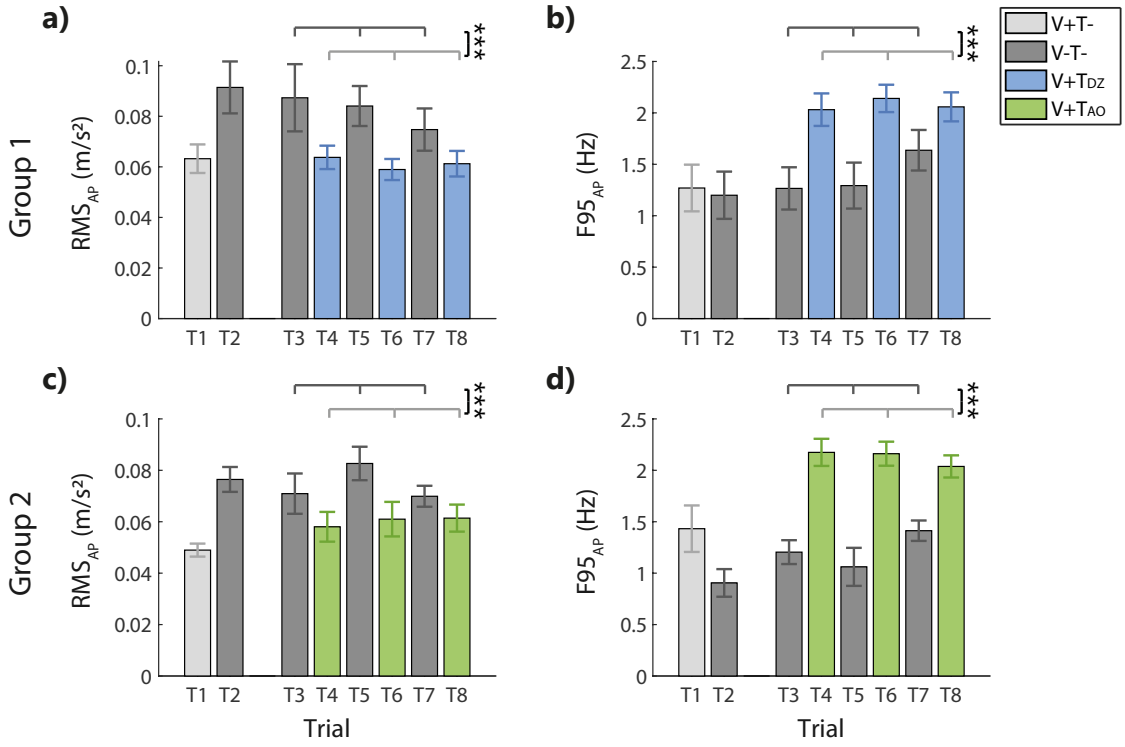

Figure 6.5 RMS and F95 parameters in the AP direction for group 1 (DZ method) in panel A and B, and for group 2 (AO method) in panel C and D, respectively. The errorbars represent the standard error of the mean obtained for all the participants. *** Indicates significant differences of rm-ANOVA: p<0.001.

ML direction

In the ML direction, i.e. the direction not encoded in the supplemental feedback, the vibration produced only a significant increase of the frequency (F95: $F_{1,22}$=14.17, p=0.001, Fig. 6.6b and 6.6d), not followed by a significant change of the amplitude of the accelerometric signal (RMS: $F_{1,22}$=1.54, p=0.228, Fig. 6.6a and 6.6c).

The sham feedback changes the postural sway differently from the synchronized feedback

To verify that the reduction of the postural sway above described was effectively due to the information embedded in the feedback related to the accelerometric measurement, we compared the performance in the sham trial (T10) with the performance in the last trial with the always-on feedback method (T8) and the two trials without vibration before (T9) and after (T11) it.

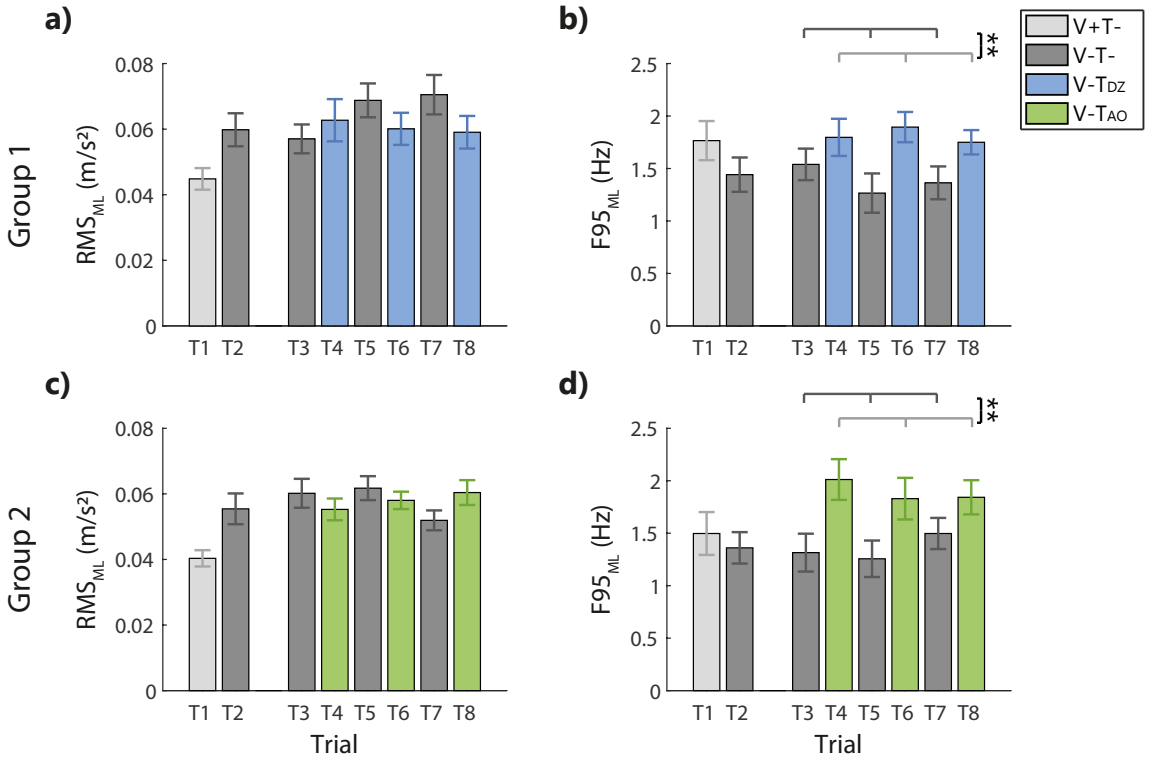

Figure 6.6 RMS and F95 parameters in the ML direction for group 1 (DZ method) in panel a and b, and for group 2 (AO method) in panel c and d, respectively. The errorbars represent the standard error of the mean obtained for all the participants. ** Indicates significant differences of rm-ANOVA: p<0.01.

We found that the unsynchronized sham feedback determined different changes in the postural sway with respect to the feedback encoding a combination of the actual position and acceleration of the body center of mass in the anterior-posterior direction. The acceleration signals from a representative participant in a trial with the sham feedback are reported in Fig. 6.4c. AP direction. Indeed, the sham feedback increased the amplitude of the accelerometric signal in the AP direction, with respect to all the tested conditions, i.e. both the no vibration trials (RMS: T9-T10: p=0.011; T10-T11: p=0.035, the latter was not robust to Bonferroni-Holm correction), and the last trial with AO method (RMS: T8-T10: p=0.002; Fig. 6.7a). For the F95 in the AP direction, the sham, differed from the trial with the AO method (T8-T10 p<0.001), while not significant differences were observed with respect to the no vibration trials (T9-T10 and T10-T11 p>0.54; Fig. 6.7b). ML direction. Instead, the F95 of the ML component was higher with respect to the last no-vibration trial before the exposure to vibration (T9-T10: p=0.039, not robust to Bonferroni-Holm correction; Fig. 6.7d).

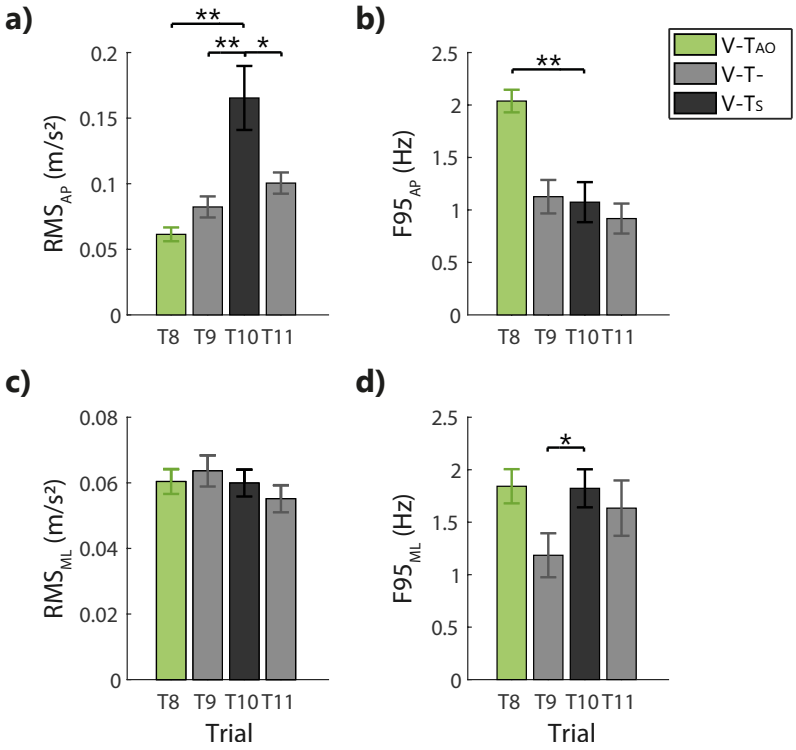

Figure 6.7 Effects of the sham feedback (V-T_S; T10) in comparison with the performance in the last trial V-T_{AO}; T8) and in the two no vibration trials before and after the sham trial (V-T-; T9, T11). RMS and F95 for the AP direction are reported in panels a and b, respectively. RMS and F95 for the ML direction are reported in panels c and d, respectively. The errorbars represent the standard error of the mean obtained for all the participants. * Indicates significant differences of rm-ANOVA: * p<0.05, **p<0.01.

For all the other comparisons and the RMS in this direction (Fig. 6.7c), not significant differences were observed (all p>0.34).

Effects related to repetition: both synchronized encoding methods determined no learning effect, but they led to different after effects

Learning effects in trials with vibration

Comparing the trials with the vibrotactile feedback during the test (T4-T6-T8), we found that for both parameters and both groups there were not significant differences among the three repetitions (Fisher's LSD test: all condition p>0.25).

After effects in trials without vibration

In the trials, without vibrotactile feedback (T3-T5-T7) the postural sway changed when comparing the performance before (T3) and after (T7) exposure to vibration (T7), and these changes depending on the encoding method.

Encoding method effect

The amplitude of the acceleration in the ML direction increased for the DZ method, but not for the AO method, which led to a not significant effect of the encoding method factor (interaction effect 'Vibration*Repetition*Encoding method' $F_{2,44}$=6.23, p=0.004; post-hoc analysis: V-T_{DZ}: T3-T7 p<0.001; V-T_{AO}: T3-T7 p=0.093). In the AP direction, instead, there were not significant after-effects for the sway amplitude ('Vibration*Repetition*Encoding method' interaction: p=0.854), although we observed that the RMS parameter decreased in 8 participants of group 1. We observed after-effects also in the frequency domain, where the F95 parameter for the no vibration trials increased across repetitions in the AP direction for the DZ method (Vibration*Repetition: $F_{2,44}$=11.42, p<0.001, post hoc analysis: V-T_{DZ}: T3-T7 p<0.001), while the trend was less clear for the AO method, with changes that did not reach a threshold of significance (V-T_{AO}: T3-T7 p=0.065).

6.4 Discussion

To investigate the effects of vibrotactile feedback on standing balance, we built a device with two vibration motors, one placed on the back at the L5 level and the other on the correspondent location of the abdomen. The vibration was synchronized with an accelerometric signal

encoding a combination of the position and acceleration of the body center of mass in the anterior-posterior direction. We expected that blindfolded unimpaired participants, when exposed to this vibration (1), would modify their postural sway in dependence of the encoding method (AO vs. DZ); (2) the changes depended on the information encoded by the vibration method, i.e. they were not a mere effect of vibration; (3) the vibration did not induce after-effects on the natural postural sway in absence of vibration. In short, the results partially matched the expectations: we found that independently from the encoding method, the presence of vibration synchronized with the accelerometric signal decreased the sway amplitude in the AP direction while increasing its frequency in both directions. The participants accounted for the information encoded in the vibration since the sham vibration did not produce the same effects. Surprisingly, we found significant after-effects of the vibration for the participants that were exposed to the DZ method. In the following sections, we discuss in detail the results.

All participants modified their postural sways vibrotactile feedback with informational content, independently from the feedback method

When exposed to supplemental vibrotactile feedback synchronized with an accelerometric signal encoding a combination of the position and acceleration of the body center of mass in the anterior-posterior direction, all participants modified their postural sways, independently from the method used to provide this information. Both encoding methods were able to modify the performance of all participants. Indeed, they reduced the amplitude and increased the frequency of the AP accelerometric signal. These changes can be interpreted as a reduction of the postural sway, i.e., smaller and more frequent postural corrections [321]. This effect is consistent with the previous studies, e.g. in [325] where supplemental vibrotactile feedback was able to modify the postural sway in healthy young participants. The main novelty of these results was that:

1. the changes were mainly on the direction of application of the stimuli, that was also the direction encoded in the supplemental feedback;

2. the presence or absence of a zone without vibration around the natural stance posture had not a specific effect on the postural sway;

3. these changes were obtained by using a simple and low-cost device based only on two vibrator motors, while [332], most studies use an array of several vibrator motors.

As for the first result, directional effects on the postural sway were described for the auditory [321] or multimodal (e.g., vibrotactile, auditory, and visual [344, 345] feedback, but to the best of our knowledge similar results were not reported for the vibration feedback with only two motors. Notice that this directional effect could be due to both the information encoded in the vibration or to the positions of the vibration motors that are on the front and the back of the participants could have influenced differently the AP and ML direction, as discussed in the following paragraph.

As for the second, the encoding methods with the idea that participants might attend to the supplemental feedback only outside a certain region of the natural postural sway [332] or above a certain threshold of the stimuli. If this is the case, the DZ method would have the advantage to drive the participants' attention to the stimuli only when it is needed could have beneficial effects. The findings that the participants did not have different responses during the exposure of the two encoding methods seems to support this hypothesis

These results suggest that the proposed simple and low-cost device was able to influence significantly the postural sway, from the initial exposure. Thus independently of the encoding method, the use of the proposed device was intuitive and effective, i.e., the central nervous system was able to incorporate the supplementary feedback [189] without requiring a long adaptation process. If the informational content was important (see next paragraph), then the process could have been enhanced by the fact that in both cases, the vibrotactile feedback were designed to elicit a repulsive strategy i.e. participants should reduce or silence the vibration intensity for decreasing the postural sway and this method, provided with other more complex matrix of vibration motors, was found to be more effective than that of the attractive strategy [239, 346].

Although these results are interesting and promising, future studies are necessary to verify the effectiveness of this approach. Also in the presence of internal and external perturbations that challenge the balance ability and to verify if different results would be obtained changing the amplitude of the dead zone or how the information of the AP CoM oscillations are encoded in the vibration intensity.

The sham feedback led to different sways patterns

The sham feedback led to different sways patterns than the vibrotactile feedback encoding a combination of the actual position and acceleration of the body center of mass in the anterior-posterior direction The lack of effect on the postural sway of the two different encoding methods described above could be due to the exposure to vibration, with different

directional effects because the vibrator motors are located on the front/back of the participants, i.e. the vibration was provided along the AP direction. It is well known that also a low-level noise vibrotactile stimulation increases the detection of the stimuli, leading to improvements in postural control [330, 331, 340–342]. To verify whether or not the participants in this experiment integrated their neural control of the informational content encoded in the vibration, we added a trial where the participants of group 2 were exposed to sham feedback. In other words, we tested if the modification of the postural sway was the same with unsynchronized feedback with actual postural sway, but with similar amplitude and frequency content. The exposure to the sham feedback had different effects than the synchronized informative feedback, determining an increase of the amplitude of the AP direction associated with a decrease of the frequency of the ML direction, with respect to the signal recorded in absence of supplemental feedback. Therefore, our participants when exposed to synchronized informative feedback reduced the amplitude of the AP oscillations and increased their frequency content, by integrating the information encoded in the vibration. These results are not in contrast with [339], where participants with bilateral vestibular loss improved equally with the informative and uninformative vibration. We specifically tested if our participants accounted for the informational content of vibration when exposed to informative feedback, and the experiment was not designed to verify whether or not informative feedback would lead to the same changes in postural control. In particular, the increased AP acceleration amplitude in presence of the uninformative vibration was probably due not to the mere effect of our sham feedback, but to the fact that the participants have learned to integrate into their postural control loop, the vibration informational content experienced in the previous trials. Thus, when the feedback becomes uninformative, its integration into the control loop decreased the postural stability. This result supports the hypothesis that participants were able to integrate the proposed supplemental feedback in their postural loop control, accounting for its informational content, after a short time from the initial exposure. Thus, this result encourages further investigation and exploits the possibility of applying this technology and supplemental vibrotactile feedback in long-term training and rehabilitation of postural control abilities.

The exposure to DZ feedback method led short term after effects

The vibrotactile feedback determined changes on the natural postural sway, depending on the encoding method: the exposure to the DZ feedback method led to short-term after-effects. To investigate the after-effects of the exposure to supplemental feedback is important:

if present, they modify, either in a positive or negative way, the postural responses of the participants either in the short or in the long term [328]. This could have relevant implications in the sensory substitution domain, e.g. for amputees [327], and is a central issue when the technology is used with applications with rehabilitation goals, e.g. in [347, 348]. However, the study of after-effects of exposure to vibrotactile feedback has received limited attention [305]. Here we made a first step in the direction of investigating this problem, limiting the study to short-term effects due to a short exposure to the vibrotactile stimuli. Surprisingly, we found that even a short exposure of few minutes (the entire experiment lasted about 15 minutes) can induce short-term changes in the natural oscillation patterns of the CoM in absence of vibration and these changes depend on the encoding method. Indeed, only the DZ feedback method modified the natural oscillation pattern leading to an increased frequency in the AP direction and, most importantly, to an increased amplitude in the acceleration component of the ML direction. The increase in postural oscillations in the ML direction is usually a negative effect associated with instability. Therefore, this finding needs to be investigated further, extending the study to long-term exposure and long-term after-effects of the vibrotactile feedback. As it is, this result seems to suggest that providing feedback method as always on instead of one as a dead zone is preferable since it allows avoiding undesired after-effects. Notice that based only on the observation of the effect during the exposure to the stimuli we would have concluded that the DZ feedback method would be preferable because it reduces the exposure to the stimuli [313]. However, the observation of the after effect seems to suggest that the best choice is to keep the vibration always on to avoid undesirable effects when the stimuli are turned off. We acknowledge that these are only preliminary results related to the proposed device and protocol. They highlighted the importance to investigate also the after-effects of the stimuli, and deeper and larger investigations are needed to drive general conclusions.

Vibrotactile synchronized feedback and light touch

In the early 90's it was discovered by [349] that "fingertip contact influences human postural control". In particular, it was found that such additional tactile information allowed the subjects to significantly reduce the size of sway movements: very small contact forces, of the order of 1N, could elicit this phenomenon and, at such level of interaction, purely biomechanical explanations would not match the findings while suggesting a multi-sensory integration process, somehow related to the effect investigated in this study. The initial demonstrations mentioned above involved the tandem Romberg standing posture, which is

particularly unstable in the frontal plane, however a following study [350] obtained similar effects with normal bipedal stance: they also found a positive correlation between the contact force and the reduced oscillation of the center of pressure in support of the idea of synchronized feedback for the reduction of postural sway. Moreover, it was found that such reduction does not necessarily need to involve the hand but also occurs when different parts of the swaying body (e.g. leg or shoulder) experience a light contact with an environmental referent [351]. In any case, it is mandatory that tactile information is not inhibited by any means, such as anaesthetization of the hand [352]. By comparing the effect of different levels of light touch, namely the fact that the stronger the touch the better the sway reduction, it was suggested by [353] that "heavier contact provides clearer sensory information about sway allowing faster and more accurate compensatory balance adjustments". In other words, it seems plausible to postulate that the solution adopted by the brain for stabilizing standing upright, in the sense of minimizing as much as possible the unavoidable body sway, is to carry out a multi-sensory data fusion for obtaining the most accurate estimation of the oscillation of the CoM that is essential for closing the stabilization loop. We need to take into account that such critical information is not accessible directly through a specific sensory channel but indirectly through different noisy channels: visual, proprioceptive, and vestibular, in the natural situation. Light touch or synchronized vibrotactile stimulation are artificial channels that can complement the natural ones for improving the accurate evaluation of the CoM sway that is necessary for minimizing its amplitude. There are indeed reasons to believe that sway movements during quiet standing are not noise-driven around a point attractor (the nominal equilibrium posture) but are the results of an intermittent stabilization process attracted by a limit-cycle whose size depends on the inaccuracy of CoM estimation [354, 355]. From this point of view light touch and vibrotactile synchronized feedback are somehow equivalent. However, the latter one lends itself much more naturally to clinical applications that will be the target of a further development of this study.

Limitations

We did not found any difference due to the two encoding methods (AO and DZ) during exposure to the supplemental feedback, thus we added a test with sham feedback to verify if the participants took into account the informational content encoded in the vibration. If this were not the case, we would conclude that the lack of difference between the encoding methods was due simply to the fact that participants used the vibration without accounting for the informational content. The results of the test with sham feedback allowed us to reject this

hypothesis highlighting that the participants previously exposed to the AO feedback method were indeed using the informational content of the vibration. We also expect a similar effect for the DZ method, but this specific test was not included in the present protocol and could be part of a future extension of the research line. An additional potential effect that was not covered by the protocol used in this study is a 'bias effect'. The fact that participants were exposed to sham feedback after being exposed to the informative feedback might create a bias: the increased oscillations observed in presence of sham feedback were due to the previous exposure to the informative feedback since participants were trying to use the vibration information also during exposure to the sham feedback. To verify the effects of this sham feedback per se, we should have added a group that would have been exposed only to sham feedback (or at least exposed first to the sham feedback). Pursuing this extension of the line of research performed by the current study we should also have taken into account that the relation between the body sway and the intensity of vibratory noise has a U-like shape, thus only specific levels of noise might induce a decrease of postural performance [340–342]. However, this was not our goal, but we just wanted to verify the mechanisms underlying the changes in the postural sway due to the vibration we provided encoding the CoM information, as in [42] for the upper limb supplemental feedback. Finally, with the proposed paradigm, alternating short trials with and without vibration, we specifically aimed at verifying if participants accounted for the vibrotactile feedback we provided in a short time frame (i.e. trial of 50 seconds) and if that short exposure could determine any modification of the natural oscillation patterns observed before the exposure. Notice that the participants were aware that in the 'No vibration trials' the vibration was off. The short exposure to only one of our feedback modalities determined after effects and we believe that, while different protocols could lead to different after effects, their existence was not due to our protocol. However, this point should be further verified in future studies and we acknowledge that the paradigm we choose could have influenced the learning and the related after-effects i.e. a different paradigm could have led to different results.

Chapter 7

Study II: Effect of short-term exposure to supplemental vibrotactile feedback on goal-directed movements after stroke

This study has been published in: Ballardini G., Krueger A., Giannoni P., Marinelli L., Casadio M., Scheidt R. A. *'Effect of short-term exposure to supplemental vibrotactile kinesthetic feedback on goal-directed movements after stroke: a proof of concept case series'*, Sensors 21(4): 1519 (2021). doi.org/10.3390/s21041519

7.1 Introduction

Recently, empirical evidence has demonstrated the potential benefit of vibratory stimuli for improving neurorehabilitation [27–34]. Indeed, few of them increase performance in the contralesional side [28] or upper-limb symmetry [33] conveying information only on the ipsilesional limb. However, to the best of our knowledge, no studies to date have investigated the use of real-time supplemental vibrotactile kinesthetic feedback into the ongoing control of goal-directed movements and stabilization of the arm and hand after stroke.

This study aims to fill this gap, assessing the feasibility of using vibrotactile feedback to enhance the accuracy and precision of goal-directed stabilization and reaching tasks performed without visual feedback by survivors of stroke in the chronic stage of recovery. We tested the hypothesis that chronic stroke survivors without cognitive impairment can readily interpret the informative content of vibrotactile feedback and use it to solve reaching and stabilization tasks. We also examined the hypothesis that performance would be con-

sistently better with an error encoding scheme vs. state encoding, as found previously for neurologically-intact participants in [42].

7.2 Material and methods

7.2.1 Participants

A convenience sample of three chronic stroke survivors (aged 57 to 68 years; 2 females; see Table 7.1 for details) provided written and informed consent to participate in a series of experimental sessions designed to evaluate the immediate utility and usability of supplemental kinesthetic feedback for enhancing the control of stabilization and reaching movements of the arm and hand. Inclusion criteria included: (i) diagnosis of a single stroke event confirmed by brain imaging; (ii) within the chronic stage of recovery (i.e., more than six months post-stroke); (iii) capability to perform upper limb movement exceeding 10 cm in presence of counterbalance support; (iv) capability to understand and follow basic two-step instructions: Folstein Mini-Mental State Examination score [356] above 28; and (v) normal or corrected-to-normal vision. Exclusion criteria included: (i) absence of vibration sensation in the ipsilesional arm; (ii) neurological impairments that prohibit informed consent and the understanding of the tasks; (iii) presence of hemispatial neglect. All participants were enrolled by a qualified physiotherapist and a neurologist. All procedures were approved by the local Ethical Committee serving the University of Genoa (ASL3 Genovese) and the Institutional Review Board of Marquette University (HR-3044) in accord with the 1964 Declaration of Helsinki. The study required one visit to the lab for clinical testing and then two separate 1-hour experimental sessions, all within three weeks.

Table 7.1 Demographic and clinical data for the stroke survivors

	Sex	Age	Type	PS	TSS(ys)	Lesion location
S01	F	68	I	R	12.5	L basal ganglia, internal capsule, occipital lobe
S02	M	57	I	L	1	R basal ganglia, temporal lobe, insula
S03	F	65	H	L	16	R occipital lobe

Abbreviations: F: female; M: male; I: ischemic; H: hemorrhagic; PS: paretic side; R: right; L: left; TSS: time since stroke.

Clinical evaluations

A licensed physiotherapist evaluated the motor, functional and proprioceptive status of each participant using a series of clinical assessments (Table 7.2 and 7.3). These included: (i) the motor and somatosensory sections of FMA-UE in the contralesional arm. Higher FMA-UE scores indicate less impairment; (ii) the Modified Ashworth Scale (MAS) to quantify stiffness; higher scores of MAS indicate more spasticity; (iii) the 13-item Chedoke Arm and Hand Activity Inventory (CAHAI), which is a test of sensorimotor function. Higher CAHAI scores mean better functional ability in activities of daily living; (iv) the kinesthetic and stereognosis portions of the Nottingham Sensory Assessment (NSA) in the contralesional arm. Higher scores indicate better somatosensory capability; (v) a tuning fork assessment of vibrotactile sensation in both arms. Higher scores indicate better sensation.

Table 7.2 Clinical test results - Part 1

	FMA-UE		MAS					
	A-D (0-66)	H (0-12)	Sho (0-4)	Elb (0-4)	For (0-4)	Wri (0-4)	Fin (0-4)	Thu (0-4)
S01	57	11	1	0	0	0	0	1
S02	6	7	1+	1+	2	3	3	3
S03	42	7	1	1	1	2	1	1

Abbreviations: FMA-UE: Upper Extremity portion of the Fugl-Meyer Assessment; A-D: motor sections; H: sensory section; MAS: Modified Ashworth Scale; Sho: shoulder; Elb: elbow; For: forearm; Wri: Wrist; Fin: Finger; Thu: thumb.

Table 7.3 Clinical test results - Part 2

	CAHAI	NSA		Tuning Fork Test			
		P	D	Contra		Ipsi	
	(0-91)	(0-3)	(0-2)	Elb	Wri	Elb	Wri
S01	80	3	2	6	6	6	6
S02	13	0	0	6	5.5	7	7.5
S03	24	1	0	5	6	6	6

Abbreviations: CAHAI: the 13-item Chedoke Arm and Hand Activity Inventory; NSA: Nottingham Sensory Assessment; P: proprioception; S: stereognosis; Contra: contralesional arm, Ipsi: ipsilesional arm; Elb: elbow; Wri: Wrist.

7.2.2 Experimental set-up

Subjects were seated comfortably in a high-backed chair with a flat footrest in front of a horizontal planar robotic manipulandum (7.1a; see [357] for a detailed description). The contralesional hand grasped the robotic handle, which has an integrated lightweight and rigid arm support that was strapped to the forearm. The arm support provided gravity compensation and free motion of the forearm in the horizontal plane. The ipsilesional arm rested comfortably on a horizontal support mounted below the robot's plane of motion. An opaque shield was placed over the workspace to block the participant's view of the moving arm and the robotic apparatus. The chair was adjusted to align the left/right horizontal center of the robot's workspace with the participant's midline. The participant was positioned near the edge of the opaque shield, so the anterior/posterior range of the robot was within the participant's reach. The seat height was adjusted such that the abduction angle of the shoulder was between 75° and 85°. A vertical screen was placed in direct view, 70 cm from the participant; it always provided visual cues of target position and hand motion when appropriate (see subsection 7.2.5). The spatial mapping from handle movement to cursor movement was 1:1. Before starting each experimental session, participants were provided descriptions of the tasks they would be asked to perform and encouraged to ask questions. Subjects were also encouraged to give verbal feedback about the ongoing experience at any time during the experimental sessions.

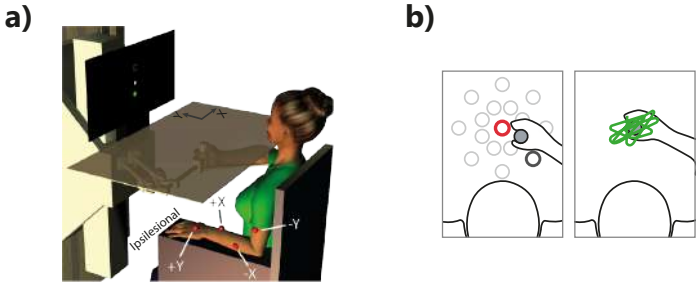

Figure 7.1 Experimental set-up and tasks. A) Subject seated in a high-backed chair holding the end effector of a planar manipulandum with the contralesional hand. An opaque screen prevented direct visual feedback of the moving arm and end effector. The four actuators vibrotactile display interface was fixed to the ipsilesional arm. The default locations of the vibration motors are shown by red spheres. Each motor was activated by hand displacement in one of four directions. A vertical screen was placed in front of the participant for providing visual feedback of the target position and of the hand motion. B) Tasks - Left: example of a reaching movement from the starting target (black) to the final target (red). All possible target locations are shown here in gray. Right: example of hand stabilization against robotic perturbations at the center of the robot workspace. Hand displacements are shown in green.

7.2.3 Experimental task

We focused on two actions that are fundamental to the performance of many activities of daily living: reaching and stabilizing with the arm and hand ([5, 358, 359]).

Reaching

In each block of the reaching task, participants were asked to perform center-out-and-then-back reaches to 16 targets, for a total of 32 discrete reaching movements. Each movement was considered a unique trial. The 16 targets were equally spaced around two concentric circles centered on the center of the robot's workspace (Fig 7.1b, left). This design allows testing of 16 movement directions (22.5° apart) and two movement extents: 5 and 10 cm for the eight targets fixed to the inner and the outer circles, respectively. To equalize the difficulty of reaching targets placed at different distances, we scaled the target size according to Fitts' Law, which predicts that the time required to rapidly move to a target area is a function of the ratio between the distance to the target and the target size [360]. According to that, the target radius was 1 cm for the close targets and 2 cm for the far targets. Target presentation order was pseudo-randomized within each block. Subjects were instructed to "Capture the target as quickly and accurately as possible." As a reminder to capture the target quickly, reach targets turned from red to blue 1 second after they appeared. Upon completing the reach, the participant announced that they thought they had arrived at the target and the experimenter registered that event (i.e., the end of the movements) by pressing a button. Subjects were allowed a maximum of 20 seconds to complete each trial.

Stabilizing

In each block of the stabilization task, participants attempted to hold the robot handle steady at the center of the workspace for 60 seconds against time-varying sum-of sinusoid force perturbations (Fig. 7.1b, right). The perturbations contained both a low frequency and several high frequency components (Eq. 7.1):

$$\begin{cases} F_x = 0.75 \cdot cos(2\pi \cdot 1.75t) + 0.75 \cdot sin(2\pi \cdot 1.2t) + 6 \cdot cos(2\pi \cdot 0.25t) \\ F_y = 0.75 \cdot sin(2\pi \cdot 1.65t) + 0.75 \cdot sin(2\pi \cdot 1.1t) + 6 \cdot sin(2\pi \cdot 0.25t) \end{cases} \tag{7.1}$$

Accordingly, hand force perturbations had peak magnitudes of approximately 10 N.

7.2.4 Vibrotactile interface

Supplemental kinesthetic feedback about the moving hand was provided using a two-channel (four-actuator) vibrotactile interface attached to the non-moving ipsilesional arm. Each actuator was an Eccentric Rotating Mass (ERM) micromotor with an operational frequency range of 50-250 Hz (Pico Vibe 310-117; Precision Microdrives, Inc.). The ERM actuators have a vibrational amplitude range is 0.20–0.97 N that covaries with vibrational frequency (see [42] for more details). The fact that vibration frequency and amplitude are coupled in ERM actuators is well-suited for the purpose of implementing a vibrotactile interface because as shown previously by [336], people perceive vibrotactile stimuli better when the amplitude and frequency of vibration increase or decrease coherently. For simplicity in the text to follow, we will refer to correlated changes in the amplitude and frequency of vibrotactile stimuli as changes in vibration intensity. The actuators were initially arranged with a standard configuration designed such that inter-actuator spacing exceeded two-point discrimination thresholds for dermatomal regions of the arm and forearm as reported by [361]. In the standard configuration, the actuators - represented in Fig. 7.1a by red spheres - were placed at least 6 cm apart as in [336]. One actuator (Y+) was placed on the back of the hand approximately 1 cm proximal to the first and second finger metacarpophalangeal joints. Two actuators were placed on the forearm between 3 to 7 cm distal to the cubital fossa, one on each side of the forearm (X- on the left, X+ on the right with respect to the participant's reference frame). One actuator (Y-) was placed on the biceps muscle belly about 5 cm proximal to the cubital fossa. Each actuator was secured by an elastic band. The actuators were used to encoded hand motion into vibratory stimuli as a vector, with each dimension of Cartesian space mapped onto one pair of the actuators.

Before each experimental session, we performed a set-up procedure for the vibrotactile interface that lasted approximately 5-10 minutes: We adjusted the actuator locations if necessary so that the participant could indicate reliably which actuator or pair of actuators was activated at any given time. The vibration of all actuators was zero at the center of the workspace. We assessed the ability of participants to correctly perceive vibratory stimuli with the hand at three distances from this point corresponding to low, middle, and high-intensity vibrations (approximately 10%, 40%, and 90% Full-Scale Range (FSR: 75-250Hz), respectively). Set-up began with the participant placing the cursor at each of the four corners of the screen (corresponding to displacements of 15 cm from the center) and then reporting which actuators were vibrating (at $\sim$90% FSR). This was repeated two additional times, once near the center of the screen ($\sim$10% FSR) and once approximately mid-way between the center and the edge of the screen ($\sim$40% FSR). Next, the participant was asked to place the

cursor at the center of the screen, and then, to move away from that location and back again in each cardinal direction. If the participant could not give a clear and correct indication as to which actuator was active and/or the appropriate direction of intensity change, we adjusted the corresponding actuator locations to the nearest area where the vibrotactile stimuli were correctly perceived with a minimum distance of 6 cm between the actuators ([336]). It happens only in one participant for the actuators located in the upper arm and the internal forearm, in both cases they were moved less than 3 cm from the default location.

Supplementary feedback encoding schemes

Subjects experienced two different forms of supplemental kinesthetic feedback during the experiments: a vibrotactile encoding of limb state feedback and encoding of hand position error feedback. Both types of feedback conveyed meaningful information about the participant's performance in that the vibration encoded the motion of the hand with respect to either the center of the workspace (state feedback) or the current target (error feedback). In both cases, motion with respect to the reference point in the rightward/leftward and forward/backward directions resulted in vibrations of the +X/-X and the +Y/-Y actuators, respectively.

State feedback In this encoding scheme, the intensity of vibration was a weighted linear combination of hand position and velocity information as per [42] (Eq. 7.2):

$$\gamma(t) = 0.2 \cdot \dot{p}(t) + 0.8 \cdot (t) \tag{7.2}$$

where, p(t) and $\dot{p}$(t) represent hand position and velocity vectors in extrinsic coordinates, and γ(t) represents the vector of vibration intensity that is mapped into the four-actuators vibrotactile interface as a function of time. Indeed, the sign and the value of each element of γ(t) determined which actuator was turned on and its vibration intensity, since each actuator coded a certain direction (see subsection 7.2.4). This particular weighting of position and velocity information was found to yield optimal performance during reaching and stabilizing tasks performed by neurologically-intact individuals [42]. The center of the vibrotactile workspace (i.e., the point where the vibration of all actuators was zero if the hand was held in that position) was aligned with both the center of the visual screen and the center of the robot's workspace. Vibratory stimulation reached 90% FSR when the hand was held at the bounds of the visual display, 60% FSR at the far targets, and 30% FSR at the close targets.

Error feedback Here, vibratory stimuli encoded information about the signed error between the hand's instantaneous location and the current target's location. The vibration was zero when the hand was at the center of the current target, and its intensity increased in

proportion to the Euclidean distance from that target. Vibratory stimulation reached 90%, 60%, and 30% FSR when the hand was 15, 10, and 5 cm respectively from the then-current target. With error feedback, the vibratory stimuli conveyed no information about hand velocity. Error feedback provided information only about hand position relative to the target, which changed from one trial to the next in the reaching task.

7.2.5 Protocol

Each participant took part in two experimental sessions in two separate days lasting up to 90 minutes each. One participant volunteered to participate in a third session, which assessed the possibility of day-over-day performance improvements (i.e., sensorimotor learning) in the integration of supplemental vibrotactile kinesthetic feedback into the control of reaching movements after stroke. All sessions were performed within three weeks of the clinical evaluation. During each session, the type of vibrotactile feedback (state or error) did not change within an experimental session: in the first session, all participants experienced state feedback, while all participants experienced error feedback in the second (and later) session(s). In each session, the participants performed several blocks of trials in three experimental phases, each with different visual feedback conditions and purposes. These phases included familiarization, practice, and assessment. Each phase was composed of one or more trial blocks wherein participants performed stabilization and/or reaching tasks under a specific combination of vibroTactile (T) and Visual (V) feedback. The protocol performed by each participant varied in the number of blocks performed within each phase due to differing levels of stamina between participants and across testing sessions (see Table 7.4 for details).

Familiarization (V+T-)

In the familiarization phase, participants completed the reaching and the stabilization tasks without vibrotactile feedback (T-). They were provided visual feedback of hand position (V+) through a 0.5 cm radius cursor that was continuously visible on the computer screen. This block was performed in the first experimental session; it was intended to ensure that participants understood the two tasks. It was offered to all participants to repeat this phase at the beginning of the later session(s) but all declined, indicating that they understood and were comfortable repeating the reaching and stabilization tasks.

Table 7.4 The sequence of testing conditions in each participant

	Day:Encoding	Familiarization V+T-	Practice V_{KR}T+		V-T-	Baseline V-T+	Test
S01	Day1:State	R+S	R	R		R+S	R+S
	Day2:Error		R	R		R+S	R+S
S02	Day1:State	R+S	R	R	R	R+S	R+S
	Day2:Error		R	R	R		R+S
S03	Day1:State	R+S	R			R+S	
	Day2:Error		R	R	R		R+S
	Day3:Error		R	R	R	R+S	R+S

The order of the blocks corresponds to the timeline in which the blocks were presented in the experimental session; Abbreviations: V+T-:concurrent visual feedback without vibrotactile feedback; R: reaching, S: stabilization; V_{KR}T+: vibrotactile feedback and visual knowledge of results; V-T-: neither visual nor vibrotactile feedback; V-T+: only vibrotactile feedback.

Practice (V_{KR}T+)

In the practice phase, the participant performed at least two blocks of the reaching task with the vibrotactile feedback always on (T+). The practice phase did not include the stabilization task. Real-time visual feedback of hand position was provided on the screen only after the end of each trial (i.e., Knowledge of Results (KR); V_{KR}). Subjects were encouraged to use the terminal visual feedback to correct any target capture error that may have accrued during the initial reach. The goal of this phase was to encourage participants to learn the mapping between hand position and the information encoded in the vibrotactile feedback.

Assessment (V-)

After practice, participants underwent an assessment phase, wherein they performed the reaching and stabilization tasks without any visual feedback (V-) during or after each reach. The cursor representing hand position/motion was never displayed on the screen, knowledge of results was not provided, and actual vision of the hand was precluded by the opaque shield (see Fig. 7.1a). This phase was divided into two separate blocks, one with vibrotactile feedback and the other without. In the first block (Baseline), the participants did not receive any external visual or vibrotactile feedback (V-T-). The goal of this block was to assess the baseline capability of the participants to complete the tasks using only their residual inherent proprioception. In the second block (Generalization), the vibrotactile feedback was turned back on (V-T+). The goal of this block was to test the participant's ability to generalize what

they learned during practice with vibrotactile feedback (state or error) and visual KR to a condition entirely devoid of visual feedback.

7.2.6 Self-report evaluation of vibrotactile feedback

At the end of each experimental session, we encouraged participants to orally report their participantive perceptions by asking three open questions regarding the use of the vibrotactile encoding scheme experienced in the session. We focused on two main aspects of the participantive user experience: usability, and user satisfaction. To assess usability, we asked participants 'how easy it was to perceive changes in the vibrotactile signals' and 'how easy it was to use those cues to achieve the goals in each task'. To assess user satisfaction, we asked participants 'on which the extent the vibrotactile feedback system was comfortable to use'.

7.2.7 Data analysis

Hand position data were recorded at 1kHz. The resulting data were subsequently filtered with a zero-phase fourth-order Butterworth low-pass filter with a cut-off frequency of 12 Hz. We computed the following performance measures for each trial for each participant under the two vibrotactile encoding schemes. In the reaching task, we computed the final position error as the Euclidean distance between the final hand position and the center of the current target. The final hand position was taken as the hand's location either when the participant indicated that the target had been reached or when the time for completing the trial had expired, whichever came first. In the stabilization task, we computed root-mean-square-error to assess how well participants could maintain the hand at the desired target. To compute RMSE, we discarded the first 10 seconds of each 60-second trial to eliminate potential start-up transients caused by the onset of hand force perturbations (cf., [42]). We then divided the trial into five non-overlapping 10-second segments and computed the RMSE between the hand's instantaneous location and the stabilization target (i.e., the center of the workspace). We evaluated the trial RMSE using the mean and standard error values computed from the RMSE values obtained in the five 10-second segments. We used a single-subject-design analysis to evaluate changes in task performance due to the presence of the vibrotactile feedback. Our primary focus was on the assessment blocks performed without visual feedback. We investigated differences in performance between trials with and without supplemental vibrotactile feedback (i.e., between the Generalization and Baseline blocks), and between Generalization blocks with different vibrotactile feedback encoding schemes (i.e., error vs. state feedback). Secondarily, we focused on the practice blocks,

to investigate learning effects as participants practiced reaching with vibrotactile feedback within and across days.

7.3 Results

Subjective evaluation of supplemental vibrotactile feedback

User satisfaction

All three participants tolerated the vibratory stimuli with no complaints of hypersensitivity or discomfort. When we asked participants to report on the extent to which the vibrotactile feedback system was comfortable to use, all three stated that using the supplemental vibrotactile feedback to guide the arm was an overall mild positive experience. One participant (S03) did report mild annoyance when vibrations were at their highest intensity levels, saying that the vibrations felt like "a bright light or a loud noise" and that they were a little "distracting".

Usability

All three participants reported that they were able to perceive the vibrotactile feedback applied to the ipsilesional arm. For two of the participants, vibration perception was satisfactory with the actuators placed in their default locations. One of the participants (S01) experienced initial difficulty perceiving vibrations on the external forearm and the upper arm. We, therefore, adjusted the position of these actuators by moving them approximately two centimeters in different directions until the participant could reliably perceive changes in vibration intensity. We also adjusted the elastic band on the internal forearm actuator to increase the applied pressure to allow this participant to more effectively perceive the vibration stimuli. When we asked how easy it was to perceive changes in the vibrotactile signals, all of them responded that error feedback was easier to understand and use than state feedback. S02 remarked that his vibrotactile sensitivity improved with practice, whereas the other two participants reported a modest perceived degradation in vibrotactile sensitivity after approximately one hour of continuous practice. S02 and S03 reported an increase in alertness or general body awareness while using the supplemental vibrotactile feedback, and that this effect persisted for some time after the experimental session was over. However, these same two participants also reported difficulty in dividing attention between "feeling" the vibration on one limb and executing movements with the other. S01 and S03 both expressed difficulty in integrating

simultaneous visual and vibrotactile inputs, as occurred in between trials in the Practice blocks (V_{KR}T+).

General observations on kinematic performance with and without ongoing visual feedback

All three participants demonstrated sufficient motor capability to perform the reaching task with small target capture errors (i.e., with final position error less than 1 cm) and with stereotypically-straight hand paths when they were provided visual feedback of ongoing performance (Fig.7.2a; Familiarization phase, F: V+T-). All three were also able to stabilize their hand with small positioning errors when provided visual feedback of ongoing performance (Fig.7.2b; F: V+T-); despite the force perturbations in the stabilization task, average RMSE values did not exceed 2.5 cm when ongoing cursor feedback was provided. By contrast, kinematic performance degraded dramatically during both reaching and stabilizing when all extrinsic feedback was eliminated (Fig.7.2; Baseline assessment, B: V-T-). As we will show, the participants exhibited varied levels of success when interpreting and using supplemental state- and error-feedback for closed-loop control of the contralesional arm. No systematic improvements in baseline performance without visual feedback were observed from one day to the next.

Effects of supplemental kinesthetic feedback on the performance of reaching and stabilizing tasks

All participants learned to interpret and use at least one of the vibration feedback encodings to successfully perform the reaching and/or stabilizing tasks. Some were able to use the vibrotactile information to control the arm more readily, whereas others required more time and practice to do so. There were striking differences between participants regarding the effects of supplemental kinesthetic feedback on task performance and regarding the effects of practice using the supplemental feedback. We, therefore, describe the pattern of results separately for each case in the paragraphs to follow.

S01

Reaching. During baseline assessment (i.e., in the absence of all extrinsic feedback), S01 performed inaccurate reaches that were generally shorter than those required to perform the cued task. These movements were also shifted relative to the intended start and goal

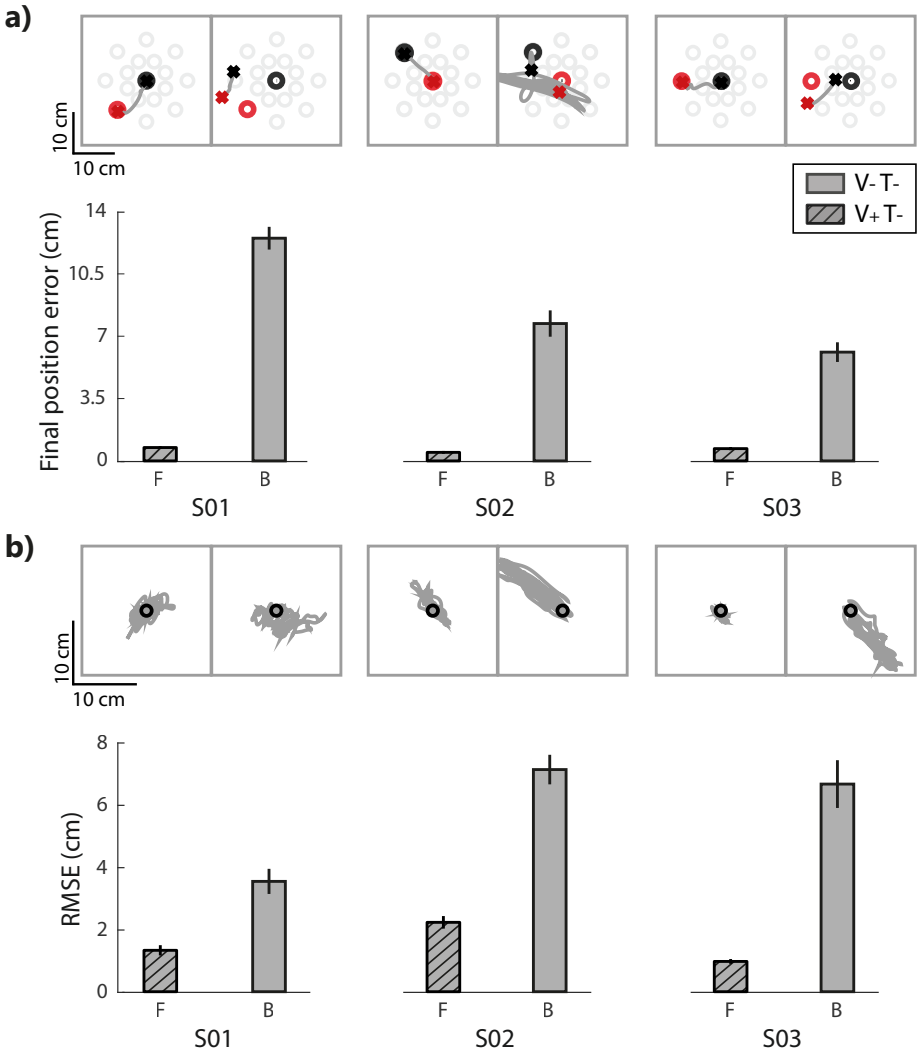

Figure 7.2 Familiarization and baseline phase performance for the reaching and stabilizing tasks for each participant. a) Reaching task performance. Top row: examples of hand paths for the Familiarization block (F; left) performed with only visual feedback and the Baseline block (B; right) performed in absence of extrinsic feedback. Results for each participant are presented in separate columns. Start and stop targets are represented by black and red 'o' symbols, respectively. The start and stop positions of the corresponding hand movements are represented by 'x' symbols. Bar charts on the bottom row: Final position error averaged within the familiarization and baseline blocks. Error bars: mean ± SE. b) Stabilization task performance. Top row: the black circle in the center of the workspace where the hand should be stabilized. Hand paths during the stabilization period are shown in grey. Bottom row: root mean square error (RMSE) averaged across consecutive 10 second stabilization intervals. Results for each participant are presented in separate columns.

targets (Fig. 7.3a; Baseline, B). This result is consistent with previous observations of "proprioceptive drift" [362], which is thought to arise due to an accumulating misalignment of visual and proprioceptive representations of limb position. Adding visual KR to either form of real-time supplemental vibrotactile feedback mitigated the drift effect to a large extent, primarily by shifting the initial hand position back to the desired starting location (Fig. 7.3a; Practice, P). This mitigation was evidently due to the visual KR and not to the presence of supplemental kinesthetic feedback because drift in the hand's initial position re-established rapidly when only vibrotactile feedback was provided (Fig. 7.3a; Generalization, G). These single-trial observations were consistent within each testing day (i.e., for both encoding schemes of vibrotactile feedback; Fig. 7.3c). Note that this participant decreased final position error in the generalization blocks by 16.1% with error feedback relative to her baseline trials (which are represented by the upper grey horizontal band in Fig. 7.3c), whereas final position errors increased by 6.3% with state feedback relative to baseline performance.

Stabilization. Fig. 7.3b shows individual stabilization trials for each phase in the two experimental sessions. Differences in generalization block performance between the two vibrotactile feedback encodings were more dramatic in stabilization than in reaching. Hand deflections were smaller in magnitude and less shifted with respect to the center of the workspace when this participant stabilized the hand with error feedback as compared to state feedback. These observations were reflected in the RMSE values, which decreased by 41.6% with error feedback relative to baseline and increased by 67.2% in the state feedback test block relative to baseline (Fig. 7.3d). The increase in RMSE with state feedback testing was largely due to a reappearance of hand positioning errors accruing in the absence of visual feedback.

In summary, S01 was able to interpret and use vibrotactile error feedback to enhance closed-loop control of contralesional arm reaching and stabilization actions in just one experimental session. By contrast, limb state feedback did not as rapidly enable improved performance in the absence of visual feedback on either task relative to V-T- baseline trials.

S02

Reaching. S02 persistently made multiple corrective movements when reaching in the absence of concurrent visual feedback - with or without supplemental kinesthetic feedback. Reach performance degraded substantially when vision was removed, and this participant was unable to capitalize on either form of supplemental kinesthetic feedback to reduce target capture errors (Fig. 7.4a). Even adding visual KR in the practice blocks failed to mitigate the performance degradation within a single session of practice with either kinesthetic encoding

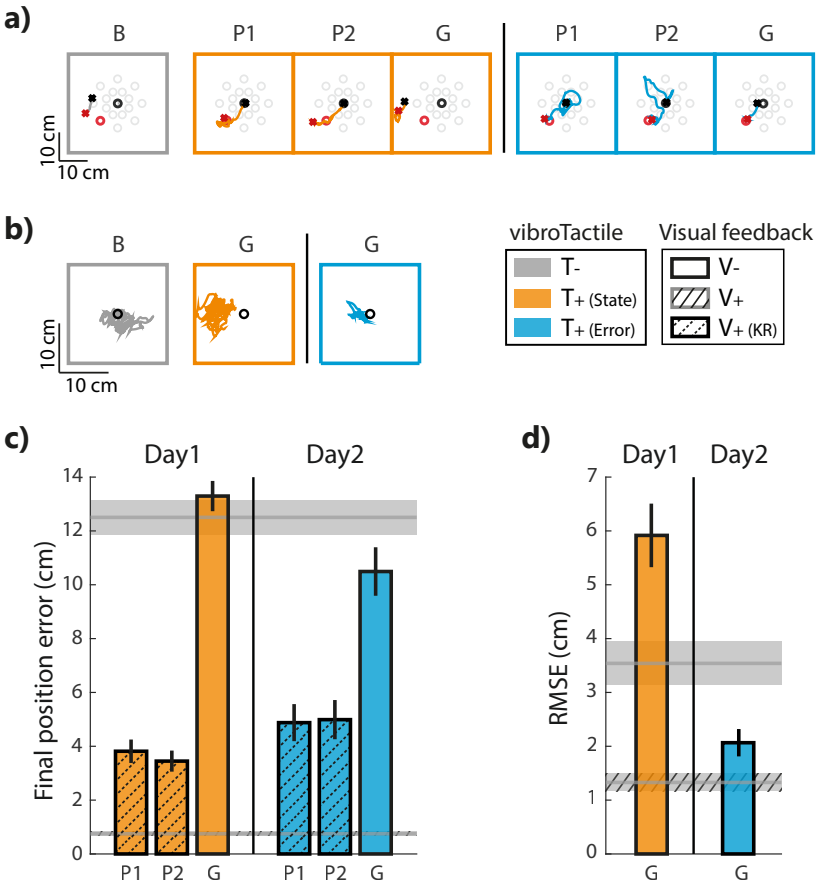

Figure 7.3 Individual results for S01. a) example hand paths for the Baseline (B), Practice (P), and Generalization (G) blocks in the reaching task. b) example hand paths for the Baseline (B) and Generalization (G) blocks in the stabilization task. Orange: state feedback condition; Blue: error feedback condition; Gray: no vibrotactile or visual feedback. c) Mean ± SE final position error for the reaching task; d) Mean ± SE root mean square error for the stabilization task. As before, color coding indicates the type of vibrotactile feedback provided. Upper horizontal gray patch: mean ± SE of performance in the Baseline block of trials without visual or vibrotactile feedback. Lower (dashed) horizontal gray patch: mean ± SE of performance in the familiarization block of trials (i.e., with concurrent visual feedback).

scheme. Error feedback appeared to confound this participant more than state feedback during reaching (Fig. 7.4c).

Stabilization. The performance also degraded in the stabilization task during baseline assessment without concurrent visual feedback; hand deflections became larger and displaced relative to the center of the workspace (Fig. 7.4b). In contrast to this participant's performance in the reaching task, stabilization improved markedly using state vibrotactile feedback (a

40.2% reduction in RMSE relative to the no-feedback baseline trial), mainly by reducing hand position drift (Fig. 7.4d, Day 1). By contrast, error feedback led to a 13.2% increase in RMSE relative to baseline trials. While both encodings convey information primarily about the hand's position relative to the center of workspace in this task, only state feedback includes velocity information that accentuates changes in hand position, which may have helped this participant perform more effective error correction when stabilizing.

Thus, while S02 was able to exploit supplemental limb state feedback to improve stabilization of the contralesional arm, he was unable to use error feedback effectively in that task. S02 was unable to use either encoding scheme to improve performance in the reaching task.

S03

When S03 experienced state feedback during the first experimental session, she tried to nullify the vibratory stimulation as if she were receiving error feedback. This behavior was persistent; even after repeated explicit instructions on how to use state feedback, S03 declared that state feedback was confusing, that it required high cognitive effort, and that she preferred not to continue using state feedback. The experience did not dampen S03's willingness to participate in the study because she agreed to perform the second experimental session with error feedback and she also volunteered to attend the third session. The Day 3 session repeated the Day 2 protocol using error feedback.

Reaching. As for the other two participants, removing continuous visual feedback strongly degraded S03's reaching performance, resulting in longer and shifted hand paths relative to the desired start and final positions. With state feedback, S03 hardly moved from the starting point in the first experimental session (Fig. 7.5a) clustering most of the final hand positions close to the center, i.e., where the vibration was absent. When presented on Days 2 and 3 with supplementary error feedback and concurrent visual KR, this participant improved reach performance within each experimental session. The final position error in the third practice block was lower by 19.2% with respect to the first practice block on day 2, and by 22.7% on day 3 (Fig. 7.5c). In the last practice block on Day 3, the final position error averaged 20.2% lower than during baseline assessment. Any beneficial effect of practice was likely due to the presence of terminal visual KR for this participant because removing visual KR during the generalization trials effectively eliminated the positive training effect observed during the practice blocks. Performance in the generalization assessment block did not differ from baseline (with final position errors being only 7.4% and 1.1% lower in the generalization assessments of day 2 and 3, respectively). We observed no clear day-over-day improvements in reach performance during practice with error feedback in this participant.

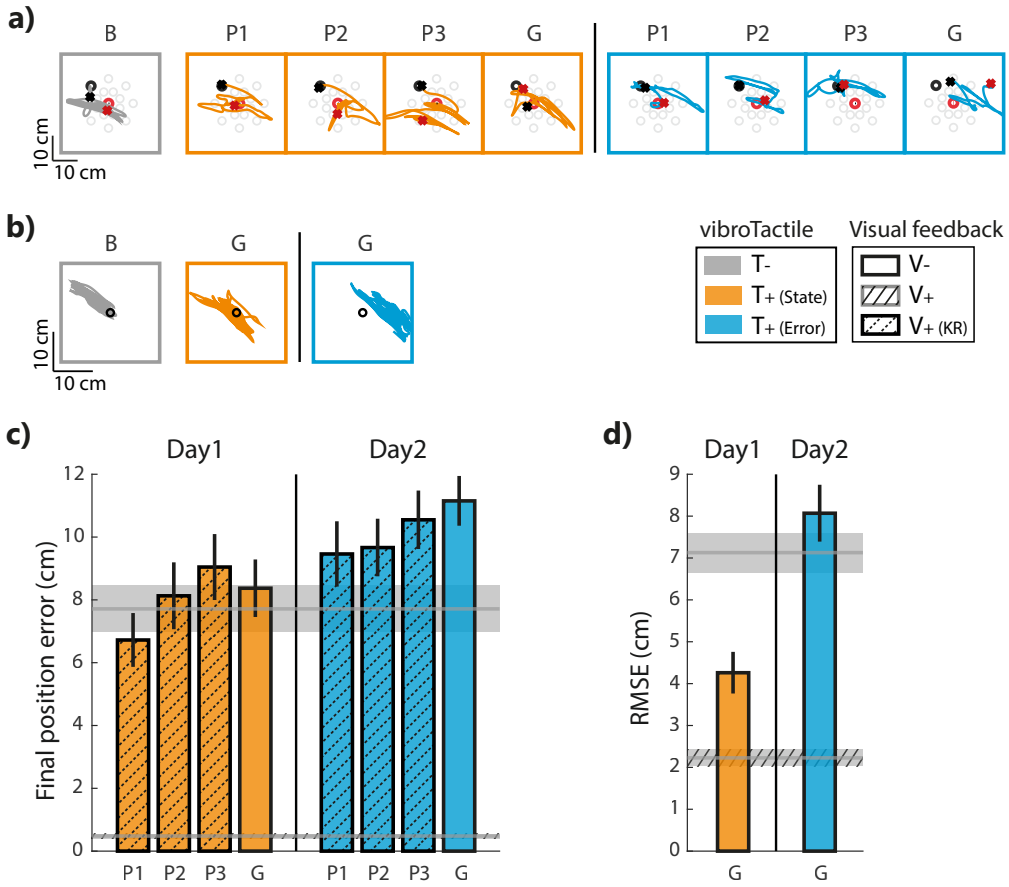

Figure 7.4 Individual results for S02. a) example hand paths for the Baseline (B), Practice (P), and Generalization (G) blocks in the reaching task. b) example hand paths for the Baseline (B) and Generalization (G) blocks in the stabilization task. Orange: state feedback condition; Blue: error feedback condition; Gray: no vibrotactile or visual feedback. c) Mean ± 1 SE final position error for the reaching task; d) Mean ± SE root mean square error for the stabilization task. As before, color coding indicates the type of vibrotactile feedback provided. Upper horizontal gray patch: mean ± SE of performance in the Baseline block of trials without visual or vibrotactile feedback. Lower (dashed) horizontal gray patch: mean ± SE of performance in the familiarization block of trials (i.e., with concurrent visual feedback).

Stabilization. In the stabilization task - as in reaching - this participant relied heavily on visual feedback. During baseline assessment (i.e., in the absence of all extrinsic feedback), hand deflections became larger with respect to the familiarization trial block and displaced relative to the central target (Fig. 7.5b; Baseline assessment, B). The application of supplementary error feedback partially mitigated this effect, leading to a lower RMSE in the generalization block (19.1% lower than in the baseline block; Fig. 7.5d). With repeated practice using error

feedback (i.e., on Day 3), the hand's position was much better stabilized on the workspace center, leading to an RMSE 48.8% lower than in the baseline trials, reflecting a substantial day-over-day learning effect.

In summary, while S03 was confounded by supplemental limb state feedback, she was able to properly interpret error feedback and use it to improve arm stabilization performance to a modest extent after a single day's training, and to a larger extent after two days of training.

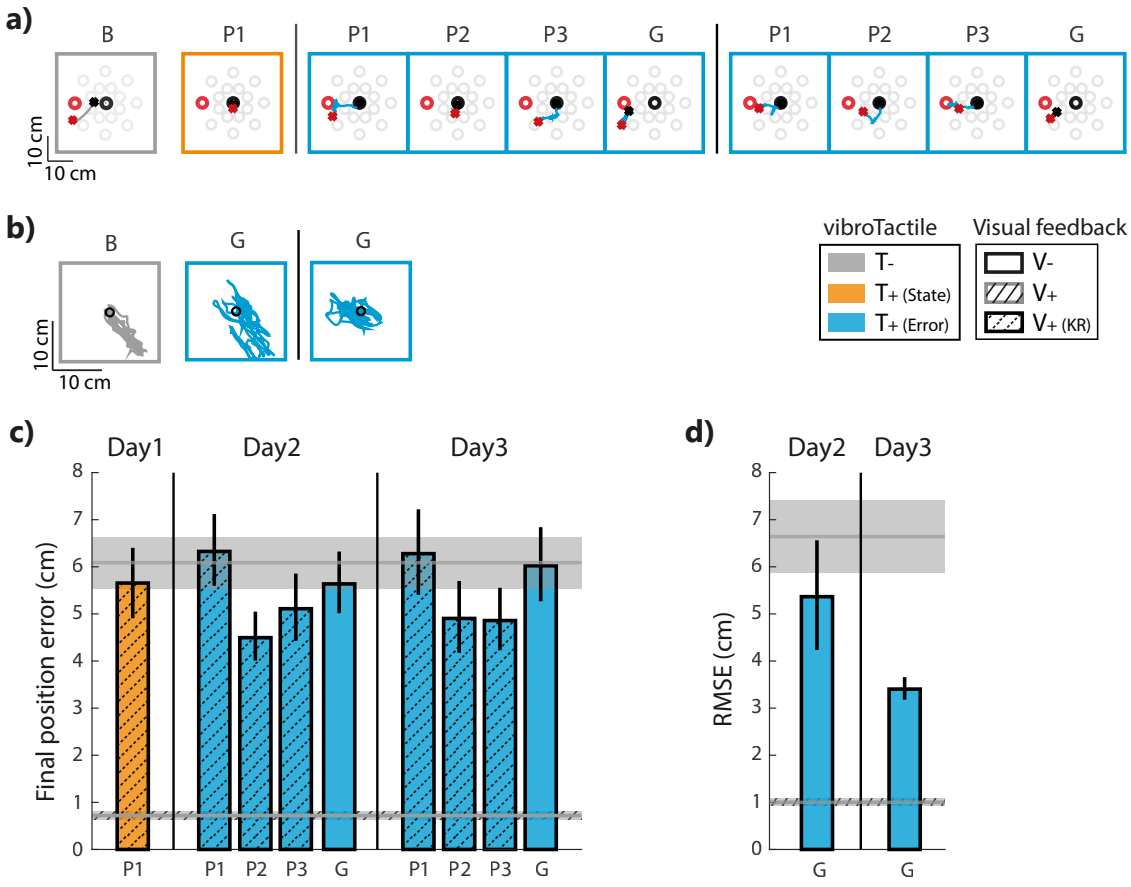

Figure 7.5 Individual results for S03. a) example hand paths for the Baseline (B), Practice (P), and Generalization (G) blocks in the reaching task. b) example hand paths for the Baseline (B) and Generalization (G) blocks in the stabilization task. Orange: state feedback condition; Blue: error feedback condition; Gray: no vibrotactile or visual feedback. c) Mean ± SE final position error for the reaching task; d) Mean ± SE root mean square error for the stabilization task. As before, color coding indicates the type of vibrotactile feedback provided. Upper horizontal gray patch: mean ± 1 SE of performance in the Baseline block of trials without visual or vibrotactile feedback. Lower (dashed) horizontal gray patch: mean ± SE of performance in the familiarization block of trials (i.e., with concurrent visual feedback).

7.4 Discussion

This study evaluated the ability of three stroke survivors to interpret and use supplemental vibrotactile feedback to enhance the accuracy and precision of stabilizing and reaching actions performed with the contralesional arm and hand in the absence of visual feedback. The supplemental kinesthetic feedback had objective utility in the sense that after only minutes of practice, each of the participants was able to interpret and use at least one type of feedback to improve performance in one task. However, the participants differed with regards to which form of information encoding enhanced performance. One participant demonstrated the ability to interpret and use error feedback to improve the accuracy of reaches; none of them successfully used state feedback to improve reach accuracy within the short 1-hour time frame of a single experimental session. In the stabilization task, where the two feedback is similar except for the hand velocity information, which is included only in the state feedback, one of the participants performed best when vibrations encoded hand position and velocity, whereas the other two performed better when vibrations were encoded only hand position errors. For two stroke survivors, who experienced both feedback modalities in both tasks, the subjective preference for one feedback modality over the other is consistent between the two tasks, this could be related to a preference for the information content and/or it may be related to the participants' motor ability. For example, [42] found that the absence of velocity information yielded to superior performance in healthy participants performing stabilization task and here, the stroke survivor with the higher motor ability had the same results. Nevertheless, all three participants reported that using supplemental vibrotactile kinesthetic feedback yielded a positive user experience. When asked to compare the two encoding schemes, all three participants reported that error feedback was easier than state feedback to understand and use. Improvement of stabilization performance across repeated sessions in one participant suggests that the integration of supplemental kinesthetic feedback into the ongoing control of the arm is a skill that can be learned with practice. Taken together, these results demonstrate that a wearable system providing supplemental kinesthetic feedback can have objective utility for enhancing the control of reaching and stabilizing actions performed with the arm and hand after stroke, while also providing a favorable user experience.

Human performance enhancement through vibrotactile cueing

A growing body of research has sought to use vibrotactile stimuli to enhance human performance in healthy individuals (e.g., [363, 364]) or to overcome sensorimotor deficits in

patients (e.g., [205, 365, 366]. In some cases, uninformative "noisy" stimuli have been used to enhance somatosensory sensitivity to faint stimuli through stochastic resonance ([309]) or to improve motor coordination by enhancing cortical modulation of spinal reflex activity (c.f., [30]). In other cases, important aspects of task performance were encoded into vibrotactile "alerts" intended to increase the user's situational awareness [239, 363, 367], or into a continuous stream of vibrotactile cues intended to either teach desirable skills that should persist after the vibrotactile stimuli are removed [206, 365, 368, 369] or to enhance sensorimotor performance through permanent feedback devices designed to be used indefinitely like a prosthesis [370]. The system tested in this study is of the last type in that it is intended to be worn continuously as a real-time sensorimotor control aid, and to provide continuous benefit while worn. We found that after only minutes of practice, all three stroke survivors were able to interpret and use vibrotactile cues to enhance modestly the control of upper limb reaching and/or stabilizing actions in the absence of concurrent visual feedback. How is this possible?

A recent review of sensory augmentation applied to human balance control highlights four potential mechanisms of action [371], which we now consider as potential means by which supplemental vibrotactile kinesthetic feedback might have enhanced control of upper limb reaching and stabilization in this study.

A first possibility, "sensory restoration", implies the full restoration of missing sensory information [371]. In the case of upper limb reaching and stabilizing, this would require the restoration of proprioceptive feedback pathways serving muscle spindle primary (Ia) and secondary (II) afferents, Golgi tendon organs, and the various cutaneous mechanoreceptors (cf. [52]). While our limb state feedback encoding was inspired by the biological encoding of displacement and rate-of-displacement information by muscle spindle primary afferents [42], the application of vibrotactile stimuli in our studies is optimized to preferentially excite Pacinian corpuscles [42, 43] rather than directly engaging muscle spindles, tendon organs and their afferent pathways. We do not suggest that we somehow reactivate injured somatosensory feedback pathways through the application of supplemental vibrotactile feedback. The effectiveness of our approach was not driven by sensory restoration.

A second possibility, "sensory integration", refers to the optimization of sensorimotor control through a guided re-weighting of intact afferent signal pathways [371]. Exposure to supplemental kinesthetic feedback during the performance of specific actions would provide the CNS with task-related vibrotactile stimuli that are strongly correlated with residual (intact) afferent signals. Repeated success on tasks performed with supplemental kinesthetic stimuli would promote increased weighting of the intact sensory channels, thereby promoting increased reliance on residual intrinsic pathways during the performance of the

practiced tasks, and possibly during the performance of unpracticed tasks. It is expected therefore that training with sensory augmentation would lead to beneficial changes in sensory integration that are maintained even without continued use of the sensory prosthesis [371]. We do not believe that sensory integration contributed significantly to the effectiveness of supplemental kinesthetic feedback in our current study because participants demonstrated enhanced performance after just a few minutes of practice. This does not seem to be a sufficient amount of time to drive substantially increased reliance on residual afferent signals. Moreover, we did not observe systematic improvements in baseline performance from one day to the next, as would be expected if short bouts of training with the supplemental kinesthetic feedback had led to greater reliance on residual (intact) proprioceptive afferent signals.

A third possibility, "sensory substitution", refers to the synthesis and delivery of artificial motion information replacing that of a damaged source [371]. The idea here is to circumvent injured sensorimotor feedback pathways by encoding motion information into stimuli that the CNS can integrate into the implicit planning and control of the action. Ideally, the supplemental stimulus encoding would sufficiently replicate the information lost due to injury such that the CNS would draw upon the supplemental information source instead. Likely, however, is the case that the supplemental stimuli will differ in meaningful and significant ways from the lost intrinsic signals - such as with respect to the embedded reference frame (e.g., retinocentric vs. body-centered encodings; [372]). In this case, participants would need to learn novel mappings between changes in motor variables (e.g., muscle activations), movement kinematics (joint rotations), and changes in the supplemental kinesthetic feedback (e.g., [373–375]). While people can learn visuomotor rotations after some tens of movements [376, 377] and they can learn truly novel visuomotor mappings for planar target capture tasks after several hundred movement attempts (c.f., [374, 375]), we expect that full integration of vibrotactile feedback into the ongoing control of reaching and stabilization will be a skill that will likely require hours of practice to fully acquire. A recent study [378] on stroke survivors highlighted that in 1D tracking task, a 2-day training with supplementary vibrotactile feedback encoding the position and velocity of the cursor with respect to the target, can induce measurable improvement in the perceptive ability. However, they used different actuators for encoding the position and velocity (i.e., two actuator for encoding the 1D position of the cursor with respect to the target on the arm used for performing the task and an additional actuator on the other arm to encode the velocity of the cursor). This decoupling of the positional and velocity information could play an important role in the efficacy of the feedback. Differently from this study, they focused on the improvement in

term of perceptive ability, while we focused on the motor outcome of the proprioception. Hence, they did not found evidence that the somatosensory learning transfers to untrained motor tasks.

In this study sensory substitution might have played some role - especially for participant S03 as described below - however, the fourth possibility, "cognitive processing", most likely conferred immediate utility to supplemental vibrotactile kinesthetic feedback for stabilization (all three participants) and reaching (S02) with the contralesional arm.

"Cognitive processing", refers to the development of conscious associations and rules governing voluntary response to the supplemental vibrotactile kinesthetic stimuli. The same set-up procedure that allowed us to verify that participants could perceive unique vibrotactile stimuli at each of the four stimulus locations also allowed the participants to learn how the intensity of vibration at each location mapped onto hand deviations from the desired location. At the end of the set-up procedure, each participant was required to place the cursor at the center of the screen, and then, move away from that location in each cardinal direction to begin to learn the mapping between changes in hand position and changes in vibrotactile stimulation. Indeed, at the end of reach testing, S02 described how he implemented a specific cognitive strategy to independently and sequentially resolve performance errors along each cardinal axis of the vibrotactile interface. First, he moved in the left/right direction so that he could attend to one pair of vibrators, and then he moved in the anterior/posterior direction so that he could attend to the other set of vibrators. This "decomposition strategy" for minimizing target capture errors was adopted also by healthy individuals in a prior study using the same vibrotactile display [43].

S03 also described strategic cognitive strategies for solving the reaching and stabilization tasks. Specifically, S03 reported that performing the reaching and stabilization tasks imposed a cognitive load like a dual-task. While S03 indicated that she was able to feel the vibrations at the beginning of the study, and while she could correctly describe what the vibrations meant, she had difficulty transferring the information from perception to action: “as if my brain does ’feel vibration’ and ’moves arm’ separately". However, with practice, S03 solved this problem with different strategies for the two tasks. When reaching, she stated that she focused her attention on the vibrations instead of the residual sensation of movement. During stabilization, by contrast, she stated that she focused her attention on the moving arm without paying as much attention to the vibrations. This outcome is remarkable because, despite her low scores on the clinical NSA tests of somatosensation, two days of practice with supplemental vibrotactile kinesthetic feedback led to stabilization test trial performance that was markedly better than baseline performance without the vibrotactile stimuli. As noted by

[371], more than one of the sensory augmentation mechanisms can occur simultaneously, and we speculate that the strategic focus of S03 on residual sensations in her contralesional moving arm may have promoted mechanisms of sensory substitution and/or sensory integration. In any event, these promising pilot results motivate future controlled studies designed to quantify the potential contributions of sensory integration, sensory substitution, and cognitive processing to the benefits of supplemental vibrotactile kinesthetic feedback that may accrue as participants practice reaching and stabilizing with their contralesional arm after stroke.

Limitations

This study had several notable limitations in addition to the small number of participants, which limits the possibility to draw a general conclusion. First, all the participants were exposed to state feedback on the first testing day and error feedback on the second (and later) testing day(s). We acknowledge that this ordering could have biased subjective assessments and objective performance toward error feedback because participants had more practice on the tasks overall by the time they were introduced to error feedback. Future studies comparing the utility and usability of state and error feedback encoding should counterbalance their presentation order across participants to mitigate potential order effects. A second limitation is that each participant performed a slightly different protocol from the others (see Table 7.4), e.g., one participant performed a different number of practice blocks and another participant did not perform stabilization with state feedback. Future studies should be designed with a fixed number of blocks of trials, which will allow being performed in a reasonable amount of time. A third limitation is that the current study was structured only to test whether a convenience sample of chronic stroke survivors could find supplemental vibrotactile kinesthetic feedback useful and usable for enhancing the kinematic performance of reaching and stabilizing behaviors performed with the contralesional arm. The study was not designed to elucidate potential mechanisms by which supplemental vibrotactile kinesthetic feedback may enhance kinematic performance. Future studies should include additional test conditions and several days of training to determine the extent to which observed benefits of supplemental feedback may be due to sensory integration, sensory substitution, and/or cognitive processes. For example, by including V-T- baseline blocks of trials before and after each day of VKRT+ training on a given encoding scheme, it would be possible to determine the time course and extent to which supplemental kinesthetic feedback training leads to improved performance through a beneficial re-weighting of residual task-relevant somatosensory signals (pathways). By including appropriate dual-task testing

conditions and extended periods of training, it would be possible to determine the time course and extent to which integration of supplemental feedback into the planning and ongoing control of movement becomes automatic (i.e., less dependent on strategic cognitive transformations from perception to action dependent on attentional resources; c.f., [302]). Reducing cognitive load would make the proposed technology easier to use and more practical for applications where users must also be responsive to the external and uncontrolled environment. The results presented here in a small cohort of participants suggest that many stroke survivors can perceive vibrotactile stimulation applied to the ipsilesional arm, can come to understand how to interpret it to control goal-directed behaviors performed with the contralesional arm, and that performance improvement in reaching are seen across multi-day practice sessions. Future multi-session learning studies will need to be conducted to extend these results to a larger cohort of stroke survivors, to minimize potential order effects, and to allow participants the time to develop the skill needed to autonomously integrate supplemental kinesthetic feedback into ongoing control of the arm and hand while performing real-world tasks in unstructured environments. We are encouraged in this goal because all three stroke survivors enrolled in this study found the vibrotactile feedback to be a positive experience, and some even reported secondary benefits in terms of alertness or body awareness. Such outcomes, if replicated in a larger cohort of stroke survivors, would support and encourage the use of vibrotactile feedback devices moving forward.

Discussion

The ability to coordinate force and position in bimanual tasks is essential for many daily-living activities. However, despite their importance and interconnection, in the usual formulation of assessment protocols, either in research or clinical environments, position and force sense are mainly evaluated separately while their possible interactions or interference have received less attention. Furthermore, in the current formulation of the neurological assessment protocol, proprioceptive functions are most often subjectively assessed by clinicians using qualitative clinical scales [7, 9] and the two arms are mainly evaluated separately without taking into account the bimanual coordination. This assessment limits the evaluation of the possible interactions or interference that arise from the inter-limb coordination [10, 12]. In addition to that, even if it is well known that the proprioceptive deficits interfere with motor planning, control and learning and lead sub-optimal functional recovery [3–8]. Rehabilitative treatments are more focus on motor retraining [379, 380], with only limited attention paid to mitigating proprioceptive deficits [381].

The findings of Ph.D. research project are a step to fulfill those gaps assessing different aspects of proprioception using different types of device and investigate how to enhance proprioception using supplementary vibrotactile feedback.

Hence, in my Ph.D. I characterized the bimanual proprioception using passive and actuated system in stroke survivors and unimpaired participants. The choice of using both passive and actuated device allowed me to assess different aspects of the proprioceptive ability. In fact, it is well known that proprioception differs in active and passive tasks due to many factors like, for example, the difference sources of signals, i.e., performance in passive movements resulted primarily from processing of afferent inputs, while during active movement also the efferent copy of the motor commands plays a key-role [168]. Thanks to that, we found that in bimanual passive tasks on unimpaired participants the position sense is influenced by the symmetry of the loading condition, while force control is mostly affected by the position of the non-dominant hand. Indeed, this latter findings is not

determined by handedness, but more likely by the specialization of the brain hemispheres even if handedness influenced the overall proprioceptive performance. In bimanual passive tasks on stroke survivors, we found that stroke affect the ability to match a level of force required, even when it is tailored on their capability, but not the ability to maintain it. Stroke also affect the ability to lift an object, in fact stroke survivors applied more force than age-matched unimpaired participants, while the timing in which the forces were applied was not significantly affected. An actuated device, instead, were used to assess proprioception without the motor component, i.e., the device performed the movement for the participants. This improve the repeatability of the stimuli and solve the lack of motion capacity of the participants. This actuated device was used to assess the position sense of the ipsilesional arm in stroke survivors, finding that t the ipsilesional arm of stroke survivors had similar matching accuracy but higher precision than the contralesional arm. The accuracy of the two arms inter-correlated in the left and central regions of the peripersonal space for all the stroke survivors independently of the location of the brain lesion.

The final goals of functional assessment is helping the understanding of the disease and the progress of the rehabilitative treatment. However, it is also important to tailor a rehabilitative treatment to restore proprioception. An effective and intuitive way to do so is applying a supplementary vibrotactile feedback. However, an important parameter of such type of feedback is how the information is encoded in the vibration. To better exploit this point in my Ph.D. research project I compared the effect of different method to encode the task performance in the vibration in stroke survivors and unimpaired participants. Furthermore, we found that the vibrotactile feedback encoding information on postural performance significantly improved the postural control, while vibration uncorrelated with the performance led to the opposite results, highlighting the importance of the encoded information. In a second study on stroke survivors, we found that the stroke survivors were able to perceive the vibrotactile feedback and to perform the motor tasks (i.e., reaching and stabilization) when it was applied, but they reached various levels of capability in distinguishing and using it during the motor tasks. These preliminary results encourage investigating the effects of a longer multi-session training with a personalized vibrotactile feedback design, based on preliminary proprioceptive assessment.

The work carried out in my Ph.D. research project highlighted the importance of assessing proprioception in both unimpaired participants and people with sensorimotor deficits. My findings enlarge the actual knowledge on interaction between the upper limb position sense and force control, and its asymmetries related to handedness and how it is affected after stroke. My Ph.D. research project also provide evidences to support the need to a assess both

ipsilesional and contralesional proprioceptive deficits separately and concurrently during bimanual tasks. This assessment is also fundamental for tailoring a rehabilitative protocol and an effective supplementary feedback.

References

[1] E. R. Kandel, J. H. Schwartz, T. M. Jessell, S. A. Siegelbaum, and J. A. Hudspeth, *Principles of neural science*. McGraw-hill New York, 4 ed., 2000.

[2] R. S. Johansson and R. J. Flanagan, "Coding and use of tactile signals from the fingertips in object manipulation tasks," *Nature Reviews Neuroscience*, vol. 10, no. 5, pp. 345–359, 2009.

[3] C. Ghez, J. Gordon, and M. F. Ghilardi, "Impairments of reaching movements in patients without proprioception. II. Effects of visual information on accuracy," *Journal of neurophysiology*, vol. 73, no. 1, pp. 361–372, 1995.

[4] J. E. Aman, N. Elangovan, I.-L. Yeh, and J. Konczak, "The effectiveness of proprioceptive training for improving motor function: a systematic review," *Frontiers in Human Neuroscience*, vol. 8, no. January, p. 1075, 2015.

[5] R. L. Sainburg, H. Poizner, and C. Ghez, "Loss of proprioception produces deficits in interjoint coordination," *Journal of neurophysiology*, vol. 70, no. 5, pp. 2136–2147, 1993.

[6] F. R. Sarlegna, G. M. Gauthier, C. Bourdin, J. L. Vercher, and J. Blouin, "Internally driven control of reaching movements: A study on a proprioceptively deafferented subject," *Brain Research Bulletin*, vol. 69, no. 4, pp. 404–415, 2006.

[7] S. P. Dukelow, T. M. Herter, K. D. Moore, M. J. Demers, J. I. Glasgow, S. D. Bagg, K. E. Norman, and S. H. Scott, "Quantitative assessment of limb postion sense following stroke," *Neurorehabilitation and Neural Repair*, vol. 24, no. 2, pp. 178–187, 2010.

[8] B. D. Cameron, C. De La Malla, and J. López-Moliner, "The role of differential delays in integrating transient visual and proprioceptive information.," *Frontiers in psychology*, vol. 5, no. February, p. 50, 2014.

[9] S. P. Dukelow, T. M. Herter, S. D. Bagg, and S. H. Scott, "The independence of deficits in position sense and visually guided reaching following stroke," *Journal of neuroengineering and rehabilitation*, vol. 9, no. 1, p. 72, 2012.

[10] S. P. Swinnen, "Intermanual coordination: from behavioural principles to neural-network interactions," *Nature Reviews Neuroscience*, vol. 3, no. 5, p. 348, 2002.

[11] R. G. Carson, S. Riek, and N. Shahbazpour, "Central and peripheral mediation of human force sensation following eccentric or concentric contractions," *Journal of physiology*, vol. 539, no. 3, pp. 913–925, 2002.

[12] J. E. Schaffer, F. R. Sarlegna, and R. L. Sainburg, "A rare case of deafferentation reveals an essential role of proprioception in bilateral coordination," *Neuropsychologia*, vol. 160, p. 107969, 2021.

[13] T. J. Boll, "Right and left cerebral hemisphere damage and tactile perception: Performance of the ipsilateral and contralateral sides of the body," *Neuropsychologia*, vol. 12, no. 2, pp. 235–238, 1974.

[14] J. P. Essing, J. W. Gersten, and P. Yarnell, "Light touch thresholds in normal persons and cerebral vascular disease patients: Bilateral deficit after unilateral lesion," *Stroke*, 1980.

[15] H. G. Vaughan and L. D. Costa, "Performance of patients with lateralized cerebral lesions. II: Sensory and motor tests," *Journal of Nervous and Mental Disease*, 1962.

[16] N. M. Lima, K. C. Menegatti, É. Yu, N. Y. Sacomoto, T. D. Oberg, and D. C. Honorato, "Motor and sensory effects of ipsilesional upper extremity hypothermia and contralesional sensory training for chronic stroke patients," *Topics in stroke rehabilitation*, 2015.

[17] S. Y. Schaefer, K. Y. Haaland, and R. L. Sainburg, "Ipsilesional motor deficits following stroke reflect hemispheric specializations for movement control," *Brain*, 2007.

[18] S. Y. Schaefer, P. K. Mutha, K. Y. Haaland, and R. L. Sainburg, "Hemispheric specialization for movement control produces dissociable differences in online corrections after stroke," *Cerebral Cortex*, 2012.

[19] S. Mani, P. K. Mutha, A. Przybyla, K. Y. Haaland, D. C. Good, and R. L. Sainburg, "Contralesional motor deficits after unilateral stroke reflect hemisphere-specific control mechanisms," *Brain*, vol. 136, no. 4, pp. 1288–1303, 2013.

[20] S. M. Son, Y. H. Kwon, N. K. Lee, S. H. Nam, and K. Kim, "Deficits of movement accuracy and proprioceptive sense in the ipsi-lesional upper limb of patients with hemiparetic stroke," *Journal of Physical Therapy Science*, 2013.

[21] E. L. Bustrén, K. S. Sunnerhagen, and M. Alt Murphy, "Movement Kinematics of the Ipsilesional Upper Extremity in Persons with Moderate or Mild Stroke," *Neurorehabilitation and Neural Repair*, 2017.

[22] S. Subramaniam, R. Varghese, and T. Bhatt, "Influence of chronic stroke on functional arm reaching: quantifying deficits in the ipsilesional upper extremity," *Rehabilitation Research and Practice*, 2019.

[23] D. B. Carvalho, S. M. Freitas, F. A. Alencar, M. L. Silva, and S. R. Alouche, "Performance of discrete, reciprocal, and cyclic movements of the ipsilesional upper limb in individuals after stroke," *Experimental Brain Research*, 2020.

[24] L. Nielsen, R. Khurana, A. Coats, S. Frokjaer, J. Brange, S. Vyas, V. N. Uversky, and A. L. Fink, "Effect of environmental factors on the kinetics of insulin fibril formation: elucidation of the molecular mechanism," *Biochemistry*, vol. 40, no. 20, pp. 6036–6046, 2001.

[25] C. Pacchierotti, S. Sinclair, M. Solazzi, A. Frisoli, V. Hayward, and D. Prattichizzo, "Wearable haptic systems for the fingertip and the hand: taxonomy, review, and perspectives," *IEEE Transactions on Haptics*, vol. 10, no. 4, pp. 580–600, 2017.

[26] H. Culbertson, S. B. Schorr, and A. M. Okamura, "Haptics: the present and future of artificial touch sensations," *Annu. Rev. Control Robot. Auton. Syst*, vol. 11225, no. 1, pp. 1–12, 2018.

[27] D. L. Jaffe, D. A. Brown, C. D. Pierson-Carey, E. L. Buckley, and H. L. Lew, "Stepping over obstacles to improve walking in individuals with poststroke hemiplegia.," *Journal of Rehabilitation Research and Development*, vol. 41, 2004.

[28] C. X. Rosado and L. Simone, "Translational haptic feedback for post-stroke rehabilitation," in *2007 IEEE 33rd Annual Northeast Bioengineering Conference*, pp. 259–260, IEEE, 2007.

[29] Q. Qiu, G. G. Fluet, S. Saleh, I. Lafond, A. S. Merians, and S. V. Adamovich, "Integrated versus isolated training of the hemiparetic upper extremity in haptically rendered virtual environments," in *2010 Annual International Conference of the IEEE Engineering in Medicine and Biology*, pp. 2255–2258, IEEE, 2010.

[30] M. O. Conrad, R. A. Scheidt, and B. D. Schmit, "Effects of wrist tendon vibration on targeted upper-arm movements in poststroke hemiparesis.," *Neurorehabilitation and neural repair*, vol. 25, pp. 61–70, jan 2011.

[31] M. R. Afzal, H. Y. Byun, M. K. Oh, and J. Yoon, "Effects of kinesthetic haptic feedback on standing stability of young healthy subjects and stroke patients," *Journal of NeuroEngineering and Rehabilitation*, vol. 12, no. 1, pp. 1–11, 2015.

[32] M. O. Conrad, B. Gadhoke, R. A. Scheidt, and B. D. Schmit, "Effect of tendon vibration on hemiparetic arm stability in unstable workspaces," *PLoS ONE*, 2015.

[33] C.-T. Hung, E. A. Croft, and M. H. F. Van der Loos, "A wearable vibrotactile device for upper-limb bilateral motion training in stroke rehabilitation: a case study," in *2015 37th Annual International Conference of the IEEE Engineering in Medicine and Biology Society (EMBC)*, pp. 3480–3483, IEEE, 2015.

[34] M. R. Afzal, H. Lee, A. Eizad, C. H. Lee, M. K. Oh, and J. Yoon, "Effects of vibrotactile biofeedback coding schemes on gait symmetry training of individuals with stroke," *IEEE Transactions on Neural Systems and Rehabilitation Engineering*, 2019.

[35] M. Takahashi, S. Kuroki, H. Nii, N. Kawakami, and S. Tachi, "Environmental type electro-tactile display for touchpanel interface," in *JSME Conference on Robotics and Mechatronics, 1P1-G05*, 2009.

[36] G. Wilson, M. Halvey, S. A. Brewster, and S. A. Hughes, "Some like it hot: thermal feedback for mobile devices," in *Proceedings of the SIGCHI Conference on Human Factors in Computing Systems*, pp. 2555–2564, 2011.

[37] I. Rakkolainen, A. Sand, and R. Raisamo, "A survey of mid-air ultrasonic tactile feedback," in *2019 IEEE International Symposium on Multimedia (ISM)*, pp. 94–944, 2019.

[38] M. Koehler, N. S. Usevitch, and A. M. Okamura, "Model-Based Design of a Soft 3-D Haptic Shape Display," *IEEE Transactions on Robotics*, 2020.

[39] T. K. Ferris and N. Sarter, "Continuously informing vibrotactile displays in support of attention management and multitasking in anesthesiology," *Human Factors*, 2011.

[40] O. B. Kaul and M. Rohs, "HapticHead: a spherical vibrotactile grid around the head for 3D guidance in virtual and augmented reality," in *Conference on Human Factors in Computing Systems - Proceedings*, 2017.

[41] V. Cobus, B. Ehrhardt, S. Boll, and W. Heuten, "Vibrotactile alarm display for critical care," in *Proceedings of the 7th ACM International Symposium on Pervasive Displays*, pp. 1–7, 2018.

[42] A. R. Krueger, P. Giannoni, V. A. Shah, M. Casadio, and R. A. Scheidt, "Supplemental vibrotactile feedback control of stabilization and reaching actions of the arm using limb state and position error encodings," *Journal of NeuroEngineering and Rehabilitation*, vol. 14, no. 1, p. 36, 2017.

[43] N. Risi, V. A. Shah, L. A. Mrotek, M. Casadio, and R. A. Scheidt, "Supplemental vibrotactile feedback of real-time limb position enhances precision of goal-directed reaching," *Journal of neurophysiology*, vol. 122, no. 1, pp. 22–38, 2019.

[44] S. A. Brewster and L. M. Brown, "Tactons: structured tactile messages for non-visual information display," in *Conference on Australasian user interface*, pp. 15–23, Australian Computer Society, Inc., 2004.

[45] C. B. Walter and S. P. Swinnen, "Asymmetric interlimb interference during the performance of a dynamic bimanual task," *Brain and Cognition*, vol. 14, no. 2, pp. 185–200, 1990.

[46] J. Diedrichsen, E. Hazeltine, W. K. Nurss, and R. B. Ivry, "The role of the corpus callosum in the coupling of bimanual isometric force pulses," *Journal of Neurophysiology*, vol. 90, no. 4, pp. 2409–2418, 2003.

[47] X. Hu and K. M. Newell, "Asymmetric interference associated with force amplitude and hand dominance in bimanual constant isometric force," *Motor Control*, vol. 16, no. 3, pp. 297–316, 2012.

[48] T. Tazoe, S. Sasada, M. Sakamoto, and T. Komiyama, "Modulation of interhemispheric interactions across symmetric and asymmetric bimanual force regulations," *European Journal of Neuroscience*, vol. 37, no. 1, pp. 96–104, 2013.

[49] K. M. Zackowski, A. W. Dromerick, S. A. Sahrmann, W. T. Thach, and A. J. Bastian, "How do strength, sensation, spasticity and joint individuation relate to the reaching deficits of people with chronic hemiparesis?," *Brain*, vol. 127, no. 5, pp. 1035–1046, 2004.

[50] R. A. Scheidt and T. Stoeckmann, "Reach adaptation and final position control amid environmental uncertainty following stroke," *Journal of neurophysiology*, vol. 97, no. 4, pp. 2824–2836, 2007.

[51] J. L. Taylor, "Proprioception," *Encyclopedia of Neuroscience*, pp. 1143–1149, 2009.

[52] U. Proske and S. C. Gandevia, "The proprioceptive senses: their role in sigaling body shape, body position and movement, and muscle force," *Physiological reviews*, pp. 1651–1697, 2012.

[53] J. C. Tuthill and E. Azim, "Proprioception," *Current Biology*, vol. 28, no. 5, pp. R194–R203, 2018.

[54] S. C. Gandevia, J. L. Smith, M. Crawford, U. Proske, and J. L. Taylor, "Motor commands contribute to human position sense," *Journal of Physiology*, vol. 571, no. 3, pp. 703–710, 2006.

[55] L. E. Sergio and J. F. Kalaska, "Changes in the temporal pattern of primary motor cortex activity in a directional isometric force versus limb movement task," *Journal of neurophysiology*, vol. 80, no. 3, pp. 1577–1583, 1998.

[56] L. E. Sergio, C. Hamel-Pâquet, and J. F. Kalaska, "Motor cortex neural correlates of output kinematics and kinetics during isometric-force and arm-reaching tasks," *Journal of neurophysiology*, vol. 94, no. 4, pp. 2353–2378, 2005.

[57] C. Hamel-Pâquet, L. E. Sergio, and J. F. Kalaska, "Parietal area 5 activity does not reflect the differential time-course of motor output kinetics during arm-reaching and isometric-force tasks," *Journal of neurophysiology*, vol. 95, no. 6, pp. 3353–3370, 2006.

[58] D. Phillips and A. Karduna, "No relationship between joint position sense and force sense at the shoulder," *Journal of motor behavior*, vol. 50, no. 2, pp. 228–234, 2018.

[59] B. L. Luu, B. L. Day, J. D. Cole, and R. C. Fitzpatrick, "The fusimotor and reafferent origin of the sense of force and weight," *The Journal of physiology*, vol. 589, no. 13, pp. 3135–3147, 2011.

[60] J. Brooks, T. J. Allen, and U. Proske, "The senses of force and heaviness at the human elbow joint," *Experimental brain research*, vol. 226, no. 4, pp. 617–629, 2013.

[61] G. Savage, T. J. Allen, and U. Proske, "The senses of active and passive forces at the human ankle joint," *Experimental brain research*, vol. 233, no. 7, pp. 2167–2180, 2015.

[62] B. Niespodziński, A. Kochanowicz, J. Mieszkowski, E. Piskorska, and M. Żychowska, "Relationship between joint position sense, force sense, and muscle strength and the impact of gymnastic training on proprioception," *BioMed research international*, vol. 2018, 2018.

[63] N. Elangovan, A. Herrmann, and J. Konczak, "Assessing proprioceptive function: evaluating joint position matching methods againist psychophysical thresholds," *Phys Therapy*, vol. 94, pp. 553–561, 2014.

[64] S. Hillier, M. Immink, and D. Thewlis, "Assessing proprioception: a systematic review of possibilities," *Neurorehabilitation and Neural Repair*, vol. 29, no. 10, pp. 933–949, 2015.

[65] D. J. Goble, "Proprioceptive acuity assessment via joint position matching: from basic science to general practice," *Physical therapy*, vol. 90, no. 8, pp. 1176–1184, 2016.

[66] F. Marini, V. Squeri, P. Morasso, C. Campus, J. Konczak, and L. Masia, "Robot-aided developmental assessment of wrist proprioception in children," *Journal of neuroengineering and rehabilitation*, vol. 14, no. 1, p. 3, 2017.

[67] C. L. Martin, B. A. Phillips, T. J. Kilpatrick, H. Butzkueven, N. Tubridy, E. Mcdonald, and M. P. Galea, "Gait and balance impairment in early multiple sclerosis in the absence of clinical disability," *Multiple Sclerosis Journal*, vol. 12, no. 5, pp. 620–628, 2006.

[68] D. E. Adamo and B. J. Martin, "Position sense asymmetry," *Experimental Brain Research*, vol. 192, no. 1, pp. 87–95, 2009.

[69] L. B. Bagesteiro and R. L. Sainburg, "Nondominant arm advantages in load compensation during rapid elbow joint movements," *Journal of Neurophysiology*, vol. 90, no. 3, pp. 1503–1513, 2003.

[70] S. Scotland, D. E. Adamo, and B. J. Martin, "Sense of effort revisited: relative contributions of sensory feedback and efferent copy," *Neuroscience Letters*, vol. 561, pp. 208–212, 2014.

[71] L. B. Bagesteiro and R. L. Sainburg, "Handedness: dominant arm advantages in control of limb dynamics," *Journal of Neurophysiology*, vol. 88, no. 5, pp. 2408–2421, 2006.

[72] D. J. Goble and S. H. Brown, "The biological and behavioral basis of upper limb asymmetries in sensorimotor performance," *Neuroscience and Biobehavioral Reviews*, vol. 32, no. 3, pp. 598–610, 2008.

[73] K. Amunts, G. Schlaug, A. Schleicher, H. Steinmetz, A. Dabringhaus, P. E. Roland, and K. Zilles, "Asymmetry in the human motor cortex and handedness," *Neuroimage*, vol. 4, no. 3, pp. 216–222, 1996.

[74] W. J. Triggs, B. Subramanium, and F. Rossi, "Hand preference and transcranial magnetic stimulation asymmetry of cortical motor representation," *Brain research*, vol. 835, no. 2, pp. 324–329, 1999.

[75] H. Liu, S. M. Stufflebeam, J. Sepulcre, T. Hedden, and R. L. Buckner, "Evidence from intrinsic activity that asymmetry of the human brain is controlled by multiple factors," *Proceedings of the National Academy of Sciences*, vol. 106, pp. 20499–20503, dec 2009.

[76] M. Mitchell, B. J. Martin, and D. E. Adamo, "Upper limb asymmetry in the sense of effort is dependent on force level," *Frontiers in Psychology*, vol. 8, no. APR, pp. 1–8, 2017.

[77] G. E. Ansems, T. J. Allen, and U. Proske, "Position sense at the human forearm in the horizontal plane during loading and vibration of elbow muscles," *Journal of Physiology*, vol. 576, no. 2, pp. 445–455, 2006.

[78] S. J. A. Kelso, K. G. Holt, P. Rubin, and P. N. Kugler, "Patterns of human interlimb coordination emerge from the properties of non-linear, limit cycle oscillatory processes: Theory and data," *Journal of motor behavior*, vol. 13, no. 4, pp. 226–261, 1981.

[79] S. J. A. Kelso, "Phase transitions and critical behavior in human bimanual coordination," *American Journal of Physiology-Regulatory, Integrative and Comparative Physiology*, vol. 246, no. 6, pp. R1000–R1004, 1984.

[80] C. De Oliveira, "The neuronal basis of bimanual coordination: recent neurophysiological evidence and functional models," *Acta Psychologica*, vol. 110, pp. 139–159, 2002.

[81] R. C. Oldfield, "The assessment and analysis of handedness: the Edinburgh inventory," *Neuropsychologia*, vol. 9, no. 1, pp. 97–113, 1971.

[82] S. J. A. Kelso, D. L. Southard, and D. Goodman, "On the coordination of two-handed movements," *Journal of Experimental Psychology: Human Perception and Performance*, vol. 5, no. 2, p. 229, 1979.

[83] H. Heuer, T. Kleinsorge, W. Spijkers, and C. Steglich, "Static and phasic cross-talk effects in discrete bimanual reversal movements," *Journal of Motor Behavior*, vol. 33, no. 1, pp. 67–85, 2001.

[84] X. Hu and K. M. Newell, "Dependence of asymmetrical interference on task demands and hand dominance in bimanual isometric force tasks," *Experimental Brain Research*, vol. 208, no. 4, pp. 533–541, 2011.

[85] R. A. Schmidt, H. N. Zelaznik, B. Hawkins, J. S. Frank, and J. T. Quinn Jr, "Motor-output variability: a theory for the accuracy of rapid motor acts.," *Psychological review*, vol. 86, no. 5, p. 415, 1979.

[86] E. A. Franz, H. N. Zelaznik, and G. McCabe, "Spatial topological constraints in a bimanual task," *Acta Psychologica*, vol. 77, no. 2, pp. 137–151, 1991.

[87] U. Proske, "What is the role of muscle receptors in proprioception?," *Muscle and Nerve*, vol. 31, no. 6, pp. 780–787, 2005.

[88] J. A. Winter, T. J. Allen, and U. Proske, "Muscle spindle signals combine with the sense of effort to indicate limb position," *Journal of physiology*, vol. 568, no. 3, pp. 1035–1046, 2005.

[89] V. Hatzitaki and P. McKinley, "Effect of single-limb inertial loading on bilateral reaching: Interlimb interactions," *Experimental Brain Research*, vol. 140, no. 1, pp. 34–45, 2001.

[90] D. J. Goble and S. H. Brown, "Upper limb asymmetries in the matching of proprioceptive versus visual targets," *Journal of Neurophysiology*, vol. 99, no. 6, pp. 3063–3074, 2008.

[91] R. L. Sainburg, "Handedness: differential specializations for control of trajectory and position," *Exercise and Sport Sciences REviews*, vol. 33, no. 4, pp. 206–213, 2005.

[92] P. B. De Freitas, V. Krishnan, and S. Jaric, "Force coordination in static manipulation tasks: Effects of the change in direction and handedness," *Experimental Brain Research*, vol. 183, no. 4, pp. 487–497, 2007.

[93] R. S. Johansson, A. Theorin, G. Westling, M. Andersson, Y. Ohki, and L. Nyberg, "How a lateralized brain supports symmetrical bimanual tasks," *PLoS biology*, vol. 4, p. e158, 2006.

[94] R. L. Sainburg, "Evidence for a dynamic-dominance hypothesis of handedness," *Experimental brain research*, vol. 142, no. 2, pp. 241–258, 2002.

[95] S. C. Gandevia, "The perception of motor commands or effort during muscular paralysis," *Brain: a journal of neurology*, vol. 105, no. Pt 1, pp. 151–159, 1982.

[96] S. C. Gandevia, D. I. McCloskey, and D. Burke, "Kinaesthetic signals and muscle contraction," *Trends in Neurosciences*, vol. 15, no. 2, pp. 62–65, 1992.

[97] M. Papadatou-Pastou, E. Ntolka, J. Schmitz, M. Martin, M. R. Munafò, S. Ocklenburg, and S. Paracchini, "Human handedness: a meta-analysis," *Psychological bulletin*, vol. 146, no. 6, p. 481, 2020.

[98] D. Elliott and R. Chua, "Manual asymmetries in goal-directed movement," *Manual asymmetries in motor performance*, pp. 143–158, 1996.

[99] D. J. Goble, J. P. Coxon, N. Wenderoth, A. Van Impe, and S. P. Swinnen, "Proprioceptive sensibility in the elderly: degeneration, functional consequences and plastic-adaptive processes," *Neuroscience and Biobehavioral Reviews*, vol. 33, no. 3, pp. 271–278, 2009.

[100] J. Han, G. Waddington, R. Adams, and J. Anson, "Bimanual proprioceptive performance differs for right- and left-handed individuals," *Neuroscience Letters*, vol. 542, pp. 37–41, 2013.

[101] R. Leib, I. Rubin, and I. Nisky, "Force feedback delay affects perception of stiffness but not action, and the effect depends on the hand used but not on the handedness," *Journal of neurophysiology*, vol. 120, no. 2, pp. 781–794, 2018.

[102] G. Buckingham, N. S. Ranger, and M. A. Goodale, "Handedness, laterality and the size-weight illusion," *Cortex*, vol. 48, no. 10, pp. 1342–1350, 2012.

[103] T. W. Anderson and D. A. Darling, "A test of goodness of fit," *Journal of the American statistical association*, vol. 49, no. 268, pp. 765–769, 1954.

[104] G. F. Templeton, "A two-step approach for transforming continuous variables to normal: Implications and recommendations for IS research," *Communications of the Association for Information Systems*, 2011.

[105] N. Kang and J. H. Cauraugh, "Bimanual force variability and chronic stroke: asymmetrical hand control," *PloS one*, vol. 9, no. 7, p. e101817, 2014.

[106] D. Mitrovic, S. Klanke, R. Osu, M. Kawato, and S. Vijayakumar, "A computational model of limb impedance control based on principles of internal model uncertainty," *PloS one*, vol. 5, no. 10, 2010.

[107] J. K. Shim, B. S. Lay, V. M. Zatsiorsky, and M. L. Latash, "Age-related changes in finger coordination in static prehension tasks," *Journal of Applied Physiology*, vol. 97, no. 1, pp. 213–224, 2004.

[108] V. L. Feigin, "Anthology of stroke epidemiology in the 20th and 21st centuries: Assessing the past, the present, and envisioning the future," *International Journal of Stroke*, 2019.

[109] P. Langhorne, F. Coupar, and A. Pollock, "Motor recovery after stroke: a systematic review," *The Lancet Neurology*, vol. 8, 2009.

[110] J. M. Veerbeek, A. C. Langbroek-Amersfoort, E. E. H. Van Wegen, C. G. M. Meskers, and G. Kwakkel, "Effects of robot-assisted therapy for the upper limb after stroke: a systematic review and meta-analysis," *Neurorehabilitation and neural repair*, vol. 31, no. 2, pp. 107–121, 2017.

[111] S. S. Kessner, U. Bingel, and G. Thomalla, "Somatosensory deficits after stroke: a scoping review," *Topics in Stroke Rehabilitation*, vol. 23, no. 2, pp. 136–146, 2016.

[112] E. Abela, J. Missimer, R. Wiest, A. Federspiel, C. Hess, M. Sturzenegger, and B. Weder, "Lesions to primary sensory and posterior parietal cortices impair recovery from hand paresis after stroke," *PloS one*, vol. 7, no. 2, 2012.

[113] E. C. van Lieshout, I. G. van de Port, R. M. Dijkhuizen, and J. M. Visser-Meily, "Does upper limb strength play a prominent role in health-related quality of life in stroke patients discharged from inpatient rehabilitation?," *Topics in Stroke Rehabilitation*, 2020.

[114] S. Wetter, J. L. Poole, and K. Y. Haaland, "Functional implications of ipsilesional motor deficits after unilateral stroke," *Archives of Physical Medicine and Rehabilitation*, 2005.

[115] G. H. Kitsos, I. J. Hubbard, A. R. Kitsos, and M. W. Parsons, "The ipsilesional upper limb can be affected following stroke," *The Scientific World Journal*, 2013.

[116] A. Sunderland, M. P. Bowers, S. M. Sluman, D. J. Wilcock, and M. E. Ardron, "Impaired dexterity of the ipsilateral hand after stroke and the relationship to cognitive deficit," *Stroke*, 1999.

[117] H. Y. Jung, J. S. Yoon, and B. S. Park, "Recovery of proximal and distal arm weakness in the ipsilateral upper limb after stroke.," *NeuroRehabilitation*, 2002.

[118] A. Brodal, "Self-observations and neuro-anatomical considerations after a stroke," *Brain*, 1973.

[119] F. Chollet, V. Dipiero, R. J. Wise, D. J. Brooks, R. J. Dolan, and R. S. Frackowiak, "The functional anatomy of motor recovery after stroke in humans: A study with positron emission tomography," *Annals of Neurology*, 1991.

[120] Y. H. Kwon, C. S. Kim, and S. H. Jang, "Ipsi-lesional motor deficits in hemiparetic patients with stroke," *NeuroRehabilitation*, 2007.

[121] J. S. Kim and S. Choi-Kwon, "Discriminative sensory dysfunction after unilateral stroke," *Stroke*, 1996.

[122] M. H. Niessen, D. J. H. Veeger, P. A. Koppe, M. H. Konijnenbelt, J. van Dieën, and T. W. Janssen, "Proprioception of the Shoulder After Stroke," *Archives of Physical Medicine and Rehabilitation*, 2008.

[123] S. Corkin, B. Milner, and T. Rasmussen, "Effects of different cortical excisions on sensory thresholds in man," *Transactions of the American Neurological Association*, 1964.

[124] G. Gainotti and C. Tiacci, "Homolateral and controlateral disturbances in the tactile discrimination of the hemispheric lesions," *Rivista di neurologia*, 1975.

[125] A. Carmon, "Disturbances of tactile sensitivity in patients with unilateral cerebral lesions," *Cortex*, 1971.

[126] J. P. Brasil-Neto and A. C. De Lima, "Sensory deficits in the unaffected hand of hemiparetic stroke patients," *Cognitive and Behavioral Neurology*, 2008.

[127] A. Yelnik, I. Bonan, M. Debray, E. Lo, F. Gelbert, and B. Bussel, "Changes in the execution of a complex manual task after ipsilateral ischemic cerebral hemispheric stroke," *Archives of Physical Medicine and Rehabilitation*, 1996.

[128] B. P. Cunha, S. M. S. F. de Freitas, and P. B. de Freitas, "Assessment of the Ipsilesional Hand Function in Stroke Survivors: The Effect of Lesion Side," *Journal of Stroke and Cerebrovascular Diseases*, 2017.

[129] T. Isa, M. Kinoshita, and Y. Nishimura, "Role of direct vs. indirect pathways from the motor cortex to spinal motoneurons in the control of hand dexterity," *Frontiers in Neurology*, 2013.

[130] C. Maenza, D. C. Good, C. J. Winstein, D. A. Wagstaff, and R. L. Sainburg, "Functional Deficits in the Less-Impaired Arm of Stroke Survivors Depend on Hemisphere of Damage and Extent of Paretic Arm Impairment," *Neurorehabilitation and Neural Repair*, 2020.

[131] S. Y. Schaefer, K. Y. Haaland, and R. L. Sainburg, "Hemispheric specialization and functional impact of ipsilesional deficits in movement coordination and accuracy," *Neuropsychologia*, 2009.

[132] K. Y. Haaland and D. L. Harrington, "Hemispheric control of the initial and corrective components of aiming movements," *Neuropsychologia*, vol. 27, no. 7, pp. 961–969, 1989.

[133] K. Y. Haaland and D. L. Harrington, "Limb-sequencing deficits after left but not right hemisphere damage," *Brain and cognition*, vol. 24, no. 1, pp. 104–122, 1994.

[134] C. J. Winstein and P. S. Pohl, "Effects of unilateral brain damage on the control of goal-directed hand movements," *Experimental brain research*, vol. 105, no. 1, pp. 163–174, 1995.

[135] K. Y. Haaland and D. Harrington, "The role of the hemispheres in closed loop movements," *Brain and cognition*, vol. 9, no. 2, pp. 158–180, 1989.

[136] M. T. Banich, "Hemispheric Specialization and Cognition," pp. 1081–1086, Oxford: Academic Press, 2009.

[137] J. L. Ringo, R. W. Doty, S. Demeter, and P. Y. Simard, "Time is of the essence: a conjecture that hemispheric specialization arises from interhemispheric conduction delay," *Cerebral Cortex*, vol. 4, no. 4, pp. 331–343, 1994.

[138] M. Kinsbourne, "Hemispheric specialization and the growth of human understanding.," *American Psychologist*, vol. 37, no. 4, p. 411, 1982.

[139] P.-Y. Hervé, L. Zago, L. Petit, B. Mazoyer, and N. Tzourio-Mazoyer, "Revisiting human hemispheric specialization with neuroimaging," *Trends in cognitive sciences*, vol. 17, no. 2, pp. 69–80, 2013.

[140] D. J. Serrien, R. B. Ivry, and S. P. Swinnen, "Dynamics of hemispheric specialization and integration in the context of motor control," *Nature Reviews Neuroscience*, vol. 7, no. 2, pp. 160–166, 2006.

[141] K. J. Friston, "Models of brain function in neuroimaging," *Annu. Rev. Psychol.*, vol. 56, pp. 57–87, 2005.

[142] K. E. Stephan, G. R. Fink, and J. C. Marshall, "Mechanisms of hemispheric specialization: insights from analyses of connectivity," *Neuropsychologia*, vol. 45, no. 2, pp. 209–228, 2007.

[143] R. W. Sperry, "Lateral specialization in the surgically separated hemispheres," *The neurosciences third study program*, pp. 5–19, 1974.

[144] J. Pujol, J. Deus, J. M. Losilla, and A. Capdevila, "Cerebral lateralization of language in normal left-handed people studied by functional MRI," *Neurology*, vol. 52, no. 5, p. 1038, 1999.

[145] S. Knecht, B. Dräger, M. Deppe, L. Bobe, H. Lohmann, A. Flöel, E.-B. Ringelstein, and H. Henningsen, "Handedness and hemispheric language dominance in healthy humans," *Brain*, vol. 123, no. 12, pp. 2512–2518, 2000.

[146] V. Yadav and R. L. Sainburg, "Limb dominance results from asymmetries in predictive and impedance control mechanisms," *PloS one*, vol. 9, no. 4, p. e93892, 2014.

[147] G. Vallar, G. Antonucci, C. Guariglia, and L. Pizzamiglio, "Deficits of position sense, unilateral neglect and optokinetic stimulation," *Neuropsychologia*, 1993.

[148] L. Santisteban, M. Térémetz, J. P. Bleton, J. C. Baron, M. A. Maier, and P. G. Lindberg, "Upper limb outcome measures used in stroke rehabilitation studies: A systematic literature review," *PLoS ONE*, 2016.

[149] J. Bernard-Espina, M. Beraneck, M. A. Maier, and M. Tagliabue, "Multisensory Integration in Stroke Patients: A Theoretical Approach to Reinterpret Upper-Limb Proprioceptive Deficits and Visual Compensation," *Frontiers in Neuroscience*, 2021.

[150] J. Han, G. Waddington, R. Adams, J. Anson, and Y. Liu, "Assessing proprioception: a critical review of methods," *Journal of Sport and Health Science*, vol. 5, no. 1, pp. 80–90, 2016.

[151] I. Cusmano, I. Sterpi, A. Mazzone, S. Ramat, C. Delconte, F. Pisano, and R. Colombo, "Evaluation of upper limb sense of position in healthy individuals and patients after stroke," *Journal of Healthcare Engineering*, 2014.

[152] N. Gurari, J. M. Drogos, and J. P. Dewald, "Individuals with chronic hemiparetic stroke can correctly match forearm positions within a single arm," *Clinical Neurophysiology*, 2017.

[153] N. Gurari, J. M. Drogos, and J. P. Dewald, "Investigation of how accurately individuals with hemiparetic stroke can mirror their forearm positions," *PLoS ONE*, 2021.

[154] D. Campolo, P. Tommasino, K. Gamage, J. Klein, C. M. Hughes, and L. Masia, "H-Man: A planar, H-shape cabled differential robotic manipulandum for experiments on human motor control," *Journal of Neuroscience Methods*, 2014.

[155] S. Contu, A. Hussain, L. Masia, and D. Campolo, "A preliminary study for quantitative assessment of upper limb proprioception," in *Engineering in Medicine and Biology Society (EMBC)*, pp. 4614–4617, IEEE, 2016.

[156] A. Cherpin, S. Kager, A. Budhota, S. Contu, D. A. Vishwanath, C. W. Kuah, C. Y. Ng, L. H. Yam, L. Xiang, A. Hussain, C. Karen, and D. Campolo, "A preliminary study on the relationship between proprioceptive deficits and motor functions in chronic stroke patients," in *IEEE International Conference on Rehabilitation Robotics*, 2019.

[157] A. Budhota, K. S. G. Chua, A. Hussain, S. Kager, A. Cherpin, S. Contu, D. Vishwanath, C. W. K. Kuah, C. Y. Ng, and L. H. L. Yam, "Robotic Assisted Upper Limb Training Post Stroke: A Randomized Control Trial Using Combinatory Approach Toward Reducing Workforce Demands," *Frontiers in neurology*, vol. 12, 2021.

[158] S. Contu, F. Marini, and L. Masia, "Robotic assessment of the contribution of motor commands to wrist position sense," in *IEEE International Conference on Rehabilitation Robotics*, 2017.

[159] A. Hussain, A. Budhota, C. M. L. Hughes, W. D. Dailey, D. A. Vishwanath, C. W. Kuah, L. H. Yam, Y. J. Loh, L. Xiang, K. S. Chua, E. Burdet, and D. Campolo, "Self-paced reaching after stroke: A quantitative assessment of longitudinal and directional sensitivity using the H-man planar robot for upper limb neurorehabilitation," *Frontiers in Neuroscience*, 2016.

[160] L. M. Rea and R. A. Parker, *Designing and conducting survey research a comprehensive guide*. 2014.

[161] N. Leibowitz, N. Levy, S. Weingarten, Y. Grinberg, A. Karniel, Y. Sacher, C. Serfaty, and N. Soroker, "Automated measurement of proprioception following stroke," *Disability and Rehabilitation*, 2008.

[162] M. D. Rinderknecht, O. Lambercy, V. Raible, I. Büsching, A. Sehle, J. Liepert, and R. Gassert, "Reliability, validity, and clinical feasibility of a rapid and objective assessment of post-stroke deficits in hand proprioception," *Journal of NeuroEngineering and Rehabilitation*, 2018.

[163] D. J. Goble, B. C. Noble, and S. H. Brown, "Proprioceptive target matching asymmetries in left-handed individuals," *Experimental brain research*, vol. 197, no. 4, pp. 403–408, 2009.

[164] A. Ferlinc, E. Fabiani, T. Velnar, and L. Gradisnik, "The Importance and Role of Proprioception in the Elderly: a Short Review," *Materia Socio Medica*, 2019.

[165] C. Weiller, M. Jüptner, S. Fellows, M. Rijntjes, G. Leonhardt, S. Kiebel, S. Müller, H. C. Diener, and A. F. Thilmann, "Brain representation of active and passive movements," *NeuroImage*, 1996.

[166] J. A. Semrau, T. M. Herter, S. H. Scott, and S. P. Dukelow, "Examining differences in patterns of sensory and motor recovery after stroke with robotics," *Stroke*, vol. 46, no. 12, pp. 3459–3469, 2015.

[167] S. E. Findlater and S. P. Dukelow, "Upper Extremity Proprioception After Stroke: Bridging the Gap Between Neuroscience and Rehabilitation," *Journal of Motor Behavior*, 2017.

[168] V. Gritsenko, N. I. Krouchev, and J. F. Kalaska, "Afferent input, efference copy, signal noise, and biases in perception of joint angle during active versus passive elbow movements," *Journal of Neurophysiology*, 2007.

[169] R. J. Van Beers, A. C. Sittig, and J. J. Denier Van Der Gon, "The precision of proprioceptive position sense," *Experimental Brain Research*, 1998.

[170] C. T. Fuentes and A. J. Bastian, "Where is your arm? Variations in proprioception across space and tasks," *Journal of Neurophysiology*, vol. 103, no. 1, pp. 164–171, 2010.

[171] R. Iandolo, V. Squeri, D. De Santis, P. Giannoni, P. Morasso, and M. Casadio, "Testing proprioception in intrinsic and extrinsic coordinate systems: is there a difference?," in *Engineering in Medicine and Biology Society (EMBC)*, pp. 6961–6964, IEEE, 2014.

[172] S. Contu, A. Hussain, S. Kager, A. Budhota, D. A. Vishwanath, C. W. Kuah, L. H. Yam, L. Xiang, K. S. Chua, L. Masia, and D. Campolo, "Proprioceptive assessment in clinical settings: Evaluation of joint position sense in upper limb post-stroke using a robotic manipulator," *PLoS ONE*, 2017.

[173] S. H. Scott and G. E. Loeb, "The computation of position sense from spindles in mono- and multiarticular muscles," *Journal of Neuroscience*, 1994.

[174] J. P. Roll, M. Bergenheim, and E. Ribot-Ciscar, "Proprioceptive population coding of two-dimensional limb movements in humans: II. Muscle-spindle feedback during 'drawing-like' movements," *Experimental Brain Research*, 2000.

[175] K. E. Jones, J. Wessberg, and Å. B. Vallbo, "Directional tuning of human forearm muscle afferents during voluntary wrist movements," *Journal of Physiology*, 2001.

[176] J. E. Schaffer, C. Maenza, D. C. Good, A. Przybyla, and R. L. Sainburg, "Left hemisphere damage produces deficits in predictive control of bilateral coordination," *Experimental Brain Research*, 2020.

[177] R. Sterzi, G. Bottini, M. G. Celani, E. Righetti, M. Lamassa, S. Ricci, and G. Vallar, "Hemianopia, hemianaesthesia, and hemiplegia after right and left hemisphere damage. A hemispheric difference.," *Journal of Neurology, Neurosurgery & Psychiatry*, vol. 56, no. 3, pp. 308–310, 1993.

[178] C. Grefkes and G. R. Fink, "Reorganization of cerebral networks after stroke: New insights from neuroimaging with connectivity approaches," 2011.

[179] R. Sleimen-Malkoun, J.-J. Temprado, L. Thefenne, and E. Berton, "Bimanual training in stroke: How do coupling and symmetry-breaking matter?," *BMC neurology*, vol. 11, no. 1, pp. 1–9, 2011.

[180] J. H. Cauraugh, N. Lodha, S. K. Naik, and J. J. Summers, "Bilateral movement training and stroke motor recovery progress: A structured review and meta-analysis," *Human Movement Science*, 2010.

[181] P. M. Rossini, C. Calautti, F. Pauri, and J.-C. Baron, "Post-stroke plastic reorganisation in the adult brain," *The Lancet Neurology*, vol. 2, no. 8, pp. 493–502, 2003.

[182] R. G. Carson, "Neural pathways mediating bilateral interactions between the upper limbs," *Brain Research Reviews*, vol. 49, no. 3, pp. 641–662, 2005.

[183] M. Cincotta and U. Ziemann, "Neurophysiology of unimanual motor control and mirror movements," *Clinical Neurophysiology*, vol. 119, no. 4, pp. 744–762, 2008.

[184] J. H. Cauraugh and J. J. Summers, "Neural plasticity and bilateral movements: a rehabilitation approach for chronic stroke," *Progress in neurobiology*, vol. 75, no. 5, pp. 309–320, 2005.

[185] F. Debaere, N. Wenderoth, S. Sunaert, P. Van Hecke, and S. P. Swinnen, "Cerebellar and premotor function in bimanual coordination: parametric neural responses to spatiotemporal complexity and cycling frequency," *Neuroimage*, vol. 21, no. 4, pp. 1416–1427, 2004.

[186] P. Nachev, C. Kennard, and M. Husain, "Functional role of the supplementary and pre-supplementary motor areas," *Nature Reviews Neuroscience*, vol. 9, no. 11, pp. 856–869, 2008.

[187] J. Fagard, I. Hardy-Léger, C. Kervella, and A. Marks, "Changes in interhemispheric transfer rate and the development of bimanual coordination during childhood," *Journal of experimental child psychology*, vol. 80, no. 1, pp. 1–22, 2001.

[188] C. Shirota, J. Jansa, J. Diaz, S. Balasubramanian, S. Mazzoleni, N. A. Borghese, and A. Melendez-Calderon, "On the assessment of coordination between upper extremities: towards a common language between rehabilitation engineers, clinicians and neuroscientists," *Journal of neuroengineering and rehabilitation*, vol. 13, no. 1, pp. 1–14, 2016.

[189] L. J. F. Janssen, L. L. Verhoeff, C. G. C. Horlings, and J. H. J. Allum, "Directional effects of biofeedback on trunk sway during gait tasks in healthy young subjects," *Gait and posture*, vol. 29, no. 4, pp. 575–581, 2009.

[190] N. Wenderoth, F. Debaere, S. Sunaert, P. van Hecke, and S. P. Swinnen, "Parieto-premotor areas mediate directional interference during bimanual movements," *Cerebral Cortex*, vol. 14, no. 10, pp. 1153–1163, 2004.

[191] S. A. Mutalib, M. Mace, and E. Burdet, "Bimanual coordination during a physically coupled task in unilateral spastic cerebral palsy children," *Journal of neuroengineering and rehabilitation*, vol. 16, no. 1, pp. 1–11, 2019.

[192] E. Galofaro, G. Ballardini, S. Boggini, F. Foti, I. Nisky, and M. Casadio, "Assessment of bimanual proprioception during an orientation matching task with a physically coupled object," in *IEEE International Conference on Rehabilitation Robotics*, vol. 2019-June, 2019.

[193] M. Kok, J. D. Hol, and T. B. Schön, "Using inertial sensors for position and orientation estimation," *arXiv preprint arXiv:1704.06053*, 2017.

[194] N. Smania, S. Paolucci, M. Tinazzi, A. Borghero, P. Manganotti, A. Fiaschi, G. Moretto, P. Bovi, and M. Gambarin, "Active finger extension: a simple movement predicting recovery of arm function in patients with acute stroke," *Stroke*, vol. 38, no. 3, pp. 1088–1090, 2007.

[195] N. Lodha, S. K. Naik, S. A. Coombes, and J. H. Cauraugh, "Force control and degree of motor impairments in chronic stroke," *Clinical Neurophysiology*, vol. 121, no. 11, pp. 1952–1961, 2010.

[196] M. E. Galganski, A. J. Fuglevand, and R. M. Enoka, "Reduced control of motor output in a human hand muscle of elderly subjects during submaximal contractions," *Journal of neurophysiology*, vol. 69, no. 6, pp. 2108–2115, 1993.

[197] G. Ballardini, V. Ponassi, E. Galofaro, L. Pellegrino, C. Solaro, M. Muller, and M. Casadio, "Bimanual control of position and force in people with multiple sclerosis: preliminary results," in *2019 IEEE 16th International Conference on Rehabilitation Robotics (ICORR)*, vol. 2019-June, pp. 1147–1152, IEEE, 2019.

[198] J. García-Piqueras, Y. García-Mesa, L. Cárcaba, J. Feito, I. Torres-Parejo, B. Martín-Biedma, J. Cobo, O. García-Suárez, and J. A. Vega, "Ageing of the somatosensory system at the periphery: Age-related changes in cutaneous mechanoreceptors," *Journal of anatomy*, vol. 234, no. 6, pp. 839–852, 2019.

[199] A. M. Hedman, N. E. M. van Haren, H. G. Schnack, R. S. Kahn, and H. E. Hulshoff Pol, "Human brain changes across the life span: a review of 56 longitudinal magnetic resonance imaging studies," *Human brain mapping*, vol. 33, no. 8, pp. 1987–2002, 2012.

[200] C. C. Bowerman, J. A. Semrau, Z. Kiss, and S. P. Dukelow, "The importance of somatosensory deficits in neurological disease," in *International Functional Electrical Stimulation Society (IFESS) Conference*, pp. 2–5, 2012.

[201] V. Dietz and K. Fouad, "Restoration of sensorimotor functions after spinal cord injury," *Brain*, vol. 137, no. 3, pp. 654–667, 2014.

[202] S. B. Zandvliet, G. Kwakkel, R. H. M. Nijland, E. E. H. van Wegen, and C. G. M. Meskers, "Is recovery of somatosensory impairment conditional for upper-limb motor recovery early after stroke?," *Neurorehabilitation and neural repair*, vol. 34, no. 5, pp. 403–416, 2020.

[203] I. Serrada, B. Hordacre, and S. L. Hillier, "Does sensory retraining improve sensation and sensorimotor function following stroke: a systematic review and meta-analysis," *Frontiers in neuroscience*, vol. 13, p. 402, 2019.

[204] P. Bach-y Rita and S. W. Kercel, "Sensory substitution and the human–machine interface," *Trends in cognitive sciences*, vol. 7, no. 12, pp. 541–546, 2003.

[205] K. Bark, E. Hyman, F. Tan, E. Cha, S. A. Jax, L. J. Buxbaum, and K. J. Kuchenbecker, "Effects of vibrotactile feedback on human learning of arm motions," *IEEE Transactions on Neural Systems and Rehabilitation Engineering*, vol. 23, no. 1, pp. 51–63, 2014.

[206] J. Lieberman and C. Breazeal, "TIKL: Development of a wearable vibrotactile feedback suit for improved human motor learning," in *IEEE Transactions on Robotics*, 2007.

[207] T. Bao, W. J. Carender, C. Kinnaird, V. J. Barone, G. Peethambaran, S. L. Whitney, M. Kabeto, R. D. Seidler, and K. H. Sienko, "Effects of long-term balance training with vibrotactile sensory augmentation among community-dwelling healthy older adults: a randomized preliminary study," *Journal of neuroengineering and rehabilitation*, vol. 15, no. 1, pp. 1–13, 2018.

[208] V. A. Shah, N. Risi, G. Ballardini, L. A. Mrotek, M. Casadio, and R. A. Scheidt, "Effect of dual tasking on vibrotactile feedback guided reaching–a pilot study," in *International Conference on Human Haptic Sensing and Touch Enabled Computer Applications*, pp. 3–14, Springer, 2018.

[209] P. Galambos, "Vibrotactile feedback for haptics and telemanipulation: survey, concept and experiment," *Acta Polytechnica Hungarica*, 2012.

[210] P. J. Standen, K. Threapleton, L. Connell, A. Richardson, D. J. Brown, S. Battersby, C. J. Sutton, and F. Platts, "Patients' use of a home-based virtual reality system to provide rehabilitation of the upper limb following stroke," *Physical therapy*, vol. 95, no. 3, pp. 350–359, 2015.

[211] R. Strong and B. Gaver, "Feather, scent and shaker: supporting simple intimacy," in *Proceedings of CSCW*, vol. 96, pp. 29–30, 1996.

[212] S. Brave and A. Dahley, "inTouch: a medium for haptic interpersonal communication," in *CHI'97 Extended Abstracts on Human Factors in Computing Systems*, pp. 363–364, 1997.

[213] M. A. Eid and H. Al Osman, "Affective haptics: Current research and future directions," *IEEE Access*, vol. 4, pp. 26–40, 2015.

[214] H. Culbertson, C. M. Nunez, A. Israr, F. Lau, F. Abnousi, and A. M. Okamura, "A social haptic device to create continuous lateral motion using sequential normal indentation," in *2018 IEEE Haptics Symposium (HAPTICS)*, pp. 32–39, IEEE, 2018.

[215] C. M. Nunez, S. R. Williams, A. M. Okamura, and H. Culbertson, "Understanding continuous and pleasant linear sensations on the forearm from a sequential discrete lateral skin-slip haptic device," *IEEE transactions on haptics*, vol. 12, no. 4, pp. 414–427, 2019.

[216] M. A. Baumann, K. E. MacLean, T. W. Hazelton, and A. McKay, "Emulating human attention-getting practices with wearable haptics," in *2010 IEEE Haptics Symposium*, pp. 149–156, IEEE, 2010.

[217] T. L. Baldi, G. Paolocci, D. Barcelli, and D. Prattichizzo, "Wearable haptics for remote social walking," *IEEE transactions on haptics*, vol. 13, no. 4, pp. 761–776, 2020.

[218] F. A. Saunders, "Recommended procedures for electrocutaneous displays," in *Functional electrical stimulation: Applications in neural prostheses*, pp. 303–309, Marcel Dekker, 1977.

[219] A. Y. Szeto and F. A. Saunders, "Electrocutaneous stimulation for sensory communication in rehabilitation engineering.," *IEEE Transactions on Biomedical Engineering*, vol. 29, pp. 300–308, apr 1982.

[220] A. Higashiyama and M. Hayashi, "Localization of electrocutaneous stimuli on the fingers and forearm: effects of electrode configuration and body axis," *Perception and psychophysics*, vol. 54, no. 1, pp. 108–120, 1993.

[221] T. Watanabe, S. Watanabe, K. Yoshino, R. Futami, and N. Hoshimiya, "A study of relevance of skin impedance to absolute threshold for stabilization of cutaneous sensation elicited by electric current stimulation," *Biomechanisms*, vol. 16, pp. 61–73, 2002.

[222] J. Gregory, N. Xi, and Y. Shen, "Towards on-line fingertip bio-impedance identification for enhancement of electro-tactile rendering," in *2009 IEEE/RSJ International Conference on Intelligent Robots and Systems*, pp. 3685–3690, IEEE, 2009.

[223] H. Kajimoto, "Electrotactile display with real-time impedance feedback using pulse width modulation," *IEEE Transactions on Haptics*, vol. 5, no. 2, pp. 184–188, 2012.

[224] C. C. Collins, "Tactile television-mechanical and electrical image projection," *IEEE Transactions on man-machine systems*, vol. 11, no. 1, pp. 65–71, 1970.

[225] K. A. Kaczmarek, J. G. Webster, and R. G. Radwin, "Maximal dynamic range electrotactile stimulation waveforms," *IEEE transactions on biomedical engineering*, vol. 39, no. 7, pp. 701–715, 1992.

[226] C. J. Poletto and C. L. Van Doren, "Elevating pain thresholds in humans using depolarizing prepulses," *IEEE transactions on biomedical engineering*, vol. 49, no. 10, pp. 1221–1224, 2002.

[227] E. Torebjörk and M. Schmelz, "Single-unit recordings of afferent human peripheral nerves by microneurography," in *Peripheral Neuropathy*, pp. 1003–1014, Elsevier Saunders, Pennsylvania, USA, 2005.

[228] L. A. Jones and S. J. Lederman, *Human hand function*. Oxford University Press, 2006.

[229] S. H. Peurala, K. Pitkänen, J. Sivenius, I. M. Tarkka, and U. of Nottingham, "Cutaneous electrical stimulation may enhance sensorimotor recovery in chronic stroke," *Clinical Rehabilitation*, vol. 16, pp. 709–716, nov 2002.

[230] G. Wilson, S. Brewster, M. Halvey, and S. Hughes, "Thermal feedback identification in a mobile environment," in *International Workshop on Haptic and Audio Interaction Design*, pp. 10–19, Springer, 2013.

[231] M. Benali-Khoudjal, M. Hafez, J.-M. Alexandre, J. Benachour, and A. Kheddar, "Thermal feedback model for virtual reality," in *MHS2003. Proceedings of 2003 International Symposium on Micromechatronics and Human Science (IEEE Cat. No. 03TH8717)*, pp. 153–158, IEEE, 2003.

[232] J. C. Stevens, "Temperature can sharpen tactile acuity," *Perception and psychophysics*, vol. 31, no. 6, pp. 577–580, 1982.

[233] H.-N. Ho and L. A. Jones, "Contribution of thermal cues to material discrimination and localization," *Perception and Psychophysics*, vol. 68, no. 1, pp. 118–128, 2006.

[234] M. Aggravi, F. Pausé, P. R. Giordano, and C. Pacchierotti, "Design and evaluation of a wearable haptic device for skin stretch, pressure, and vibrotactile stimuli," *IEEE Robotics and Automation Letters*, vol. 3, no. 3, pp. 2166–2173, 2018.

[235] J. L. Sullivan, N. Dunkelberger, J. Bradley, J. Young, A. Israr, F. Lau, K. Klumb, F. Abnousi, and M. K. O'Malley, "Multi-sensory stimuli improve distinguishability of cutaneous haptic cues," *IEEE transactions on haptics*, vol. 13, no. 2, pp. 286–297, 2019.

[236] N. Dunkelberger, J. L. Sullivan, J. Bradley, I. Manickam, G. Dasarathy, R. Baraniuk, and M. K. O'Malley, "A multisensory approach to present phonemes as language through a wearable haptic device," *IEEE Transactions on Haptics*, vol. 14, no. 1, pp. 188–199, 2020.

[237] K. Bark, J. W. Wheeler, S. Premakumar, and M. R. Cutkosky, "Comparison of skin stretch and vibrotactile stimulation for feedback of proprioceptive information," *Haptic Interfaces for Virtual Environment and Teleoperator Systems Symposium (HAPTICS)*, pp. 71–78, 2008.

[238] J. B. Van Erp, "Presenting directions with a vibrotactile torso display," *Ergonomics*, vol. 48, no. 3, pp. 302–313, 2005.

[239] B.-C. Lee, B. J. Martin, and K. H. Sienko, "Directional postural responses induced by vibrotactile stimulations applied to the torso," *Experimental brain research*, vol. 222, no. 4, pp. 471–482, 2012.

[240] L. Jiang, M. R. Cutkosky, J. Ruutiainen, and R. Raisamo, "Using haptic feedback to improve grasp force control in multiple sclerosis patients," *IEEE transactions on Robotics*, vol. 25, no. 3, pp. 593–601, 2009.

[241] A. H. Wan, D. W. Wong, C. Z. H. Ma, M. Zhang, and W. C. Lee, "Wearable vibrotactile biofeedback device allowing identification of different floor conditions for lower-limb amputees," *Archives of physical medicine and rehabilitation*, vol. 97, no. 7, pp. 1210–1213, 2016.

[242] C.-Y. Chen, Y.-Y. Chen, Y.-J. Chung, and N.-H. Yu, "Motion guidance sleeve: guiding the forearm rotation through external artificial muscles," in *Proceedings of the 2016 CHI Conference on Human Factors in Computing Systems*, pp. 3272–3276, 2016.

[243] L. A. Jones and N. B. Sarter, "Tactile displays: guidance for their design and application," *Human Factors: The Journal of the Human Factors and Ergonomics Society*, vol. 50, no. 1, pp. 90–111, 2008.

[244] V. A. Shah, M. Casadio, R. A. Scheidt, and L. A. Mrotek, "Spatial and temporal influences on discrimination of vibrotactile stimuli on the arm," *Experimental brain research*, pp. 1–12, 2019.

[245] E. J. Colgate and M. J. Brown, "Factors affecting the z-width of a haptic display," in *IEEE International Conference on Robotics and Automation*, pp. 3205–3210, IEEE, 1994.

[246] R. Ackerley, I. Carlsson, H. Wester, H. Olausson, and H. Backlund Wasling, "Touch perceptions across skin sites: differences between sensitivity, direction discrimination and pleasantness," *Frontiers in Behavioral Neuroscience*, vol. 8, no. February, pp. 1–10, 2014.

[247] B. Dandu, Y. Shao, A. Stanley, and Y. Visell, "Spatiotemporal haptic effects from a single actuator via spectral control of cutaneous wave propagation," in *2019 IEEE World Haptics Conference (WHC)*, pp. 425–430, IEEE, 2019.

[248] T. Hachisu and K. Suzuki, "Representing interpersonal touch directions by tactile apparent motion using smart bracelets," *IEEE transactions on haptics*, vol. 12, no. 3, pp. 327–338, 2019.

[249] S. Choi and K. J. Kuchenbecker, "Vibrotactile display: Perception, technology, and applications," 2013.

[250] T. A. Kern, *Engineering haptic devices: A beginner's guide for engineers*. 2009.

[251] T. Ahmaniemi, "Effect of dynamic vibrotactile feedback on the control of isometric finger force," *IEEE Transactions on Haptics*, 2012.

[252] C. I. Wall, M. S. Weinberg, P. B. Schmidt, and D. E. Krebs, "Balance prosthesis based on micromechanical sensors using vibrotactile feedback of tilt," *IEEE Transactions on Biomedical Engineering*, vol. 48, no. 10, pp. 1153–1161, 2001.

[253] A. V. Cuppone, V. Squeri, M. Semprini, L. Masia, and J. Konczak, "Robot-assisted proprioceptive training with added vibro-tactile feedback enhances somatosensory and motor performance," *PloS one*, vol. 11, no. 10, p. e0164511, 2016.

[254] C. E. Sherrick and R. Rogers, "Apparent haptic movement," *Perception and Psychophysics*, 1966.

[255] S. J. Lederman and R. L. Klatzky, "Haptic perception: a tutorial," *Attention, perception and psychophysics*, vol. 71, no. 7, pp. 1439–1459, 2009.

[256] F. A. Geldard and C. E. Sherrick, "The cutaneous "rabbit": A perceptual illusion," *Science*, 1972.

[257] G. M. Goodwin, D. I. Mccloskey, and P. B. Matthews, "Proprioceptive illusions induced by muscle vibration: Contribution by muscle spindles to perception?," *Science*, 1972.

[258] M. W. Taylor, J. L. Taylor, and T. Seizova-Cajic, "Muscle Vibration-Induced Illusions: Review of Contributing Factors, Taxonomy of Illusions and User's Guide," 2017.

[259] A. U. Alahakone and A. S. M. N. Senanayake, "Vibrotactile feedback systems: current trends in rehabilitation, sports and information display," *IEEE/ASME International Conference on Advanced Intelligent Mechatronics, AIM*, pp. 1148–1153, 2009.

[260] K. O. Sofia and L. Jones, "Mechanical and psychophysical studies of surface wave propagation during vibrotactile stimulation," *IEEE transactions on haptics*, vol. 6, no. 3, pp. 320–329, 2013.

[261] K. O. Johnson, T. Yoshioka, and F. Vega-Bermudez, "Tactile functions of mechanoreceptive afferents innervating the hand," *Journal of clinical neurophysiology*, vol. 17, no. 6, pp. 539–558, 2000.

[262] M. F. Rotella, K. Guerin, X. He, and A. M. Okamura, "Hapi bands: a haptic augmented posture interface," in *2012 IEEE Haptics Symposium (HAPTICS)*, pp. 163–170, IEEE, 2012.

[263] V. Nitsch and B. Färber, "A meta-analysis of the effects of haptic interfaces on task performance with teleoperation systems," *IEEE transactions on haptics*, vol. 6, no. 4, pp. 387–398, 2012.

[264] T. Takeuchi, M. Futatsuka, H. Imanishi, and S. Yamada, "Pathological changes observed in the finger biopsy of patients with vibration-induced white finger," *Scandinavian journal of work, environment and health*, pp. 280–283, 1986.

[265] P. M. Taylor, A. Hosseini-Sianaki, C. J. Varley, and D. M. Pollet, "Advances in an electrorheological fluid based tactile array," *IEE Colloquium on developments in tactile display*, 1997.

[266] M. Jungmann and H. F. Schlaak, "Miniaturised electrostatic tactile display with high structural compliance," in *Proceedings of Eurohaptics*, pp. 12–17, Citeseer, 2002.

[267] Y. Jansen, T. Karrer, and J. Borchers, "MudPad: localized tactile feedback on touch surfaces," in *Adjunct proceedings of the 23nd annual ACM symposium on User interface software and technology*, pp. 385–386, 2010.

[268] T.-H. Yang, H.-J. Kwon, S. S. Lee, J. An, J.-H. Koo, S.-Y. Kim, and D.-S. Kwon, "Development of a miniature tunable stiffness display using MR fluids for haptic application," *Sensors and Actuators A: Physical*, vol. 163, no. 1, pp. 180–190, 2010.

[269] G. V. Merrett, C. D. Metcalf, D. Zheng, S. Cunningham, S. Barrow, and S. H. Demain, "Design and qualitative evaluation of tactile devices for stroke rehabilitation," in *IET Seminar on Assisted Living 2011*, IET, 2011.

[270] A. A. Stanley and K. J. Kuchenbecker, "Evaluation of tactile feedback methods for wrist rotation guidance," *IEEE Transactions on Haptics*, vol. 5, no. 3, pp. 240–251, 2012.

[271] L. Meli, C. Pacchierotti, and D. Prattichizzo, "Experimental evaluation of magnified haptic feedback for robot-assisted needle insertion and palpation," *The International Journal of Medical Robotics and Computer Assisted Surgery*, vol. 13, no. 4, p. e1809, 2017.

[272] Z. F. Quek, S. B. Schorr, I. Nisky, W. R. Provancher, and A. M. Okamura, "Sensory substitution of force and torque using 6-DoF tangential and normal skin deformation feedback," in *IEEE International Conference on Robotics and Automation*, pp. 264–271, IEEE, 2015.

[273] S. B. Schorr and A. M. Okamura, "Three-dimensional skin deformation as force substitution: wearable device design and performance during haptic exploration of virtual environments," *IEEE Transactions on Haptics*, vol. 10, no. 3, pp. 418–430, 2017.

[274] J. Franks, M. O. Culjat, C. King, M. L. Franco, J. W. Bisley, W. Grundfest, and E. P. Dutson, "Pneumatic balloon actuators for tactile feedback in robotic surgery," *Industrial Robot: An International Journal*, 2008.

[275] V. Yem, M. Otsuki, and H. Kuzuoka, "Development of a wearable out-covering haptic display using ball effector for hand motion guidance," *Lecture Notes in Electrical Engineering*, vol. 277, pp. 85–89, 2015.

[276] A. Talhan and S. Jeon, "Pneumatic actuation in haptic-enabled medical simulators: a review," *IEEE Access*, vol. 6, pp. 3184–3200, 2018.

[277] M. Gabardi, M. Solazzi, D. Leonardis, and A. Frisoli, "A new wearable fingertip haptic interface for the rendering of virtual shapes and surface features," in *2016 IEEE Haptics Symposium (HAPTICS)*, pp. 140–146, IEEE, 2016.

[278] L. R. Gavrilov and E. M. Tsirulnikov, "Mechanisms of stimulation effects of focused ultrasound on neural structures: Role of nonlinear effects," *Nonlinear Acoustics at the Beginning of the 21st Century*, no. October 2015, pp. 445–448, 2002.

[279] H. Gil, H. Son, J. R. Kim, and I. Oakley, "Whiskers: Exploring the use of ultrasonic haptic cues on the face," in *Proceedings of the 2018 CHI Conference on Human Factors in Computing Systems*, pp. 1–13, 2018.

[280] S. Suzuki, R. Takahashi, M. Nakajima, K. Hasegawa, Y. Makino, and H. Shinoda, "Midair haptic display to human upper body," in *2018 57th Annual Conference of the Society of Instrument and Control Engineers of Japan (SICE)*, pp. 848–853, IEEE, 2018.

[281] B. Long, S. A. Seah, T. Carter, and S. Subramanian, "Rendering volumetric haptic shapes in mid-air using ultrasound," *ACM Transactions on Graphics*, vol. 33, no. 6, pp. 1–10, 2014.

[282] Y. Monnai, K. Hasegawa, M. Fujiwara, K. Yoshino, S. Inoue, and H. Shinoda, "Adding texture to aerial images using ultrasounds," in *Haptic Interaction*, pp. 59–61, Springer, 2015.

[283] E. Freeman, R. Anderson, J. Williamson, G. Wilson, and S. A. Brewster, "Textured surfaces for ultrasound haptic displays," in *Proceedings of the 19th ACM International Conference on Multimodal Interaction*, pp. 491–492, 2017.

[284] K. Hasegawa and H. Shinoda, "Aerial display of vibrotactile sensation with high spatial-temporal resolution using large-aperture airborne ultrasound phased array," in *World Haptics Conference (WHC)*, pp. 31–36, IEEE, 2013.

[285] T. Howard, M. Marchal, A. Lécuyer, and C. Pacchierotti, "PUMAH: Pan-Tilt Ultrasound Mid-Air Haptics for larger interaction workspace in virtual reality," *IEEE Transactions on Haptics*, vol. 13, no. 1, pp. 38–44, 2020.

[286] E. Rutten, L. Van Den Bogaert, and D. Geerts, "From initial encounter with mid-air haptic feedback to repeated use: the role of the novelty effect in user experience," *IEEE Transactions on Haptics*, 2020.

[287] M. Y. Tsalamlal, N. Ouarti, and M. Ammi, "Psychophysical study of air jet based tactile stimulation," *World Haptics Conference (WHC)*, no. March 2016, pp. 639–644, 2013.

[288] A. Glezer, "The formation of vortex rings," *The Physics of fluids*, vol. 31, no. 12, pp. 3532–3542, 1988.

[289] J. M. Romano and K. J. Kuchenbecker, "The AirWand: design and characterization of a large-workspace haptic device," in *IEEE International Conference on Robotics and Automation*, pp. 1461–1466, IEEE, 2009.

[290] M. Bianchi, J. C. Gwilliam, A. Degirmenci, and A. M. Okamura, "Characterization of an air jet haptic lump display," in *Engineering in Medicine and Biology Society (EMBC)*, pp. 3467–3470, IEEE, 2011.

[291] R. Sodhi, I. Poupyrev, M. Glisson, and A. Israr, "AIREAL: interactive tactile experiences in free air," *ACM Transactions on Graphics*, vol. 32, no. 4, p. 134, 2013.

[292] Y. Suzuki and M. Kobayashi, "Air jet driven force feedback in virtual reality," *IEEE Computer Graphics and Applications*, vol. 25, no. 1, pp. 44–47, 2005.

[293] K. Inoue, F. Kato, and S. Lee, "Haptic device using flexible sheet and air jet for presenting virtual lumps under skin," in *IEEE International Conference on Intelligent Robots and Systems*, pp. 1749–1754, IEEE, 2009.

[294] F. Arafsha, L. Zhang, H. Dong, and A. El Saddik, "Contactless haptic feedback: State of the art," in *2015 IEEE International Symposium on Haptic, Audio and Visual Environments and Games (HAVE)*, pp. 1–6, IEEE, 2015.

[295] T. Hoshi, "Development of aerial-input and aerial-tactile-feedback system," in *2011 IEEE World Haptics Conference*, pp. 569–573, IEEE, 2011.

[296] Y. Ochiai, K. Kumagai, T. Hoshi, J. Rekimoto, S. Hasegawa, and Y. Hayasaki, "Fairy lights in femtoseconds: aerial and volumetric graphics rendered by focused femtosecond laser combined with computational holographic fields," *ACM Transactions on Graphics*, vol. 35, no. 2, 2016.

[297] Y. Ochiai, K. Kumagai, T. Hoshi, S. Hasegawa, and Y. Hayasaki, "Cross-field aerial haptics: rendering haptic feedback in air with light and acoustic fields," *CHI*, pp. 3238–3247, 2016.

[298] P. Kim, S. Kim, Y.-D. Park, and S.-B. Choi, "Force modeling for incisions into various tissues with MRF haptic master," *Smart Materials and Structures*, vol. 25, no. 3, p. 35008, 2016.

[299] J.-Y. Kim, K. Jang, S.-J. Yang, J.-H. Baek, and J.-R. Park, "Simulation study of the thermal and the thermoelastic effects induced by pulsed laser absorption in human skin," *Journal of the Korean Physical Society*, vol. 68, no. 8, pp. 979–988, 2016.

[300] H. Lee, J.-S. Kim, J.-Y. Kim, S. Choi, J.-H. Jun, J.-R. Park, A.-H. Kim, H.-B. Oh, J.-H. Baek, and S.-J. Yang, "Mid-air tactile stimulation using indirect laser radiation," *IEEE Transactions on Haptics*, vol. 9, no. 4, pp. 574–585, 2016.

[301] H. Cha, H. Lee, J. Park, H.-S. Kim, S.-C. Chung, and S. Choi, "Mid-air tactile display using indirect laser radiation for contour-following stimulation and assessment of its spatial acuity," *IEEE World Haptics Conference (WHC)*, pp. 136–141, 2017.

[302] P. M. Fitts and M. I. Posner, *Human performance*. Brooks/Cole, 1967.

[303] P. M. Van Vliet and G. Wulf, "Extrinsic feedback for motor learning after stroke: what is the evidence?," *Disability and rehabilitation*, vol. 28, no. 13-14, pp. 831–840, 2006.

[304] B. T. Gleeson, S. K. Horschel, and W. R. Provancher, "Design of a fingertip-mounted tactile display with tangential skin displacement feedback," *IEEE Transactions on Haptics*, vol. 3, no. 4, pp. 297–301, 2010.

[305] C. J. Winstein and R. A. Schmidt, "Reduced frequency of knowledge of results enhances motor skill learning.," *Journal of Experimental Psychology: Learning, Memory, and Cognition*, vol. 16, no. 4, p. 677, 1990.

[306] L. Gammaitoni, "Stochastic resonance and the dithering effect in threshold physical systems," *Physical Review E*, 1995.

[307] L. Gammaitoni, P. Hänggi, P. Jung, and F. Marchesoni, "Stochastic resonance," *Reviews of Modern Physics*, 1998.

[308] F. Moss, L. M. Ward, and W. G. Sannita, "Stochastic resonance and sensory information processing: A tutorial and review of application," *Clinical Neurophysiology*, 2004.

[309] J. J. Collins, C. C. Chow, and T. T. Imhoff, "Stochastic resonance without tuning," *Nature*, 1995.

[310] J. J. Collins, A. A. Priplata, D. C. Gravelle, J. B. Niemi, J. D. Harry, and L. A. Lipsitz, "Noise-enhanced human sensorimotor function," *IEEE Engineering in Medicine and Biology Magazine*, vol. 22, no. 2, pp. 76–83, 2003.

[311] N. J. Seo, M. L. Kosmopoulos, L. R. Enders, and P. Hur, "Effect of remote sensory noise on hand function post stroke," *Frontiers in Human Neuroscience*, 2014.

[312] N. J. Seo, M. L. Woodbury, L. Bonilha, V. Ramakrishnan, S. A. Kautz, R. J. Downey, B. H. Dellenbach, A. W. Lauer, C. M. Roark, L. E. Landers, S. K. Phillips, and A. A. Vatinno, "TheraBracelet stimulation during task-practice therapy to improve upper extremity function after stroke: a Pilot randomized controlled study," *Physical Therapy*, 2019.

[313] M. Dozza, L. Chiari, F. Hlavacka, A. Cappello, and F. B. Horak, "Effects of linear versus sigmoid coding of visual or audio biofeedback for the control of upright stance," *IEEE Transactions on Neural Systems and Rehabilitation Engineering*, vol. 14, no. 4, pp. 505–512, 2006.

[314] J. Massion, "Postural control system," *Current Opinion in Neurology*, vol. 4, no. 6, pp. 877–887, 1994.

[315] Y. Ivanenko and V. S. Gurfinkel, "Human Postural Control," *Frontiers in neuroscience*, vol. 12, p. 171, mar 2018.

[316] F. B. Horak and J. M. Macpherson, "Postural orientation and equilibrium," *Handbook of physiology*, vol. 1, pp. 255–292, 1996.

[317] S.-i. Hirabayashi and Y. Iwasaki, "Developmental perspective of sensory organization on postural control," *Brain and development*, vol. 17, no. 2, pp. 111–113, 1995.

[318] R. J. Peterka and F. O. Black, "Age-related changes in human posture control: sensory organization tests," 1989.

[319] J. M. Macpherson and T. J. Inglis, "Stance and balance following bilateral labyrinthectomy," in *Progress in brain research*, vol. 97, pp. 219–228, Elsevier, 1993.

[320] M. Dozza, F. B. Horak, and L. Chiari, "Auditory biofeedback substitutes for loss of sensory information in maintaining stance," *Experimental brain research*, vol. 178, pp. 37–48, 2007.

[321] M. Dozza, L. Chiari, B. Chan, L. Rocchi, F. B. Horak, and A. Cappello, "Influence of a portable audio-biofeedback device on structural properties of postural sway," *Journal of NeuroEngineering and Rehabilitation*, vol. 2, no. 13, pp. 1–12, 2005.

[322] Y. P. Danilov, M. E. Tyler, K. L. Skinner, R. A. Hogle, and P. Bach-y Rita, "Efficacy of electrotactile vestibular substitution in patients with peripheral and central vestibular loss," *Journal of Vestibular Research*, vol. 17, no. 2, 3, pp. 119–130, 2007.

[323] K. H. Sienko, D. M. Balkwill, and C. I. Wall, "Biofeedback improves postural control recovery from multi-axis discrete perturbations," *Journal of NeuroEngineering and Rehabilitation*, vol. 9, no. 1, p. 53, 2012.

[324] L. L. Verhoeff, C. G. C. Horlings, L. J. F. Janssen, S. A. Bridenbaugh, and J. H. J. Allum, "Effects of biofeedback on trunk sway during dual tasking in the healthy young and elderly," *Gait and posture*, vol. 30, no. 1, pp. 76–81, 2009.

[325] J. Xu, T. Bao, U. H. Lee, C. Kinnaird, W. J. Carender, Y. Huang, K. H. Sienko, and P. B. Shull, "Configurable, wearable sensing and vibrotactile feedback system for real-time postural balance and gait training: proof-of-concept," *Journal of NeuroEngineering and Rehabilitation*, vol. 14, no. 102, pp. 1–10, 2017.

[326] M. E. Tyler, Y. P. Danilov, and P. Bach-Y-Rita, "Closing an open-loop control system: vestibular substitution through the tongue," *Journal of integrative neuroscience*, vol. 2, no. 02, pp. 159–164, 2003.

[327] M. Y. Lee, C. F. Lin, and K. S. Soon, "Balance control enhancement using subsensory stimulation and visual-auditory biofeedback strategies for amputee subjects," *Conference Proceedings - IEEE International Conference on Systems, Man and Cybernetics*, vol. 31, no. December, pp. 2951–2959, 2007.

[328] A. D. Goodworth, C. I. Wall, and R. J. Peterka, "Influence of feedback parameters on performance of a vibrotactile balance prosthesis," *IEEE transactions on neural systems and rehabilitation engineering*, vol. 17, no. 4, pp. 397–408, 2009.

[329] P. Loughlin, A. Mahboobin, and J. Furman, "Designing vibrotactile balance feedback for desired body sway reductions," in *2011 Annual International Conference of the IEEE Engineering in Medicine and Biology Society*, pp. 1310–1313, IEEE, 2011.

[330] D. C. Gravelle, C. A. Laughton, N. T. Dhruv, K. D. Katdare, J. B. Niemi, L. A. Lipsitz, and J. J. Collins, "Noise-enhanced balance control in older adults," *NeuroReport*, vol. 13, no. 15, pp. 1853–1856, 2002.

[331] A. A. Priplata, J. B. Niemi, J. D. Harry, L. A. Lipsitz, and J. J. Collins, "Vibrating insoles and balance control in elderly people," *The Lancet*, vol. 362, no. 9390, pp. 1123–1124, 2003.

[332] A. U. Alahakone and A. S. M. N. Senanayake, "A real-time system with assistive feedback for postural control in rehabilitation," *IEEE/ASME Transactions on Mechatronics*, vol. 15, no. 2, pp. 226–233, 2010.

[333] M. Mancini, F. B. Horak, C. Zampieri, P. Carlson-Kuhta, J. G. Nutt, and L. Chiari, "Trunk accelerometry reveals postural instability in untreated Parkinson's disease," *Parkinsonism and Related Disorders*, vol. 17, no. 7, pp. 557–562, 2011.

[334] M. Mancini, A. Salarian, P. Carlson-Kuhta, C. Zampieri, L. King, L. Chiari, and F. B. Horak, "ISway: a sensitive, valid and reliable measure of postural control," *Journal of NeuroEngineering and Rehabilitation*, vol. 9, no. 59, pp. 1–8, 2012.

[335] R. Iandolo, M. Carè, V. A. Shah, S. Schiavi, G. Bommarito, G. Boffa, P. Giannoni, M. Inglese, L. A. Mrotek, and R. A. Scheidt, "A two alternative forced choice method for assessing vibrotactile discrimination thresholds in the lower limb," *Somatosensory and motor research*, vol. 36, no. 2, pp. 162–170, 2019.

[336] C. Cipriani, M. Dalonzo, and M. C. Carrozza, "A miniature vibrotactile sensory substitution device for multifingered hand prosthetics," *IEEE Transactions on Biomedical Engineering*, vol. 59, no. 2, pp. 400–408, 2012.

[337] N. T. Dhruv, J. B. Niemi, J. D. Harry, L. A. Lipsitz, and J. J. Collins, "Enhancing tactile sensation in older adults with electrical noise stimulation," *Neuroreport*, vol. 13, no. 5, pp. 597–600, 2002.

[338] W. Liu, L. A. Lipsitz, M. Montero-Odasso, J. Bean, C. D. Kerrigan, and J. J. Collins, "Noise-enhanced vibrotactile sensitivity in older adults, patients with stroke, and patients with diabetic neuropathy," *Archives of physical medicine and rehabilitation*, vol. 83, no. 2, pp. 171–176, 2002.

[339] M. Janssen, R. Stokroos, J. Aarts, R. van Lummel, and H. Kingma, "Salient and placebo vibrotactile feedback are equally effective in reducing sway in bilateral vestibular loss patients," *Gait and Posture*, vol. 31, no. 2, pp. 213–217, 2010.

[340] F. H. Magalhães and A. F. Kohn, "Vibratory noise to the fingertip enhances balance improvement associated with light touch," *Experimental Brain Research*, vol. 209, no. 1, pp. 139–151, 2011.

[341] L. Borel and E. Ribot-Ciscar, "Improving postural control by applying mechanical noise to ankle muscle tendons," *Experimental Brain Research*, vol. 234, no. 8, pp. 2305–2314, 2016.

[342] K. Kwak, H. G. Kim, and D. W. Kim, "Variation of ankle biomechanical property according to vibro-perception threshold and vibration frequency," *Biomedical Engineering Letters*, vol. 6, no. 1, pp. 16–25, 2016.

[343] G. Marchesi, M. Casadio, G. Ballardini, A. De Luca, V. Squeri, F. Vallone, C. Giorgini, P. Crea, A. Pilotto, C. Sanfilippo, J. A. Saglia, and A. Canessa, "Robot-based assessment of sitting and standing balance: preliminary results in Parkinson's disease," *IEEE International Conference on Rehabilitation Robotics*, vol. 2019-June, 2019.

[344] J. R. Davis, M. G. Carpenter, R. Tschanz, S. Meyes, D. Debrunner, J. Burger, and J. H. J. Allum, "Trunk sway reductions in young and older adults using multi-modal biofeedback," *Gait and posture*, vol. 31, no. 4, pp. 465–472, 2010.

[345] J. L. Huffman, L. E. Norton, A. L. Adkin, and J. H. J. Allum, "Directional effects of biofeedback on trunk sway during stance tasks in healthy young adults," *Gait and posture*, vol. 32, no. 1, pp. 62–66, 2010.

[346] C. Kinnaird, J. Lee, W. J. Carender, M. Kabeto, B. J. Martin, and K. H. Sienko, "The effects of attractive vs. repulsive instructional cuing on balance performance," *Journal of NeuroEngineering and Rehabilitation*, vol. 13, no. 29, pp. 1–5, 2016.

[347] R. W. Lindeman, Y. Yanagida, K. Hosaka, and S. Abe, "The TactaPack: A wireless sensor/actuator package for physical therapy applications," in *2006 14th Symposium on Haptic Interfaces for Virtual Environment and Teleoperator Systems*, pp. 337–341, IEEE, 2005.

[348] F. Asseman, A. M. Bronstein, and M. A. Gresty, "Using vibrotactile feedback of instability to trigger a forward compensatory stepping response," *Journal of neurology*, vol. 254, no. 11, pp. 1555–1561, 2007.

[349] J. J. Jeka and J. R. Lackner, "Fingertip contact influences human postural control," *Experimental Brain Research*, vol. 79, no. 2, pp. 495–502, 1994.

[350] S. Clapp and A. M. Wing, "Light touch contribution to balance in normal bipedal stance," *Experimental brain research*, vol. 125, no. 4, pp. 521–524, 1999.

[351] M. W. Rogers, D. L. Wardman, S. R. Lord, and R. C. Fitzpatrick, "Passive tactile sensory input improves stability during standing," *Experimental Brain Research*, vol. 136, no. 4, pp. 514–522, 2001.

[352] M. Kouzaki and K. Masani, "Reduced postural sway during quiet standing by light touch is due to finger tactile feedback but not mechanical support," *Experimental brain research*, vol. 188, no. 1, pp. 153–158, 2008.

[353] A. M. Wing, L. Johannsen, and S. Endo, "Light touch for balance: influence of a time-varying external driving signal," *Philosophical Transactions of the Royal Society B: Biological Sciences*, vol. 366, no. 1581, pp. 3133–3141, 2011.

[354] A. Bottaro, M. Casadio, P. Morasso, and V. Sanguineti, "Body sway during quiet standing: Is it the residual chattering of an intermittent stabilization process?," *Human Movement Science*, vol. 24, no. 4, pp. 588–615, 2005.

[355] Y. Asai, Y. Tasaka, K. Nomura, T. Nomura, M. Casadio, and P. Morasso, "A model of postural control in quiet standing: robust compensation of delay-induced instability using intermittent activation of feedback control," *PLoS One*, vol. 4, no. 7, p. e6169, 2009.

[356] M. F. Folstein, S. E. Folstein, and P. R. McHugh, ""Mini-mental state": a practical method for grading the cognitive state of patients for the clinician," *Journal of psychiatric research*, vol. 12, no. 3, pp. 189–198, 1975.

[357] M. Casadio, V. Sanguineti, P. Morasso, and V. Arrichiello, "Braccio di Ferro: a new haptic workstation for neuromotor rehabilitation," *Technology and Health Care*, vol. 14, no. 3, pp. 123–142, 2006.

[358] R. L. Sainburg, C. Ghez, and D. Kalakanis, "Intersegmental dynamics are controlled by sequential anticipatory, error correction, and postural mechanisms," *Journal of Neurophysiology*, 1999.

[359] L. Simo, C. Ghez, L. Botzer, and R. A. Scheidt, "A quantitative and standardized robotic method for the evaluation of arm proprioception after stroke," in *Engineering in Medicine and Biology Society (EMBC)*, pp. 8227–8230, IEEE, 2011.

[360] P. M. Fitts, "The information capacity of the human motor system in controlling the amplitude of movement.," *Journal of experimental psychology*, vol. 47, no. 6, p. 381, 1954.

[361] M. F. Nolan, "Two-point discrimination assessment in the upper limb in young adult men and women," *Physical therapy*, vol. 62, no. 7, pp. 965–969, 1982.

[362] J. P. Wann and S. F. Ibrahim, "Does limb proprioception drift?," *Experimental Brain Research*, 1992.

[363] K. Bark, W. McMahan, A. Remington, J. Gewirtz, A. Wedmid, D. I. Lee, and K. J. Kuchenbecker, "In vivo validation of a system for haptic feedback of tool vibrations in robotic surgery," *Surgical Endoscopy*, 2013.

[364] A. M. Okamura, "Haptic feedback in robot-assisted minimally invasive surgery," 2009.

[365] M. K. Holden and E. Todorov, "Use of virtual environments in motor learning and rehabilitation," *Department of Brain and Cognitive Sciences, Handbook of Virtual Environments: Design, Implementation, and Applications*, pp. 999–1026, 2002.

[366] E. Tzorakoleftherakis, M. C. Bengtson, F. A. Mussa-Ivaldi, R. A. Scheidt, and T. D. Murphey, "Tactile proprioceptive input in robotic rehabilitation after stroke," in *2015 IEEE International Conference on Robotics and Automation (ICRA)*, pp. 6475–6481, IEEE, 2015.

[367] F. Wolf and R. Kuber, "Developing a head-mounted tactile prototype to support situational awareness," *International Journal of Human Computer Studies*, 2018.

[368] K. Bark, P. Khanna, R. Irwin, P. Kapur, S. A. Jax, L. J. Buxbaum, and K. J. Kuchenbecker, "Lessons in using vibrotactile feedback to guide fast arm," *IEEE World Haptics Conference (WHC)*, pp. 355–360, 2011.

[369] J. Van Der Linden, R. Johnson, J. Bird, Y. Rogers, and E. Schoonderwaldt, "Buzzing to play: Lessons learned from an in the wild study of real-time vibrotactile feedback," in *Conference on Human Factors in Computing Systems - Proceedings*, 2011.

[370] P. B. Shull and D. D. Damian, "Haptic wearables as sensory replacement , sensory augmentation and trainer – a review," *Journal of NeuroEngineering and Rehabilitation*, pp. 1–13, 2015.

[371] K. H. Sienko, R. D. Seidler, W. J. Carender, A. D. Goodworth, S. L. Whitney, and R. J. Peterka, "Potential mechanisms of sensory augmentation systems on human balance control," *Frontiers in Neurology*, 2018.

[372] M. Flanders, S. I. Helms Tillery, and J. F. Soechting, "Early stages in a sensorimotor transformation," *Behavioral and Brain Sciences*, 1992.

[373] D. Piovesan, M. Casadio, F. A. Mussa-Ivaldi, and P. Morasso, "Multijoint arm stiffness during movements following stroke: Implications for robot therapy," in *2011 IEEE International Conference on Rehabilitation Robotics*, pp. 1–7, IEEE, 2011.

[374] E. M. Mosier, T. J. Herda, M. A. Trevino, and J. D. Miller, "The influence of prolonged vibration on motor unit behavior," *Muscle and nerve*, vol. 55, no. 4, pp. 500–507, 2017.

[375] H. Liu, Z. Zhang, X. Xie, Y. Zhu, Y. Liu, Y. Wang, and S.-C. Zhu, "High-fidelity grasping in virtual reality using a glove-based system," in *2019 International Conference on Robotics and Automation (ICRA)*, pp. 5180–5186, IEEE, 2019.

[376] J. Gordon, M. F. Ghilardi, and C. Ghez, "Impairments of reaching movements in patients without proprioception. I. Spatial errors.," *Journal of neurophysiology*, vol. 73, no. 1, pp. 347–60, 1995.

[377] J. Wang and R. L. Sainburg, "Interlimb transfer of visuomotor rotations depends on handedness," *Experimental Brain Research*, vol. 175, no. 2, pp. 223–230, 2006.

[378] I. Yeh, J. Holst-Wolf, N. Elangovan, A. V. Cuppone, K. Lakshminarayan, L. Capello, L. Masia, and J. Konczak, "Effects of a robot-aided somatosensory training on proprioception and motor function in stroke survivors," *Journal of NeuroEngineering and Rehabilitation*, vol. 18, pp. 1–11, 2021.

[379] R. M. Silva, E. Sousa, P. Fonseca, A. R. Pinheiro, C. Silva, M. V. Correia, and S. Mouta, "Analysis and quantification of upper-limb movement in motor rehabilitation after stroke BT - converging clinical and engineering research on neurorehabilitation II," (Cham), pp. 209–213, Springer International Publishing, 2017.

[380] M. Coscia, M. J. Wessel, U. Chaudary, J. d. R. Millán, S. Micera, A. Guggisberg, P. Vuadens, J. Donoghue, N. Birbaumer, and F. C. Hummel, "Neurotechnology-aided interventions for upper limb motor rehabilitation in severe chronic stroke," *Brain*, vol. 142, no. 8, pp. 2182–2197, 2019.

[381] U. Gopaul, L. M. Carey, R. Callister, M. Nilsson, and P. van Vliet, "Combined somatosensory and motor training to improve upper limb function following stroke: a systematic scoping review," *Physical Therapy Reviews*, vol. 23, no. 6, pp. 355–375, 2018.

[382] D. B. Camarillo, T. M. Krummel, and K. J. Salisbury Jr, "Robotic technology in surgery: past, present, and future," *The American Journal of Surgery*, vol. 188, no. 4, pp. 2–15, 2004.

[383] G. Spinoglio, A. Marano, F. Priora, F. Melandro, and G. Formisano, "History of robotic surgery," in *Robotic Surgery*, pp. 1–12, Springer, 2015.

[384] B. M. A. Schout, A. J. M. Hendrikx, F. Scheele, B. L. H. Bemelmans, and A. J. J. A. Scherpbier, "Validation and implementation of surgical simulators: a critical review of present, past, and future," *Surgical endoscopy*, vol. 24, no. 3, pp. 536–546, 2010.

[385] A. M. Okamura, "Haptics in robot-assisted minimally invasive surgery," *The Encyclopedia of MEDICAL ROBOTICS: Volume 1 Minimally Invasive Surgical Robotics*, pp. 317–339, 2019.

[386] I. El Rassi and J.-M. El Rassi, "A review of haptic feedback in tele-operated robotic surgery," *Journal of medical engineering and technology*, vol. 44, no. 5, pp. 247–254, 2020.

[387] J. K. Koehn and K. J. Kuchenbecker, "Surgeons and non-surgeons prefer haptic feedback of instrument vibrations during robotic surgery," *Surgical endoscopy*, vol. 29, no. 10, pp. 2970–2983, 2015.

[388] C. E. Reiley, T. Akinbiyi, D. Burschka, D. C. Chang, A. M. Okamura, and D. D. Yuh, "Effects of visual force feedback on robot-assisted surgical task performance," *The Journal of thoracic and cardiovascular surgery*, vol. 135, no. 1, pp. 196–202, 2008.

[389] Y. Liang, L. Sun, Z. Du, Z. Yan, and W. Wang, "Mechanism design and optimization of a haptic master manipulator for laparoscopic surgical robots," *IEEE Access*, vol. 7, pp. 147808–147824, 2019.

[390] Z. Chua, A. M. Jarc, S. M. Wren, I. Nisky, and A. M. Okamura, "Task Dynamics of Prior Training Influence Visual Force Estimation Ability During Teleoperation," *IEEE Transactions on Medical Robotics and Bionics*, vol. 2, no. 4, pp. 586–597, 2020.

[391] J. D. Brown, J. N. Fernandez, S. P. Cohen, and K. J. Kuchenbecker, "A wrist-squeezing force-feedback system for robotic surgery training," in *2017 IEEE World Haptics Conference (WHC)*, pp. 107–112, IEEE, 2017.

[392] L. Moody, C. Baber, and T. N. Arvanitis, "Objective surgical performance evaluation based on haptic feedback," in *Medicine Meets Virtual Reality 02/10*, pp. 304–310, IOS Press, 2002.

[393] C. G. L. Cao, M. Zhou, D. B. Jones, and S. D. Schwaitzberg, "Can surgeons think and operate with haptics at the same time?," *Journal of Gastrointestinal Surgery*, vol. 11, no. 11, pp. 1564–1569, 2007.

[394] M. Mahvash, J. Gwilliam, R. Agarwal, B. Vagvolgyi, L.-M. Su, D. D. Yuh, and A. M. Okamura, "Force-feedback surgical teleoperator: Controller design and palpation experiments," in *2008 Symposium on Haptic Interfaces for Virtual Environment and Teleoperator Systems*, pp. 465–471, IEEE, 2008.

[395] A. Saracino, A. Deguet, F. Staderini, M. N. Boushaki, F. Cianchi, A. Menciassi, and E. Sinibaldi, "Haptic feedback in the da Vinci Research Kit (dVRK): a user study based on grasping, palpation, and incision tasks," *The International Journal of Medical Robotics and Computer Assisted Surgery*, vol. 15, no. 4, p. e1999, 2019.

[396] Q. Ouyang, J. Wu, S. Sun, J. Pensa, A. Abiri, E. Dutson, and J. W. Bisley, "Bio-inspired Haptic Feedback for Artificial Palpation in Robotic Surgery," *IEEE Transactions on Biomedical Engineering*, 2021.

[397] L. Bahar, Y. Sharon, and I. Nisky, "Surgeon-centered analysis of robot-assisted needle driving under different force feedback conditions," *Frontiers in neurorobotics*, vol. 13, p. 108, 2020.

[398] K. Rangarajan, H. Davis, and P. H. Pucher, "Systematic review of virtual haptics in surgical simulation: a valid educational tool?," *Journal of surgical education*, vol. 77, no. 2, pp. 337–347, 2020.

[399] A. Lelevé, T. McDaniel, and C. Rossa, "Haptic training simulation," *Frontiers in Virtual Reality*, vol. 1, p. 3, 2020.

[400] S. McKinley, A. Garg, S. Sen, R. Kapadia, A. Murali, K. Nichols, S. Lim, S. Patil, P. Abbeel, and A. M. Okamura, "A single-use haptic palpation probe for locating subcutaneous blood vessels in robot-assisted minimally invasive surgery," in *2015 IEEE International Conference on Automation Science and Engineering (CASE)*, pp. 1151–1158, Ieee, 2015.

[401] J. Hergenhan, J. Rutschke, M. Uhl, S. E. Navarro, B. Hein, and H. Worn, "A haptic display for tactile and kinesthetic feedback in a CHAI 3D palpation training scenario," in *2015 IEEE International Conference on Robotics and Biomimetics (ROBIO)*, pp. 291–296, IEEE, 2015.

[402] C. R. Wagner, R. D. Howe, and N. Stylopoulos, "The role of force feedback in surgery: analysis of blunt dissection," in *Haptic Interfaces for Virtual Environment and Teleoperator Systems Symposium (HAPTICS)*, p. 73, Citeseer, 2002.

[403] B. Demi, T. Ortmaier, and U. Seibold, "The touch and feel in minimally invasive surgery," in *IEEE international workshop on haptic audio visual environments and their applications*, pp. 6–pp, IEEE, 2005.

[404] J. Guo, S. Guo, and Y. Yu, "Design and characteristics evaluation of a novel teleoperated robotic catheterization system with force feedback for vascular interventional surgery," *Biomedical microdevices*, vol. 18, no. 5, pp. 1–16, 2016.

[405] R. L. Klatzky and B. Wu, "Visual-haptic compliance perception," in *Multisensory Softness*, pp. 17–30, Springer, 2014.

[406] G. De Gersem, H. Van Brussel, and F. Tendick, "Reliable and enhanced stiffness perception in soft-tissue telemanipulation," *The international journal of robotics research*, vol. 24, no. 10, pp. 805–822, 2005.

[407] E. Karadogan, R. L. Williams, J. N. Howell, and R. R. Conatser Jr, "A stiffness discrimination experiment including analysis of palpation forces and velocities," *Simulation in Healthcare*, vol. 5, no. 5, pp. 279–288, 2010.

[408] I. Nisky, F. Huang, A. Milstein, C. M. Pugh, F. A. Mussa-Ivaldi, and A. Karniel, "Perception of stiffness in laparoscopy–the fulcrum effect," *Studies in health technology and informatics*, vol. 173, p. 313, 2012.

[409] A. T. Maereg, A. Nagar, D. Reid, and E. L. Secco, "Wearable vibrotactile haptic device for stiffness discrimination during virtual interactions," *Frontiers in Robotics and AI*, vol. 4, p. 42, 2017.

[410] J. M. Jacinto, A. Filippeschi, C. A. Avizzano, and E. Ruffaldi, "Preliminary Stiffness Perception Assessment for a Tele-palpation Haptic Interface," in *International Conference on Human Haptic Sensing and Touch Enabled Computer Applications*, pp. 175–185, Springer, 2018.

[411] R. Gourishetti and M. Manivannan, "Improved force JND in immersive virtual reality needle insertion simulation," *Virtual Reality*, vol. 23, no. 2, pp. 133–142, 2019.

[412] I. Nisky, A. Pressman, C. M. Pugh, F. A. Mussa-Ivaldi, and A. Karniel, "Perception and action in teleoperated needle insertion," *IEEE transactions on haptics*, vol. 4, no. 3, pp. 155–166, 2011.

[413] A. Abiri, A. Tao, M. LaRocca, X. Guan, S. J. Askari, J. W. Bisley, E. P. Dutson, and W. S. Grundfest, "Visual–perceptual mismatch in robotic surgery," *Surgical endoscopy*, vol. 31, no. 8, pp. 3271–3278, 2017.

[414] H. Joodaki and M. B. Panzer, "Skin mechanical properties and modeling: A review," *Proceedings of the Institution of Mechanical Engineers, Part H: Journal of Engineering in Medicine*, vol. 232, no. 4, pp. 323–343, 2018.

[415] S. Misra, K. T. Ramesh, and A. M. Okamura, "Physically valid surgical simulators: linear versus nonlinear tissue models," *Studies in health technology and informatics*, vol. 132, p. 293, 2008.

[416] J. Reis, H. M. Schambra, L. G. Cohen, E. R. Buch, B. Fritsch, E. Zarahn, P. A. Celnik, and J. W. Krakauer, "Noninvasive cortical stimulation enhances motor skill acquisition over multiple days through an effect on consolidation," *Proceedings of the National Academy of Sciences*, vol. 106, no. 5, pp. 1590–1595, 2009.

[417] A. M. Van Rij, J. R. McDonald, R. A. Pettigrew, M. J. Putterill, C. K. Reddy, and J. J. Wright, "Cusum as an aid to early assessment of the surgical trainee," *Journal of British Surgery*, vol. 82, no. 11, pp. 1500–1503, 1995.

[418] K. Moorthy, Y. Munz, S. K. Sarker, and A. Darzi, "Objective assessment of technical skills in surgery," *Bmj*, vol. 327, no. 7422, pp. 1032–1037, 2003.

[419] I. Nisky, Y. Che, Z. F. Quek, M. Weber, M. H. Hsieh, and A. M. Okamura, "Teleoperated versus open needle driving: Kinematic analysis of experienced surgeons and novice users," in *2015 IEEE International Conference on Robotics and Automation (ICRA)*, pp. 5371–5377, IEEE, 2015.

[420] Y. Sharon, A. M. Jarc, T. S. Lendvay, and I. Nisky, "Rate of Orientation Change as a New Metric for Robot-Assisted and Open Surgical Skill Evaluation," *IEEE Transactions on Medical Robotics and Bionics*, vol. 3, no. 2, pp. 414–425, 2021.

[421] L. Shmuelof, J. W. Krakauer, and P. Mazzoni, "How is a motor skill learned? Change and invariance at the levels of task success and trajectory control," *Journal of neurophysiology*, vol. 108, no. 2, pp. 578–594, 2012.

[422] I. Nisky, A. M. Okamura, and M. H. Hsieh, "Effects of robotic manipulators on movements of novices and surgeons," *Surgical endoscopy*, vol. 28, no. 7, pp. 2145–2158, 2014.

[423] G. Marchesi, G. Ballardini, L. Barone, P. Giannoni, C. Lentino, A. De Luca, and M. Casadio, "Modified Functional Reach Test: Upper-Body Kinematics and Muscular Activity in Chronic Stroke Survivors," *Sensors*, vol. 22, no. 1, p. 230, 2022.

[424] B. Maurin, L. Barbe, B. Bayle, P. Zanne, J. Gangloff, M. De Mathelin, A. Gangi, L. Soler, and A. Forgione, "In vivo study of forces during needle insertions," in *Perspective in Image-Guided Surgery*, pp. 415–422, World Scientific, 2004.

[425] A. M. Okamura, C. Simone, and M. D. O'leary, "Force modeling for needle insertion into soft tissue," *IEEE transactions on biomedical engineering*, vol. 51, no. 10, pp. 1707–1716, 2004.

[426] A. E. Kerdok, M. P. Ottensmeyer, and R. D. Howe, "Effects of perfusion on the viscoelastic characteristics of liver," *Journal of Biomechanics*, vol. 39, no. 12, pp. 2221–2231, 2006.

[427] N. Abolhassani, R. Patel, and M. Moallem, "Needle insertion into soft tissue: A survey," *Medical Engineering and Physics*, vol. 29, no. 4, pp. 413–431, 2007.

[428] M. A. Abd, I. Gonzalez, M. Nojoumian, and E. D. Engeberg, "Trust, satisfaction and frustration measurements during human-robot interaction," in *Proceedings of the 30th Florida Conference on Recent Advances in RoboticsMay 11-12*, vol. 2107, 2017.

[429] M. Giuliani, N. Mirnig, G. Stollnberger, S. Stadler, R. Buchner, and M. Tscheligi, "Systematic analysis of video data from different human–robot interaction studies: a categorization of social signals during error situations," *Frontiers in Psychology*, 2015.

[430] J. Lazar, A. Jones, and B. Shneiderman, "Workplace user frustration with computers: An exploratory investigation of the causes and severity," *Behaviour and Information Technology*, vol. 25, pp. 239–251, may 2006.

[431] B. Weiner, "An Attributional Theory of Achievement Motivation and Emotion," *Psychological Review*, 1985.

[432] S. Fox and P. E. Spector, "A model of work frustration-aggression," *Journal of Organizational Behavior*, vol. 20, no. 6, pp. 915–931, 1999.

[433] J. Dollard, N. E. Miller, L. W. Doob, O. H. Mowrer, and R. R. Sears, *Frustration and aggression.* Yale University Press, oct 1939.

[434] Z. Cao, G. Hidalgo, T. Simon, S. E. Wei, and Y. Sheikh, "OpenPose: Realtime Multi-Person 2D Pose Estimation Using Part Affinity Fields," *IEEE Transactions on Pattern Analysis and Machine Intelligence*, vol. 43, pp. 172–186, jan 2021.

[435] T. Baltrusaitis, P. Robinson, and L. P. Morency, "OpenFace: An open source facial behavior analysis toolkit," in *2016 IEEE Winter Conference on Applications of Computer Vision, WACV 2016*, Institute of Electrical and Electronics Engineers Inc., may 2016.

[436] J. Wagner, F. Lingenfelser, T. Baur, I. Damian, F. Kistler, and E. André, "The Social Signal Interpretation (SSI) Framework Multimodal Signal Processing and Recognition in Real-Time," in *Proceedings of the 21st ACM international conference on Multimedia - MM '13*, (New York, New York, USA), ACM Press, 2013.

[437] S. Zhao, S. Wang, M. Soleymani, D. Joshi, and Q. Ji, "Affective computing for large-scale heterogeneous multimedia data: A survey," dec 2019.

[438] R. W. Picard, "Affective computing: Challenges," *International Journal of Human Computer Studies*, vol. 59, pp. 55–64, jul 2003.

[439] A. Kothig, J. Munoz, S. A. Akgun, A. M. Aroyo, and K. Dautenhahn, "Connecting Humans and Robots Using Physiological Signals – Closing-the-Loop in HRI," pp. 735–742, 2021.

[440] P. Novais and D. Carneiro, "The role of non-intrusive approaches in the development of people-aware systems," *Progress in Artificial Intelligence*, vol. 5, no. 3, pp. 215–220, 2016.

[441] H. Genno, K. Ishikawa, O. Kanbara, M. Kikumoto, Y. Fujiwara, R. Suzuki, and M. Osumi, "Using facial skin temperature to objectively evaluate sensations," *International Journal of Industrial Ergonomics*, vol. 19, pp. 161–171, feb 1997.

[442] D. Shastri, A. Merla, P. Tsiamyrtzis, and I. Pavlidis, "Imaging facial signs of neurophysiological responses," *IEEE Transactions on Biomedical Engineering*, vol. 56, pp. 477–484, feb 2009.

[443] R. Sinha, W. R. Lovallo, and O. A. Parsons, "Cardiovascular differentiation of emotions," *Psychosomatic Medicine*, vol. 54, no. 4, pp. 422–435, 1992.

[444] C. Collet, E. Vernet-Maury, G. Delhomme, and A. Dittmar, "Autonomic nervous system response patterns specificity to basic emotions," *Journal of the Autonomic Nervous System*, vol. 62, pp. 45–57, jan 1997.

[445] C. B. Cross, J. A. Skipper, and D. Petkie, "Thermal imaging to detect physiological indicators of stress in humans," in *Thermosense: Thermal Infrared Applications XXXV*, vol. 8705, p. 87050I, SPIE, may 2013.

[446] J. Stemberger, R. S. Allison, and T. Schnell, "Thermal imaging as a way to classify cognitive workload," in *CRV 2010 - 7th Canadian Conference on Computer and Robot Vision*, pp. 231–238, 2010.

[447] Y. Abdelrahman, E. Velloso, T. Dingler, A. Schmidt, and F. Vetere, "Cognitive Heat," *Proceedings of the ACM on Interactive, Mobile, Wearable and Ubiquitous Technologies*, vol. 1, pp. 1–20, sep 2017.

[448] B. A. Rajoub and R. Zwiggelaar, "Thermal Facial Analysis for Deception Detection," *IEEE Transactions on Information Forensics and Security*, vol. 9, pp. 1015–1023, jun 2014.

[449] J. P. Gee, *Good video games + good learning: collected essays on video games, learning ...*, vol. 49. New York :: Lang,, 2007.

[450] F. Chen, J. Zhou, Y. Wang, K. Yu, S. Z. Arshad, A. Khawaji, and D. Conway, *Robust multimodal cognitive load measurement*. Springer, 2016.

[451] B. Kort, R. Reilly, and R. W. Picard, "An affective model of interplay between emotions and learning: Reengineering educational pedagogy-building a learning companion," in *Proceedings IEEE international conference on advanced learning technologies*, pp. 43–46, IEEE, 2001.

[452] S. Aslam, K. Gouweleeuw, G. Verhoeven, and N. Zwart, "Classification of Disappointment and Frustration Elicited by Human-Computer Interaction: Towards Affective HCI," No. August, 2019.

[453] Z. Liu, V. Pataranutaporn, J. Ocumpaugh, and R. Baker, "Sequences of frustration and confusion, and learning," in *Educational data mining 2013*, Citeseer, 2013.

[454] D. M. C. Lee, M. M. T. Rodrigo, R. S. Baker, J. O. Sugay, and A. Coronel, "Exploring the relationship between novice programmer confusion and achievement," in *Lecture Notes in Computer Science (including subseries Lecture Notes in Artificial Intelligence and Lecture Notes in Bioinformatics)*, vol. 6974 LNCS, pp. 175–184, 2011.

[455] J. Sabourin, J. P. Rowe, B. W. Mott, and J. C. Lester, "When off-task is on-task: The affective role of off-task behavior in narrative-centered learning environments," in *AIED*, 2011.

[456] A. Weidemann and N. Rußwinkel, "The Role of Frustration in Human–Robot Interaction – What Is Needed for a Successful Collaboration?," *Frontiers in Psychology*, vol. 12, p. 707, mar 2021.

[457] B. Taylor, A. Dey, D. Siewiorek, and A. Smailagic, "Using physiological sensors to detect levels of user frustration induced by system delays," in *UbiComp 2015 - Proceedings of the 2015 ACM International Joint Conference on Pervasive and Ubiquitous Computing*, pp. 517–528, Association for Computing Machinery, Inc, sep 2015.

[458] A. Kapoor, W. Burleson, and R. W. Picard, "Automatic prediction of frustration," *International Journal of Human Computer Studies*, vol. 65, pp. 724–736, aug 2007.

[459] M. A. Abd, I. Gonzalez, M. Nojoumian, and E. D. Engeberg, "Trust , Satisfaction and Frustration Measurements During Human-Robot Interaction," *30th Florida Conference on Recent Advances in Robotics (FCRAR)*, 2017.

[460] A. Psaltis, K. Kaza, K. Stefanidis, S. Thermos, K. C. Apostolakis, K. Dimitropoulos, and P. Daras, "Multimodal affective state recognition in serious games applications," in *2016 IEEE International Conference on Imaging Systems and Techniques (IST)*, pp. 435–439, 2016.

[461] A. Fydanaki and Z. Geradts, "Evaluating OpenFace: an open-source automatic facial comparison algorithm for forensics," *https://doi.org/10.1080/20961790.2018.1523703*, vol. 3, pp. 202–209, jul 2018.

[462] J. M. Lloyd, *Thermal Imaging Systems*. Boston, MA: Springer US, 1975.

[463] T. Nguyen, K. Tran, and H. Nguyen, "Towards Thermal Region of Interest for Human Emotion Estimation," in *Proceedings of 2018 10th International Conference on Knowledge and Systems Engineering, KSE 2018*, pp. 152–157, Institute of Electrical and Electronics Engineers Inc., dec 2018.

[464] H. Nguyen, K. Kotani, F. Chen, and B. Le, "A thermal facial emotion database and its analysis," in *Lecture Notes in Computer Science (including subseries Lecture Notes in Artificial Intelligence and Lecture Notes in Bioinformatics)*, vol. 8333 LNCS, pp. 397–408, Springer Verlag, oct 2014.

[465] B. Bhushan, S. Basu, P. K. Panigrahi, and S. Dutta, "Exploring the Thermal Signature of Guilt, Shame, and Remorse," *Frontiers in Psychology*, vol. 11, p. 2874, nov 2020.

[466] S. Ioannou, V. Gallese, and A. Merla, "Thermal infrared imaging in psychophysiology: Potentialities and limits," *Psychophysiology*, vol. 51, pp. 951–963, oct 2014.

[467] M. Sorostinean, F. Ferland, and A. Tapus, "Reliable stress measurement using face temperature variation with a thermal camera in human-robot interaction," in *IEEE-RAS International Conference on Humanoid Robots*, vol. 2015-Decem, pp. 14–19, IEEE Computer Society, dec 2015.

[468] M. N. Haji Mohd, M. Kashima, K. Sato, and M. Watanabe, "Mental Stress Recognition based on Non-invasive and Non-contact Measurement from Stereo Thermal and Visible Sensors," *International Journal of Affective Engineering*, vol. 14, no. 1, pp. 9–17, 2015.

[469] S. Wang, M. He, Z. Gao, S. He, and Q. Ji, "Emotion recognition from thermal infrared images using deep boltzmann machine," *Frontiers of Computer Science*, vol. 8, no. 4, pp. 609–618, 2014.

[470] F. G. W. C. Paas and J. J. G. V. Merriënboer, "The Efficiency of Instructional Conditions: An Approach to Combine Mental Effort and Performance Measures," *Human Factors*, vol. 35, no. 4, pp. 737–743, 1993.

[471] S. van Waveren, E. J. Carter, O. Örnberg, and I. Leite, "Exploring Non-Expert Robot Programming Through Crowdsourcing," *Frontiers in Robotics and AI*, vol. 8, 2021.

[472] D. W. Fiske, "Consistency of the factorial structures of personality ratings from different sources," *Journal of Abnormal and Social Psychology*, vol. 44, pp. 329–344, jul 1949.

[473] S. G. Hart and L. E. Staveland, "Development of NASA-TLX (Task Load Index): Results of Empirical and Theoretical Research," *Advances in Psychology*, vol. 52, pp. 139–183, jan 1988.

[474] S. Cecchi, A. Piersanti, A. Poli, and S. Spinsante, "Physical Stimuli and Emotions: EDA Features Analysis from a Wrist-Worn Measurement Sensor," in *IEEE International Workshop on Computer Aided Modeling and Design of Communication Links and Networks, CAMAD*, vol. 2020-Septe, Institute of Electrical and Electronics Engineers Inc., sep 2020.

[475] J. Tao and T. Tan, "Affective Computing: A Review," *Lecture Notes in Computer Science (including subseries Lecture Notes in Artificial Intelligence and Lecture Notes in Bioinformatics)*, vol. 3784 LNCS, pp. 981–995, oct 2005.

[476] R. Chinmayi, G. J. Nair, M. Soundarya, D. S. Poojitha, G. Venugopal, and J. Vijayan, "Extracting the features of emotion from EEG signals and classify using affective computing," *Proceedings of the 2017 International Conference on Wireless Communications, Signal Processing and Networking, WiSPNET 2017*, vol. 2018-January, pp. 2032–2036, feb 2018.

[477] E. Vyzas and R. W. Picard, "Offline and online recognition of emotion expression from physiological data," in *Workshop on Emotion-Based Agent Architectures at the Third International Conference on Autonomous Agents*, vol. Technical, 1999.

[478] R. W. Picard, E. Vyzas, and J. Healey, "Toward machine emotional intelligence: Analysis of affective physiological state," *IEEE Transactions on Pattern Analysis and Machine Intelligence*, vol. 23, no. 10, pp. 1175–1191, 2001.

[479] V. Kolodyazhniy, S. D. Kreibig, J. J. Gross, W. T. Roth, and F. H. Wilhelm, "An affective computing approach to physiological emotion specificity: Toward subject-independent and stimulus-independent classification of film-induced emotions," *Psychophysiology*, vol. 48, pp. 908–922, jul 2011.

[480] P. Ekman, *Emotions revealed: recognizing faces and feelings to improve communication and emotional life*. 2003.

[481] D. Makowski, T. Pham, Z. J. Lau, J. C. Brammer, F. Lespinasse, H. Pham, C. Schölzel, and S. H. Chen, "NeuroKit2: A Python toolbox for neurophysiological signal processing," *Behavior Research Methods*, 2021.

[482] M. Nabian, Y. Yin, J. Wormwood, K. S. Quigley, L. F. Barrett, and S. Ostadabbas, "An open-source feature extraction tool for the analysis of peripheral physiological data," *IEEE Journal of Translational Engineering in Health and Medicine*, 2018.

[483] G. Menardi and N. Torelli, "Training and assessing classification rules with imbalanced data," *Data Mining and Knowledge Discovery 2012 28:1*, vol. 28, pp. 92–122, oct 2012.

[484] L. A. Jeni, J. F. Cohn, and F. De La Torre, "Facing imbalanced data–recommendations for the use of performance metrics," in *2013 Humaine Association Conference on Affective Computing and Intelligent Interaction*, pp. 245–251, 2013.

[485] A. K. Vail, J. B. Wiggins, J. F. Grafsgaard, K. E. Boyer, E. N. Wiebe, and J. C. Lester, "The affective impact of tutor questions: Predicting frustration and engagement.," *International Educational Data Mining Society*, 2016.

[486] E. Babaei, N. Srivastava, J. Newn, Q. Zhou, T. Dingler, and E. Velloso, *Faces of Focus: A Study on the Facial Cues of Attentional States*, p. 1–13. New York, NY, USA: Association for Computing Machinery, 2020.

[487] D. Kulíc and E. Croft, "Affective state estimation for human-robot interaction," in *IEEE Transactions on Robotics*, vol. 23, pp. 991–1000, oct 2007.

[488] K. Ihme, A. Unni, M. Zhang, J. W. Rieger, and M. Jipp, "Recognizing frustration of drivers from face video recordings and brain activation measurements with functional near-infrared spectroscopy," *Frontiers in human neuroscience*, vol. 12, p. 327, 2018.

[489] S. D'Mello, S. Craig, B. Gholson, S. Franklin, R. Picard, and A. Graesser, "Integrating affect sensors into an intelligent tutoring system," in *Affective interactions: The computer in the affective loop. Proceedings of the 2005 International Conference on Intelligent User Interfaces*, pp. 7–13, 2004.

[490] B. McDaniel, S. D'Mello, B. King, P. Chipman, K. Tapp, and A. Graesser, "Facial features for affective state detection in learning environments," in *Proceedings of the Annual Meeting of the Cognitive Science Society*, vol. 29, 2007.

[491] M. E. Dawson, A. M. Schell, and D. L. Filion, "The electrodermal system.," 2017.

[492] G. I. Christopoulos, M. A. Uy, and W. J. Yap, "The Body and the Brain: Measuring Skin Conductance Responses to Understand the Emotional Experience," *Organizational Research Methods*, vol. 22, no. 1, pp. 394–420, 2019.

[493] J. J. Braithwaite, D. G. Watson, R. Jones, and M. Rowe, "A guide for analysing electrodermal activity (eda) & skin conductance responses (scrs) for psychological experiments," *Psychophysiology*, vol. 49, no. 1, pp. 1017–1034, 2013.

Appendix A

Supplementary force feedback: effects of tissue stiffness on the performance of a virtual incision task

A.1 Introduction

Robot-Assisted Minimal Invasive Surgery (RAMIS) offers advantages to both patients and surgeons: it minimizes tissue trauma, complication rates, pain, post-operative infection risk, and recovery time [382, 383]. Furthermore, it improves accuracy and dexterity by reducing tremors [383, 384], muscle fatigue [384], and providing optimal hand-eye alignment and motion scaling [383]. Nevertheless, state-of-the-art RAMIS systems have several drawbacks, such as the cost and the requirement of training for surgeons and nurses [385]. A major limitation is the lack of haptic feedback [385, 386] due to the physical separation between the surgeon and the instruments [387]. Thus, haptic sensations such as resistance of tissue or tension when tying a suture are imperceptible to the surgeon [388, 389]. In order to counteract the absence of haptic feedback, surgeons rely on visual feedback. This creates a different experience from open surgery [255, 390], may create a cognitive overload [391], and increase the learning time [364, 385]. Surprisingly, despite the growing interest in developing and testing RAMIS with haptic feedback [392–396], on-going debates are related to the benefits of haptic to RAMIS [397]. Similarly, haptic feedback is important, yet not fully accepted, in surgical simulations [398, 399].

Several studies assessed the role of haptic feedback in surgical tasks as palpation [394, 400, 401, 395], incision [298, 402, 403], catheter steering [404], and needle driving and

suturing [271, 392, 397]. The success of those surgical tasks depends on the ability of the surgeon to discriminate mechanical properties of the tissues such as stiffness, which benefits from a combination and integration of visual and haptic information [405]. Yet, visual information is not always available. For example, incision and cutting require stiffness discrimination for identifying invisible embedded structures, such as vessels and nerves, that are stiffer than the surrounding tissue matrix. In this scenario, haptic feedback could help to minimize the risk of damages during incision [395]. However, stiffness discrimination during incision and cutting is not extensively investigated.

Several studies assessed the performance of expert and novice users by focusing on the perceptual ability to discriminate stiffness [406–410]. Generally, these studies employ psychophysics and measure the just noticeable difference [411] or perceptual biases [408, 412]. However, this approach requires long experiments, therefore limiting the direct application to RAMIS systems design. Furthermore, it does not quantify the effects of stiffness discrimination on the action [412].

In this study, we quantified the stiffness discrimination ability of non-expert users in a virtual incision task on a two-layer tissue using a haptic device. We seek to address two questions: (i) how the performance is affected by the mechanical properties of the tissue; (ii) whether practice leads to an improvement of performance. We directly evaluate the task performance computing metrics related to the ability in discriminating the mechanical properties of the virtual environment, yet are easy to compute at the end of the trial.

Such metrics will allow a characterization of the stiffness discrimination ability during incursion and incision movements performed with a haptic device and how it changes with practice. This information would improve the knowledge on how the stiffness discrimination ability affect the performance in incision task when people are naive in interacting with a haptic device. Furthermore, our results would highlight how and which mechanical properties of the tissue are easier to discriminate. These findings could be used for improving the efficacy of haptic feedback during RAMIS and to develop surgical simulators where the difficulty level is adapted to the users' ability.

A.2 Material and methods

A.2.1 Participants

Thirty right-handed participants (aged between 18 to 30 years) without any known history of neurological, psychiatric, or neuromuscular disorders participated in the experiment after signing an informed consent.

The inclusion criterion was to be right-handed since handedness could be a confounding factor in this experiment, i.e., handedness could influence the force and somatosensory perception and discrimination ability, as shown and discussed in Chapter 2 and in [100].

All procedures were approved by the Human Participants Research Committee of Ben-Gurion University of the Negev (Be'er-Sheva, Israel) and in accordance with the 1964 Declaration of Helsinki.

A.2.2 Experimental set-up

The participants sat in front of the experimental setup, which was composed of a Sony HMZ-T3W head-mounted display fixed on a support frame and placed above a Sigma 7 (Force Dimension) haptic device. The participants were asked to wear the display to perceive the Virtual Reality (VR) environment and to perform the task by moving the end-effector of the haptic device with their dominant hand (see the subsection A.2.3 for more details).

The height of the head-mounted display was adjusted for each participant to guarantee a comfortable posture and its orientation was fixed at 45°, which preliminary tests highlighted as the most comfortable for the participants. This angle was equal to the orientation of the haptic reference frame in the VR in order to avoid a visual-haptic mismatch that could occur whenever there is a difference between the orientations in the real and virtual world creating discomfort and increasing also the cognitive load of the task [413].

We developed the VR application in CHAI3D, which was responsible for computing visual (sample frequency of 100 Hz) and haptic (sample frequency of 4 kHz) rendering, and sending those to the hardware devices (Fig. A.1). The haptic device has 7 active degrees of freedom, but here we used only the three related to force.

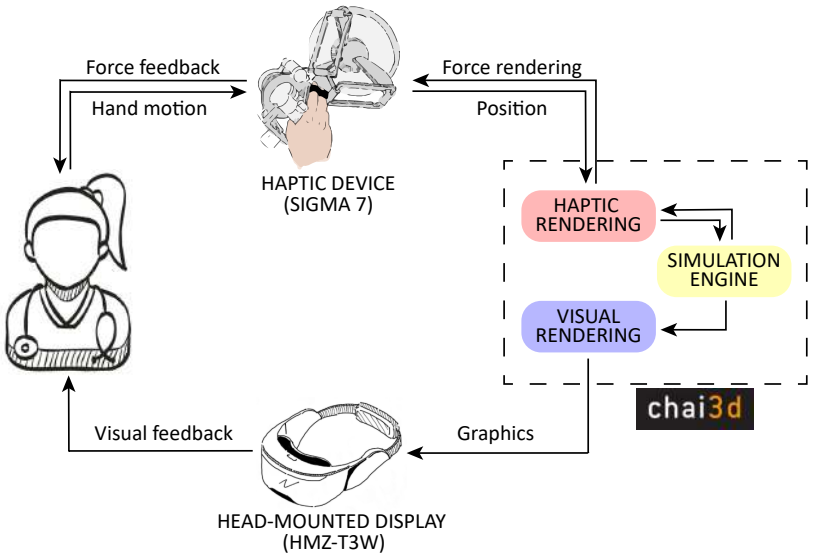

Figure A.1 System's architecture of the experimental set-up. The participants interacted with the VR using the right end-effector of the haptic device. Its position was used by the CHAI3D simulation engine to compute the visual and haptic rendering of the VR environment. The visual rendering was provided via a head-mounted display, and the haptic rendering was via a haptic device.

A.2.3 Experimental task

We focused on the incision task, which is a fundamental, delicate and recurrent surgical procedure. We designed a simplified virtual incision and quantified how performance is affected by different mechanical properties of the virtual tissue and practice.

During the task, participants interacted with a 7 cm high virtual tissue, which was fixed in the same position within the VR environment. The height of the tissue was selected in accordance with the workspace of the haptic device and higher to the real human tissue to better explore the participants' performance. The model of the tissue was composed of two layers, with the softer layer beneath, in order to have a tissue similar to the human skin like in the abdomen [414]. Each layer of the tissue was modeled as an elastic force field with different stiffness (Eq. A.1), with the top layer stiffer than the bottom ($K_1 > K_2$). This model is a good approximation of human skin when the non-viscous properties of the skin are negligible, i.e., small forces are applied [415, 414].

In each trial, participants started outside the tissue, where there were no active forces. They had to reach the top surface of the tissue (first column of Fig. A.2a, Fig. A.2b) where the start and goal (i.e., two gray spheres of 1 cm of diameter) were placed 8 cm apart. Then participants had to place the tool on the start target, which became green when reached

(second column of Fig. A.2a, Fig. A.2b), and pass vertically through the higher stiffness layer until they detected the softer layer beneath (third column of Fig. A.2a, Fig. A.2b). Then, remaining as close as possible to the interface, they had to trace a horizontal line until the goal target, which became red when reached (last column of Fig. A.2a, Fig. A.2b).

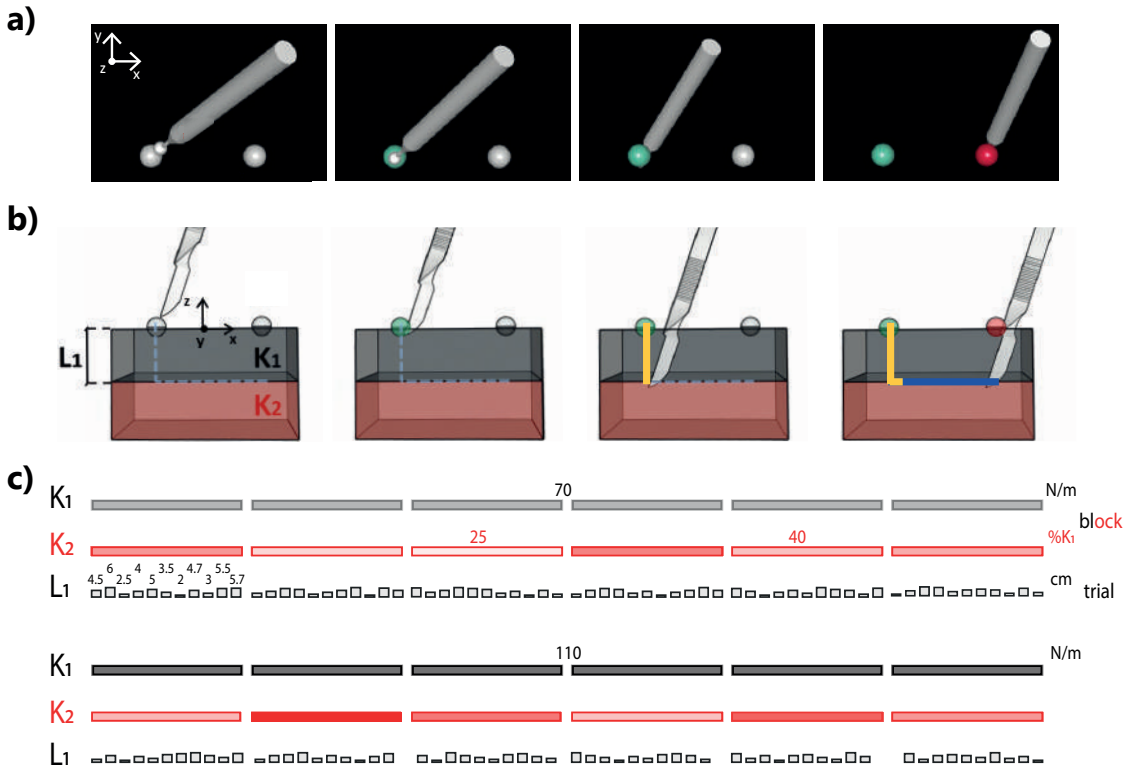

Figure A.2 Steps of the task from a) the participants' point of view, and b) the x-z side perspective. In both, the end-effector is represented by a surgical-resembling tool, and the two spheres are the start and goal targets, which were gray at the beginning, and became green and red, respectively, only after they were reached. K_1, K_2, and L_1 are the mechanical properties of the tissue, i.e., the stiffness of the two layers and the thickness of the first layer. In each column a different step of the task is depicted: (i) the surgical tool is outside the tissue; (ii) the tool reaching the start target; (iii) the tool passing through the first virtual layer until the interface (incursion phase); (iv) the tool reaching the goal target (horizontal cut phase). Here, the line in the bottom row shows the perfect trajectory. c) Graphical representation of the experimental protocol.

The haptic device applied a force F_z only in the normal direction, depending on the position of its end-effector along the z-axis:

$$\begin{cases} F_z = 0, \textit{ when } p_z > 0, \\ F_z = -K_1 \cdot p_z, \textit{ when } L_1 < p_z \leq 0, \\ F_z = -K_2 \cdot p_z, \textit{ when } L_2 \leq p_z \leq L_1, \end{cases} \tag{A.1}$$

where p_z is the z-coordinate of the end-effector, 0 and L_1 are the z-coordinates of the top surface and the interface, respectively; L_1 is the thickness of the first layer and the target depth where the horizontal cut has to be performed, and L_2 is the workspace (and model) boundary. Notice that the force rendered in the other directions will always be equal to zero, independently of the position of the end-effector.

A.2.4 Protocol

The experiment consisted of two sequential phases, namely familiarization and test. The entire experiment lasted about 30 minutes.

The familiarization phase included 30 trials, where the participants experienced different combinations of the environmental parameters (K_1, K_2 and L_1). In this phase, participants received additional information, such as the end-effector velocity, the performance score at the end of each trial - based on the distance between the end-effector and L_1. In addition to that, in the first 15 trials, they knew also the layer where the end-effector was.

The test phase included 120 trials, with a predefined combination of the environment parameters (Fig. A.2C). Trials were organized in 12 'blocks' given by the combination of two values of K_1 (70 and 110 N/m) presented sequentially and six values of K_2 (25, 40, 55, 70, 85, and 100% of K_1). The presentation order of K_1 was balanced among the participants, while the values of K_2 were presented in non-repetitive random order. Each block included ten trials, with different L_1 (2.5, 3.0, 3.5, 4.0, 4.5, 4.7, 5.0, 5.5, 5.7, and 6.0 cm), presented in non-repetitive random order to avoid bias. The number of mechanical properties tested has been chosen to span a large range of mechanical properties of the tissue, without increasing the length of the experiment.

Notice that, in the blocks where K_2 is equal to K_1, the virtual tissue was no more a two-layer model. As consequence, in those trials there was not an interface between the two layers in which was requested to perform the cut, i.e., there was no right depth to perform the

cut. For this reason, those trials were excluded from the following analysis, which is based only on 100 trials for each participant.

A.2.5 Data analysis

We divided each trial into two sequential phases, namely *incursion* and *horizontal cut*. For each phase, the ideal path (last column of Fig. A.2b) was a straight movement along a single axis, different for each phase:

1. *incursion*: movement along the z-axis, from the top surface to the interface between the two layers;

2. *horizontal cut*: movement along the x-axis along the interface from the start to the goal target.

Hence, we defined as *incursion* the trajectory performed until the last time that the end-effector passed the x coordinate of 0.75 cm (with x=0 the center of the start target). The horizontal cut was defined as the first 6 cm of the trajectory performed from the end of the incursion phase toward the goal target. If the horizontal cut was shorter than that, the trial was excluded from the analysis (we excluded a total of 23 out of 100*30 trials).

We calculated the following metrics.

For the *whole trial*, we considered (i) the trial execution time as the time up to the end of the horizontal cut, and (ii) the trial depth error as the difference between the maximum depth reached by the end-effector and the interface between the two layers.

For the *incursion*, we considered (i) the incursion peak speed, as maximum speed along the z-axis during the incursion, and (ii) the ratio between the mean and the peak speed along the z-axis, indicating the temporal smoothness of the speed profile, i.e., values close to 1 indicate a smooth velocity profile.

Finally, for the *horizontal cut*, for each trial, we found the best linear fitting of the end-effector trajectory by using the least square method. Then, we computed (i) the angular deviation of the estimated line from the desired horizontal cut line, and (ii) the maximum deviation of the measured trajectory from the estimated trajectory computed as the absolute maximum distance between them.

Statistical analysis

In order to test whether the performance was affected by the tissue mechanical properties, we grouped the metrics according to the values of K_1, K_2, and L_1.

On each of the metrics considered separately as a dependent variable, we run a repeated measures ANOVA (rm-ANOVA) with three within-subjects factors, i.e., K_1 (2 levels: 70 and 110 N/m), K_2 (5 levels: 25, 40, 55, 70 and 85 $\%K_1$), and L_1 (10 levels).

To test if performance was affected by the practice, we focused only on the metrics computed on the whole trial, i.e., trial execution time and trial depth error. We ordered the data according to the chronological order experienced by each participant, regardless of the environmental parameters. Then, we performed an rm-ANOVA with two within-subjects factors, namely blocks (10 levels, i.e., block of trials with the same K_1 and K_2), and trials within blocks (10 levels).

Before running the rm-ANOVAs, we checked the data normality by using the Anderson-Darling test. When it was rejected, i.e., for all the metrics, we normalized the data with the fractional rank method [104]. We tested the sphericity using Mauchly's test and the Greenhouse-Geisser correction was applied when the assumption of sphericity was rejected. Statistical significance was set at the family-wise error rate of α=0.05, except for the trial depth error, which was used in both the rm-ANOVAs, there we applied the Bonferroni correction and set the significance level at α=0.05/2=0.025.

Furthermore, we were interested in how performance was influenced by the stiffness of the two layers. For that reason, for the trial depth error and the incursion peak velocity, we computed the average value of each participant for each combination of K_1 and K_2. Then, we fitted those with two second-order polynomial functions, i.e., one for each K_1 by using a quartile regression. We computed the minimum of the fitted curve and the related R-square value to investigate the proportion of variance that was predictable.

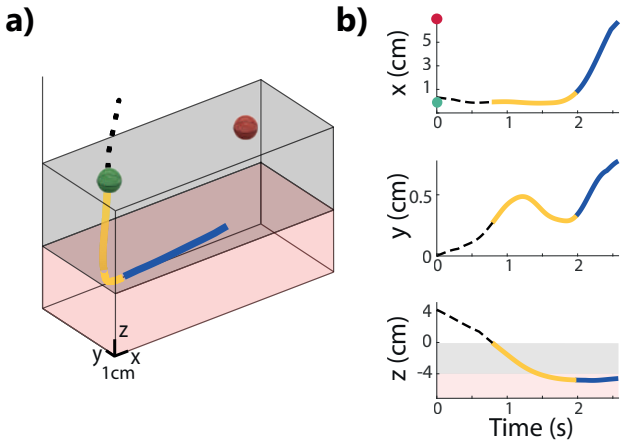

Figure A.3 a) Example of a trajectory, divided into two sequential phases: incursion (yellow) and horizontal cut (blue). b) Example of a trajectory along the three axes as function of the time, divided into incursion and horizontal cut.

A.3 Results

An example of a typical cutting path is depicted in Fig. A.2c and A.2d. The path is smooth, it starts outside the virtual tissue and goes in the start target, and performs a linear vertical incursion (in the z-axis) without changing the direction until the interface between the two levels. There, starts the horizontal cut path, which is below the interface between the two layers, almost linear along the x-axis. Herewith we discuss the effects of practice and of the tissue mechanical properties on performance.

Effects of practice

The trial execution time significantly decreased with practice both between ($F_{9,135.7} = 4.23$, $p = 0.002$) and within ($F_{9,156.6} = 8.89$, $p < 0.001$) blocks (left panel in Fig. A.4).

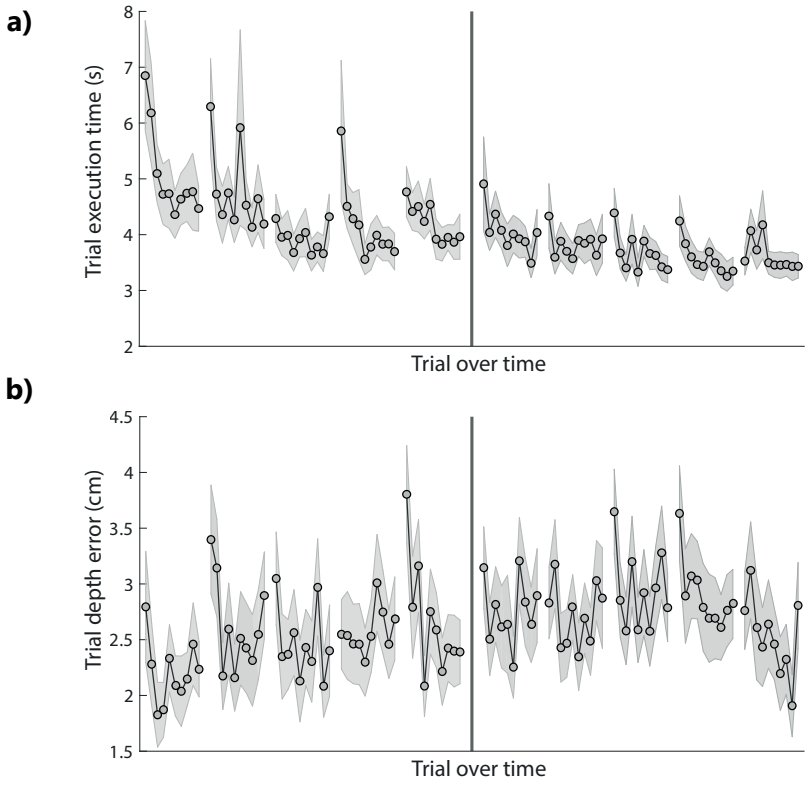

Figure A.4 Performance metrics computed on the whole trial: a) trial execution time and b) trial depth error. The trials are reported in chronological order and divided into 10 blocks of trials. The gray line divides the block of trials with the same K_1 within each participant - the presentation order of the values of K_1 was balanced among the whole population. For each trial, we reported the mean and the standard error of the population.

The trial depth error also changed with the practice both between ($F_{9,156.7} = 3.83$, $p = 0.002$) and within ($F_{9,184.8} = 6.40$, $p < 0.001$) blocks (right panel of Fig. A.4). However, the depth error decreased only within the blocks of trials with the same K_2.

Effects of tissue mechanical properties

Considering the *whole trial*, the trial depth error was significantly affected by the mechanical properties of the virtual tissue: it decreased for higher value of K_1 ($F_{1,29} = 11.71$, $p = 0.002$) and of L_1 ($F_{9,135.6} = 133.67$, $p < 0.001$). Interestingly, the trial depth error depended also on K_2 ($F_{4,116} = 13.62$, $p < 0.001$), i.e., it was U-shaped according to K_2 for each K_1, as shown in Fig. A.5.

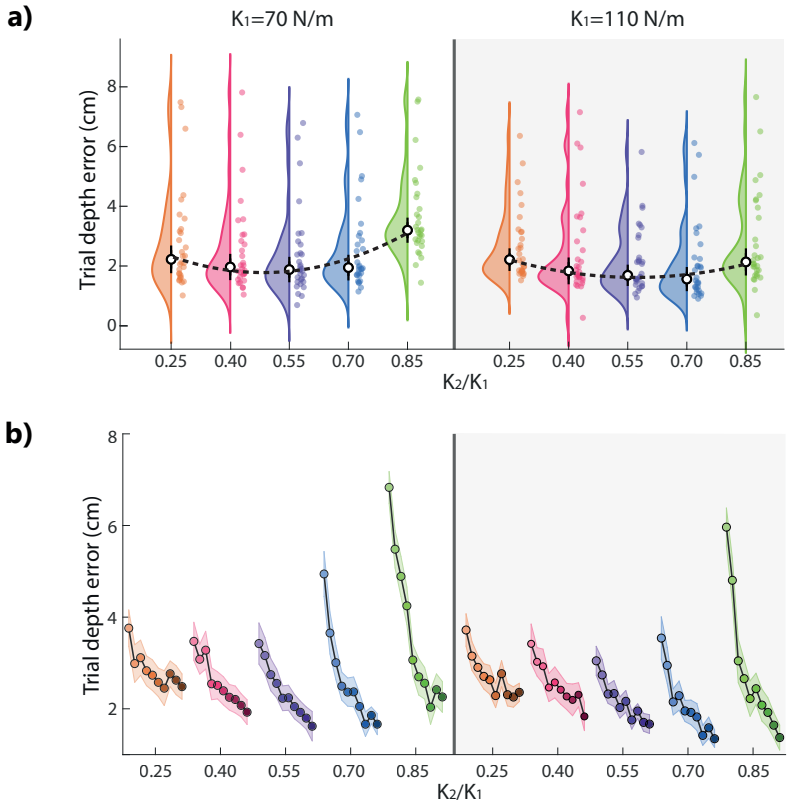

Figure A.5 a) Fitting of the population trial depth error for each K_1 condition with a different second-order polynomial function. For each condition, the smaller circles represent the mean trial depth error of each participant, while the big white circle is the median population error and its standard error. b) Population trial depth error. The trials are divided according to the mechanical properties experienced by the participants. The blocks with different K_1 are separated by the gray line, the blocks with the same K_2/K_1 are reported in the same color, and the L_1 are displayed with a darker color for a deeper interface level. For each condition, we reported the mean and the standard error of the population..

Specifically, it decreased when K_2 was in a range between 40 and 70% K_1. With the aim of investigating this dependency separately, we fitted the data with a second-order polynomial function for each value of K_1. From this analysis, we found that for K_1 = 70 N/m the fitting curve had R^2 = 0.901 and the minimum was in K_2 = 49% of K_1, and that for K_1 = 110 N/m the R^2 = 0.895 and the minimum was at K_2 = 57% of K_1.

As far as the *incursion* phase is concerned, the peak speed and the ratio between the mean and the peak speed were significantly affected by the mechanical properties of the virtual tissue. Indeed, higher thickness of the first level led to higher peak speed ($F_{9,261}$ = 2.28, p = 0.018). It was also influenced by the stiffness of both the layers (K_1 effect: $F_{1,29}$ = 9.64, p = 0.004, K_2 effect: $F_{5,71.3}$ = 15.55, $p < 0.001$), and the interaction between the two stiffness layer ($F_{4,116}$ = 4.66, p = 0.002). Furthermore, the peak speed increased when the difference in stiffness between the two layers was larger than 70% K_1 or smaller than 40% K_1. However, this trend is more evident for the lower stiffness. To deeply investigate this dependency separately, we fitted the data with a second-order polynomial function for each value of K_1. From this analysis, we found that for K_1 = 70 N/m the fitting curve had R^2 = 0.886 and the minimum was in K_2 = 59% of K_1, and that for K_1 = 110 N/m the R^2 = 0.981 and the minimum was in K_2 = 77% of K_1. The ratio between the mean and peak speed is related to how the incursion movement is performed. Indeed, it is related to the number of sub-movements performed to complete the incursion phase. we found that the strategy to accomplish the incursion phase is affected by all the mechanical properties of the tissue. Indeed, it is affected by the stiffness of both the layers separately (K_1 effect: $F_{1,29}$ = 57.84, $p < 0.001$, K_2 effect: $F_{2.4,68.6}$ = 8.17, $p < 0.001$), and the interaction between the two stiffness layer ($F_{4,116}$ = 6.20, $p < 0.001$). In addition, a higher thickness of the first level led to a lower mean-peak speed ratio ($F_{5.5,160.5}$ = 18.48, $p < 0.001$). Interestingly, the effect of the interface depth changes in accordance with the ratio between the stiffness of the two layers (Fig. A.6), in fact, it had more influence for the higher difference between the two layers.

Considering the *horizontal cut*, the performance in this phase was significantly affected by the depth of the interface, and by the stiffness of the second layer. Higher thickness and higher stiffness decreased the deviation from the horizontal line both in terms of maximum deviation (L_1 effect: $F_{9,261}$ = 4.23, $p < 0.001$; K_2 effect: $F_{4,65.9}$ = 5.80, p = 0.003) and angular deviation (L_1 effect: $F_{9,261}$ = 2.52, p = 0.009; K_2 effect: $F_{4,83.8}$ = 10.93, $p < 0.001$). The stiffness of the first layer did not significantly affect the horizontal cut movement (angular deviation: $F_{1,29}$ = 1.50, p = 0.230; maximum deviation: $F_{1,29}$ = 3.31, p = 0.079). The angular deviation from the horizontal line showed that there was a general trend of cutting below the interface between the layers (see Fig. A.3a).

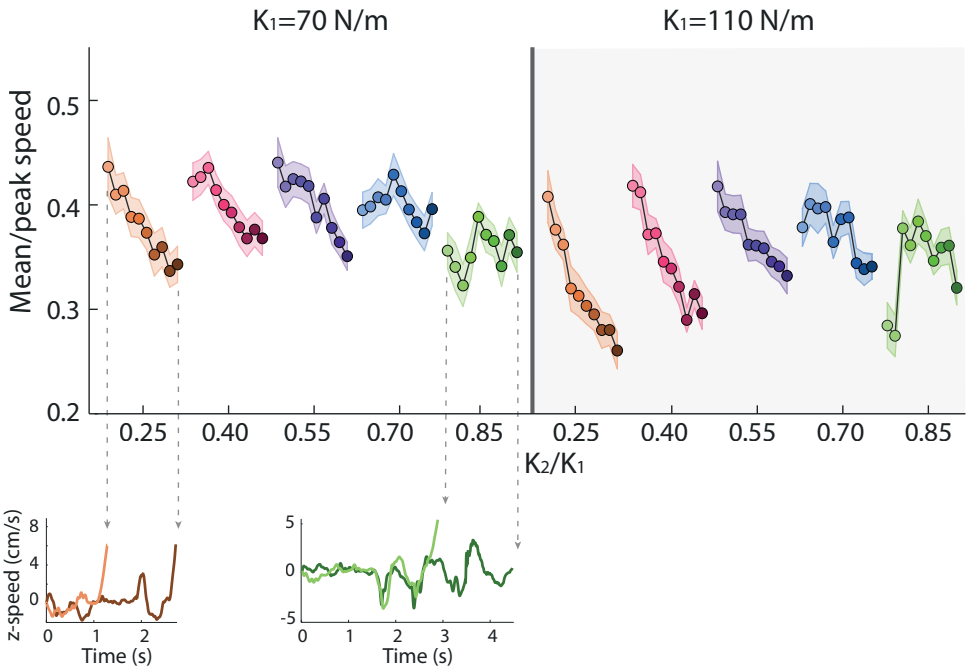

Figure A.6 (top) Population ratio between the mean and the peak speed in the incursion phase. The trials are divided according to the mechanical properties experienced by the participants.The blocks with different K_1 are separated by the gray line, the blocks with the same K_2/K_1 are reported in the same color, and the L1 is displayed with a darker color for a deeper interface level. For each condition, we reported the mean and the standard error of the population. (bottom) Four examples of speed profiles performed in the incursion phase along the z-axis by one participant.

A.4 Discussion

we found that the performance of virtual incision and cutting was significantly affected by the mechanical properties of the two-layer virtual tissue, and in particular by the relative stiffness of the two layers, and the depth of the interface between them. The best performance in discriminating the stiffness in terms of depth error and incursion speed was reached when the stiffness of the second layer was 40-70% of the first layer stiffness. With practice, the time needed to execute the task was reduced, but this reduction was not accompanied by an improvement in the ability to cut closer to the interface between the layers.

Effects of practice

An improvement in the time to execute the task may indicate that the participants became more confident in performing the task with practice (Fig. A.4), even with mechanical properties

of the model never experienced before. In our incision task, participants took more time to perform the task when a new condition was presented - in the first trial of every block the execution time increased independently on the mechanical parameters presented since their presentation order was randomized across blocks for each participant and across participants. This improvement in the time was not followed by a similar betterment of the ability to correctly perform the task. The trial depth error did not decrease with practice and continued to depend on the mechanical properties of the tissue throughout the experiment. Nevertheless, participants did not become less accurate, and hence, they still improved their skill in the sense of performing the task faster without trading-off accuracy [416].

This is consistent with many previous studies, where they reported that the trial time as an indicator of skilled performance in the surgical contexts [417–420], but not for stiffness discrimination tasks, where the perception has a predominant effect on the motor component.

Furthermore, the previous literature supports the hypothesis that in the motor task, practice leads to faster task completion time. However, even in motor tasks, the evidence related to improvement in the movement accuracy is still limited and seems to be task dependent. Specifically, the effect of practice depends on the task and the instruction given to participants, e.g., it can lead to improvement in motor accuracy and execution time [421, 422], or even only in the accuracy [423]. Moreover, our finding highlighted that in an incision task, practice leads to faster task execution time, while the accuracy, i.e., the trial depth error, did not change for our task, which is not a pure motor task, i.e., the perception ability has a predominant role on the motor performance. This specific task is less explored that motor task where the performance is less dependent on the perception ability, and it was not granted that the practice led to faster competition time but not higher accuracy. Thus, our results enlarge the present knowledge, extending previous results to the incision task.

These findings could be due to the length of the familiarization phase, i.e., 30 trials, that might have have brought to a first plateau in the learning curve. However, during this phase was performed in different task conditions (in this phase participants received online and offline visual feedback about their performance). To further investigate this effect, we analyzed the familiarization trials for a subset of participants with the same metrics. There, we found the same trend, i.e., only the trial execution time decreased, supporting the hypothesis that the length of the familiarization did not bring to a first plateau in the learning curve.

Effect of tissue mechanical properties

The stiffness of the first layer affected the trial depth error and the speed of the incursion phase, but not the horizontal cut. This was expected since participants were instructed to perform the cut in the second layer as close as possible to the interface.

In contrast, we found that the metrics computed on the whole trial and the peak speed in the incursion phase exhibited a U-shaped dependence on the ratio between the stiffness of the two layers. This relationship between the difference of the two-layers stiffness (i.e., K_2/K_1) and the trial depth error is unlikely to be related to learning (see section A.4), habitation, or boredom of the repetitive task since the presentation order of the mechanical properties was randomized among the population of participants. The depth error increased and the peak speed decreased both when the participants struggled to perceive the difference between the two layers ($K_2 > 70\%\ K_1$), and when they had difficulty in controlling the movement because of the high differences ($K_2 < 40\%\ K_1$). It is likely that for our participants it was easier to perceive and act upon the change in stiffness between the layers when their difference was between 40 and 70%. The fitting of the second-order polynomial to the trial depth error as a function of second layer stiffness revealed that the optimal K_2/K_1 ratio to minimize errors is approximately 0.50 (0.49 or 0.57 depending on K_1).

For values of K_2 close to K_1 ($> 70\%$) participants probably crossed the layers without perceiving the transition, resulting in higher depth error and peak speed. This is consistent with the findings of Kardogan et al. [407] in a palpation task. Therein, medical students had to compare the stiffness of two virtual surfaces using the force feedback given by a haptic device. For some stiffness values, they found a positive correlation between the palpation speed and the sensitivity to stiffness discrimination, meaning that higher speed is related to lower discrimination ability. However, to the best of our knowledge, it is still an open question what is the cause-effect relation of this correlation, i.e., if higher speed is the result of lower discrimination or vice versa.

For values of K_2 relevantly smaller than K_1 ($< 40\%$), the decrease in performance could be related to the significant jump in force that the user experience in the transition between the two layers. This made staying close to the interface more difficult than the discrimination task itself. we observed this for both values of K_1, but it needs further corroboration for more stiffness values in future studies.

We also found that the depth of the interface affects the performance, i.e., when it was deeper the depth error was lower. This effect could be a result of our experimental design: (1) participants had more time to become aware of the environment and respond when the interface was deeper. This explanation is in line with the results of Jacinto et al. [410] in

a palpation task, who found that a thicker first layer helps in stiffness discrimination. (2) participants were instructed to go deeper until they did not perceive the transition between the layers. If they did not find the transition, the error would have been smaller for the higher thickness of the first layer.

In addition, our results showed also that the mechanical properties of the tissue affect how the incursion phase is performed. Thus, independently on the values of the stiffness, the ratio between the mean and the peak velocity in the normal direction, is more affected by the depth of the interface when the ratio between the two layers is lower. Thus, when the difference between the stiffness of two layers is higher the incursion trajectory is more affected by the thickness of the first layer than when they had similar stiffness ($K_2 > 70\%$ K_1).

Limitations and future studies

Several extensions could deepen our understanding of virtual incisions. An extension to a wider range of stiffness values, including also K_2 higher than K_1, is necessary to reproduce and extend the implications of our findings.

Implementing a visco-elastic and nonlinear tissue model could better generalize to actual tissue, as was previously done for needle insertion [424–427]. Adding also feedback of the shear forces, i.e., the force rendering also along the other axis, could improve the realism of the incision task, especially in the horizontal cut phase, but also in the incursion.

Studying the effects of a time delay could make our findings relevant for remote applications as in RAMIS [412].

In clinical practice, surgeons perform a bi-manual incision procedure, where the non-dominant hand is holding the tissue, and the dominant hand was involved in the task. To successfully accomplish this bimanual task the Central Nervous System has to process the sensory inputs coming from both upper limbs and coordinate the actions of the two hands. For that reason, this bimanual asymmetric condition is more challenging, and the task execution, as well as the findings, could be influenced by results that depend on the interplay of many factors, such as stiffness discrimination, inter-manual coordination, or cross-modal interference [48]. We designed a protocol and experimental design to assess how the stiffness discrimination affects the motor performance in an incision task performed with the dominant hand, without the evaluation of the possible interactions or interference that arise from the coordination of the two upper limbs.

Another limitation of this study is the fact that we focused only on non-technically-skilled users. It is important to extend these studies in the future also to participants with a medical background who perform surgical procedures, including experienced users, such as surgeons, intermediate users such as surgical residents, and beginner users such as medical students. Comparing their performance and learning with those of our naive participants could enlarge our findings on the effect of the practice with haptic interface in a surgical task.

Appendix B

Automatic Frustration Detection Using Thermal Imaging

This study has been carried out at t the Robotic, Perception and Learning Division of KHT - Royal Institute of Technology in Stockholm. It has been published in: Mohamed Y., Ballardini G., Parreira M. T., Lemaignan S., Leite I. *'Automatic frustration detection using thermal imaging'*, ACM/IEEE International Conference on Human-Robot Interaction (HRI), virtual. (March 7-10, 2022)

B.1 Introduction

In collaborative environments with robots, users are prone to feeling frustration due to the robot's behavioural errors, such as social norm violations, or technical errors, like speech recognition failure [428, 429]. This can affect acceptance of the robots [429]. Furthermore, frustration can be associated with lower levels of productivity [430], motivation [431], and trust [428], and higher levels of aggression [432, 433]. If a robot can detect frustration in a user, it could proactively employ mediation strategies or abort the interaction before that state intensifies.

Although current methods can accurately extract social signals (e.g., facial landmarks, action units and pose estimation) [434–436], inferring affective states and understanding those signals can be skewed, biased, and/or subjective [437, 438]. Thus, several sensors have been introduced to detect those affective states using different physiological signals, including electrocardiography, electromyography, skin conductance and body temperature [439]. However, these sensors are usually intrusive and can affect the participants' behaviour [440], making them unsuitable for real-world scenarios.

In 1997, Hirokazu Genno [441] proposed one of the first methods to evaluate stress and fatigue using thermal cameras. In spite of technical limitations in accuracy and resolution, a high correlation was observed between reported stress levels and the measured facial temperatures. This is due to the automatic reactions of the sympathetic nervous system, which are reflected in facial temperature [442–444]. As thermal cameras are becoming more accurate and affordable, thermal imaging has been gaining attention for detecting internal states like stress [445], cognitive load [446, 447], and deception [448].

Some researchers suggest that there are different types of frustration [449]. We focus our work in the detection of frustration in two cases that we consider relevant for human-robot interaction (HRI): failure-induced frustration and cognitive load-induced frustration. Cognitively demanding situations relate to stress and anxiety [450]; moreover, failure to resolve the situation or to change that stressful state can lead to the onset of frustration [451]. Additionally, the occurrence of a repeated failure is directly related to frustration and disappointment [452]. According to [453–455], frustration might be multi-faceted and can be affected by the task's length, nature, or sequence. Hence, we have reasons to believe that, by inducing frustration in different scenarios, we can create a more general prediction of frustration.

In this work, we used an infra-red thermal camera to investigate if a machine learning model can detect frustration using facial thermal data in an HRI scenario. This will be achieved by:

- Comparing the model's performance when using RGB features, i.e. Action Units (AUs), facial thermal features and ElectroDermal Activity (EDA) features;
- Selecting the facial thermal Regions Of Interest (ROIs) that yield the highest prediction accuracy;
- Investigating the effects of aggregating the data points into time intervals of 1, 3.5 and 7 seconds (window size).

B.2 Related Work

Understanding frustration and detecting it while people are interacting with robots is an ongoing challenge. This study will be based on the advancements made in thermal imaging, affective state detection and frustration detection.

Frustration Detection

Frustration has been established as one of the most important affective states to detect in HRI [456]. Hence, several approaches have been implemented to detect frustration. Taylor et al. [457] simultaneously used three wearable sensors to detect five levels of frustration with 80% accuracy using physiological data like electrodermal activity, heat flux, heart rate, skin temperature and skin conductivity. While the results were promising, the use of three different sensors is hardly applicable outside of a laboratory setting and might affect the participants' behaviour. In addition to physiological data, other non-verbal data have also been used for classification. Kapoor el al. [458] used skin conductance, pupil tracking, posture, mouse pressure and smile probability to predict frustration in a tutoring scenario with a virtual agent. The authors highlight the importance of detecting frustration in similar scenarios and compared several machine learning approaches reaching a prediction accuracy of 79%.

A data-driven approach was taken by [452] to classify frustration and disappointment caused by the same task. The authors collected the AUs, EDA and heart rate from 18 subjects within 5 seconds of the occurrence of an event. The event was based on a web form that the participants were made to believe they had to fill out to proceed to the experiment. When the participants tried to submit the form, an error would occur. The occurrence of the first error was assumed to cause disappointment, and any successive errors were assumed to cause frustration. This assumption was supported by self-reports from the participants after the experiment. The authors then created a multi-class classifier that distinguished between neutral, frustration, and disappointment states. Using different data subsets and different machine learning algorithms, they achieved a maximum accuracy of 64%. The authors used only the tonic component of the EDA without any further processing or feature extraction, which limits their results [459]. Furthermore, they used a shuffle split for cross-validation, which does not guarantee different folds, especially for small data sets.

Affective State Detection and Thermal Imaging

Using visual sensors to detect affective states is common in the literature. In [460], the authors used a Microsoft Kinect to extract action units and body movement to predict the six basic affective states: anger, fear, disgust, happiness, surprise and sadness. The authors then fed the facial expression and body movement data streams separately to a uni-modal neural network, and they applied late fusion to determine the affective state of the participant. Their model achieved an accuracy of 93% on an acted affect data set.

Image-based methods for affective state detection, however, are heavily dependant on lighting conditions, and the accuracy of their detection can be drastically affected by the self-report measures and conflicting facial expressions [461].

Alternatively, thermal cameras use far infra-red to measure the radiation emitted by warm objects, which is independent of reflected light [462]. Hence, thermal imaging can be used to overcome an RGB camera's limitations, as the thermal spectrum is not affected by light presence and it is able to record objective measures, such as changes in skin temperature [463].

Thermal imaging primarily has been used by researchers to detect the six basic affective states. For instance, the Kotani Thermal Facial Emotion data set [464] contained visual and thermal images of 26 subjects experiencing those states. Each affective state was induced by making the participants watch an emotional video clip while measuring facial thermal changes. The baseline was collected from the participants while listening to music between clips, and each affective state was labeled based on the participants' self-reports.

More complex affective states like guilt, shame, and remorse were also investigated [465]. The authors induced them by introducing the participants to storyboards with different scenarios, each designed to induce one of those affective states. They found thermal differences between the affective states, as guilt resulted in a change of at least 0.5° C higher than shame and remorse in the forehead, cheek, and mouth regions.

In addition, stress and cognitive load have been a focus for thermal imaging, as their effects on the facial temperature are established in psychology literature [466]. For example, [447] detected cognitive load induced by the Stroop effect and reading tasks, and observed a high correlation between the difficulty of the task and the facial temperature, with an increase in the nose and decrease in the forehead region. Stress detection in HRI using thermal data was discussed in [467], where a thermal camera was mounted on a Meka robot to measure facial temperature variations while playing a card-based quiz game with the robot. Several scenarios were tested with variations in setting parameters. It was observed that the closer the robot was positioned to the participant, the higher their nose temperature. Moreover, they used the RGB camera's ROI detection and overlaid it on the calibrated thermal image. This approach can accurately detect the ROI in the thermal image while eliminating the need for advanced image processing techniques (e.g., using a bilateral filter on the thermal images to preserve edges and reduce the noise [468] or generating binary images and computing their projection curves [469]).

As such, we used an RGB camera calibrated with the thermal camera to detect ROIs, which can be done using an off-the-shelf face detection model. Furthermore, other more

complex facial features can be extracted from the RGB image, including action units, which can later aid in the creation of multi-modal systems with better prediction accuracy for affective states.

To the best of our knowledge, there is no study that examined frustration using thermal imaging, let alone with different types of frustration. In our study, we bridged this gap and used thermal imaging to detect frustration in two cases: cognitive load-induced frustration and failure-induced frustration.

B.3 Data Collection

B.3.1 Participants

A total of 25 participants (12 female, 13 male) without any known history of neurological or psychiatric disorders were recruited for the experiment. The recruitment process was through online platforms, word of mouth and flyers. Most recruits were from the surrounding area and the university campus. The age of the participants ranged from 21 to 46 years *(M = 27.80, SD = 6.18)*. The submitted work describes research with human participants and was approved by a relevant ethics committee. The data from five participants was discarded from the analysis for technical problems occurring during the experiment, as some participants did not comply with the task instructions or frequently touched their face during the data collection. The data from two participants were discarded since they self-reported (see Figure B.3.2) that they did not get frustrated in any of the tasks. For the analysis, we used data collected from 18 participants (9 female, 9 male), with ages between 21 and 39 years old *(M = 27.28, SD = 5.67)*.

B.3.2 Task Description

Participants had to complete two tasks separated by a resting period. A NAO robot provided instructions and guided the participants through the tasks. Two cameras were mounted on a table: a thermal camera and an RGB camera, positioned high enough to ensure that the participants face was always visible, as seen in Figure B.1. One task consisted of a quiz where the answers from the participant were misinterpreted by the robot, leading to frustration caused by failure; the other task involved the completion of two challenges in the laptop in front of the participant.

Figure B.1 Experimental setup.

Participants had to alternate between the two challenges when prompted by the sound of a buzzer. According to cognitive load theory, cognitive load can be reduced if the task is learned [470], hence, switching between tasks constantly is theorized to keep the participant in a constant cognitive load state. Since the participant fails to overcome the cause of the cognitive load, frustration is also expected to occur [451].

As such, the experiment consisted of four stages: baseline (B), collected before the start of the first task, cognitive load-induced frustration (TCog), rest and failure-induced frustration (TFail) (Fig. B.2). The order of the two tasks (TFail and TCog) was balanced among participants to avoid bias due to presentation order. Before each task, the NAO robot briefly explained the instructions and during the tasks a countdown was displayed on a monitor in front of participants.

Baseline. We considered as initial baseline a 1 minute time-window before the first interaction with the robot.

TFail. A simple game of trivia was played between the participants and the NAO robot. The robot was teleoperated by a human wizard. The participant was instructed that they must provide 10 correct answers in less than 5 minutes in order to increase their reward by 20 SEK, from the 80 SEK they were promised. We note that the participant would receive the full compensation of 100 SEK regardless of the performance. During the interaction, NAO asked 14 obvious general questions, e.g. *'how many hours are there in a day?'*, or referred to pictures shown on the laptop in front of the participant. The order of

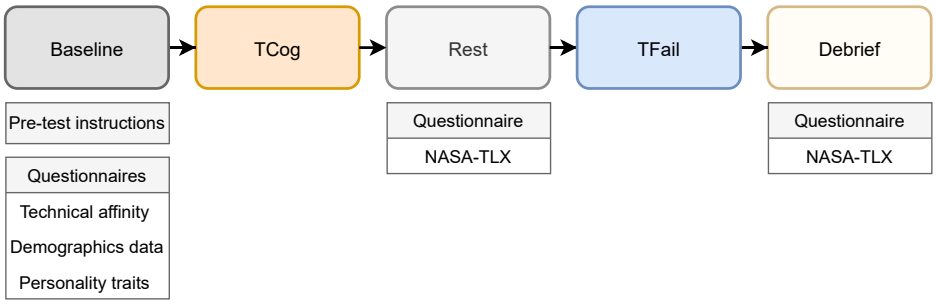

Figure B.2 Tasks procedure, the order of TCog and TFail was randomized to avoid bias.

the questions and the robot responses were predetermined. The answers to the first three questions were correctly identified by the robot, but from the fourth question onwards the robot intentionally declared an answer to be incorrect or it took time while *'processing the answer'* in order to induce frustration. This behaviour was repeated until the time was up or the participant answered all the questions. Out of the 14 questions, 8 answers were considered correct, and in 4 instances NAO took longer to process (2 ending with correct responses).

Rest. The participant was prompted to wait and listen to classical music for two minutes, in order to isolate the physiological responses from each task.

TCog. Cognitive load would be induced by a dual-task composed of a challenging coding task[1] adopted from [471] and a mental rotation task[2] for 8 minutes. In the coding task, participant had to program (using a visual programming language interface) an animated robot to move from one place to the other and its level of difficulty was based on the participant programming background. When a loud buzzer sound was played, the participant had to solve one question in the mental rotation task and after that go back to the coding task. The timing and the number of the buzzer occurrences were adapted to the performance. In general, the closer the participant would get to solving the coding task, the smaller the intervals were between buzzer rings.

Self-assessment. Four different types of self-assessment questionnaires were given to the participants. They had to digitally fill out three of them before the start of the experiment:

- demographic data,
- technical affinity,

[1]https://oscared.github.io/level_4/
[2]https://vample.com/tools/mental-rotation/

- personality traits [472].

The technical affinity questionnaire included questions about current and previous experience with robots (*'have you ever seen a robot in real life?'*). Furthermore, after each task the participants filled out the NASA-TLX [473] questionnaire, stating the amount of cognitive load and frustration felt during the previous task. We used the NASA-TLX self-reports as a manipulation check of our tasks.

B.3.3 System Implementation

The system architecture (Fig. B.3) was composed of both hardware and software components, two cameras mutually calibrated (thermal IR camera: `Optris PI 640`[3] and RGB-D camera: `RealSense D435`[4]), `NAO`[5] robot and an `EDA sensor` (embedded in the Empatica E4 wristband[6]). All of the mentioned components were synchronized in real-time using Robotic Operating System (ROS), except for the EDA sensor, which was synchronized in data post-processing. In addition, OpenCV was used for image processing and camera calibration. The frames from the thermal and RGB cameras were published to ROS (both cameras acquired 15 frames per second). Then, the RGB frames were sent into OpenFace to detect the position of the facial landmarks and the presence and intensity of 18 action units. After that, applying the calibration matrix, the landmark positions were transposed into the thermal frames (Fig. **??**) by OpenCV in order to extract the thermal ROIs, i.e., a rectangle on the thermal image based on the relevant landmark positions.

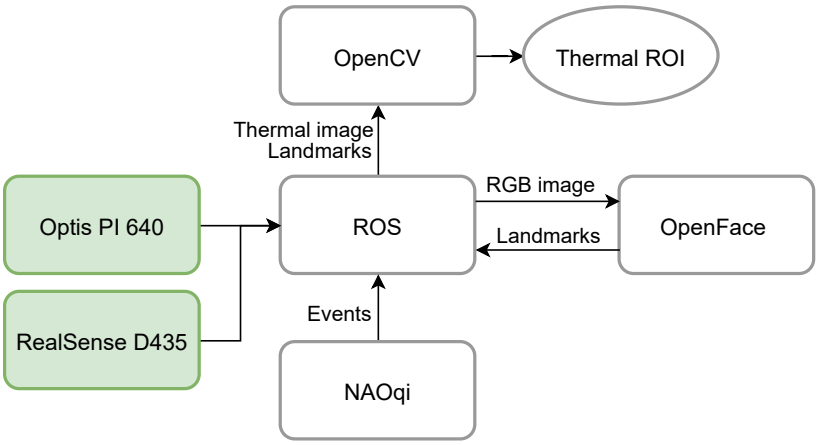

Figure B.3 System architecture.

[3]https://www.optris.global/thermal-imager-optris-pi-640
[4]https://www.intelrealsense.com/depth-camera-d435/
[5]https://www.softbankrobotics.com/emea/en/nao
[6]https://www.empatica.com/research/e4/

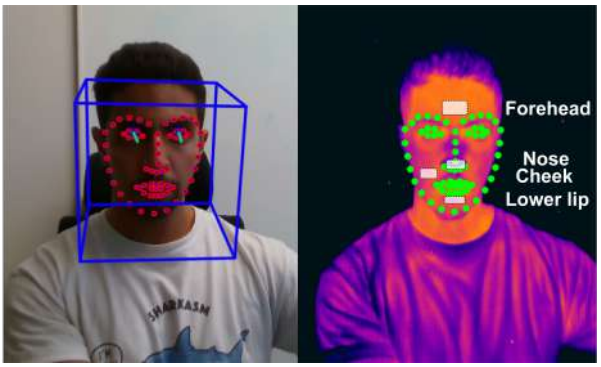

Figure B.4 (left) Landmarks positions detected in the RGB image; (right) thermal image overlaid landmarks and the ROIs, which include forehead, nose, cheek and lower lip.

Finally, an average of the thermal values within the ROIs was computed. Four facial ROIs were extracted from the thermal image: nose, forehead, cheek and lower lip, as shown in Fig. B.4. Furthermore, NAO robot's SDK (NAOqi) was used to control the robot's responses. Key responses which were considered to be important events in the interaction, e.g. instances where the robot responded with *'incorrect'*,*'correct'* and *'processing'*, were published in ROS to be synchronized with the thermal and the RGB data streams.

During the experiment, participants wore the Empatica E4 wristband on the right arm. It captures skin electrical conductance by passing a minimal alternating current between two electrodes in contact with the skin. EDA samples are measured at 4 Hz rate, with a resolution of 900 pS in a measurable range of 0.01-100 µS [474].

Frustration Prediction

For frustration prediction, our goal is to (1) inspect the effectiveness of thermal imaging in detecting frustration when compared to RGB and EDA data, as well as (2) find out optimal features to identify frustration from thermal, RGB and EDA features. The frustration classifier is based on a K-Nearest Neighbors (KNN) algorithm, which is widely used in affective computing with weighted distance tasks [475, 476]. To evaluate the model, we used cross validation of leaving one participant out. The models were trained based on the best features selected by the Sequential Forward Floating Selection (SFFS) algorithm. The SFFS is a wrapper method that uses several greedy search methods to select the features that would yield the highest accuracy in the model. The method was adopted due to its wide use in the affective computing literature [477–479], over its more simple counterpart, sequential forward selection, which does not exclude the features once they are selected.

Labeling

Input data for the classifier corresponded the participants that self-reported frustration in the NASA-TLX questionnaire in TCog *(M = 3.75, SD = 1)* and in TFail *(M = 3.3, SD = 0.9)*. For TCog, we assumed a constant state of cognitive load-induced frustration onset 30 s after the beginning of the task. As such, as we do with B for *'non-frustration'* instances, that period was subdivided into non-overlapping 'windows' of three possible lengths: 1, 3.5 or 7 s. The same windows were applied to all the modalities and used to extract the different features. The features from each window were used as instances to train the models (Table B.2). For TFail, frustration was not assumed as constant state, but inducted by failure, i.e., when the robot replied that the answer was *'incorrect'*, which occurred 6 times during the task. For that reason, in TFail frustration instances corresponded to 7-second periods after those event. The length of the period was determined as the maximum duration allowed to isolate physiological responses to frustration-inducing events, i.e., the minimum amount of time between *'incorrect'* events. Each 7-second period was then subdivided into non-overlapping windows of 1, 3.5 and 7 s. An illustration can be seen in Fig. B.5.

All three data subsets (TCog, TFail and TCog+TFail) used the same baseline (B). Classification with task separation allows for a more fine grained analysis of frustration, while the combination of both types allows for a more general prediction of frustration. The number of instances for each of the data subsets is shown in Table B.1. Furthermore, each subset was trained on four feature types: thermal, RGB, EDA and all features combined. Window sizes can be an indication of the duration of the affective state. Typically, a facial expression lasts between 0.5-4 seconds but a physiological effect lasts 5-15 seconds [480]. Accordingly, the window sizes of 1, 3.5 and 7 seconds were inspected for model training.

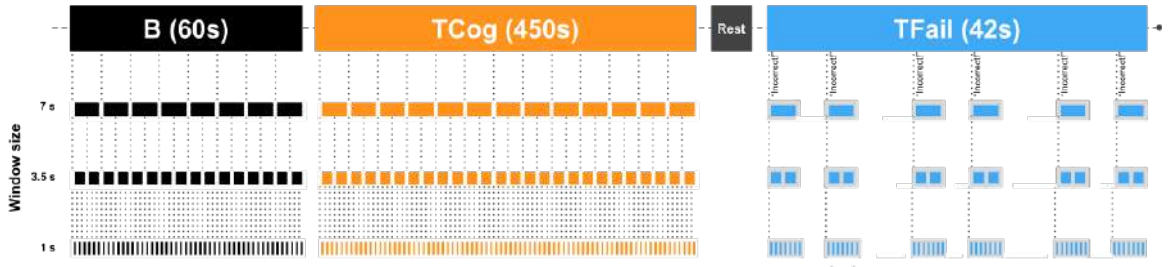

Figure B.5 The length of data of 60, 450 and 42 seconds considered in Baseline, TCog and TFail, with the window sizes to be 1, 3.5 and 7 seconds.

Table B.1 The number of instances used for training in the cases of cognitive load-induced frustration (TCog), failure induced frustration (TFail) and baseline (B).

	No. of Instances		
Window (s)	**TCog**	**TFail**	**B**
1	7692	1127	1010
3.5	2198	322	303
7	1094	161	151

Pre-processing

Thermal ROIs were standardized using `RobustScaler`, a standardization method which removes the median and scales data based on the quartile range, in order to accommodate for the presence of outliers.

Similarly, the standardization based on median and quartile was applied to the EDA data. After that, the EDA was divided into tonic and phasic components [481]. The sensor sampling rate of 4 Hz only allowed window sizes of 3.5 and 7 seconds to be included, otherwise there would not be enough peaks for meaningful results.

All the data was then labelled and split into B, TCog and TFail (as described above, see Fig. B.6 for reference).

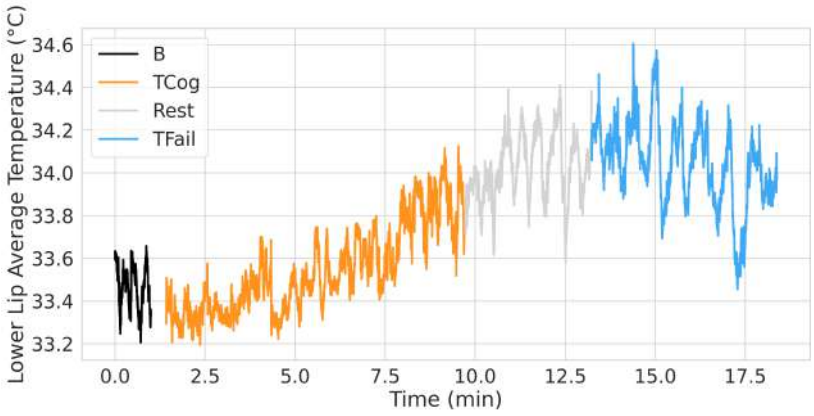

Figure B.6 An example of thermal data from lower lip from one participant, after labelling. B consists of a 60-second period.

All data processing was performed using Python's `scikit-learn`[7], `NeuroKit2`[8] and `MLxtend`[9] libraries.

Feature Extraction

For each modality, several features were extracted as seen in Table B.2.

The features for the thermal data were computed for all the four ROIs: nose, forehead, cheek and lower lip. As for the action units extracted, they corresponded to the Facial Action Coding System (FACS): 1 (inner brow raiser), 2 (outer brow raiser), 4 (brow lowerer), 5 (Upper lid raiser), 6 (cheek raiser), 7 (lid tightener), 9 (nose wrinkler), 10 (upper lip raiser), 12 (lip corner puller), 14 (dimpler), 15 (lip corner depressor), 17 (chin raiser), 20 (lip stretcher), 23 (lip tightener), 25 (lips part), 26 (jaw drop), 28 (lip suck), and 45 (blink).

For both the temperature and the AU intensity, we computed the average, the change and the maximum within each window.

In addition, the tonic component in the EDA data included the mean Skin Conductance Level (SCL), while from the peak detection analysis we extracted standard peak features, such as time interval between consecutive peaks (IPI), frequency of peak occurrence, mean peak amplitude, mean peak rise time and mean peak duration, in accordance to [482].

Table B.2 Extracted features

Modality	**Features**
Thermal	ROIs temperature average ROIs temperature change ROIs temperature maximum
RGB	AU Intensity average AU intensity change AU maximum intensity
EDA	Mean skin conductance level (SCL) Frequency of the peak occurrence Mean peak amplitude Peak rise time Mean peak duration Mean of inter-peak interval (IPI)

[7]https://scikit-learn.org
[8]https://github.com/neuropsychology/NeuroKit
[9]http://rasbt.github.io/mlxtend/

B.4 Results

To evaluate KNN models performance, both the accuracy and the weighted F1-score were computed for each modality and window size. Considering the imbalance of the data, the accuracy alone might be unreliable [483], therefore, the F1-score can be a better metric [484]. The metrics were calculated based on the average result of the cross-validation of leaving one participant out for each test-train split.

Figure B.7 describes the performance of each modality over three window sizes.

Thermal. For the TFail model, increasing the window size slightly increases the accuracy, as in the 1 second window it is 59% then increases by 5% in the 7 second window. F1-score follows accordingly, as it is the highest at 64% in the 7 second window. Similarly, in TCog accuracy is the highest in the 7 second window to 83% . In TCog+TFail, the accuracy peaks in the 7 second window at 87%.

RGB. For TFail, maximum accuracy is achieved in the 3.5 second window (81%) and the lowest in the 1 second window (69%), while in 7 second window it goes back to 71%. In TCog+TFail, the accuracy in the 1 and 3.5 second windows is constant at 89%. The accuracy in TCog gets to 89% in the 1 and 3.5 second windows.

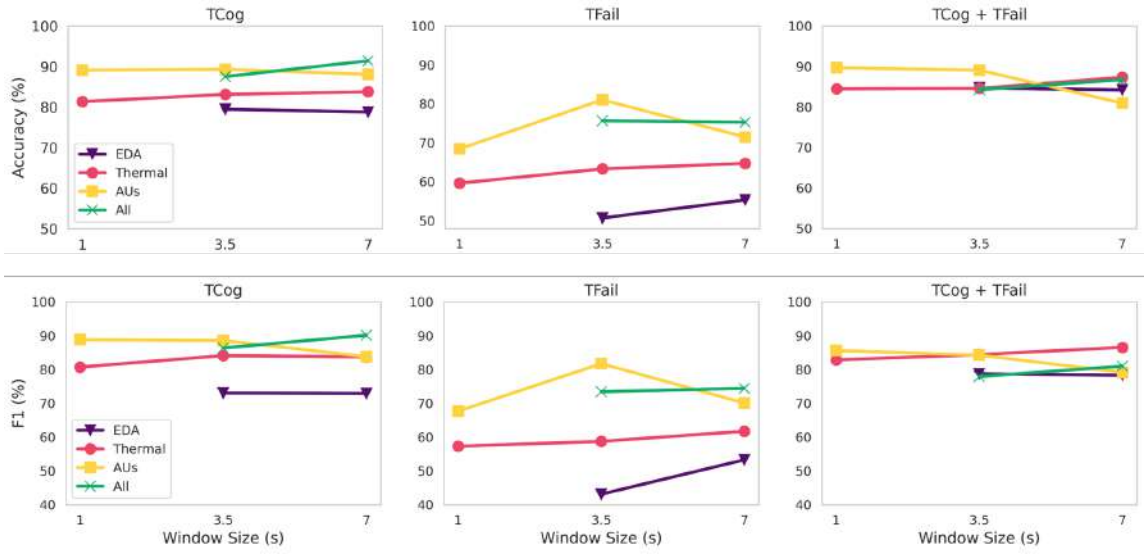

Figure B.7 KNN models performance, accuracy (top) and F1-score (bottom) for cognitive load-induced frustration (left), failure-induced frustration (center) and both data subsets concatenated (right).

F1-score follows the same trend, with a decline to 83% in the 7 second window.

EDA. The EDA data was only inspected in the 3.5 and 7 second windows, due to the low sampling rate of the wristband. In TFail, accuracy goes to 55% in the 7 second window, while the accuracy in TCog and TCog+TFail is 78% and 84% respectively and does not vary across window sizes. A similar trend can also be seen in the F1-score metric, which in TFail is 53%, while for TCog and TCog+TFail it is 73% and 78% respectively.

All modalities. When using all the modalities (thermal, RGB and EDA) to train the model, for TFail the accuracy is steady at 74% across both window sizes. On the other hand, TCog accuracy increases to 90% in the 7 second window. Similarly, when using TCog+TFail, accuracy increases in the 7 seconds to 86%. F1-scores follow the same trends overall for all three data subsets.

B.4.1 Feature Selection

In Table B.3, the best features of the SFFS are shown for each task and each modality separately. To show all three modalities, with the highest model granularity possible, the 3.5 second window was picked to illustrate the feature selection results.

Thermal. When using only the thermal data, for the TFail classifier it can be seen that the cheek region was discarded by the feature selector, selecting only the nose, forehead and lower lip for both temperature average and change. Similarly for the TCog and the TCog+TFail, the maximum temperatures of the nose and lower lip were also selected, in addition to nose temperature average and change for forehead and lower lip.

RGB. In TFail, the most relevant average intensity were AU20, AU23, AU28, AU10 and AU12, which correspond to movements in the lips, in addition to 7 and 4 which correspond to movements in the eye and brow respectively. Similarly, when using TCog the most relevant features for classification were the ones that correspond to lip and eye movements (AU07 and AU05). For the TCog+TFail subset, out of the 8 features selected, 4 were related to lip movements.

EDA. For the TFail classifier, 4 out of the 6 features were selected: mean conductance level, inter-peak interval, peak amplitude and peak duration. For the TCog, only inter-peak

Table B.3 Results for feature selection in the 3.5 second window

Task	Modality	Best Features	
TFail	**Thermal**	**Temp. average**	Nose, Forehead, Lower lip
		Temp. change	Nose, Forehead, Lower lip
	RGB	**Intensity average**	AU07, AU20, AU23, AU28, AU10, AU04, AU12
		Intensity change	AU02, AU09, AU04
		Intensity maximum	AU28
	EDA	**Tonic**	SCL
		Phasic	IPI, Peak amplitude, Peak duration
	All	**Temp. average**	Lower lip
		Intensity average	AU28, AU10, AU23, AU17, AU06
		Temp. change	Lower lip
		Intensity change	AU28, AU02, AU26
TCog	**Thermal**	**Temp. average**	Nose
		Temp. change	Forehead, Lower lip
		Temp. maximum	Nose, Lower lip
	RGB	**Intensity average**	AU06, AU07, AU02, AU10, AU05, AU12, AU26, AU28, AU20, AU14
		Intensity change	AU28, AU20, AU25, AU26
		Intensity maximum	AU28
	EDA	**Phasic**	IPI, Peak duration
	All	**Temp. average**	Nose
		Intensity average	AU45, AU06, AU20, AU10, AU23, AU28, AU07, AU25, AU12
		Temp. change	Lower lip
		Intensity change	AU28, AU04, AU12
		Intensity maximum	AU01, AU02
TCog+TFail	**Thermal**	**Temp. average**	Nose
		Temp. change	Forehead, Lower lip
		Temp. maximum	Nose, lower lip
	RGB	**Intensity average**	AU06, AU02, AU09, AU25, AU26, AU28
		Intensity change	AU28
		Intensity maximum	AU28
	EDA	**Phasic**	Peak duration, Peak rise
	All	**Intensity average**	AU28, AU06, AU02, AU23, AU25
		Intensity change	AU28
		Intensity maximum	AU28

interval and peak duration were selected. Finally, when both tasks are combined, peak rise time and peak duration were the most relevant features.

All Modalities. The most relevant thermal region across all modalities for the TFail classifier was the lower lip, as the temperature average and change. In addition, 7 action units were also selected, mostly corresponding to lip movements. In TCog, two thermal regions were relevant: the nose temperature average and the lower lip temperature change. Also, 12 action units were selected, 6 of which correspond to lip movements, 3 with brows, 2 with eyes and 1 with cheek movements. When the two tasks are combined, in TCog+TFail, only action units were selected, 3 corresponding to lip movements and 2 to brow and cheek movements.

B.5 Discussion

The window sizes comparison across all data subsets shows that using AUs as input data results in the highest accuracy in the 3.5-second window, while thermal and EDA data achieve the highest accuracies in the 7-second window. In other words, increasing the window size decreases the performance of the classifier which uses RGB features as input, while for thermal data as input the performance slightly increases, which coincides with Ekman's findings [480]. Ekman hypothesised that facial expressions last between 0.5 to 4 seconds after a stimuli, but the physiological reaction might take 5 to 15 seconds to completely deteriorate.

Feature selection on the thermal data shows that, among the ROIs provided, the nose, forehead and lower lip are the most relevant to detect frustration. In previous works, the cheek region has been related only to the startle affective state [466], while the other three regions were associated mainly with negative affective states like stress, fear and anxiety [466]. This could explain the correlation that we found with frustration, which is considered a negative state. Furthermore, the classifiers based on only one task (TFail or TCog) selected different features out of the thermal data. In fact, the detectors for TCog and TCog+TFail also used the maximum temperature for the nose and lower lip. This could imply that the thermal facial reaction can be dependant on the type of frustration, since TCog instances are assumed to be more related to cognitive load-induced frustration and the TFail instances to failure-induced frustration. For the classifier which uses instances from both tasks, the features selected are more similar to those of the TCog detector, which could imply these are more evidently

distinguishable from a baseline state, when compared to the failure-induced frustration. However, this effect may be also related to our experimental design and processing, future investigations are needed to better address this point.

The selected features for AUs for both tasks are mainly focused on lip movements, and the common AUs across the three data subsets are AU28 (lip suck) and AU02 (outer brow raiser). As stated by [485], AU28 is associated with fidgeting and can be directly related to negative affective states. The occurrence of AU02 is explained in [486], which states that it is mainly associated with focus. Furthermore, the presence of AU04 (brow lowerer) and AU07 (lid tightner) in both the TCog and TFail detectors can indicate the occurrence of confusion [487]. Nonetheless, for the combined (TCog+TFail) classifier neither of these AUs are selected by the SFFS. According to the literature [488–490], there is no common consensus on which AUs relate to frustration, as it is task-dependent. However, some of the AUs mentioned were AU09, AU10, AU12, AU14, AU23 and AU24, which can be seen among the features selected for each task. Nonetheless, AU28 was repeatedly selected as one of the most relevant action units in our work.

Peak duration is the common selected feature across all data subsets in the EDA modality, in addition to peak rise time in the TCog+TFail detector. According to [491, 492], the tonic component (SCL) might be less useful to detect affective states, while the phasic component is more reactive to external stimuli. This coincides with the fact that only phasic components were selected in the TCog+TFail and TCog detectors.

Combining all the modalities can yield higher accuracies, as is the case across all detectors in the 7 second window size. However, the feature selector discarded EDA data from all the subsets, which indicates that the best combination of modalities would be AUs and thermal data.

The trained model can be extracted and used in real-time, the limiting factor for each window size is the amount of data that would be needed to give one prediction. The time window for the highest accuracy using thermal imaging is 7 seconds, in contrast to the RGB models which reach the highest accuracy in 3.5 seconds. Although, as model reactivity is a priority while running it in real-time, the increase of 3% in accuracy might be a valid compromise for faster reactivity. Furthermore, that does not hinder the capabilities of thermal imaging models as it still can detect frustration in scenarios where it is not visible to RGB cameras. Furthermore, a rolling window can be used to mitigate that effect and increase reactivity in real time retaining the accuracy.

Overall, using the thermal modality yields the highest accuracy when using larger window sizes in TCog+TFail, which is the more general model. Using RGB features for models with

shorter window sizes will lead to better performance, as the KNN model had the highest accuracy at the 3.5 second window.

Limitations

Considering that phasic features were extracted from EDA data, the sampling rate of 4 Hz of the used wristband is not sufficient for small window sizes [493].

Furthermore, allowing for a longer period of rest between tasks (TCog and TFail) could have provided some insight on how much time is necessary to return to a neutral state after becoming frustrated. In TFail, we have assumed that frustration would occur within 7 seconds of each frustrating event; nonetheless, the use of external annotators could have provided a more reliable ground truth for frustration.

Although we have tried to make the interactions as natural as possible while collecting the data, a more robust model would be trained on data collected outside of a lab setting.

In future work, we would like to collect a larger data set with more types of frustration and more participants, which would result in a more general and reliable model. In addition, insuring that the data in granular enough to test smaller and larger window sizes, as the thermal data might perform even better on window sizes larger than 7 seconds.